

University of Alberta

Flavonoids in Saskatoon Fruits, Blueberry Fruits, and Legume Seeds

by

Lihua Jin

A thesis submitted to the Faculty of Graduate Studies and Research
in partial fulfillment of the requirements for the degree of

Doctor of Philosophy
in
Plant Science

Department of Agricultural, Food and Nutritional Science

©Lihua Jin
Fall 2011
Edmonton, Alberta

Permission is hereby granted to the University of Alberta Libraries to reproduce single copies of this thesis and to lend or sell such copies for private, scholarly or scientific research purposes only. Where the thesis is converted to, or otherwise made available in digital form, the University of Alberta will advise potential users of the thesis of these terms.

The author reserves all other publication and other rights in association with the copyright in the thesis and, except as herein before provided, neither the thesis nor any substantial portion thereof may be printed or otherwise reproduced in any material form whatsoever without the author's prior written permission.

Abstract

Flavonoids are a large group of plant secondary metabolites. Three main subclasses of flavonoids are anthocyanins, flavonols, and proanthocyanidins (PAs). In order to improve our understanding of flavonoid biosynthesis and accumulation, and their roles in fruits and seeds, we studied the developmental profiles of anthocyanins, flavonols, and PAs in developing and mature saskatoon (*Amelanchier alnifolia* Nutt.) and highbush blueberry (*Vaccinium corymbosum* L.) fruits and seeds, as well as in the seeds of grain legumes including pea (*Pisum sativum* L.), faba bean (*Vicia faba* L.), and lentil (*Lens culinaris* L.). Levels of these flavonoids were correlated with the visual or histological localization of these compounds in the developing seeds and fruits. A biphasic and tissue-specific pattern of flavonoid production was observed in the fruits. Flavonol and PA concentrations in saskatoon and blueberry fruits were high during early fruit development localizing throughout the ovary tissues. As the fruit matured, flavonol and PA levels declined and localized to only specific ovary tissues and the seed coat. In contrast, anthocyanin concentration was low during early fruit development and dramatically increased as the fruit ripened. For blueberry fruit, flavonoid gene expression was also correlated with flavonoid end-products and end-product localization over development. In the seeds of specific pea cultivars, PA concentration peaked in the seed coats at mid-development, and then declined as the seed matured. PAs were localized to the epidermal and ground-parenchyma layers of the seed coat. Flavonoid type and concentration varied over development, and with organ (fruit or seed), species and within species. Overall,

these data demonstrate that these flavonoid pathways are controlled both spatially and temporally suggesting important functions for these compounds in these organs, including serving as protective agents throughout development.

Acknowledgements

I would like to take this opportunity to thank the many people who have contributed to my graduate research. First, I would like to thank my supervisor Dr. Jocelyn Ozga for her unstinting guidance and support: it is because of her encouragement and patience that I am able to say that I have really enjoyed my graduate studies and my research. Many thanks go as well to Dr. Randall Weselake, Dr. Andreas Schieber, and Dr. Liang Li (from Department of Chemistry) for serving on my committee and for giving me appropriate direction. I would also like to thank my current and previous lab mates who were cheerful companions during my graduate studies. Special thanks are extended to the people in Dr. Weselake's group and Dr. Schieber's group for allowing me to use their specialized equipment. Indeed I was also lucky to meet numerous other nice people, including Dr. Reinecke, Gabor Botar, Szidonia Botar, Gary Sedgwick, Len Steele, Randy Mandryk, Arlene Oatway, Dr. Nakano, and Bruce Alexander, who were always ready with their generous help and encouragement. Further thanks are due to my collaborators at the University of Victoria, to Dr. Peter Constabel and Michael Zifkin for their work on the blueberry project, and to Dr. Dae-Kyun Ro and Kiva Ferraro at University of Calgary for their work on the pea project.

Last but not least, I would like to thank my family and my friends. My mother's endless love and support allowed me put all my time and effort into my study and research. My husband, Peter Li, has shown tremendous patience and sacrifice in support of my graduate studies, dealing with my research-related stresses in truly commendable fashion. My daughter's sweet love and trust never failed to encourage me to continue my course of study. Finally, my friend's steadfast encouragement and sharing helped keep my life as a graduate student joyous and ever optimistic.

Table of Contents

| | Page |
|--|------|
| List of Figures | |
| List of Tables | |
| List of Abbreviations | |
| Chapter 1 Thesis Introduction | 1 |
| Chapter 2 Literature Review | 3 |
| Flavonoid classification..... | 3 |
| <i>Anthocyanins</i> | 5 |
| <i>Flavonols</i> | 6 |
| <i>Proanthocyanidins</i> | 7 |
| Flavonoid biosynthesis..... | 9 |
| Flavonoid trafficking..... | 13 |
| Flavonoid localization..... | 15 |
| Flavonoid chemical analysis..... | 17 |
| Saskatoon fruits..... | 22 |
| <i>Plant characteristic</i> | 22 |
| <i>Fruit maturity stages</i> | 23 |
| <i>Flavonoid complement</i> | 24 |
| Blueberry fruits..... | 24 |
| <i>Plant characteristic</i> | 24 |
| <i>Fruit maturity stages</i> | 25 |
| <i>Flavonoid complement</i> | 26 |
| Legume seeds..... | 27 |
| <i>Plant characteristic</i> | 27 |
| <i>Flavonoid complement</i> | 27 |
| Literature Cited..... | 28 |
| Chapter 3 Anthocyanin and Flavonol Profiles of Saskatoon Fruits (<i>Amelanchier alnifolia</i> Nutt.) during Development and at Maturity | 41 |

| | |
|---|--|
| Introduction..... | 41 |
| Materials and Methods..... | 42 |
| <i>Plant material</i> | 42 |
| <i>Chemicals</i> | 42 |
| <i>Extraction and purification of anthocyanins and flavonols</i> | 43 |
| <i>HPLC analysis</i> | 43 |
| <i>LC-MS analysis</i> | 44 |
| <i>Histology</i> | 44 |
| Results and Discussion..... | 45 |
| <i>Fruit growth and development</i> | 45 |
| <i>Anthocyanin and flavonol profiles during fruit development</i> | 48 |
| <i>Localization of flavonols during fruit development</i> | 59 |
| Conclusions..... | 61 |
| Literature Cited..... | 61 |
| Chapter 4 | Characterization of Proanthocyanidins in Saskatoon Fruits (<i>Amelanchier alnifolia</i> Nutt.) during Development and at Maturity |
| | 66 |
| Introduction..... | 66 |
| Materials and Methods..... | 67 |
| <i>Plant material</i> | 67 |
| <i>Chemicals</i> | 67 |
| <i>Extraction and purification of PAs</i> | 68 |
| <i>Phloroglucinolysis of PAs</i> | 69 |
| <i>Identification and quantitation of PAs</i> | 70 |
| <i>Histochemical localization of PAs</i> | 72 |
| Results and Discussion..... | 74 |
| <i>Kinetic studies on phloroglucinolysis of PAs from saskatoon fruits</i> | 74 |
| <i>Characterization and quantitation of PAs</i> | 76 |

| | | |
|------------------|---|-----------|
| | <i>Localization of PAs in saskatoon fruits</i> | 84 |
| | Conclusions..... | 87 |
| | Literature Cited..... | 88 |
| Chapter 5 | Gene expression and metabolite profiling of developing highbush blueberry (<i>Vaccinium corymbosum</i> L.) fruit indicates transcriptional regulation of flavonoid metabolism and ripening-associated activation of abscisic acid metabolism | 91 |
| | Introduction..... | 91 |
| | Materials and Methods..... | 96 |
| | <i>Plant material and developmental staging criteria</i> | 96 |
| | <i>cDNA library construction and EST sequencing</i> | 96 |
| | <i>Annotation and phylogenetic analysis of blueberry ESTs</i> | 98 |
| | <i>RNA isolation and cDNA synthesis for qRT-PCR gene expression analysis</i> | 98 |
| | <i>Primer design</i> | 99 |
| | <i>Real time qRT-PCR</i> | 100 |
| | <i>Reference gene selection and optimization of qRT-PCR expression normalization</i> | 101 |
| | <i>Soluble proanthocyanidin (PA) quantification and determination of PA subunit composition and mean degree of polymerization (mDP)</i> | 102 |
| | <i>Quantification of anthocyanidins and flavonol aglycone</i> | 105 |
| | <i>Histological procedures and PA and flavonol tissue localization</i> | 107 |
| | <i>Quantification of abscisic acid and its catabolites</i> | 108 |
| | Results..... | 109 |
| | <i>Phenology of blueberry fruit development</i> | 109 |
| | <i>Construction, annotation and analysis of blueberry ESTs</i> | 111 |
| | <i>Identification of genes for blueberry flavonoid</i> | |

| | |
|---|-----|
| <i>biosynthesis</i> | 112 |
| <i>PA biosynthetic genes are expressed very early in blueberry fruit development</i> | 116 |
| <i>Quantification and chemical characterization of PAs</i> ... | 119 |
| <i>General flavonoid and anthocyanin-specific transcript profiles and end product accumulation are distinct from those in PA synthesis</i> | 121 |
| <i>PAs, flavonols, and flavonoid gene transcripts are localized to distinct regions of blueberry fruit</i> | 125 |
| <i>Abscisic acid biosynthesis and metabolism throughout blueberry development</i> | 130 |
| Discussion..... | 133 |
| <i>PA synthesis is developmentally and spatially delimited in blueberry fruit</i> | 134 |
| <i>PA subunit composition reflects biosynthetic gene expression and suggests transcriptional control of PA synthesis</i> | 135 |
| <i>Coexpression of VcUFGT, VcF3'5'H, and VcCytob₅ implicate these genes in anthocyanin synthesis in blueberry</i> | 137 |
| <i>VcMYB1 phylogeny and expression pattern suggest a broad role in regulation of flavonoid synthesis</i> | 138 |
| <i>Activation of ABA metabolism during blueberry ripening</i> | 139 |
| Conclusion..... | 141 |
| Literature Cited..... | 141 |
| Chapter 6 Characterization of Proanthocyanidins in Pea (<i>Pisum sativum</i> L.), Lentil (<i>Lens culinaris</i> L.), and Faba bean (<i>Vicia faba</i> L.) | |
| Seeds | 151 |
| Introduction..... | 151 |
| Materials and Methods..... | 152 |

| | |
|---|-----|
| <i>Plant material</i> | 152 |
| <i>Chemicals</i> | 154 |
| <i>Extraction and purification of PAs</i> | 154 |
| <i>Phloroglucinolysis and HPLC analysis of PA subunits</i> ... | 155 |
| <i>Identification of PA subunits by LC-MS</i> | 156 |
| <i>PA localization in pea seed coats</i> | 156 |
| Results and Discussion..... | 158 |
| <i>PA subunit composition and quantitation in mature pea seeds</i> | 158 |
| <i>PA subunit composition and quantitation in developing pea seed coats</i> | 162 |
| <i>PA subunit composition and quantitation in lentil seeds</i> | 163 |
| <i>PA subunit composition and mDP in faba bean seeds</i> | 164 |
| <i>Phloroglucinolysis product confirmation by LC-MS</i> | 165 |
| <i>Localization of PAs in developing 'Courier' pea seed coats</i> | 169 |
| <i>Localization of PAs in 'Courier' and 'Canstar' seed coats</i> | 170 |
| Conclusions..... | 171 |
| Literature Cited..... | 172 |
| Chapter 7 Summary and Conclusions | 175 |
| Appendix A | 180 |
| Appendix B | 181 |
| Appendix C | 189 |

List of Tables

| Table | Page |
|--|-------------|
| 3.1 Mean fresh fruit weight and diameter of saskatoon fruit during development..... | 48 |
| 3.2 Total anthocyanin concentration during fruit development (mg per 100 grams fresh weight) | 53 |
| 3.3 Characteristic retention time and the fragment ion masses of quercetin triglycosides in saskatoon fruit extracts as determined by LC-MS analysis..... | 55 |
| 4.1 A developmental profile of saskatoon fruit PA subunit composition following phloroglucinolysis of cultivars Altaglo, Honeywood, Northline, Pembina, and Thiessen..... | 81 |
| 4.2 Characterization of proanthocyanidin phloroglucinolysis products of ‘Northline’ stage 1 saskatoon fruits, and cranberry fruit and grape skin standards by LC-MS..... | 83 |
| 5.1 Blueberry fruit cDNA library statistics..... | 111 |
| 5.2 Blueberry unigenes used for qRT-PCR analysis..... | 113 |
| 5.3 Summary of blueberry PA subunit composition following acid hydrolysis and phloroglucinol derivatization..... | 120 |
| 6.1 Summary of PA subunit composition following phloroglucinolysis and RP-HPLC-DAD analysis in the seeds of pea, lentil and faba bean..... | 158 |
| 6.2 Summary of PA subunit composition following phloroglucinolysis of ‘Courier’ pea seed coats over development..... | 162 |
| 6.3 Characterization of phloroglucinolysis products from pea, faba bean and lentil seeds using LC-MS analysis..... | 167 |
| A1 Total flavonol concentration over fruit development (mg/100 g fwt) ... | 180 |
| B1 Top 40 represented unigenes in the two blueberry fruit EST libraries.... | 186 |
| B2 Reference genes evaluated for qRT-PCR transcript abundance normalization..... | 187 |
| B3 Reference gene statistics, stability values and rankings..... | 187 |

| | | |
|-----------|---|-----|
| B4 | LC-MS retention time and characteristic ions of stage 3 (S3) blueberry fruit PA acid-cleavage phloroglucinol derivatization products..... | 188 |
| B5 | Gene-specific primers used for qRT-PCR..... | 188 |

List of Figures

| Figure | Page |
|---------------|---|
| 2.1 | Flavonoid classification.....4 |
| 2.2 | Structures of common anthocyanidins.....5 |
| 2.3 | The chemical structure of common flavonol aglycones.....6 |
| 2.4 | The chemical structure of common flavan-3-ols.....7 |
| 2.5 | The chemical structures of B-type polymeric PAs and an A-type dimer.....8 |
| 2.6 | Flavonoid biosynthesis pathway.....10 |
| 2.7 | The flavonoid products derived from hydroxylation of naringenin by F3'H or F3'5'H.....12 |
| 2.8 | Vanillin reaction with catechin to form a red-coloured product.....16 |
| 2.9 | The reaction mechanism of PA acid-catalyzed cleavage and phloroglucinol derivatization.....22 |
| 2.10 | 'Northline' saskatoon fruit sorted into 9 maturity stages.....23 |
| 2.11 | Whole and bisected blueberry fruit (cv. Rubel) sorted into 8 maturity stages.....26 |
| 3.1 | Whole and bisected fruits of saskatoon cv. Pembina and Altaglo over development.....47 |
| 3.2 | An HPLC-DAD profile of a stage 9 'Pembina' saskatoon fruit flavonoid extract.....51 |
| 3.3 | Type and content of anthocyanins in the fruits of (A) 'Altaglo', (B) 'Honeywood', (C) 'Northline', (D) 'Pembina', and (E) 'Thiessen' during development (stages 1, 4, 5, 7 and 9).....52 |
| 3.4 | Type and content of flavonols in the fruits of (A) 'Altaglo', (B) 'Honeywood', (C) 'Northline', (D) 'Pembina', and (E) 'Thiessen' during fruit development (stages 1, 4, 5, 7 and 9).....54 |
| 3.5 | Mass spectrum of flavonol-type compound 2c.....55 |
| 3.6 | Mass spectrum of flavonol-type compound 2g.....56 |
| 3.7 | Flavonol concentration in 100 g fresh fruit weight (ffw) basis and flavonol |

| | | |
|------------|---|-----|
| | content per fruit basis over the development of saskatoon fruit..... | 58 |
| 3.8 | Flavonol accumulation in ‘Altaglo’ fruit over development..... | 60 |
| 4.1 | A schematic of a typical fruit section (5-10 mm) used for histological fixation for stage 5, 7, and 9 fruits | 72 |
| 4.2 | Effect of phloroglucinolysis reaction time on the production of flavan-3-ols and flavan-3-ol-phloroglucinol adducts..... | 75 |
| 4.3 | RP-HPLC chromatograms (monitored at 280 nm) of the phloroglucinolysis products of PAs from ‘Northline’ stage 1 saskatoon fruits, cranberry fruit standard, and grape skin standard..... | 77 |
| 4.4 | Chemical structures of subunit products following phloroglucinolysis of saskatoon fruit, grape skin, and cranberry fruit PA extracts..... | 78 |
| 4.5 | PA content in saskatoon fruit expressed as mg per 100 gram fresh weight and mg per fruit over fruit development..... | 82 |
| 4.6 | Possible fragmentation patterns of A ₂ -P and A ₂ in a negative ion mode LC-MS system..... | 84 |
| 4.7 | Light microscopic images of ‘Altaglo’ saskatoon fruit cross-sections stained with DMACA for PA visualization..... | 86 |
| 4.8 | Light microscopic images of ‘Pembina’ saskatoon seed cross-sections stained with DMACA for PA visualization..... | 87 |
| 5.1 | General flavonoid biosynthesis pathway leading to flavonols, anthocyanins and proanthocyanidins (PAs) | 94 |
| 5.2 | Developmental stages of blueberry (cv. Rubel) fruit and flowers used for molecular, chemical, and histological analyses..... | 110 |
| 5.3 | Phylogeny of F3’H and F3’5’H – the cytochrome P450 flavonoid hydroxylases..... | 114 |
| 5.4 | Phylogeny of dihydroflavonol reductase (DFR) and anthocyanidin reductase (ANR) protein family..... | 115 |
| 5.5 | Proanthocyanidin gene transcript abundance during blueberry fruit development and ripening..... | 118 |
| 5.6 | Proanthocyanidin accumulation during blueberry fruit development..... | 121 |
| 5.7 | Transcript abundance of genes involved in general flavonoid metabolism | |

| | | |
|-------------|---|-----|
| | including B-ring hydroxylation and anthocyanin synthesis..... | 123 |
| 5.8 | Anthocyanin and flavonol aglycone concentrations in blueberry fruit over development..... | 125 |
| 5.9 | Localization of PAs in blueberry fruit at major developmental stages..... | 126 |
| 5.10 | Flavonol localization in blueberry fruit cross-sections during development..... | 128 |
| 5.11 | Tissue-specific flavonoid gene expression..... | 129 |
| 5.12 | ABA metabolism and related gene expression in ripening blueberry fruit..... | 131 |
| 6.1 | Mature legume grain seeds from pea (<i>Pisum sativum</i> L.), lentil (<i>Lens culinaris</i> L.), and faba bean (<i>Vicia faba</i> L.) used in this study..... | 153 |
| 6.2 | RP-HPLC-DAD chromatograms of the phloroglucinolysis products from pea ('Courier', 'Lan3017', and 'Canstar'; A), lentil ('LeMay'; B), and faba bean ('Fatima'; B) seeds..... | 159 |
| 6.3 | The changes of PA concentration and mDP over pea seed coat development..... | 163 |
| 6.4 | Chemical structures of catechin-(4 α →2)-phloroglucinol and putative catechin-(4 α →2)-phloroglucinol isomer..... | 166 |
| 6.5 | Proposed MS fragmentation patterns of galocatechin-(4 α →2)-phloroglucinol, catechin-(4 α →2)-phloroglucinol, galocatechin, and catechin..... | 168 |
| 6.6 | Cotyledon mid-region cross sections of 'Courier' pea seed coats..... | 170 |
| 6.7 | Micrographs of 'Courier' and 'Canstar' seed coats stained with DMACA and observed under a Nomarski microscope..... | 171 |
| B1 | Gene ontology (GO) categorization of blueberry unigenes..... | 181 |
| B2 | Phylogeny of a subset of the flavonoid-O-glycosyltransferase family...182 | |
| B3 | Phylogeny of the flavonoid R2R3-MYB transcription factor family.....183 | |
| B4 | Evaluation of reference genes for qPCR..... | 184 |
| B5 | Fluorescence microscopy images of Stage 6 fruit cross-sections..... | 184 |

| | | |
|------------|---|-----|
| B6 | Concentrations of ABA and ABA catabolites from pooled fruit tissue (also used for RNA extractions) for the 2008 (A) and 2009 (B) growing seasons..... | 185 |
| C.1 | Micrographs of ‘Canstar’ seed coat cross sections over pea seed development (4 to 30 DAA) | 190 |
| C.2 | Micrographs of ‘Courier’ seed coat cross sections over pea seed development (4 to 30 DAA) | 191 |

List of Abbreviations

| Abbreviation | Definition |
|---------------------|--|
| 4CL | 4-coumarate: CoA ligase |
| A ₂ -P | A ₂ -phloroglucinol |
| ABA | Abscisic acid |
| ABA-GE | Abscisic acid-glucose ester |
| ABC | ATP-binding cassette |
| ANOVA | Analysis of Variance |
| ANR | Anthocyanidin reductase |
| ANS | Anthocyanidin synthase |
| APCI | Atmospheric pressure chemical ionization |
| AS | Aureusidin synthase |
| bHLH | Basic helix-loop-helix |
| C | (+)-Catechin |
| C4H | Cinnamate 4-hydroxylase |
| CCC | Countercurrent chromatography |
| CD | Dichroism spectroscopy |
| cDNA | Complementary deoxyribonucleic acid |
| CDC | Crop Development centre |
| CE | Collision energy |
| CHI | Chalcone isomerase |
| CHS | Chalcone synthase |
| CID | Collision-induced dissociation |
| CLMS | Confocal laser scanning microscope |
| CoA | Coenzyme A |
| C-P | Catechin-(4 α →2)-phloroglucinol |
| C _q | Quantification cycle |
| CTAB | Cetyl-trimethyl-ammonium bromide |
| CV | Coefficient of variation |
| CXP | Collision exit potential |

| | |
|--------------|--|
| DAA | Days after anthesis |
| DAD | Photodiode array detector |
| DFR | Dihydroflavonol 4-reductase |
| DMACA | 4-(dimethylamino)-cinnamaldehyde |
| DP | Declustering potential |
| DPA | Dihydrophaseic acid |
| DPBA | Diphenylboric acid 2-aminoethyl ester |
| EC | (-)-Epicatechin |
| EC-P | Epicatechin-(4 β →2)-phloroglucinol |
| EDTA | Ethylenediaminetetraacetic acid |
| EF | Elongation factor |
| EGC | (-)-Epigallocatechin |
| EGC-P | Epigallocatechin-(4 β →2)-phloroglucinol |
| EMS | Enhanced MS |
| EP | Entrance potential |
| EPI | Enhanced product ion |
| ER | Endoplasmic reticulum |
| ESI | Electrospray ionization |
| EST | Expressed sequence tag |
| EGC | Epigallocatechin |
| ESI | Electrospray ionization |
| F3H (or FHT) | Flavanone 3 β -hydroxylase |
| F3'H | Flavonoid 3' hydroxylase |
| F3'5'H | Flavonoid 3'5' hydroxylase |
| FFW | Fresh fruit weight |
| FLS | Flavanone synthase |
| FS1 | Flavone Synthase 1 |
| FS2 | Flavone Synthase 2 |
| GAPDH | Glyceraldehyde-3-phosphate dehydrogenase |
| GC | Gallocatechin |
| GC-P | Gallocatechin-(4 α →2)-phloroglucinol |

| | |
|---------|---|
| gDNA | Genomic deoxyribonucleic acid |
| GO | Gene oncology |
| GPC | Gel permeation chromatography |
| GST | Glutathione S-transferase |
| HPLC | High performance liquid chromatography |
| IDA | Information dependent acquisition |
| LAR | Leucoanthocyanidin reductase |
| LDOX | Leucoanthocyanidin dioxygenase |
| LOQ | Limit of quantification |
| MALDI | Matrix assisted laser desorption ionization |
| MATE | Multidrug and toxic compound extrusion |
| mDP | Mean degree of polymerization |
| mRNA | Messenger ribonucleic acid |
| MS | Mass spectrometry |
| MS/MS | Tandem mass spectrometry |
| NMR | Nuclear magnetic resonance |
| NRT | No reverse transcriptase |
| NTC | No template |
| OMT | Anthocyanin- <i>O</i> -methyltransferase |
| PA | Proanthocyanidin |
| PAL | Phenylalanine ammonia-lyase |
| PEM | Paraplast [®] Tissue Embedding Medium |
| PIPES | Piperazine-N, N'-bis(2-ethanesulfonic acid) |
| PPO | Polyphenol oxidase |
| qRT-PCR | Quantitative real-time reverse transcriptase polymerase chain reaction |
| RP-HPLC | Reversed phase HPLC |
| RT | Room temperature |
| SPE | Solid phase extraction |
| SSP | solvent-solvent partitioning |
| TAL | Tyrosine ammonia lyase |

| | |
|--------|--|
| TAIR | The Arabidopsis Information Resource |
| TEM | Transmission electron microscope |
| TFA | Trifluoroacetic acid |
| TLC | Thin layer chromatography |
| TOF | Time of flight |
| t_R | Retention time |
| UBQ | Polyubiquitin |
| UDP | Uridine diphosphate |
| UGT | UDP-glucose: flavonoid-3-O-glycosyltransferase |
| UV-Vis | Ultra violet-visible |

Chapter 1

Thesis Introduction

The general hypotheses tested in this thesis were:

- 1) Flavonoid synthesis and accumulation in the fruits of *Amelanchier alnifolia* (saskatoon) and *Vaccinium corymbosum* (blueberry), and seeds of *Pisum sativum* (pea) are developmentally and spatially regulated.
- 2) Variation exists in type and amount of specific flavonoids between different cultivars of the same species (among fruits of *Amelanchier alnifolia* [saskatoon] and among seeds of *Pisum sativum* [pea]), as well as among seeds of different species within the grain legume crops (pea, faba bean and lentil).

To this end, the products of three major flavonoid classes (proanthocyanins [PAs], flavonols, and anthocyanins) were identified and the flavonoid profiles and distribution in the fruit and seed tissues were determined over development. From these data, various mechanisms are postulated that may be involved in the production of the observed variation in the flavonoid type, levels, and location in the various tissues over development and among cultivars of the same species.

This thesis is organized as follows:

- Chapter 2: Literature Review: introduces the structure, biosynthesis, and accumulation of flavonoids in different plants, reviews literature on characterization of flavonoids using chemical analysis and histological methods, and summarizes literature on plant characteristics, development patterns, and flavonoid complement of saskatoon fruits, blueberry fruits, and seeds of pea, faba bean, and lentil.
- Chapter 3 reports work on the characterization of anthocyanins and flavonols in the fruits from five different cultivars of saskatoon during development and at maturity.
- Chapter 4 presents work on the characterization of PAs in the fruits from five different cultivars of saskatoon during development and at maturity.

- Chapter 5 presents work on flavonoid biosynthesis gene expression and flavonoid profiling of developing highbush blueberry (*Vaccinium corymbosum* L.) fruit and a ripening-associated activation of abscisic acid metabolism. This chapter represents collaborative work with the labs of Dr. Peter Constabel at the University of Victoria and Dr. Sue Abrams at the Plant Biotechnology Institute (Saskatoon).
- Chapter 6 presents work on the characterization of PAs in pea (*Pisum sativum* L.), lentil (*Lens culinaris* L.), and faba bean (*Vicia faba* L.) seeds.
- Chapter 7: summarizes the research reported in this thesis, provides overall conclusions obtained from the work, and discusses possible future research directions.
- Appendix A, B, and C: Supplemental data are reported in these sections.

Chapter 2

Literature Review

Flavonoid classification

Flavonoids are a large group of phytochemical compounds synthesized by many higher plants as secondary metabolites. With a common phenolic carbon 6-carbon 3-carbon 6 (C6-C3-C6) skeleton, flavonoids from many different plant species, tissues, and organs display a wide range of diversified structures. By 2004, around 9,000 flavonoids were identified (Williams and Grayer, 2004), and more flavonoids have been reported in more recent years. This huge number of flavonoid compounds can be grouped into different subclasses. The classification of flavonoids can vary depending on the definition of the backbone flavonoid structure. If the flavonoid backbone is defined as two benzene rings (A-ring and B-ring) and one pyran ring (C-ring), flavonoids can be divided into three main subgroups according to the B-ring attachment position on the C-ring as follows: flavonoids (B-ring attached to the C2 position of the C-ring), isoflavonoids (B-ring attached to the C3 position of the C-ring), and neoflavonoids (B-ring attached to the C4 position of the C-ring) (**Figure 2.1**). The flavonoid subgroup can be further divided into 8 subclasses according to C-ring saturation and oxidation as follows: flavones, flavanones, flavonols, flavanonols, anthocyanins, flavan-3,4-diols, flavan-3-ols (and their polymers, proanthocyanidins), and flavan-4-ols (and their polymers, phlobaphenes). Usually chalcones and aurones are not considered to be flavonoids since chalcones do not contain a pyran ring and aurones contain a furan ring instead of a pyran ring (**Figure 2.1**). However, some scientists still like to include chalcones (with a non-cyclized three carbon structure linking the two benzene rings) and aurones among flavonoids (Williams and Grayer, 2004; Ono et al., 2006) because they also have a C6-C3-C6 backbone structure and their biosynthesis pathway shares enzymes with that of the recognized flavonoids. Flavonoids have attracted great scientific interest because of their structural diversity, physiological functions, and purported positive health beneficial effects.

My PhD research focuses on three subclasses of flavonoids, the anthocyanins, flavonols, and the flavan-3-ol oligomers and polymers called proanthocyanidins.

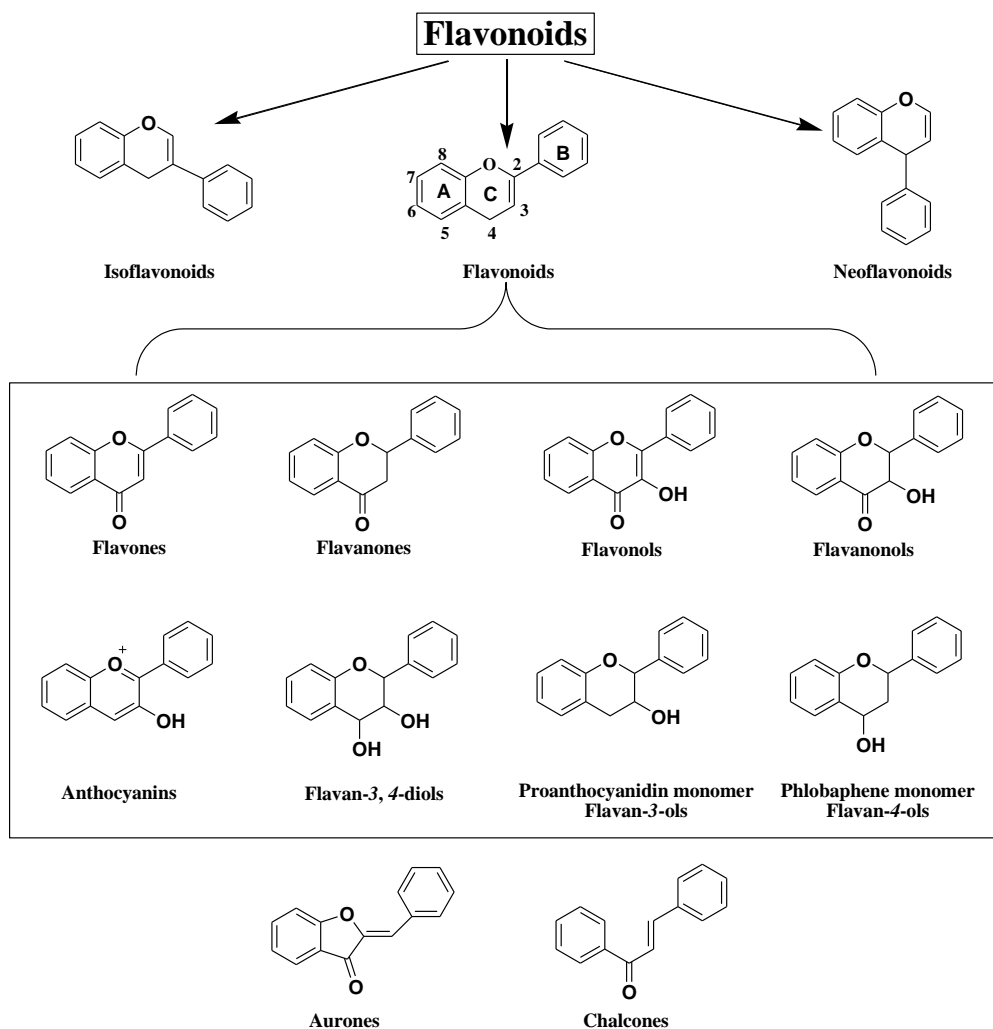


Figure 2.1: Flavonoid classification. Flavonoids can be divided into 3 main subgroups according to the B-ring attachment position on the C-ring leading to the subclasses of flavonoids, isoflavonoids, and neoflavonoids. The flavonoid subgroup can be further divided into 8 subclasses (within the box) according to C-ring saturation and oxidation. Usually chalcones and aurones are not considered to be flavonoids as they do not contain the flavonoid backbone of two benzene rings (A-ring and B-ring) and one pyran ring (C-ring).

Anthocyanins

Anthocyanins are glycosides of anthocyanidins (anthocyanin aglycones). Anthocyanidins contain a flavylium ion in their chemical structure and the differences between individual anthocyanidins are the result of variations in the number and position of methoxyl and hydroxyl units in the anthocyanidin backbone structure (**Figure 2.2**). Among the 19 anthocyanidins already identified (Iwashina, 2000), pelargonidin, cyanidin, delphinidin, peonidin, petunidin, and malvidin are the six most common. Glycosylation usually occurs in one or more positions of carbon 3, 5, 7, 3', 4', and 5' of the anthocyanidins to form anthocyanins. Glucose, galactose, rhamnose, and arabinose are the most common sugars bonded to anthocyanidins (Iwashina, 2000). Phenolic acids such as caffeic acid, gallic acid, and ferulic acid can also be conjugated to the sugar units of anthocyanins to form more complex anthocyanin structures (Iwashina, 2000). *O*-glycosylations are the most common form of attachment of sugar units to anthocyanidins, but *C*-glycosylations have also been found in the C8 position of anthocyanins (Williams and Grayer, 2004).

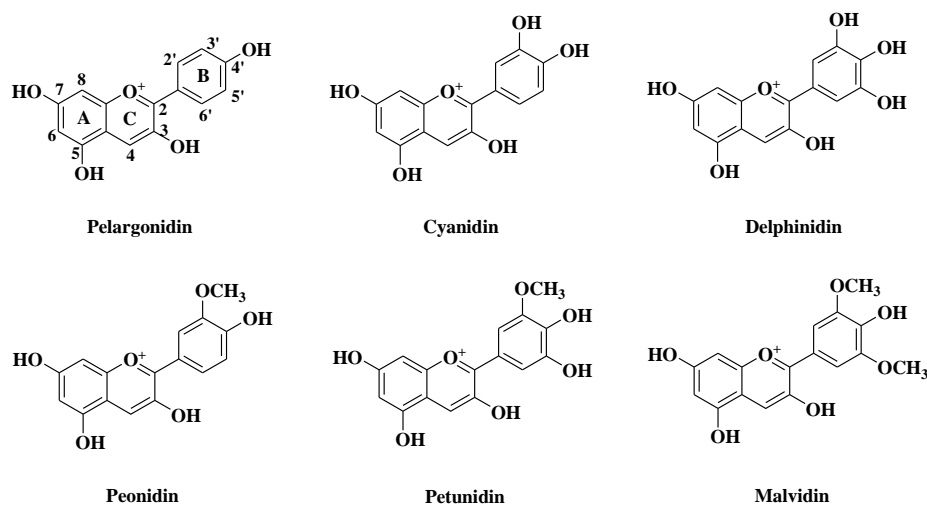


Figure 2.2: Structures of common anthocyanidins.

Anthocyanins are natural pigments producing bright colours such as red, pink, and purple in the flowers, leaves, seeds, stems, and fruits of many plants. The colour of anthocyanins can change with the pH of their environment (Goto and Kondo, 1991). Anthocyanin colour also varies with the number of hydroxyl

groups in the anthocyanin B-ring and the methylation of those hydroxyl groups in the B-ring (Moore and Vodopich, 1987). An increased number of hydroxyl groups in B-ring shifts anthocyanin colour towards the blue, whereas methylation in one or two of these hydroxyl groups has the opposite effect. Anthocyanins in floral structures can aid in the attraction of pollinating insects and birds, and in fruits they can help seed dispersal by attracting animals visually. Also, they have been associated with pathogen- and stress-resistance in some plant species (Chalker-Scott, 1999; Close and Beadle, 2003). Anthocyanins have many reported health benefits such as antioxidant, anti-carcinogenic, and antidiabetic activities (Zafra-Stone et al., 2007). The abundance of anthocyanins in plants raises the possibility that anthocyanins could substitute for synthetic dyes in processed foods and beverages, thereby addressing consumer preferences for more natural products (Lowry and Chew, 1974).

Flavonols

Flavonols that accumulate in plants are normally *O*-glycosides of 3-hydroxyl flavones (flavonol aglycones). Glycosylation can also occur at one or more positions of the flavonol molecule including carbon 3, 7, 3', and 4', with different combinations of various sugar units such as glucose, galactose, xylose, and rhamnose. The differences among flavonol aglycones are determined by the positions and numbers of hydroxyl and methoxyl groups attached to the A- and B-rings. The common flavonol aglycones found in plants are kaempferol, quercetin, myricetin, and isorhamnetin (**Figure 2.3**).

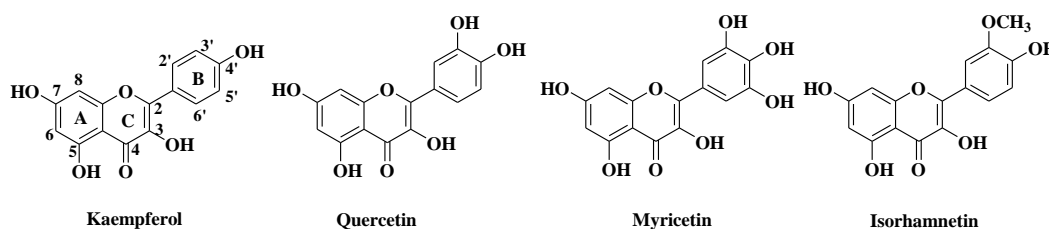


Figure 2.3: The chemical structure of common flavonol aglycones.

Flavonols are present in many plant species and in plant organs such as flowers, leaves, and fruits. Flavonols function as a UV-light filter protecting plant

organs from UV light damage by absorbing UV light (Middleton and Teramura, 1993; Kolb et al., 2003). Flavonols are normally pale yellow or colourless but in flowers they are readily recognized by insects and can thus aid in the pollination process. Flavonols also coexist as pigments with anthocyanins in flowers, shifting flower colours by molecular stacking or hydrogen bonding to ones more easily recognized by certain pollinators (Goto and Kondo, 1991; Mol et al., 1998). Flavonols are present in the cells of cultivated vascular plants such as onions, berries and apples, which are quite common in our daily dietary intake. Flavonols also have many positive health benefits for humans, as do anthocyanins (Lam et al., 2010).

Proanthocyanidins

Proanthocyanidins (PAs), also known as condensed tannins, are oligomeric and polymeric flavan-3-ols. Among approximately 80 kinds of reported flavan-3-ols, the most well-known flavan-3-ols are catechin and epicatechin. The flavan-3-ols can be further subdivided into 2, 3-*cis*-flavan-3-ols and 2, 3-*trans*-flavan-3-ols (Dixon et al., 2005).

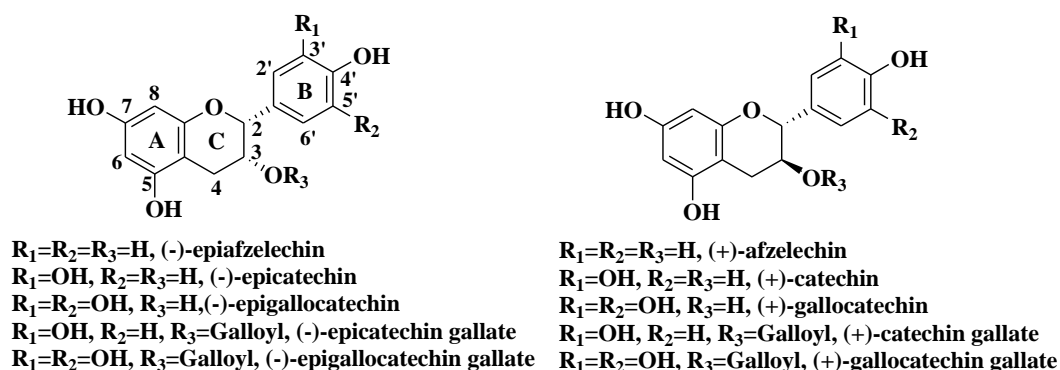


Figure 2.4: The chemical structure of common flavan-3-ols.

The structure of PAs vary by several factors: the nature (stereochemistry and hydroxylation pattern) of the flavan-3-ols in the extension and terminal units of the oligomer or polymer, the linkages between subunits, the degree of polymerization, and the presence or absence of modifications such as esterification of the C3 hydroxyl group with gallic acid or sugar units (Dixon et al.,

2005). Generally, PA subunit linkages are between the C4 of the ‘upper’ unit and the C8 or C6 positions of the ‘lower’ unit. These types of PA subunit linkages are called B-type (**Figure 2.5**). In the case of A-type PAs, both C2 and C4 of the upper unit and the oxygen at C7 and C6 or C8 are doubly linked (**Figure 2.5**). PA trimers with two C4→C8 interflavan linkages between flavan-3-ols are called C-type trimers (Aron and Kennedy, 2008). Depending on the major subunits that make up the PA extension and terminal units, they also can be called procyanidins, prodelphinidins, or propelargonidins. For example, PAs consisting of catechin and epicatechin are named procyanidins. If most subunits in the PAs are gallicocatechin and/or epigallocatechin, the PAs are prodelphinidins.

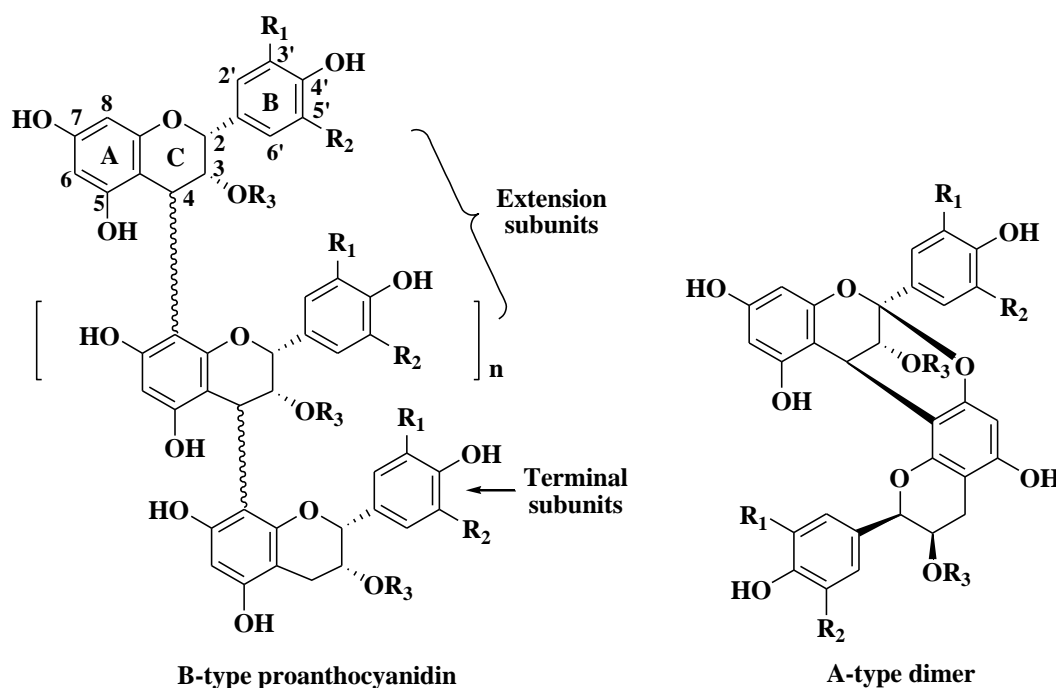


Figure 2.5 The chemical structures of B-type polymeric PAs and an A-type dimer. $R_1 = \text{OH}$ or H ; $R_2 = \text{OH}$ or H ; $R_3 = \text{H}$ or galloyl.

PAs are present in the fruits, leaves, and seeds of many woody plants, where they provide protection against microbial pathogens, insects, and larger herbivores (Ayres et al., 1997; Mellway et al., 2009). They are also present in common processed foods such as cereals, chocolates, wines, beers, coffee, and teas (Gu et al., 2003). Recently, PAs have attracted the attention of researchers in the fields of

nutrition and medicine for their reported human-health benefits. A variety of physiological responses have been attributed to PAs including antioxidant, antimicrobial, anti-carcinogenic, anti-diabetic, and anti-hypertensive activities, as demonstrated by in-vivo and in-vitro assays (Steinberg et al., 2003; Lee et al., 2008; Crozier et al., 2009). For example, A-type proanthocyanidin extracts from cranberry fruits have been found to be effective in the inhibition of urinary tract infections (Foo et al., 2000).

Flavonoid biosynthesis

Most flavonoids are believed to be synthesized in a complex of metabolic enzymes located on the cytoplasmic surface of the endoplasmic reticulum (ER) of plant cells (Burbulis and Winkel-Shirley, 1999). On the other hand, some flavonoids (flavonols and flavanols) and a few flavonoid biosynthesis enzymes (CHS, CHI, and ANS) have also been found in the nuclei of plant cells (Wang et al.; Saslowsky et al., 2005; Polster et al., 2006). This suggests that flavonoids are synthesized in different cell compartments in order to support specific physiological functions. Flavonoid biosynthesis has been extensively studied in seeds of model plants such as *Arabidopsis thaliana*, *Medicago truncatula*, and *Oryza sativa* (Lepiniec et al., 2006; Pang et al., 2007; Reddy et al., 2007). Flavonoid biosynthesis has also been studied in economic fruit crops such as grapes, apples, and small fruits in order to more fully understand the biosynthesis pathway and the mechanisms that regulate it, and to further our ability to enhance the production of flavonoids in those fruits by using metabolic engineering (Jaakola et al., 2002; Espley et al., 2007; Deluc et al., 2008). Flavonoid biosynthesis shares starting materials with primary metabolite biosynthesis, such as phenylalanine, tyrosine, and malonyl-CoA. The B-ring and C-ring (three-carbon bridge) precursors of flavonoids (C6-C3-C6) are synthesized from amino acids bearing benzene side chains such as phenylalanine (Winkel-Shirley, 2001) and (rarely) tyrosine (Watts et al., 2004). The A-ring is synthesized by a condensation reaction requiring three malonyl-CoA molecules, forming an aromatic ring (**Figure 2.6**).

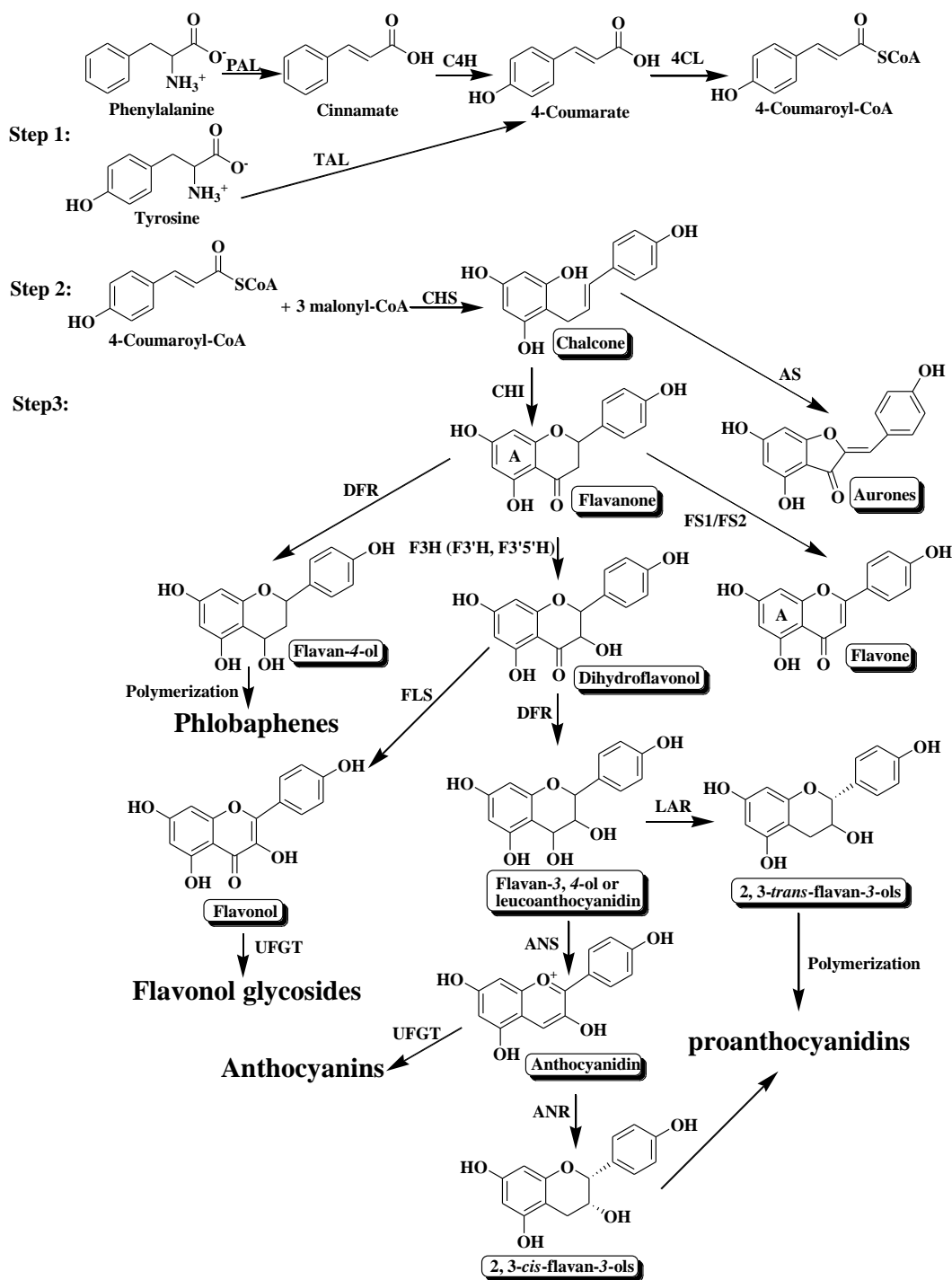


Figure 2.6: Flavonoid biosynthesis pathway. Flavonoid biosynthesis can be divided into 3 steps. Step 1: Formation of 4-coumaroyl-CoA from amino acids bearing benzene side chains (usually phenylalanine). Step 2: Formation of chalcone from 4-coumaroyl-CoA. Step 3: Formation of various subclasses of flavonoids from a chalcone. PAL, phenylalanine ammonia-lyase; C4H, cinnamate

4-hydroxylase; 4CL, 4-coumarate: CoA ligase; TAL, tyrosine ammonia-lyase; CHS, chalcone synthase; CHI, chalcone isomerase; AS, aureusidin synthase; FS1/FS2, flavone synthase 1/ flavone synthase 2; F3H, flavanone 3 β -hydroxylase; F3'H, flavonoid 3'-hydroxylase; F3'5'H, flavonoid 3'5'-hydroxylase; DFR, dihydroflavonol reductase; FLS, flavonol synthase; ANS, anthocyanidin synthase; LAR, leucoanthocyanidin reductase; ANR, anthocyanidin reductase; UFGT, UDP-glucose:flavonoid-3-O-glycosyltransferase.

Flavonoid biosynthesis is a complex process, with many enzymes (or enzyme complexes) and regulatory genes involved. Although the biosynthesis of flavonoids has been extensively studied in the last three decades, there are still parts of the biosynthesis pathway that are unresolved (Dixon et al., 2005). Flavonoid biosynthesis can be divided into 3 steps. In Step 1, phenylalanine ammonia-lyase (PAL) removes an amine group from phenylalanine, forming cinnamate. Cinnamate 4-hydroxylase (C4H) then adds a hydroxyl group to the C-4 position of cinnamate, forming 4-coumarate; this can be one enzymatic process if tyrosine is a starting material for biosynthesis. Then 4-coumarate: CoA ligase (4CL) adds a CoA to 4-coumarate to produce 4-coumaroyl-CoA. In Step 2, chalcone synthase (CHS) catalyzes the condensation reaction between 3 molecules of malonyl-CoA and 1 molecule of 4-Coumaroyl-CoA to produce 1 chalcone molecule. In Step 3, the biosynthesis of various flavonoid subclasses is catalyzed by subclass-specific enzymes (**Figure 2.6**). Chalcone isomerase (CHI) catalyzes the stereo-specific isomerization of chalcone to flavanone. Studies on the cellular location of CHS and CHI (two important enzymes in the early part of the flavonoid biosynthetic pathway), suggest that flavanones are synthesized in the cytoplasm, closely associated with the endoplasmic reticulum (ER) membrane (Saslowky and Winkel-Shirley, 2001). Aurones are synthesized in some plant species via aureusidin synthase (AS) activity in the vacuoles of flower petal cells (Nakayama et al., 2001). Flavone Synthase 1 and flavone synthase 2 (FS1 and FS2) are two distinctive enzymes from different flavone-accumulating plant species that catalyze the formation of flavones from flavanones (Martens and

Mithofer, 2005). Flavanone 3 β -hydroxylase (F3H) catalyzes the stereospecific hydroxylation of flavanone. The presence of the two enzymes, flavonoid 3' hydroxylase (F3'H) and flavonoid 3', 5' hydroxylase (F3'5'H), controls the B-ring hydroxylation pattern of the different subclasses of flavonoid (**Figure 2.7**). The B-ring hydroxylation pattern is an important factor in flavonoid studies since it impacts colour and physiological activity of specific classes of flavonoids (Bogs et al., 2006).

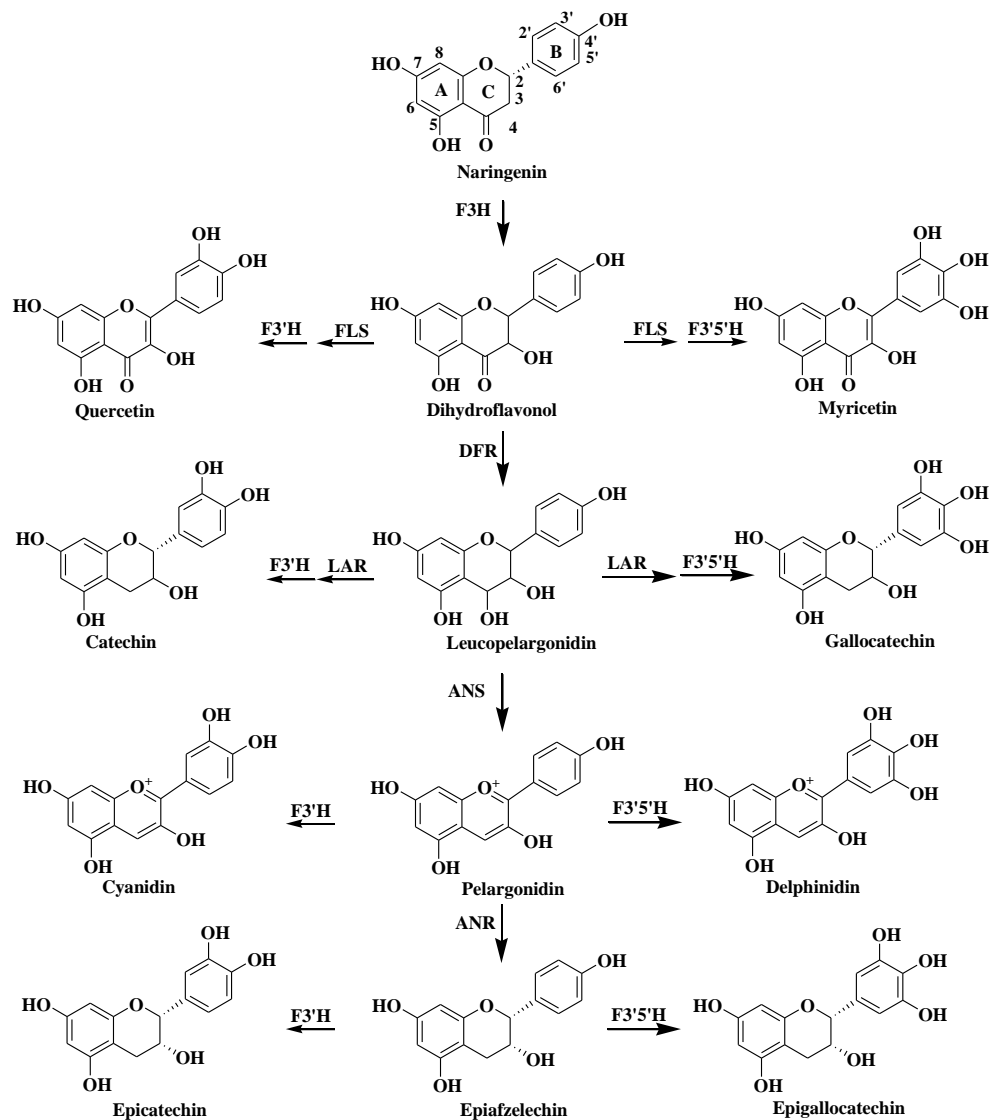


Figure 2.7: The flavonoid products derived from hydroxylation of naringenin by F3'H or F3'5'H. ANR, anthocyanidin reductase; ANS, anthocyanidins synthase; DFR, dihydroflavonol reductase; F3H, flavanone-3 β -hydroxylase; F3'H,

flavonoid 3' hydroxylase; F3'5'H, flavonoid 3', 5' hydroxylase; FLS, flavonol synthase; LAR, leucoanthocyanidin reductase.

Flavonol synthase (FLS) is a key enzyme in the biosynthesis of flavonols. Dihydroflavonols (flavanonols) are reduced to leucoanthocyanidins by dihydroflavonol 4-reductase (DFR) in the course of biosynthesis of anthocyanidins and flavan-3-ols. DFR also participates in the biosynthesis of flavan-4-ols and phlobaphens (Himi and Noda, 2004). Leucoanthocyanidin reductase (LAR) and anthocyanidins reductase (ANR) are two important enzymes in the biosynthesis of stereo-specific flavan-3-ols and PAs. Research supports that anthocyanidin synthase (ANS) and ANR converts leucoanthocyanidins to 2, 3-*cis* flavan-3-ols, and LAR converts them to 2, 3-*tran* flavan-3-ols (Dixon et al., 2005; Pang et al., 2007). UDP-glucose: flavonoid-3-O-glycosyltransferase (UFGT) is an enzyme essential for glycosylation of flavonols and anthocyanins (Boss et al., 1996). Flavonoid glycosylation occurs in the latter stage of flavonoid biosynthesis and it plays many important roles in flavonoid biosynthesis such as flavonoid aglycone stabilization, solubilisation, and detoxification (Jones and Vogt, 2001). Beyond the enzymes mentioned above, there are other enzymes that participate in flavonoid biosynthesis, increasing the diversity of flavonoids found in plants. Flavonoid biosynthesis depends not only on the above-mentioned enzyme activities, but also on controlling transcription factors. Transcription factors that regulate flavonoid biosynthesis have been studied not only in model plants such *Arabidopsis* (Nesi et al., 2001), rice (Ithal and Reddy, 2004), and *Medicago* (Peel et al., 2009), but also in economic fruit crops such as apples (Espley et al., 2007), grapes (Deluc et al., 2008), and tomato (Adato et al., 2009).

Flavonoid trafficking

Data suggests that flavonoids are compounds synthesized by plants for interacting with their surrounding environment (Mellway et al., 2009). After synthesis, flavonoids need to be efficiently transported from the site of synthesis to functioning or storage sites (such as vacuoles, which are the most common cell

component used for this purpose). Flavonoid movement can be intracellular or intercellular, and may involve crossing many membrane barriers until the secondary metabolites reach their targets. Flavonoid transport mechanisms have been extensively studied by metabolic engineers for optimizing flavonoid production (Grotewold, 2004; Winkel, 2004; Zhao and Dixon, 2010). This research is driven by two major hypotheses. The first hypothesis, called the membrane-protein-transporter hypothesis assumes specific proteins are used for flavonoid transport (Zhao and Dixon, 2010). Three major types of protein transporters are known to participate in flavonoid movement: ATP-binding cassette transporters (ABC transporters), glutathione S-transferase transporters (GST transporters), and multidrug-and-toxic-compound-extrusion transporters (MATE transporters). ABC-type transporters contribute to the movement of metal ions and plant metabolites on the basis of their trans-membrane structure (Rea, 2007). GST transporters can bind to flavonoids to form flavonoid-GST complexes that then take flavonoids to the storage site (Mueller et al., 2000). MATE transporters move flavonoids on the basis of cation (H^+ or Na^+) differences (Yazaki, 2005). The second hypothesis in flavonoid movement is known as the vesicle-mediated-transport hypothesis. This is based on microscopic observation of anthocyanoplasts (anthocyanin-containing vesicles) and their fusion to cell wall or central vacuole membranes (Yazaki, 2005). Another example of vesicle-mediated transport, as observed via transmission electron microscopy (TEM), is seen in PA-accumulating multiple small vesicles scattered in the endothelial cells of *tds4-1* mutant seeds (Abrahams et al., 2003). The vesicle-mediated-flavonoid-transport hypothesis requires additional experimentation for confirmation, especially in response to questions such as how these vesicles are formed, how these vesicles move in certain directions, and how these vesicles are recognized and can be fused with other sub-cellular membranes (Zhao and Dixon, 2010). Indeed, further research on the overall topic of flavonoid transport is warranted.

Flavonoid localization

After effective biosynthesis and transport, flavonoids accumulate in certain tissues or cell compartments and become involved in various physiological functions. The study of flavonoid location in plants is pivotal for a better understanding of when, where, and how flavonoids play their biological and ecological roles. Flavonoid localization has been investigated with histological and histochemical techniques that involve many steps such as tissue fixation, dehydration, infiltration, and microscopic observation (Gutmann and Feucht, 1991). The first step in such a localization study is tissue fixation, which can be further divided into chemical fixation and frozen fixation (an alternative to chemical fixation which needs a rapid-freezing device.) The purpose of tissue fixation is to maintain the structural integrity of tissues and protect the tissues from degradation caused by enzymatic or bacterial activity. Glutaraldehyde, osmium tetroxide (OsO_4 , for electron microscopy samples), and paraformaldehyde are commonly-used fixatives in chemical fixation (Kiernan, 2000). Various tissue sections (cross sections, longitudinal sections, or tangential sections) need to be merged into a fixing solution that contains phosphate or piperazine-N, N'-bis (2-ethanesulfonic acid) (PIPES) buffer and one or more fixatives. After fixation, tissues need to be dehydrated with a series of ethanol or acetone solutions to remove most of the water from the tissues; the remaining water can then be completely removed with a few changes of anhydrous ethanol or propylene oxide (Brorson, 1996). The dehydrated tissues then need to be infiltrated with different clearing reagents such as toluene, xylene, and Histo-ClearTM (Luchtel et al., 1998). With the help of fluid-state embedding reagents, tissues are then embedded in paraffin or various plastic resins (for example: Spurr's resin, Histo-resionTM, or LR whiteTM resin) (Yeung, 1999). Embedded tissues can be sectioned with microtomes in micrometer (μm)-level thicknesses and then mounted on glass slides in preparation for staining. The staining process is designed to improve colour contrast when tissues are viewed under a microscope. There are various staining reagents available for staining PAs, with differing features such as selectivity, the colour of staining reaction products, and

sensitivity upon reaction with PAs. Aromatic aldehydes, 4-dimethylamino-cinnamaldehyde (DMACA, stains PAs blue-purple) and 4-hydroxy-3-methoxy-benzaldehyde (vanillin, stains PAs pink-red), react with PAs via a phenol-aldehyde condensation reaction under acidic conditions to form different chromophores (Treutter, 1989). For example, vanillin reacts with flavan-3-ol (A-ring C-6 position) to produce the red-coloured product presented in **Figure 2.8**.

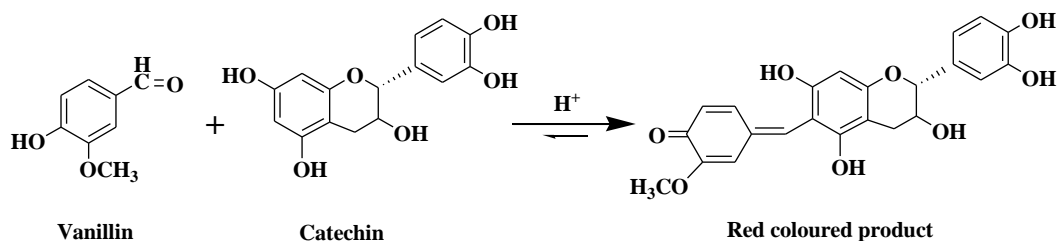


Figure 2.8: Vanillin reaction with catechin to form a red-coloured product.

Sulfuric-acid staining is based on the PA hydrolysis reaction under acidic conditions that forms red-coloured anthocyanins (Gutmann, 1993). The sulphuric-acid staining method does not stain flavan-3-ol monomers, whereas the DMACA-HCl method and Vanillin-HCl method stain both monomeric and polymeric flavanols. Therefore, the sulphuric-acid method can screen out monomeric flavan-3-ol interference from PA localization. Both vanillin- and sulphuric-acid staining produce a red colour with PAs and these staining methods should therefore not be used when plant tissues contain anthocyanins (Lees et al., 1993). The most widely-used staining reagent for PAs and flavan-3-ols is DMACA-HCl because of its high sensitivity and distinct blue-staining colour when compared with other staining reagents (Feucht et al., 1994; Li et al., 1996). As one of the major subclasses of flavonoids, anthocyanins have their natural bright colours and can be easily visualized in localization studies. The study of anthocyanin accumulation in an annual herbaceous plant (*Impatiens balsamina* L.) showed red anthocyanins to be clearly visible in vacuoles of specific tissue cells of plant parts such as node, leaf, and petal (Aras et al., 2007). Anthocyanin localization was also confirmed in seeded and seedless grapes by their natural colour and using their

colour-changing properties under different pH conditions (e.g., NH_3 gas turns anthocyanins blue) (Barcelo et al., 1994). Flavonols show auto-fluorescence and can be seen under a fluorescence microscope or a confocal laser-scanning microscope (CLSM) (Schnitzler et al., 1996). It should be noted that other compounds in plant cells such as lignin (De Micco and Aronne, 2007), chlorophyll (Rolfe and Scholes), and some proteins (Hraska et al., 2006) also show auto-fluorescence which can interfere with flavonol localization. Diphenylboric acid 2-aminoethyl ester (DPBA) can enhance flavonol auto-fluorescence and has been used for staining flavonols in different plant tissues (Schnitzler et al., 1996; Polster et al., 2006). Light microscopy, CLSM, and electron microscopy are all widely used for observing flavonoid localization in different plant tissues. Flavonoid accumulation in a plant tissue depends on many factors such as species, developmental stage, and environmental stresses. PAs accumulate in the fruit skin of apples and berries, especially in vacuoles of parenchyma layers close to fruit epidermis or in vacuoles of the hypodermal layer (Feucht et al., 1994; Lees et al., 1995). PA accumulation patterns in Arabidopsis seeds have been shown to vary according to seed developmental stages (Debeaujon et al., 2003). Poplar leaves under wounding and light stress accumulated higher levels of PAs than those from nonstressed conditions (Mellway et al., 2009). A study of flavonoid deposition in cell walls of *lisianthus* flower petals found that flavonols not only accumulate in vacuoles as do other flavonoids, but also in cell walls and even in the cuticular wax layer (Markham et al., 2000). Flavanols (PA monomers) have also been found to accumulate in nuclei of tea flower cells (Feucht et al., 2004) and cells of the seed wings of coniferous tree species (Polster et al., 2006). Flavonoid accumulation in certain tissues and cell compartments is likely related to flavonoid functions at these sites.

Flavonoid chemical analysis

After flavonoids have accumulated in certain organs or tissues, they carry out diversified tasks in plant survival, growth, and development. To improve our understanding of specific flavonoid functions, flavonoid synthesis and

accumulation patterns over development in target plant tissues and organs need to be investigated. Both chemical analyses for precise characterization and quantification, and localization studies based on histological and histochemical techniques are required to characterize the flavonoid complement within specific plant tissues. Chemical analysis includes many steps such as extraction, purification, and techniques for identification and quantitation. As mentioned before, flavonoids are diversified polyphenolic compounds. Some flavonoids are labile and can be easily degraded under ambient conditions such as high moisture, strong sunlight, and moderate temperature (Woodward et al., 2009). Also, most flavonoids are readily oxidized in the presence of polyphenoloxidase (PPO) (Pourcel et al., 2007).

Special care needs to be taken in the chemical analysis of flavonoids. The first step in this analysis is the preparation of sample material, i.e. sample collection, storage, and grinding. After field collection, plant samples need to be immediately frozen or dehydrated for reducing flavonoid degradation by enzymes during storage. Plant samples also can be ground for extraction right after collection. However, the grinding process can break cell membranes and release PPO. PPO activity can be inhibited by grinding the plant sample in the presence of liquid nitrogen to lower the grinding temperature and thus retard enzyme activity. The second step in flavonoid chemical analysis is extraction of flavonoids from prepared samples via a solvent system. Extraction solvents are chosen on the basis of the polarity of the targeted flavonoid compounds. Commonly used solvents in flavonoid extraction are water or mixtures of water, methanol, and acetone (Ozga et al., 2007). Maximum extraction efficiency depends on optimized sample particle size, solvent polarity, pH, sample/solvent ratio, time, temperature, applied force (sonication, shaking, or vortexing), sample matrix-binding property, and other factors (Andersen, 2006). Anthocyanins and flavonols that accumulate in plant tissues are usually in the glycoside form (tending to be water-soluble), with anthocyanins being unstable at high pH (Woodward et al., 2009). Thus, polar solvents (mixture of water, methanol, acetone, and formic acid) with a low pH are used for extracting these compounds (Ozga et al., 2007). PAs are a mixture of

flavan-3-ol oligomers and polymers. Aqueous acetone (approximately 70% v/v) is an efficient solvent system for extracting PAs (Hussein et al., 1990) and widely used to extract PAs from various plant materials (Tits et al., 1992; Kennedy and Jones, 2001; Taylor et al., 2003). During the extraction process, it is desirable to exclude oxygen, avoid strong light, and perhaps add chemical reagents to protect the targeted compounds from degradation.

Flavonoid extracts from plant samples contain flavonoids and other primary and secondary plant metabolites such as organic acids, sugars, chlorophylls, and lipids. These non-flavonoid compounds need to be removed. The most commonly used methods for purification of the extract are solid-phase extraction (SPE) and solvent-solvent partitioning (SSP) (Andersen, 2006). The latter method uses two immiscible solvent systems to separate out non-flavonoid compounds from flavonoids. The SPE method is based on the partition of flavonoids into two phases (mobile phase and solid stationary phase). The plant extract is applied to the stationary phase that is conditioned with aqueous organic solvent to allow the flavonoids to bind to it. Subsequently, the extract-stationary phase matrix is washed with washing solvent to remove the extraneous material. The target flavonoids are then eluted from the stationary phase with the proper solvent system (usually methanol or acetone).

The last key steps in chemical analysis are quantitative and qualitative analyses. Depending on the purpose of the study, different analytical methods can be used. The most commonly used quantification methods for measuring flavonoid content are colourimetric assays (Zhishen et al., 1999) and high-performance-liquid chromatography (HPLC) coupled with diode-array detector (HPLC-DAD) analysis (Merken and Beecher, 2000; Prati et al., 2007). Various flavonoid subfamilies can be quantified by different colourimetric methods. For example, the pH differential method has been used to determine total anthocyanins (Giusti and Wrolstad, 1996) and the vanillin-HCl method has been used to measure total PA content (Price et al., 1978). These colourimetric methods usually give values equivalent to standard compounds, and they are relatively simple and good for fast screening for comparing flavonoid content among plant

species, cultivars, or tissues. They are not suitable when specific flavonoid profiles need to be determined. Flavonoids are chromophores and each subgroup of flavonoids has its distinct absorbance according to its C-ring oxidation and saturation pattern (Andersen, 2006). This character allows flavonoid content to be easily determined in HPLC-DAD analysis. The HPLC technique can effectively be used to separate individual flavonoids from each other and when coupled to a DAD detector, the flavonoids can be monitored at characteristic specific wavelengths as they elute from the column (Ozga et al., 2007). Historically, thin-layer chromatography (TLC) was widely used for flavonoid separation (Heimler, 1986). Nowadays, HPLC is more favoured for the separation work since it can lead to greater compound separation capacity due to the higher number of theoretical plates than TLC and HPLC can be coupled with UV-Vis spectra, mass spectrometry (MS), and nuclear magnetic resonance (NMR) for online identification of flavonoid compounds. Countercurrent chromatography (CCC) is a promising technique in the separation of flavonoids (Leitao et al., 2005) since it can accomplish small- and large-scale compound separation with good recovery.

After effective separation, flavonoid compounds can be identified by MS, circular dichroism spectroscopy (CD), and NMR. MS can detect charged molecular ions or fragment ions produced by different ionization methods and this information is essential for identifying flavonoid structures. Soft ionization methods such as electrospray ionization (ESI) (Ozga et al., 2007), atmospheric-pressure chemical ionization (APCI) (Grayer et al., 2000), and matrix-assisted laser desorption ionization (MALDI) (Wang et al., 2000) have been preferred for flavonoid identification since they give clear information about molecular ions, sugar units, and flavonoid aglycones. For coupling with such ionization techniques, different mass-spectrometry analyzers such as quadrupole, tandem (MS/MS), and time-of-flight (TOF) have been used for flavonoid analysis. The most intensive use of MS in flavonoid analysis is HPLC-MS for complete separation, identification, and quantification at the same time (Andersen, 2006). However, MS cannot give definite structural identification results unless standard reference compounds are available. NMR has been extensively used for flavonoid

identification since authentic standards are not available for all flavonoids and NMR is one of the most powerful techniques for structure determination in analytical chemistry. For NMR analysis, samples need to be in a pure form and in sufficient amounts (milligram levels). These requirements have restricted NMR applications in some flavonoid analysis work. Recently, improvements in NMR techniques and coupling NMR with HPLC have greatly extended the use of NMR in flavonoid analysis (Welch et al., 2008). CD also has its relevance to flavonoid analysis since some flavonoids have chiral isomers (Xie et al., 2003). PAs are present in a plant extract as mixtures of oligomers and polymers. The oligomers can be separated by TLC or normal-phase HPLC and further identified by MS or NMR. Unfortunately, current separation and identification techniques have their limits when one works with the high molecular weight polymeric PAs.

There are at present two main approaches for characterizing PA composition. One approach is applying pre-purified PA extracts to SPE (Sephadex LH-20) and collecting fractions by gradually changing the polarity of the column-washing solvents (a series of aqueous methanol and acetone solutions) to fractionate PAs into different polymer size classes. The average polymer size in each fraction is then measured by gel-permeation chromatography (GPC) (Kennedy and Taylor, 2003) or calculated by the derivatization method (Duenas et al., 2003). Another approach to PA identification and quantification is cleaving PAs under acidic conditions and derivatizing cleaved and unstable subunits with nucleophilic compounds such as phloroglucinol and benzyl mercaptan (Prieur et al., 1994). Phloroglucinol is preferred as a derivatization reagent since benzyl mercaptan has a strong unpleasant odour and must be used in a fume hood. A reaction using phloroglucinol as a derivatization reagent is presented in **Figure 2.9**. Flavan-3-ols in the extension units form phloroglucinol adducts at their C4 positions, while terminal flavan-3-ol units are released as flavan-3-ol monomers (**Figure 2.9**). After HPLC, LC-MS, and NMR confirmation of the reaction products, the mean degree of polymerization (mDP), conversion yield, and subunit composition of PAs can be calculated (Kennedy and Jones, 2001).

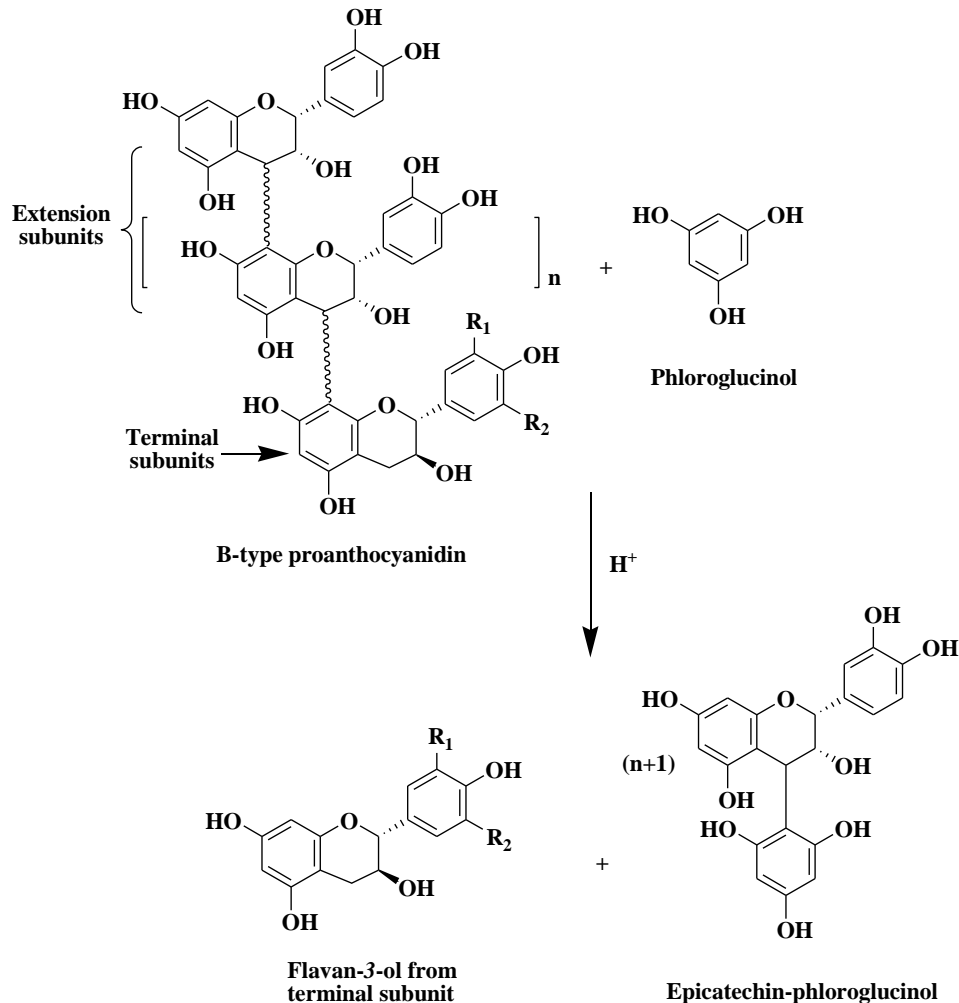


Figure 2.9: The reaction of PA acid-catalyzed cleavage and phloroglucinol derivatization. Terminal subunits of the PA polymers are released as free flavan-3-ols and PA extension subunits form stable flavan-3-ol-phloroglucinol adducts at the C4 position.

Saskatoon fruits

Plant characteristics

Saskatoon (*Amelanchier alnifolia* Nutt.) fruit is a native small fruit of the Western Canadian prairie that has excellent flavour and moderate sweetness (St-Pierre, 1992). Although the appearance (shape, colour and size) of saskatoon fruits are similar to that of blueberries, saskatoon fruit belong to the Rosaceae family and are pome fruits (similar to apple fruits) (St-Pierre and Steeves, 1990). Saskatoon shrubs have been successfully cultivated in the Western Canadian

prairies (especially in Alberta and Saskatchewan) and are capable of producing substantial amounts of fruit for many years since they can tolerate low temperatures and drought (St-Pierre, 1997). There are many different cultivars of saskatoon shrubs developed from natural selections from the wild (St-Pierre et al., 2005), and fruit size and taste vary slightly among the cultivars (McGarry et al., 1998, 2001).

Fruit maturity stages

Saskatoon fruit can be reliably sorted into 9 maturity stages over development (Rogiers and Knowles, 1997; Ozga et al., 2006). The fruit from stages 1 through 4 is mostly green and sorted by size and firmness (**Figure 2.10**). Stage 5 fruit is light green (because of a decrease in chlorophyll) to pink, while stage 6 fruit is mostly pink. Stage 7 fruits are distinguished by red colour, and stage 8 and 9 fruit are redish-blue and blue-purple, respectively, as a result of high anthocyanin content (**Figure 2.10**).

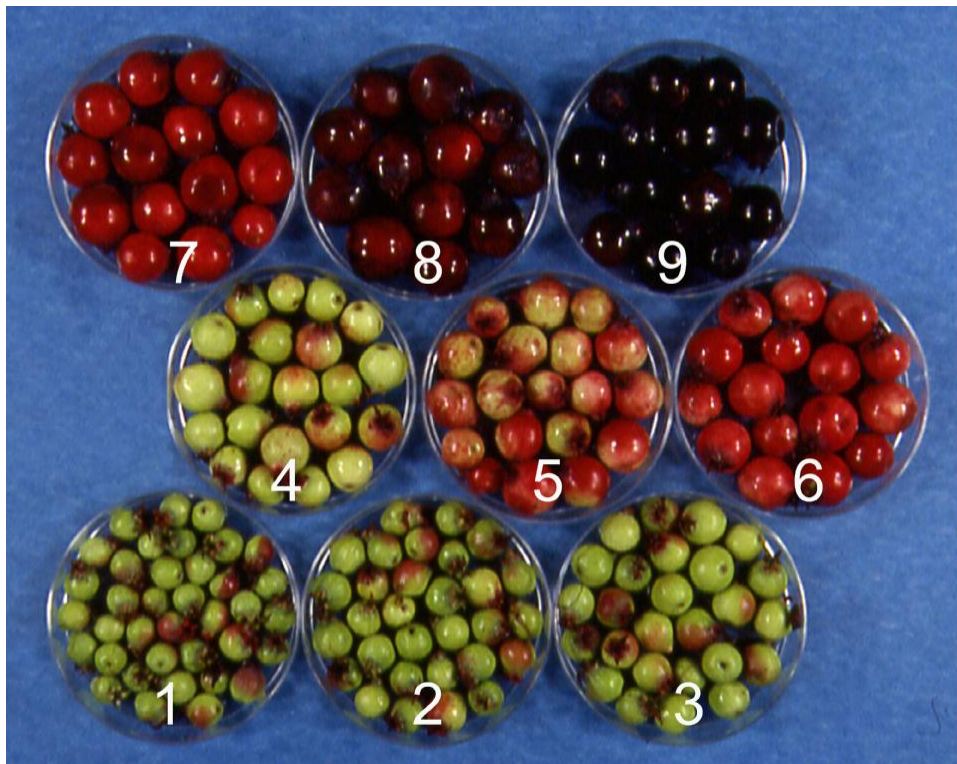


Figure 2.10: ‘Northline’ saskatoon fruit sorted into 9 maturity stages. (From Ozga et al., 2006, by permission).

Flavonoid complement

Currently, saskatoon fruits are consumed in North America as fresh fruit or in processed food products such as pies, jams, and jellies. The demand for saskatoon fruit is increasing in both domestic and international markets (Ozga et al., 2006) because of their excellent flavour and reported health benefits attributed to the flavonoid content (Adhikari et al., 2005; Hu et al., 2005). Developing flavonoid profiles for the different existing and emerging cultivars of saskatoon would allow for a targeted approach to increase fruit flavonoid content. Most flavonoid identification and quantification studies are limited to mature fruit of saskatoon (Hellstrom et al., 2007; Hosseinian et al., 2007; Ozga et al., 2007; Bakowska-Barczak and Kolodziejczyk, 2008), with minimal attention paid to developing fruit (Ozga et al., 2006). Previous studies on the anthocyanin and flavonol profiles of mature saskatoon fruit have found cyanidin to be a major anthocyanin aglycone; the major sugar units attached at the C3 position of cyanidin in an *O*-glycosylation form are galactose, glucose, arabinose, and xylose (Mazza, 1986; Ozga et al., 2007; Bakowska-Barczak and Kolodziejczyk, 2008). Total anthocyanin content was different among cultivars in these studies. Indeed, anthocyanin levels differed in the same cultivars between studies. This might be due to differences in growing conditions (including soil type and water availability), year of harvest, and the length of storage period (Mazza, 1993). Quercetin was found to be the major flavonol aglycone and quercetin 3-*O*-galactoside was the most abundant flavonol in the fruit of most saskatoon cultivars. PA analysis of saskatoon fruit has shown that epicatechin is the dominant subunit in both extension and terminal units, with B-type linkage between flavan-3-ol subunits (Hellstrom et al., 2007). The mDP of PAs varied (5 to 13) among the cultivars studied (Bakowska-Barczak and Kolodziejczyk, 2008).

Blueberry fruits

Plant characteristics

Blueberries belong to the genus *Vaccinium* within the Ericaceae family, as do cranberries. Blueberries are represented by several different species that range in

size from dwarf (0.1 meters) to tall (4 meters) habit (Riihinen et al., 2008). Among these various blueberry species, highbush blueberries (*Vaccinium corymbosum* L.) and lowbush blueberries (*Vaccinium angustifolium* L.) are the two main species extensively grown in North America. Blueberries are one of the major fruit crops in Canada. Currently, blueberry fruit is popular worldwide and it is consumed in many developed and developing countries not just for its taste but also for its reported health benefits. These include antioxidant (Kay and Holub, 2002), anticarcinogenic (Seeram et al., 2006), and anti-diabetic (Martineau et al., 2006) activities. The positive health effects of blueberries are believed to be due to the presence of substantial amounts of phytochemicals such as flavonoids in fresh fruits and in fruit extracts.

Fruit maturity stages

Blueberry fruits can be sorted into 8 maturity stages during development, according to a previously published paper (Ballinge.We and Kushman, 1970) (**Figure 2.11**). Stage 1 to 4 blueberry fruit are mainly green and sorted by increasing size. There is less chlorophyll on the surface of fruit from stages 5 and 6, which become increasingly red due to anthocyanin accumulation on the fruit surface. Stage 7 fruit are reddish-purple and stage 8 fruit are blue-purple (**Figure 2.11**). The construction of flavonoid profiles during fruit development will be useful for understanding flavonoid accumulation, and this knowledge will further contribute to metabolic engineers' efforts to improve flavonoid levels in blueberries.



Figure 2.11: Whole and bisected blueberry fruit (cv. Rubel) sorted into 8 maturity stages. (Provided by Dennis Reinecke, 2011)

Flavonoid complement

Anthocyanin profiles in both highbush and lowbush blueberry fruits have been extensively studied, while less information exists on the profiles of flavonols and PAs (Prior et al., 2001; Cho et al., 2005). Mature blueberry fruit contain the five common anthocyanidins (delphinidin, cyanidin, peonidin, petunidin, and malvidin), and most of the anthocyanidin glycosides have glucose, galactose, or arabinose attached at the C3 position in an *O*-glycosylation form (Wu and Prior, 2005). Total anthocyanins were estimated by the pH differential method and the results showed that anthocyanin levels varied among cultivars from 0.89 to 3.25 mg per gram fresh fruit weight (Ehlenfeldt and Prior, 2001). Quercetin and myricetin are two flavonol aglycones that have been found in blueberry fruits, and glycosylation occurs exclusively at the C3 position of the flavonol aglycones (Cho et al., 2005). Flavonol concentrations differed slightly among genotypes and total flavonol levels ranged from 0.19 to 0.32 mg per g fresh fruit weight in the Cho et al. (2005) study. PAs in blueberry fruits were determined with both normal-phase and reversed-phase HPLC-MS methods and the results show that the PA extension subunits consist of mainly epicatechin and the terminal PA subunits consist of epicatechin and catechin (Gu et al., 2002). This study also found that B-type linkage is the most common linkage between PA subunits, and only a small

proportion of A-type linkages were detected in oligomeric PAs, but no specific data on detection or quantification of the A-type PAs were reported. In general, most flavonoid studies in blueberry fruits are focused on mature blueberry fruits (Ehlenfeldt and Prior, 2001; Harris et al., 2007). Limited information is reported for type, concentration, and tissue-specific accumulation of flavonoids during blueberry fruit development (Castrejon et al., 2008).

Legume seeds

Plant characteristics

Peas (*Pisum sativum* L.), lentils (*Lens culinaris* L.), and faba beans (*Vicia faba* L.) belong to the *Fabaceae* family (also called *Leguminosae* or the legume family). *Fabaceae* is one of the largest families of flowering plants and many important food crops, in addition to the above species, belong to this family (such as soybeans, peanuts, and dry beans). Peas, faba beans, and lentils (also called seed grain legumes or pulses) are widely grown in Western Canada since they are well adapted to the dry and cool climates. Seeds of these legumes are good dietary sources of proteins, fibre, and other nutrients such as vitamins, minerals, and phenolic compounds. Pea, faba bean, and lentil seeds have been in the diet of Middle-Eastern and Asian cultures since ancient times (Singh et al., 2007).

Flavonoid complement

It is important to understand the structural diversity, tissue-specific accumulation, and bioactivity of flavonoids in these legume seeds for extended use of these foods in human and animal nutrition. Flavonoid subclasses such as isoflavonoids from some legume species are intensively studied for their purported benefits to human and animal health (Aoki et al., 2000). PAs are one of the major flavonoid subclasses to be found in the seeds of peas, faba beans, and lentils (they accumulate in the seed coat; Duenas et al., 2002; Duenas et al., 2004; Merghem et al., 2004). The oxidation of PAs in these seeds brings a brown oxidation colour to their seed coats and an astringent flavour caused by interaction between salivary protein and the PAs in the mouth (Ariga et al., 1981). This is one

of the reasons why PAs in legume seeds were once considered to be anti-nutritional compounds, and at that time seed consumption by humans and animals was discouraged (Martintanguy et al., 1977). Even today, some legume seeds are utilized only after removal of the seed coats. Recent nutritional studies have shown many beneficial health effects of PAs from common fresh fruits (e.g. grapes, blueberries, persimmon), wines, grape-seed extract, and chocolate (Bagchi et al., 2000; Murphy et al., 2003; Seeram et al., 2006; Lee et al., 2008). This has brought renewed interest in the PAs contained in legume seeds and further research in this area. The current information available pertaining to legume seed PAs, including structure, amount, and accumulation during seed development and bioactivity is very limited. PA structural confirmation, specific localization within the seed coat, and the construction of flavonoid profiles during seed development will be useful for understanding flavonoid accumulation, and this knowledge could be used to explore the possibilities of increasing PA levels in the seeds and aid in introducing high-PA containing legume seeds or seed-coat fractions to the human or animal diet for potential health beneficial effects.

Literature Cited

- Abrahams S, Lee E, Walker AR, Tanner GJ, Larkin PJ, Ashton AR** (2003) The Arabidopsis TDS4 gene encodes leucoanthocyanidin dioxygenase (LDOX) and is essential for proanthocyanidin synthesis and vacuole development. *Plant Journal* **35**: 624-636
- Adato A, Mandel T, Mintz-Oron S, Venger I, Levy D, Yativ M, Dominguez E, Wang ZH, De Vos RCH, Jetter R, Schreiber L, Heredia A, Rogachev I, Aharoni A** (2009) Fruit-surface flavonoid accumulation in tomato is controlled by a *SIMYB12*-regulated transcriptional network. *Plos Genetics* **5**: e1000777
- Adhikari DP, Francis JA, Schutzki RE, Chandra A, Nair MG** (2005) Quantification and characterisation of cyclooxygenase and lipid peroxidation inhibitory anthocyanins in fruits of Amelanchier. *Phytochemical Analysis* **16**: 175-180
- Andersen ØM** (2006) *Flavonoids: Chemistry, Biochemistry, and Applications*. CRC, Taylor & Francis

- Aoki T, Akashi T, Ayabe S** (2000) Flavonoids of leguminous plants: structure, biological activity, and biosynthesis. *Journal of Plant Research* **113**: 475-488
- Aras A, Cevahir G, Yentur S, Eryilmaz F, Sarsag M, Cag S** (2007) Investigation of anthocyanin localization in various parts of *Impatiens balsamina* L. *Biotechnology & Biotechnological Equipment* **21**: 69-73
- Ariga T, Asao Y, Sugimoto H, Yokotsuka T** (1981) Studies on a stringent components in legume seeds. 1. Occurrence of astringent oligomeric proanthocyanidins in legume seeds. *Agricultural and Biological Chemistry* **45**: 2705-2708
- Aron PM, Kennedy JA** (2008) Flavan-3-ols: Nature, occurrence and biological activity. *Molecular Nutrition & Food Research* **52**: 79-104
- Ayres MP, Clausen TP, MacLean SF, Redman AM, Reichardt PB** (1997) Diversity of structure and antiherbivore activity in condensed tannins. *Ecology* **78**: 1696-1712
- Bagchi D, Bagchi M, Stohs SJ, Das DK, Ray SD, Kuszynski CA, Joshi SS, Pruess HG** (2000) Free radicals and grape seed proanthocyanidin extract: importance in human health and disease prevention. *Toxicology* **148**: 187-197
- Bakowska-Barczak AM, Kolodziejczyk P** (2008) Evaluation of Saskatoon Berry (*Amelanchier alnifolia* Nutt.) Cultivars for their polyphenol content, antioxidant properties, and storage stability. *Journal of Agricultural and Food Chemistry* **56**: 9933-9940
- Ballinge. We, Kushman LJ** (1970) Relationship of stage of ripeness to composition and keeping quality highbush blueberries. *Journal of the American Society for Horticultural Science* **95**: 239-242
- Barcelo AR, Calderon AA, Zapata JM, Munoz R** (1994) The histochemical-localization of anthocyanins in seeded and seedless grapes (*Vitis-Vinifera*). *Scientia Horticulturae* **57**: 265-268
- Bogs J, Ebadi A, McDavid D, Robinson SP** (2006) Identification of the flavonoid hydroxylases from grapevine and their regulation during fruit development. *Plant Physiology* **140**: 279-291
- Boss PK, Davies C, Robinson SP** (1996) Expression of anthocyanin biosynthesis pathway genes in red and white grapes. *Plant Molecular Biology* **32**: 565-569

- Brorson SH** (1996) Improved immunogold labeling of epoxy sections by the use of propylene oxide as additional agent in dehydration, infiltration and embedding. *Micron* **27**: 345-353
- Burbulis IE, Winkel-Shirley B** (1999) Interactions among enzymes of the Arabidopsis flavonoid biosynthetic pathway. Proceedings of the National Academy of Sciences of the United States of America **96**: 12929-12934
- Castrejon ADR, Elchholz I, Rohn S, Kroh LW, Huyskens-Keil S** (2008) Phenolic profile and antioxidant activity of highbush blueberry (*Vaccinium corymbosum* L.) during fruit maturation and ripening. *Food Chemistry* **109**: 564-572
- Chalker-Scott L** (1999) Environmental significance of anthocyanins in plant stress responses. *Photochemistry and Photobiology* **70**: 1-9
- Cho MJ, Howard LR, Prior RL, Clark JR** (2005) Flavonol glycosides and antioxidant capacity of various blackberry and blueberry genotypes determined by high-performance liquid chromatography/mass spectrometry. *Journal of the Science of Food and Agriculture* **85**: 2149-2158
- Close DC, Beadle CL** (2003) The ecophysiology of foliar anthocyanin. *Botanical Review* **69**: 149-161
- Crozier A, Jaganath IB, Clifford MN** (2009) Dietary phenolics: chemistry, bioavailability and effects on health. *Natural Product Reports* **26**: 1001-1043
- De Micco V, Aronne G** (2007) Combined histochemistry and autofluorescence for identifying lignin distribution in cell walls. *Biotechnic & Histochemistry* **82**: 209-216
- Debeaujon I, Nesi N, Perez P, Devic M, Grandjean O, Caboche M, Lepiniec L** (2003) Proanthocyanidin-accumulating cells in Arabidopsis testa: Regulation of differentiation and role in seed development. *Plant Cell* **15**: 2514-2531
- Deluc L, Bogs J, Walker AR, Ferrier T, Decendit A, Merillon JM, Robinson SP, Barrieu F** (2008) The transcription factor VvMYB5b contributes to the regulation of anthocyanin and proanthocyanidin biosynthesis in developing grape berries. *Plant Physiology* **147**: 2041-2053
- Dixon RA, Xie DY, Sharma SB** (2005) Proanthocyanidins - a final frontier in flavonoid research? *New Phytologist* **165**: 9-28

- Duenas M, Hernandez T, Estrella I** (2002) Phenolic composition of the cotyledon and the seed coat of lentils (*Lens culinaris* L.). *European Food Research and Technology* **215**: 478-483
- Duenas M, Sun BS, Hernandez T, Estrella I, Spranger MI** (2003) Proanthocyanidin composition in the seed coat of lentils (*Lens culinaris* L.). *Journal of Agricultural and Food Chemistry* **51**: 7999-8004
- Duenas M, Estrella I, Hernandez T** (2004) Occurrence of phenolic compounds in the seed coat and the cotyledon of peas (*Pisum sativum* L.). *European Food Research and Technology* **219**: 116-123
- Ehlenfeldt MK, Prior RL** (2001) Oxygen radical absorbance capacity (ORAC) and phenolic and anthocyanin concentrations in fruit and leaf tissues of highbush blueberry. *Journal of Agricultural and Food Chemistry* **49**: 2222-2227
- Espley RV, Hellens RP, Putterill J, Stevenson DE, Kutty-Amma S, Allan AC** (2007) Red colouration in apple fruit is due to the activity of the MYB transcription factor, MdMYB10. *Plant Journal* **49**: 414-427
- Feucht W, Christ E, Treutter D** (1994) Flavanols as defense barriers of the fruit surface. *Angewandte Botanik* **68**: 122-126
- Feucht W, Dithmar H, Polster J** (2004) Nuclei of tea flowers as targets for flavanols. *Plant Biology* **6**: 696-701
- Foo LY, Lu YR, Howell AB, Vorsa N** (2000) A-type proanthocyanidin trimers from cranberry that inhibit adherence of uropathogenic P-fimbriated *Escherichia coli*. *Journal of Natural Products* **63**: 1225-1228
- Giusti MM, Wrolstad RE** (1996) Characterization of red radish anthocyanins. *Journal of Food Science* **61**: 322-326
- Goto T, Kondo T** (1991) Structure and molecular stacking of anthocyanins - flower colour variation. *Angewandte Chemie-International Edition in English* **30**: 17-33
- Grayer RJ, Kite GC, Abou-Zaid M, Archer LJ** (2000) The application of atmospheric pressure chemical ionisation liquid chromatography-mass spectrometry in the chemotaxonomic study of flavonoids: characterisation of flavonoids from *Ocimum gratissimum* var. *gratissimum*. *Phytochemical Analysis* **11**: 257-267
- Grotewold E** (2004) The challenges of moving chemicals within and out of cells: insights into the transport of plant natural products. *Planta* **219**: 906-909

- Gu LW, Kelm M, Hammerstone JF, Beecher G, Cunningham D, Vannozzi S, Prior RL** (2002) Fractionation of polymeric procyanidins from lowbush blueberry and quantification of procyanidins in selected foods with an optimized normal-phase HPLC-MS fluorescent detection method. *Journal of Agricultural and Food Chemistry* **50**: 4852-4860
- Gu LW, Kelm MA, Hammerstone JF, Beecher G, Holden J, Haytowitz D, Prior RL** (2003) Screening of foods containing proanthocyanidins and their structural characterization using LC-MS/MS and thiolytic degradation. *Journal of Agricultural and Food Chemistry* **51**: 7513-7521
- Gutmann M, Feucht W** (1991) A new method for selective localization of flavan-3-ols in plant-tissues involving glycolmethacrylate embedding and microwave irradiation. *Histochemistry* **96**: 83-86
- Gutmann M** (1993) Localization of proanthocyanidins using in situ - hydrolysis with sulfuric-acid. *Biotechnic & Histochemistry* **68**: 161-165
- Harris CS, Burt AJ, Saleem A, Le PM, Martineau LC, Haddad PS, Bennett SAL, Arnason JT** (2007) A single HPLC-PAD-APCI/MS method for the quantitative comparison of phenolic compounds found in leaf, stem, root and fruit extracts of *Vaccinium angustifolium*. *Phytochemical Analysis* **18**: 161-169
- Heimler D** (1986) High-performance thin-layer chromatography of selected flavonoid aglycones on ready-for-use layers of silanized silica-gel. *Journal of Chromatography* **366**: 407-411
- Hellstrom J, Sinkkonen J, Karonen M, Mattila P** (2007) Isolation and structure elucidation of procyanidin oligomers from saskatoon berries (*Amelanchier alnifolia*). *Journal of Agricultural and Food Chemistry* **55**: 157-164
- Himi E, Noda K** (2004) Isolation and location of three homoeologous dihydroflavonol-4-reductase (DFR) genes of wheat and their tissue-dependent expression. *Journal of Experimental Botany* **55**: 365-375
- Hosseinian FS, Li W, Hydamaka AW, Tsopmo A, Lowry L, Friel J, Beta T** (2007) Proanthocyanidin profile and ORAC values of manitoba berries, chokecherries, and seabuckthorn. *Journal of Agricultural and Food Chemistry* **55**: 6970-6976
- Hraska M, Rakousky S, Curn V** (2006) Green fluorescent protein as a vital marker for non-destructive detection of transformation events in transgenic plants. *Plant Cell Tissue and Organ Culture* **86**: 303-318

- Hu C, Kwok BHL, Kitts DD** (2005) Saskatoon berries (*Amelanchier alnifolia* Nutt.) scavenge free radicals and inhibit intracellular oxidation. *Food Research International* **38**: 1079-1085
- Hussein L, Fattah MA, Salem E** (1990) Characterization of pure proanthocyanidins isolated from the hulls of faba beans. *Journal of Agricultural and Food Chemistry* **38**: 95-98
- Ithal N, Reddy AR** (2004) Rice flavonoid pathway genes, *OsDfr* and *OsAns*, are induced by dehydration, high salt and ABA, and contain stress responsive promoter elements that interact with the transcription activator, OsC1-MYB. *Plant Science* **166**: 1505-1513
- Iwashina T** (2000) The structure and distribution of the flavonoids in plants. *Journal of Plant Research* **113**: 287-299
- Jaakola L, Maatta K, Pirttila AM, Torronen R, Karenlampi S, Hohtola A** (2002) Expression of genes involved in anthocyanin biosynthesis in relation to anthocyanin, proanthocyanidin, and flavonol levels during bilberry fruit development. *Plant Physiology* **130**: 729-739
- Jones P, Vogt T** (2001) Glycosyltransferases in secondary plant metabolism: tranquilizers and stimulant controllers. *Planta* **213**: 164-174
- Kay CD, Holub BJ** (2002) The effect of wild blueberry (*Vaccinium angustifolium*) consumption on postprandial serum antioxidant status in human subjects. *British Journal of Nutrition* **88**: 389-397
- Kennedy JA, Jones GP** (2001) Analysis of proanthocyanidin cleavage products following acid-catalysis in the presence of excess phloroglucinol. *Journal of Agricultural and Food Chemistry* **49**: 1740-1746
- Kennedy JA, Taylor AW** (2003) Analysis of proanthocyanidins by high-performance gel permeation chromatography. *Journal of Chromatography A* **995**: 99-107
- Kiernan JA** (2000) Formaldehyde, formalin, paraformaldehyde and glutaraldehyde: What they are and what they do? *Microscopy Today*: 8-12
- Kolb CA, Kopecky J, Riederer M, Pfundel EE** (2003) UV screening by phenolics in berries of grapevine (*Vitis vinifera*). *Functional Plant Biology* **30**: 1177-1186
- Lam TK, Rotunno M, Lubin JH, Wacholder S, Consonni D, Pesatori AC, Bertazzi PA, Chanock SJ, Burdette L, Goldstein AM, Tucker MA, Caporaso NE, Subar AF, Landi MT** (2010) Dietary quercetin,

quercetin-gene interaction, metabolic gene expression in lung tissue and lung cancer risk. *Carcinogenesis* **31**: 634-642

- Lee YA, Cho EJ, Yokozawa T** (2008) Effects of proanthocyanidin preparations on hyperlipidemia and other biomarkers in mouse model of type 2 diabetes. *Journal of Agricultural and Food Chemistry* **56**: 7781-7789
- Lees GL, Suttill NH, Gruber MY** (1993) Condensed tannins in sainfoin. 1. A histological and cytological survey of plant-tissues. *Canadian Journal of Botany-Revue Canadienne De Botanique* **71**: 1147-1152
- Lees GL, Wall KM, Beveridge TH, Suttill NH** (1995) Localization of condensed tannins in apple fruit peel, pulp, and seeds. *Canadian Journal of Botany-Revue Canadienne De Botanique* **73**: 1897-1904
- Leitao GG, El-Adji SS, de Melo WAL, Leitao SG, Brown L** (2005) Separation of free and glycosylated flavonoids from *Siparuna guianensis* by gradient and isocratic CCC. *Journal of Liquid Chromatography & Related Technologies* **28**: 2041-2051
- Lepiniec L, Debeaujon I, Routaboul JM, Baudry A, Pourcel L, Nesi N, Caboche M** (2006) Genetics and biochemistry of seed flavonoids. *Annual Review of Plant Biology* **57**: 405-430
- Li YG, Tanner G, Larkin P** (1996) The DMACA-HCl protocol and the threshold proanthocyanidin content for bloat safety in forage legumes. *Journal of the Science of Food and Agriculture* **70**: 89-101
- Lowry JB, Chew L** (1974) Use of extracted anthocyanin as a food dye. *Economic Botany* **28**: 61-62
- Luchtel DL, Boykin JC, Bernard SL, Glenny RW** (1998) Histological methods to determine blood flow distribution with fluorescent microspheres. *Biotechnic & Histochemistry* **73**: 291-309
- Markham KR, Ryan KG, Gould KS, Rickards GK** (2000) Cell wall sited flavonoids in *lisianthus* flower petals. *Phytochemistry* **54**: 681-687
- Martens S, Mithofer A** (2005) Flavones and flavone synthases. *Phytochemistry* **66**: 2399-2407
- Martineau LC, Couture A, Spoor D, Benhaddou-Andaloussi A, Harris C, Meddah B, Leduc C, Burt A, Vuong T, Le PM, Prentki M, Bennett SA, Arnason JT, Haddad PS** (2006) Anti-diabetic properties of the Canadian lowbush blueberry *Vaccinium angustifolium* Ait. *Phytomedicine* **13**: 612-623

- Martintanguy J, Guillaume J, Kossa A** (1977) Condensed tannins in horse bean-seeds - chemical-structure and apparent effects on poultry. *Journal of the Science of Food and Agriculture* **28**: 757-765
- Mazza G** (1986) Anthocyanins and other phenolic compounds of saskatoon berries (*Amelanchier alnifolia* Nutt). *Journal of Food Science* **51**: 1260-1264
- Mazza GaM, E.** (1993) Anthocyanins in fruits, vegetables, and grains. CRC Press, Boca Raton, FL.
- McGarry R, Ozga JA, Reinecke DM** (1998) Patterns of saskatoon (*Amelanchier alnifolia* Nutt.) fruit and seed growth. *Journal of the American Society for Horticultural Science* **123**: 26-29
- McGarry R, Ozga JA, Reinecke DM** (2001) Differences in fruit development among large- and small-fruited cultivars of saskatoon (*Amelanchier alnifolia*). *Journal of the American Society for Horticultural Science* **126**: 381-385
- Mellway RD, Tran LT, Prouse MB, Campbell MM, Constabel CP** (2009) The Wound-, Pathogen-, and Ultraviolet B-Responsive *MYB134* Gene Encodes an R2R3 MYB Transcription Factor That Regulates Proanthocyanidin Synthesis in Poplar. *Plant Physiology* **150**: 924-941
- Merghem R, Jay M, Brun N, Voirin B** (2004) Qualitative analysis and HPLC isolation and identification of procyanidins from *Vicia faba*. *Phytochemical Analysis* **15**: 95-99
- Merken HM, Beecher GR** (2000) Measurement of food flavonoids by high-performance liquid chromatography: A review. *Journal of Agricultural and Food Chemistry* **48**: 577-599
- Middleton EM, Teramura AH** (1993) The role of flavonol glycosides and carotenoids in protecting soybean from Ultraviolet-B damage. *Plant Physiology* **103**: 741-752
- Mol J, Grotewold E, Koes R** (1998) How genes paint flowers and seeds. *Trends in Plant Science* **3**: 212-217
- Moore R, Vodopich DS** (1987) The influence of pH on the colour of anthocyanins and betalains. *American Biology Teacher* **49**: 111-112

- Mueller LA, Goodman CD, Silady RA, Walbot V** (2000) AN9, a petunia glutathione S-transferase required for anthocyanin sequestration, is a flavonoid-binding protein. *Plant Physiology* **123**: 1561-1570
- Murphy KJ, Chronopoulos AK, Singh I, Francis MA, Moriarty H, Pike MJ, Turner AH, Mann NJ, Sinclair AJ** (2003) Dietary flavanols and procyanidin oligomers from cocoa (*Theobroma cacao*) inhibit platelet function. *American Journal of Clinical Nutrition* **77**: 1466-1473
- Nakayama T, Sato T, Fukui Y, Yonekura-Sakakibara K, Hayashi H, Tanaka Y, Kusumi T, Nishino T** (2001) Specificity analysis and mechanism of aurone synthesis catalyzed by aureusidin synthase, a polyphenol oxidase homolog responsible for flower colouration. *Febs Letters* **499**: 107-111
- Nesi N, Jond C, Debeaujon I, Caboche M, Lepiniec L** (2001) The Arabidopsis *TT2* gene encodes an R2R3 MYB domain protein that acts as a key determinant for proanthocyanidin accumulation in developing seed. *Plant Cell* **13**: 2099-2114
- Ono E, Hatayama M, Isono Y, Sato T, Watanabe R, Yonekura-Sakakibara K, Fukuchi-Mizutani M, Tanaka Y, Kusumi T, Nishino T, Nakayama T** (2006) Localization of a flavonoid biosynthetic polyphenol oxidase in vacuoles. *Plant Journal* **45**: 133-143
- Ozga JA, Saeed A, Reinecke DM** (2006) Anthocyanins and nutrient components of saskatoon fruits (*Amelanchier alnifolia* Nutt.). *Canadian Journal of Plant Science* **86**: 193-197
- Ozga JA, Saeed A, Wismer W, Reinecke DM** (2007) Characterization of cyanidin- and quercetin-derived flavonoids and other phenolics in mature saskatoon fruits (*Amelanchier alnifolia* Nutt.). *Journal of Agricultural and Food Chemistry* **55**: 10414-10424
- Pang YZ, Peel GJ, Wright E, Wang ZY, Dixon RA** (2007) Early steps in proanthocyanidin biosynthesis in the model legume *Medicago truncatula*. *Plant Physiology* **145**: 601-615
- Peel GJ, Pang YZ, Modolo LV, Dixon RA** (2009) The LAP1 MYB transcription factor orchestrates anthocyanidin biosynthesis and glycosylation in *Medicago*. *Plant Journal* **59**: 136-149
- Polster J, Dithmar H, Burgemeister R, Friedemann G, Feucht W** (2006) Flavonoids in plant nuclei: detection by laser microdissection and pressure catapulting (LMPC), in vivo staining, and uv-visible spectroscopic titration. *Physiologia Plantarum* **128**: 163-174

- Pourcel L, Routaboul JM, Cheynier V, Lepiniec L, Debeaujon I** (2007) Flavonoid oxidation in plants: from biochemical properties to physiological functions. *Trends in Plant Science* **12**: 29-36
- Prati S, Baravelli V, Fabbri D, Schwarzinger C, Brandolini V, Maietti A, Tedeschi P, Benvenuti S, Macchia M, Marotti I, Bonetti A, Catizone P, Dinelli G** (2007) Composition and content of seed flavonoids in forage and grain legume crops. *Journal of Separation Science* **30**: 491-501
- Price ML, Vanscoyoc S, Butler LG** (1978) Critical evaluation of vanillin reaction as an assay for tannin in sorghum grain. *Journal of Agricultural and Food Chemistry* **26**: 1214-1218
- Prieur C, Rigaud J, Cheynier V, Moutounet M** (1994) Oligomeric and polymeric procyanidins from grape seeds. *Phytochemistry* **36**: 781-784
- Prior RL, Lazarus SA, Cao GH, Muccitelli H, Hammerstone JF** (2001) Identification of procyanidins and anthocyanins in blueberries and cranberries (*Vaccinium spp.*) using high-performance liquid chromatography/mass spectrometry. *Journal of Agricultural and Food Chemistry* **49**: 1270-1276
- Rea PA** (2007) Plant ATP-Binding cassette transporters. *Annual Review of Plant Biology* **58**: 347-375
- Reddy AM, Reddy VS, Scheffler BE, Wienand U, Reddy AR** (2007) Novel transgenic rice overexpressing anthocyanidin synthase accumulates a mixture of flavonoids leading to an increased antioxidant potential. *Metabolic Engineering* **9**: 95-111
- Riihinen K, Jaakola L, Karenlampi S, Hohtola A** (2008) Organ-specific distribution of phenolic compounds in bilberry (*Vaccinium myrtillus*) and 'northblue' blueberry (*Vaccinium corymbosum x V angustifolium*). *Food Chemistry* **110**: 156-160
- Rogiers SY, Knowles NR** (1997) Physical and chemical changes during growth, maturation, and ripening of saskatoon (*Amelanchier alnifolia*) fruit. *Canadian Journal of Botany-Revue Canadienne De Botanique* **75**: 1215-1225
- Rolfe SA, Scholes JD** Chlorophyll fluorescence imaging of plant-pathogen interactions. *Protoplasma* **247**: 163-175
- Saslowsky D, Winkel-Shirley B** (2001) Localization of flavonoid enzymes in Arabidopsis roots. *Plant Journal* **27**: 37-48

- Saslowsky DE, Warek U, Winkel BSJ** (2005) Nuclear localization of flavonoid enzymes in Arabidopsis. *Journal of Biological Chemistry* **280**: 23735-23740
- Schnitzler JP, Jungblut TP, Heller W, Kofferlein M, Hutzler P, Heinzmann U, Schmelzer E, Ernst D, Langebartels C, Sandermann H** (1996) Tissue localization of uv-B-screening pigments and of chalcone synthase mRNA in needles of Scots pine seedlings. *New Phytologist* **132**: 247-258
- Seeram NP, Adams LS, Zhang YJ, Lee R, Sand D, Scheuller HS, Heber D** (2006) Blackberry, black raspberry, blueberry, cranberry, red raspberry, and strawberry extracts inhibit growth and stimulate apoptosis of human cancer cells in vitro. *Journal of Agricultural and Food Chemistry* **54**: 9329-9339
- Singh RJ, Chung GH, Nelson RL** (2007) Landmark research in legumes. *Genome* **50**: 525-537
- St-Pierre RG, Steeves TA** (1990) Observations on shoot morphology, anthesis, flower number, and seed production in the saskatoon, *Amelanchier alnifolia* (Rosaceae). *Canadian Field-Naturalist* **104**: 379-386
- St-Pierre RG** (1992) The development of native fruit species as horticultural crops in Saskatchewan. *Hortscience* **27**: 866
- St-Pierre RG** (1997) Growing saskatoons - a manual for orchardists. Fifth edition. Department of Horticulture Science, University of Saskatchewan, Saskatoon, SK. 338 pp.
- St-Pierre RG, Zatylny AM, Tulloch HR** (2005) Evaluation of growth and fruit production characteristics of 15 saskatoon (*Amelanchier alnifolia* Nutt.) cultivars at maturity. *Canadian Journal of Plant Science* **85**: 929-932
- Steinberg FM, Bearden MM, Keen CL** (2003) Cocoa and chocolate flavonoids: Implications for cardiovascular health. *Journal of the American Dietetic Association* **103**: 215-223
- Taylor AW, Barofsky E, Kennedy JA, Deinzer ML** (2003) Hop (*Humulus lupulus* L.) proanthocyanidins characterized by mass spectrometry, acid catalysis, and gel permeation chromatography. *Journal of Agricultural and Food Chemistry* **51**: 4101-4110
- Tits M, Angenot L, Poukens P, Warin R, Dierckxsens Y** (1992) Prodelphinidins from *Ribes nigrum*. *Phytochemistry* **31**: 971-973

- Treutter D** (1989) Chemical-reaction detection of catechins and proanthocyanidins with 4-dimethylaminocinnamaldehyde. *Journal of Chromatography* **467**: 185-193
- Wang HL, Wang W, Zhang P, Pan QH, Zhan JC, Huang WD** Gene transcript accumulation, tissue and subcellular localization of anthocyanidin synthase (ANS) in developing grape berries. *Plant Science* **179**: 103-113
- Wang J, Kalt W, Sporns P** (2000) Comparison between HPLC and MALDI-TOF MS analysis of anthocyanins in highbush blueberries. *Journal of Agricultural and Food Chemistry* **48**: 3330-3335
- Watts KT, Lee PC, Schmidt-Dannert C** (2004) Exploring recombinant flavonoid biosynthesis in metabolically engineered *Escherichia coli*. *Chembiochem* **5**: 500-507
- Welch CR, Wu QL, Simon JE** (2008) Recent advances in anthocyanin analysis and characterization. *Current Analytical Chemistry* **4**: 75-101
- Williams CA, Grayer RJ** (2004) Anthocyanins and other flavonoids. *Natural Product Reports* **21**: 539-573
- Winkel-Shirley B** (2001) Flavonoid biosynthesis. A colourful model for genetics, biochemistry, cell biology, and biotechnology. *Plant Physiology* **126**: 485-493
- Winkel BSJ** (2004) Metabolic channeling in plants. *Annual Review of Plant Biology* **55**: 85-107
- Woodward G, Kroon P, Cassidy A, Kay C** (2009) Anthocyanin stability and recovery: implications for the analysis of clinical and experimental samples. *Journal of Agricultural and Food Chemistry* **57**: 5271-5278
- Wu XL, Prior RL** (2005) Systematic identification and characterization of anthocyanins by HPLC-ESI-MS/MS in common foods in the United States: Fruits and berries. *Journal of Agricultural and Food Chemistry* **53**: 2589-2599
- Xie DY, Sharma SB, Paiva NL, Ferreira D, Dixon RA** (2003) Role of anthocyanidin reductase, encoded by *BANYULS* in plant flavonoid biosynthesis. *Science* **299**: 396-399
- Yazaki K** (2005) Transporters of secondary metabolites. *Current Opinion in Plant Biology* **8**: 301-307

Yeung EC (1999) The use of histology in the study of plant tissue culture systems - Some practical comments. *In Vitro Cellular & Developmental Biology-Plant* **35**: 137-143

Zafra-Stone S, Yasmin T, Bagchi M, Chatterjee A, Vinson JA, Bagchi D (2007) Berry anthocyanins as novel antioxidants in human health and disease prevention. *Molecular Nutrition & Food Research* **51**: 675-683

Zhao J, Dixon RA (2010) The 'ins' and 'outs' of flavonoid transport. *Trends in Plant Science* **15**: 72-80

Zhishen J, Mengcheng T, Jianming W (1999) The determination of flavonoid contents in mulberry and their scavenging effects on superoxide radicals. *Food Chemistry* **64**: 555-559

Chapter 3

Anthocyanin and Flavonol Profiles of Saskatoon Fruits (*Amelanchier alnifolia* Nutt.) during Development and at Maturity

Introduction

Flavonoid compounds in fruits have recently attracted much interest due to their reported antioxidant properties and perceived health benefits, including potential anti-cancer, anti-diabetic, anti-inflammatory and vascular protective effects (Prior, 2004; Martineau et al., 2006; Crozier et al., 2009). Saskatoon (*Amelanchier alnifolia* Nutt.) fruit, a native small fruit of North America (St-Pierre, 1997), contain significant levels of the anthocyanin and flavonol classes of flavonoids in the mature fruit (Ozga et al., 2007; Bakowska-Barczak and Kolodziejczyk, 2008). Total anthocyanin concentration in saskatoon fruits is comparable with that of blueberry and higher than that in other small fruit species such as raspberry, chokeberry, and strawberry (Hosseinian and Beta, 2007). Anthocyanins are the natural pigments chiefly responsible for the blue-purple colour of the mature fruits (Mazza, 1986; Rogiers and Knowles, 1997; McGarry et al., 2005) likely functioning to attract certain animals to aid in seed dispersal (Schaefer et al., 2004). Previous studies have identified cyanidin 3-*O*-galactoside, cyanidin 3-*O*-glucoside, cyanidin 3-*O*-arabinoside, and cyanidin 3-*O*-xyloside as the four most abundant anthocyanins in mature saskatoon fruits (*Amelanchier alnifolia* Nutt.; Ozga et al. 2007). Flavonols are compounds that can act as UV-light filters in plant tissues and protect plants from UV light damage (Middleton and Teramura, 1993; Kolb et al., 2003). They also have been implicated as signal molecules in animal-plant interactions (c.f. Mol et al., 1998). The major flavonols identified in mature saskatoon fruit include the quercetin-diglycosides (quercetin 3-*O*-rutinoside, quercetin 3-*O*-robinobioside, and quercetin 3-*O*-arabinoglucoside) and the quercetin-mono-glycosides (quercetin 3-*O*-galactoside, quercetin 3-*O*-

glucoside, quercetin 3-*O*-arabinoside, and quercetin 3-*O*-xyloside; Ozga et al., 2007). Although the major anthocyanin and flavonol compounds in mature saskatoon fruit have been identified by Ozga et al. (2007), minimal information exists on the temporal and spatial accumulation patterns of these two classes of flavonoids over fruit development. These data would further our understanding of the regulation of these two branches of the flavonoid pathway during fruit development in this species, and aid breeding efforts to optimize flavonoid content and specific flavonoid compound classes for health beneficial effects. Therefore, in order to further our understanding of the flavonoid biosynthesis pathway, its regulation, and flavonoid accumulation in saskatoon fruits, identification, quantitation, and tissue-specific accumulation of anthocyanins and flavonols were determined in four pigmented-fruit cultivars and a white mutant fruit cultivar (white-coloured fruit at maturity) of saskatoons over fruit development.

Materials and Methods

Plant material

Saskatoon fruit of the cultivars Northline, Pembina, Thiessen, Honeywood, and Altaglio were collected from the University of Alberta Experimental Farm, Edmonton, Alberta, Canada. Fruit samples for chemical analyses were harvested onto dry ice in the field, sorted on dry ice in the laboratory to remove any debris and damaged fruit and to separate fruit into maturity classes according to a 9-stage system (Rogiers and Knowles, 1997; McGarry et al., 1998, 2005). After sorting on dry ice, the fruits were immediately stored at -80 °C. Fruits for the histological studies were selectively harvested onto ice in the field, transported on ice to the laboratory, and dissected immediately in the laboratory for tissue fixation.

Chemicals

The anthocyanin and flavonol standards (cyanidin 3-*O*-galactoside chloride, cyanidin 3-*O*-glucoside chloride, quercetin 3-*O*-glucoside, quercetin 3-*O*-galactoside, quercetin 3-*O*-rutinoside, and quercetin 3-*O*-arabinoglucoside) were

purchased from Extrasynthese (Genay, France), 5-*O*-caffeoylquinic acid (chlorogenic acid), diphenylboric acid 2-aminoethyl ester (DPBA), and Triton X-100 from Sigma (Oakville, ON), and the glutaraldehyde and paraformaldehyde from Electron Microscopy Sciences (Hatfield, PA). All the HPLC grade solvents and 1-butanol were from Fisher Scientific (Ottawa, ON).

Extraction and purification of anthocyanins and flavonols

Fruit samples (2 to 4 g) were removed from -80 °C storage and immediately ground in a commercial Blender (New Hartford, Connecticut, U.S.A.). The ground tissue was extracted with 8 mL of the HPLC grade solvent mixture (acetone:methanol:water:formic acid, 40:40:20:0.1, v/v/v/v). The extract was vortexed for 2 min then filtered through Whatman #1 filter paper in a Büchner funnel under moderate vacuum. The residue was washed three times with 4 mL of solvent mixture, and the extract and wash was pooled and evaporated to near dryness in a SpeedVac vacuum concentrator (AES 200, Savant, Farmingdale, NY). The extract was brought up to 10 mL using deionized water (Milli-Q) and a 1 mL aliquot was loaded onto a Sep-Pak C18 cartridge (Waters, Mississauga, Ontario, Canada), which had been preconditioned with 2 mL of 100% methanol followed by 5 mL deionized water. The column was then washed with 5 mL deionized water to remove sugars and organic acids. Anthocyanins and flavonols were subsequently eluted from the column with 10 mL of 0.1% formic acid in methanol (v/v) and this eluent was evaporated under vacuum to near dryness. The residue was completely dried down under a stream of nitrogen. The dried methanolic fraction containing the anthocyanins and flavonols was resuspended in 200 µL of methanol: water (50:50, v/v) and a 20 µL aliquot was subjected to HPLC analysis.

HPLC analysis

The extracts were injected on to a Zorbex SB-C18, 4.6 x 250 mm (5 µm; Agilent) C18 column fitted with a Zorbex SB-C18, 4.6 x 12.5 mm (5 µm; Agilent) guard column, using a HPLC system (Agilent 1200, USA) equipped with a photodiode array (DAD; Agilent G1315B) detector. The samples were eluted at a

flow rate of 1 mL min⁻¹ using a linear gradient of 5% aqueous formic acid (solvent A) and 100% methanol (solvent B) following the protocol of Ozga et al. (2007) as follows: 17% B at 0 min, 23% B by 25 min; isocratic at 23% B from 25 to 45 min; 47% B by 55 min; isocratic at 47% B from 55 to 66 min, 17% B by 67 min, and isocratic at 17% B from 67 to 70 min. The column temperature was stable at 30 °C. The quantitation of anthocyanins and flavonols was determined using absorption at 520 nm for anthocyanins and 350 nm for flavonols.

Commercial authentic standards of anthocyanins and flavonols were used for comparison of HPLC retention times, mass spectra and UV-VIS absorption spectra, and for construction of standard curves at the HPLC step for quantitation.

A 'Honeywood' stage 9 fruit extract was selected for collecting the putative quercetin triglycoside compound (HPLC peak 2c, retention time of 10.5 min) for further identification. An HPLC 1200 Analyt FC fraction collector connected to the above HPLC system was used for collecting the compound using the HPLC analytical column and conditions as described above.

LC-MS analysis

Further identification of the putative quercetin triglycosides (HPLC peaks 2c and 2g, retention times of 10.5 and 32.7 min) was conducted using an Agilent 1100 LC-MS system fitted with electrospray ionization (ESI) interface. LC-MS column and conditions were the same as previously reported by Ozga et al. (2007).

Histology

Fresh whole fruits from stages 1 to 4 and tissue cross sections (approximately 5 mm thick) from stages 5 to 9 fruits were immediately immersed into a fixing solution containing 3.2 % paraformaldehyde (v/v), 1% glutaraldehyde (v/v), 2 mM CaCl₂, and 10 mM sucrose in a 25 mM PIPES buffer (pH 7.5). After 5 days of fixing solution infiltration under vacuum at room temperature, tissues were rinsed 3 times with 25 mM PIPES buffer and dehydrated using a graded ethanol series of 30% and 50% ethanol in 25 mM PIPES buffer (pH 7.5; v/v), followed by 70% and 96% ethanol in water for 25 min each. The tissues were further

dehydrated with two changes in 100% ethanol. After dehydration, specimens were sequentially infiltrated with 2.5%, 5%, 10%, 20%, 50%, 75% 1-butanol in ethanol (v/v) for 20 min each and the infiltration was completed with three washes of 100% 1-butanol for 20 min each. With gradual changes to Paraplast® Tissue Embedding Medium (Fisher Scientific, Houston, TX) as described by O' Brien and McCully (1981), tissues from the infiltration were embedded in paraffin blocks using a Tissue-TEK II Embedding centre (Tissue Tek, USA). Tissues were sliced into 10 to 20 µm-thick cross sections using a rotary microtome (Reichaert Histo STAT 820), stretched in a 40 °C water bath, affixed onto slides, and placed at 37 °C to dry overnight.

Tissue cross-sections from the same fruit block were mounted on clean slides and these slides were separated into two groups. In one group of slides, the paraffin was removed with two changes of toluene and cover slides were mounted on the slides using DPX mounting media (BDH Chemicals, NY, USA) for observing flavonol auto-fluorescence. In the other group of slides, the paraffin was removed in the same manner as above, then the tissues were stained with 0.1 % (w/v) DPBA staining solution (containing 0.025% Triton X-100) for 5 min, then washed with distilled water to remove any excess staining solution. The nearly dried sections were covered with cover slides using Fluoro Mount G (Electron Microscopy Sciences, USA) mounting media. The micrographs of whole fruit cross sections were taken using a Leica DMRXA microscope (Leica, Germany) (bright field option) mounted with a Nikon camera (DXM1200, Japan). The fruit pericarp, placenta, and seed fluorescence micrographs were obtained using the same equipment described above under the fluorescence microscopy configuration (Green: Excitation filter/BP 420-490; Dichromatic mirror/510; suppression filter: LP 515).

Results and Discussion

Fruit growth and development

Among the nine ripeness stages of saskatoon fruit reported by Rogiers and Knowles (1997), stages 1, 4, 5, 7, and 9 were selected to represent the major developmental stages over fruit development (**Figure 3.1**). Saskatoon fruit increased in size throughout development, with the greatest increases in fruit fresh weight occurring at the latter stages of fruit development (**Table 3.1**; McGarry et al., 1998). Of the cultivars studied, ‘Honeywood’ and ‘Thiessen’ had the largest fruit fresh weight at maturity (**Table 3.1**). For the pigmented-fruit cultivars, from stage 1 to 4, the mainly green fruit increased in size. Stage 5 fruits are lighter green and intermittent pink colour occurs on the fruit surface. By stage 7, the fruit turn red in colour having transitioned into the ripening stage, and by stage 9 the fruit are blue-purple and fully mature (**Figure 3.1**). For ‘Altaglo’, the early stages of fruit development (stages 1-5) were similar to that of the pigmented cultivars except for the substantially smaller fruit size at stage 1 (**Figure 3.1**; **Table 3.1**). However, with the transition to ripening (stage 7), minimal colouration occurred in ‘Altaglo’ fruits, and the fruits were white-coloured at maturity (stage 9; **Figure 3.1**).

Saskatoon fruits have 5 locules, similar to that of apple, and each locule can produce up to two seeds (Rogiers, 1997); however, at maturity the number of developed seeds are usually substantially lower than 10 (between 3 and 5) (McGarry et al. 1998; **Figure 3.1**).

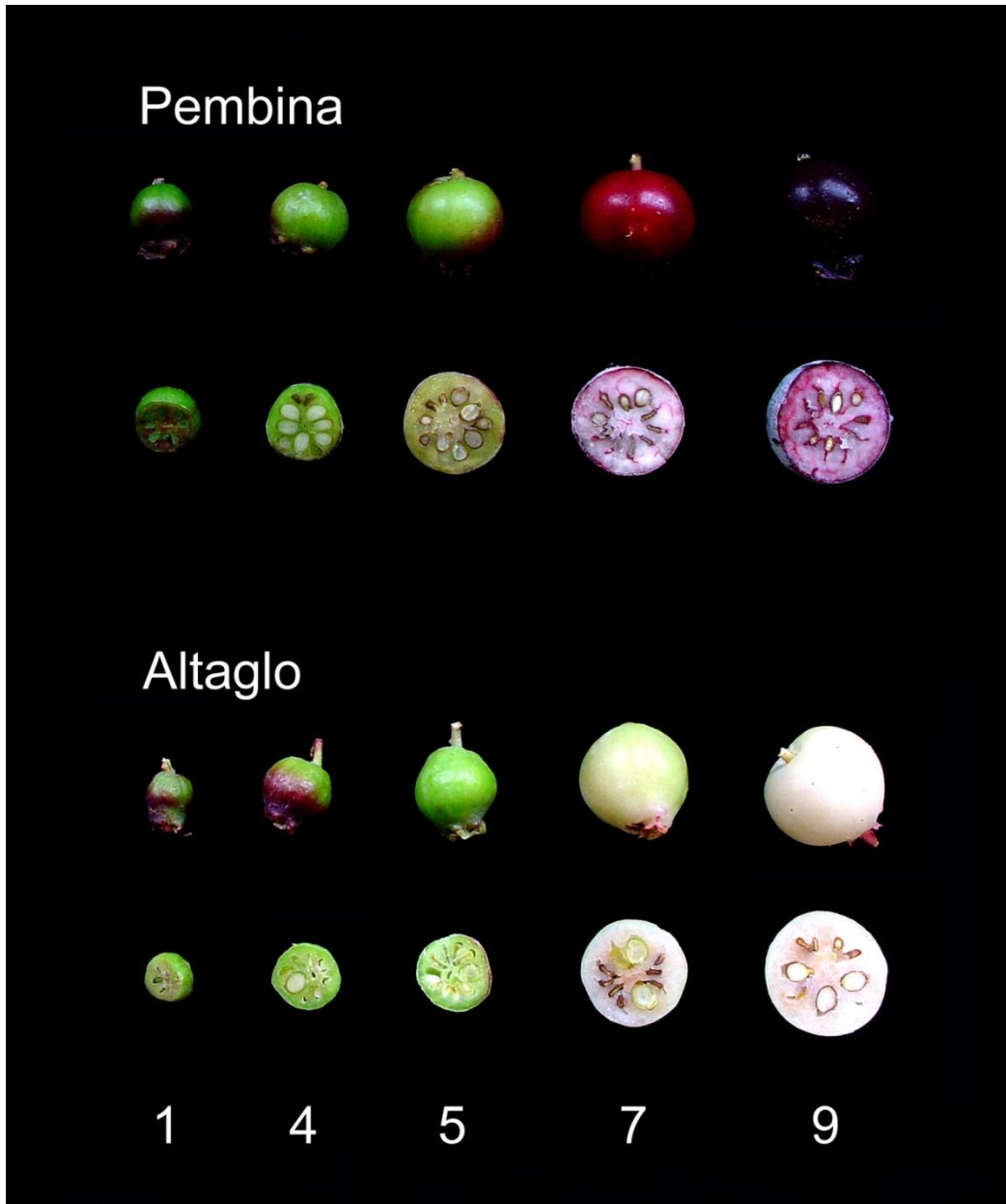


Figure 3.1: Whole and bisected fruits of saskatoon cv. Pembina and Altaglo over development. In ‘Pembina’ fruits, stage 1, small green fruit; stage 4, larger green fruit; stage 5, light green to pink fruit; stage 7, red fruit; stage 9, mature blue-purple fruit. In ‘Altaglo’ fruits, stages 1, 4, and 5, green fruit in the order of ascending fruit size; stage 7, light green to white fruit; stage 9, white fruit. The development of other pigmented cultivars of saskatoon fruits was similar to ‘Pembina’.

Table 3.1: Mean fresh fruit weight and diameter of saskatoon fruit during development.

| Cultivar | Fresh fruit diameter (mm) | | | | |
|-------------|---------------------------|--------------|--------------|--------------|----------------|
| | Stage 1 | Stage 4 | Stage 5 | Stage 7 | Stage 9 |
| ‘Northline’ | 6.9 ± 0.3* | 9.1 ± 0.1 | 10.4 ± 0.4 | 12.2 ± 0.3 | 13.4 ± 0.3 |
| ‘Honeywood’ | 6.5 ± 0.2 | 8.7 ± 0.4 | 11.7 ± 0.1 | 13.2 ± 0.2 | 15.5 ± 0.4 |
| ‘Pembina’ | 6.9 ± 0.2 | 7.6 ± 0.2 | 9.5 ± 0.3 | 11.5 ± 0.5 | 12.9 ± 0.2 |
| ‘Thiessen’ | 7.8 ± 0.2 | 8.3 ± 0.4 | 11.1 ± 0.3 | 12.8 ± 0.3 | 13.8 ± 0.3 |
| ‘Altaglo’ | 4.2 ± 0.0 | 9.2 ± 0.2 | 10.6 ± 0.3 | 11.6 ± 0.3 | 13.3 ± 0.3 |
| | Fresh fruit weight (mg) | | | | |
| ‘Northline’ | 181.3 ± 9.0 | 327.9 ± 23.2 | 475.3 ± 27.2 | 830.3 ± 14.1 | 1122.4 ± 27.4 |
| ‘Honeywood’ | 153.7 ± 2.8 | 291.1 ± 23.2 | 642.8 ± 40.7 | 981.4 ± 66.8 | 1865.8 ± 19.2 |
| ‘Pembina’ | 188.3 ± 4.2 | 242.3 ± 14.0 | 373.8 ± 21.6 | 666.3 ± 76.7 | 957.6 ± 27.5 |
| ‘Thiessen’ | 234.2 ± 3.6 | 387.1 ± 61.5 | 623.2 ± 45.8 | 948.6 ± 23.1 | 1522.4 ± 126.3 |
| ‘Altaglo’ | 52.0 ± 3.1 | 345.7 ± 17.7 | 521.4 ± 34.9 | 667.6 ± 35.2 | 1030.0 ± 92.1 |

* Data are means ± SE, n= 5.

Anthocyanin and flavonol profiles during fruit development

Anthocyanins

A typical HPLC-DAD chromatogram of a flavonoid extract from ‘Pembina’ stage 9 fruit monitored at 520 nm for anthocyanin detection is presented in **Figure 3.2 A**. Four anthocyanin peaks were detected, cyanidin 3-*O*-galactoside (cyn-gal, 1a), cyanidin-3-*O*-glucoside (cyn-glu, 1b), cyanidin 3-*O*-arabinoside (cyn-arb, 1c), and cyanidin 3-*O*-xyloside (cyn-xyl, 1d) respectively, as previously determined by Ozga et al. (2007) for cultivars Honeywood and Smoky. Cyn-gal, cyn-glu and cyn-arb were detected throughout development in fruits from all pigmented-cultivars tested (stages 1 to 9), with cyn-gal predominating the profile throughout development (**Figure 3.3 B-E**). Thus, cyn-gal is likely responsible for the reddish colouration on the mainly green-coloured fruit skin early in development (**Figure 3.1**). As the fruit transitioned into the ripening phase (stage 7), anthocyanin

content dramatically increased and cyn-xyl was detected (**Figure 3.3 B-E**). Anthocyanin levels peaked at fruit maturity (stage 9) in all pigmented-cultivars tested. The dramatic increase in anthocyanin levels in the latter fruit developmental stages suggests that as part of the ripening process, increased expression of transcription factors that are specific to up-regulating the transcript abundance of genes in the anthocyanin biosynthesis pathway occurs, as observed in grape berries (Deluc et al., 2008). The high anthocyanin levels that occur in mature fruit might function to alleviate oxidative stress as the fruit ripens (Rogiers et al., 1998), and/or the intense colouration of the fruit can function to attract animals for seed dispersal (Schaefer et al., 2004). Anthocyanin localization was carried out by cross sectioning whole fruits and visually observing tissue colouration. The typical red colour of anthocyanin appeared on some parts of the fruit exocarp (skin) throughout the earlier developmental stages (stages 1-5; **Figure 3.1A**). The fruit exocarps' red colour intensified as the fruit transitioned into the ripening stage (stage 7), and redish-purple pigmentation was also observable in the cells of the mesocarp, vascular traces, and the fruit locule margins. This colouration pattern intensified in the mature fruit (**Figure 3.1A**). In this study, the total anthocyanin concentration (mg per 100 g fresh fruit weight) was relatively similar in the mature fruits of 'Honeywood' (158), 'Pembina' (154), and 'Thiessen' (158); however, 'Northline' (201) contained higher levels (**Table 3.2**). The overall levels of anthocyanins in the mature pigmented saskatoon fruit are comparable to those found in other small fruits such as blueberry, cranberry, and sweet cherry (Wu et al., 2006). In general, saskatoon fruits have a relatively simple anthocyanin profile (4 major anthocyanins, all cyanidin-3-*O*-monoglucosides) compared to that of other common small fruits (for example, blueberries have over 13 anthocyanins; Prior et al., 2001). Qualitative and quantitative analysis of the anthocyanin profile in the non-pigmented saskatoon fruit cultivar 'Altglo' (white-coloured fruit at maturity) was also carried out over fruit development in order to gain a better understanding of flavonoid biosynthesis and accumulation in this fruit. Cyn-gal and cyn-arb were found in 'Altglo' fruits at levels comparable to that of the other pigmented cultivars during early fruit

development (stage 4; **Figure 3.3; Table 3.2**), demonstrating that the structural genes in the flavonoid pathway required to produce these anthocyanins are present and functioning during this developmental phase. However, as ‘Altaglo’ fruit continued to develop and transition into the ripening phase (stage 7), the dramatic increase in anthocyanin levels did not occur as observed in the pigmented cultivars, and only minimal levels of anthocyanins were detected at maturity (stage 9; **Figure 3.3; Table 3.2**). Thus, it is unlikely that the white-fruited ‘Altaglo’ is the result of a mutation in a key enzyme(s) for anthocyanin biosynthesis. It is more likely that the white-fruit phenotype is due to a mutation in a transcription factor (s) that regulate the coordinated up-regulation of anthocyanin biosynthesis gene expression during the ripening phase of fruit development, as documented in fruits of other plant species such as grape and apple (Jaakola et al., 2002; Espley et al., 2007; Deluc et al., 2008).

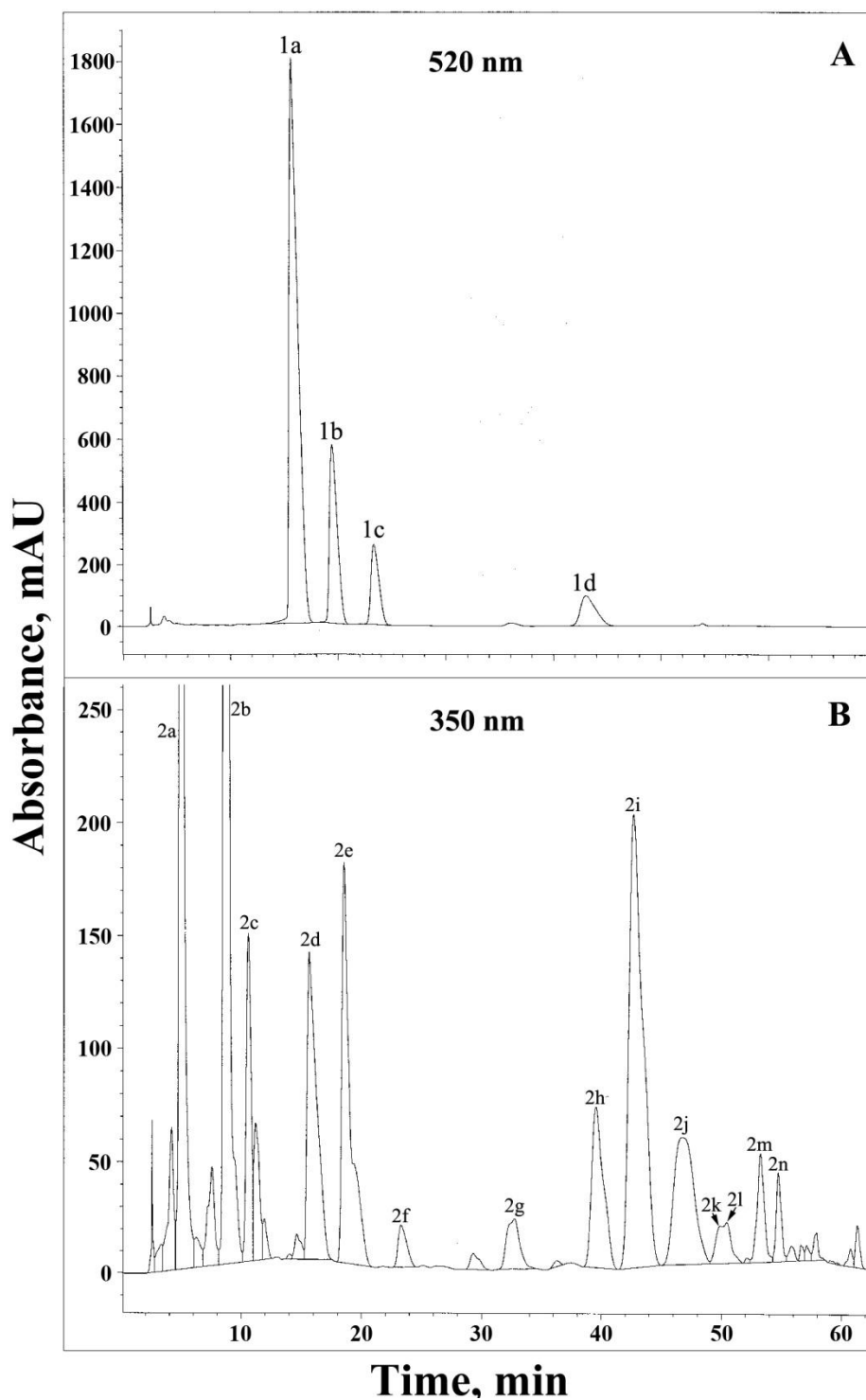


Figure 3.2: An HPLC-DAD profile of a stage 9 'Pembina' saskatoon fruit flavonoid extract. **(A)** Profile of anthocyanins monitored at 520 nm. **(B)** Profile of flavonols monitored at 350 nm. 1a (15.7 min), cyanidin 3-*O*-galactoside; 1b (19.4 min), cyanidin 3-*O*-glucoside; 1c (23.3 min), cyanidin 3-*O*-arabinoside; 1d (43.0 min), cyanidin 3-*O*-xyloside; 2a (4.9 min), 3-*O*-caffeoylquinic acid; 2b (8.7 min), 5-*O*-caffeoylquinic acid; 2c (10.6 min), putative quercetin triglycoside; 2d (15.7

min), cyanidin 3-*O*-galactoside; 2e (18.6 min), unknown chlorogenic acid isomer; 2f (23.3 min), cyanidin 3-*O*-arabinoside; 2g (32.7 min), putative quercetin triglycoside; 2h (39.6 min), quercetin 3-*O*-arabinoglucoside; 2i (42.7 min), quercetin 3-*O*-galactoside; 2j (46.8 min), quercetin 3-*O*-glucoside; 2k + 2l (50.4 min), quercetin 3-*O*-robinobioside + quercetin 3-*O*-rutinoside; 2m (53.3 min), quercetin 3-*O*-arabinoside; 2n (54.7 min), quercetin 3-*O*-xyloside.

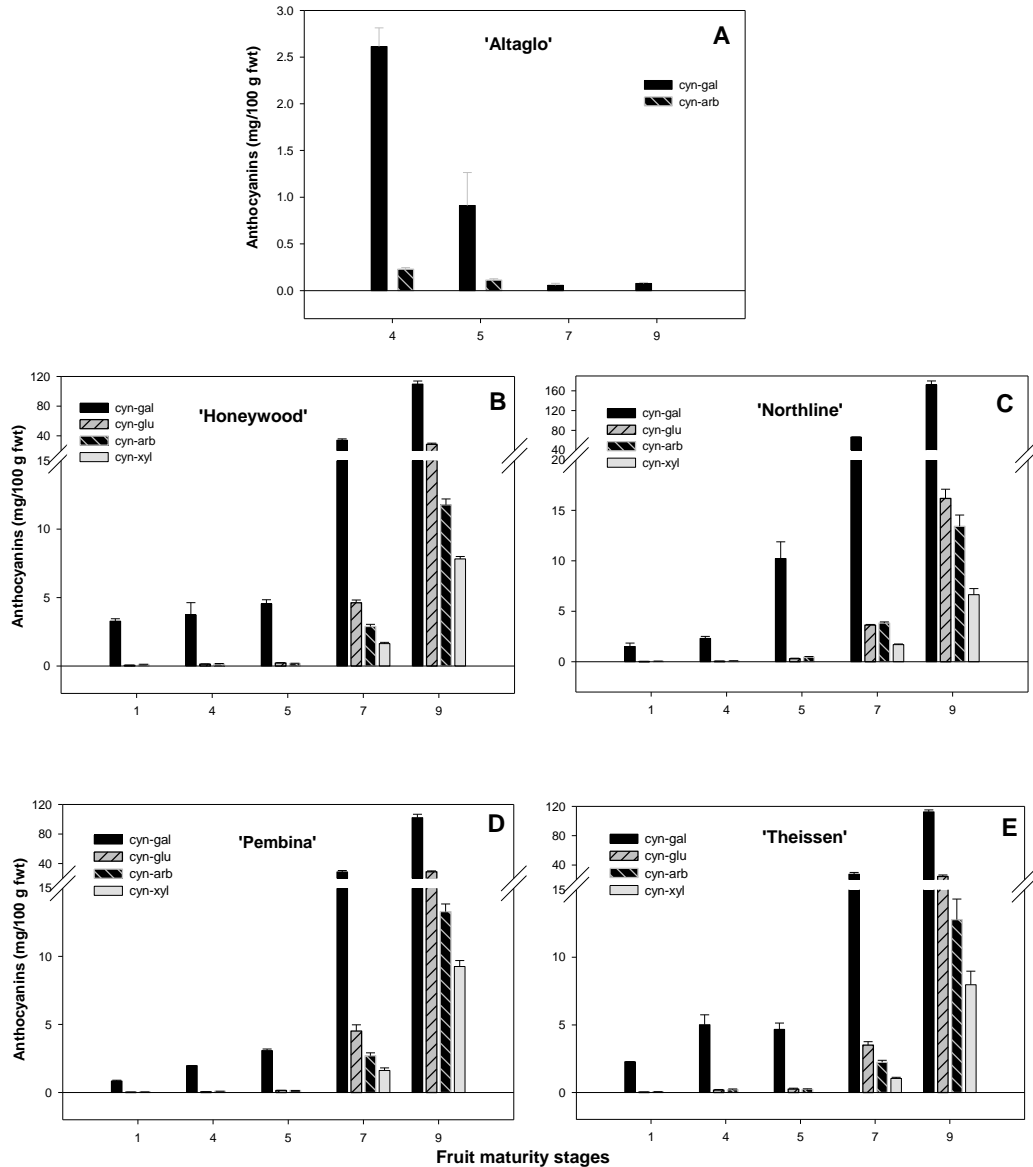


Figure 3.3: Type and content of anthocyanins in the fruits of (A) 'Altaglio', (B) 'Honeywood', (C) 'Northline', (D) 'Pembina', and (E) 'Thiessen' during development (stages 1, 4, 5, 7 and 9). Cyn-gal, cyanidin 3-*O*-galactoside; cyn-glu, cyanidin 3-*O*-glucoside; cyn-arb, cyanidin 3-*O*-arabinoside; cyn-xyl, cyanidin 3-*O*-xyloside.

Table 3.2: Total anthocyanin concentration during fruit development (mg per 100 grams fresh weight)^a.

| Cultivar | Stage 1 | Stage 4 | Stage 5 | Stage 7 | Stage 9 |
|-----------|-----------------|------------------------|------------|-------------|--------------|
| Altaglo | nd ^b | 2.8 ± 0.2 ^c | 1.0 ± 0.4 | 0.06 ± 0.02 | 0.08 ± 0.01 |
| Honeywood | 3.4 ± 0.2 | 4.0 ± 0.9 | 4.9 ± 0.3 | 43.3 ± 2.2 | 157.9 ± 5.6 |
| Northline | 1.6 ± 0.4 | 2.5 ± 0.2 | 11.0 ± 1.8 | 75.4 ± 0.5 | 200.9 ± 14.5 |
| Pembina | 0.90 ± 0.07 | 2.1 ± 0.0 | 3.4 ± 0.1 | 37.4 ± 2.8 | 153.5 ± 6.9 |
| Thiessen | 2.4 ± 0.0 | 5.4 ± 0.8 | 5.2 ± 0.6 | 34.4 ± 2.9 | 157.5 ± 7.2 |

^a Content estimated as cyanidin 3-*O*-galactoside (cyn-gal, cyn-arb, and cyn-xy) and cyanidin 3-*O*-glucoside (cyn-glu) equivalents;

^b nd=not determined;

^c Data are means ± SE, n=2 to 4.

Flavonols

A representative HPLC-DAD chromatogram of a flavonoid extract from ‘Pembina’ stage 9 fruit monitored at 350 nm for flavonol detection is presented in **Figure 3.2 B**. Seven main flavonols were detected as follows: quercetin 3-*O*-arabinoglucoside (2h), quercetin 3-*O*-galactoside (2i), quercetin 3-*O*-glucoside (2j), quercetin 3-*O*-robinobioside (2k) and quercetin 3-*O*-rutinoside (2l), quercetin 3-*O*-arabioside (2m), and quercetin 3-*O*-xyloside (2n) in all pigmented-cultivars studied, as previously determined in ‘Honeywood’ and ‘Smoky’ fruits by Ozga et al. (2007). Additionally, in ripening and mature fruit (stage 7 and 9) of the pigmented-cultivars, the presence of a strongly hydrophilic flavonol-type compound was observed (peak 2c; **Figure 3.2 B**; **Figure 3.4**) that had maximum absorbance at 343 nm. After isolation of this compound by collecting the HPLC 2c fraction, an LC-MS analysis was completed. The MS fragmentation pattern suggests that peak 2c is a quercetin triglycoside with characteristic aglycone ion masses of 303 (quercetin + H⁺ ion) and 812 (162 × 3 + 302 + 22 + 1 + 1 = hexose × 3 + quercetin + sodium ion + H + 1; **Table 3.3** and **Figure 3.5**). Strongly polar quercetin triglycosides have been reported in Italian red onion and cauliflower (Llorach et al., 2003; Bonaccorsi et al., 2005). These quercetin triglycosides were

glycosylated at carbons 3, 7 or 4' (Figure 2.3). As the polarity of this compound was much stronger than the other flavonols detected (eluted at 10.5 min in our HPLC system; **Figure 3.2 B**), it is reasonable to propose that the glycosylation pattern of this flavonol likely differs from the other flavonols, with a hexose sugar attached at carbon 3 and 7 or 4'. Nuclear magnetic resonance (NMR) studies would be required to determine the exact chemical structure of this quercetin triglycoside.

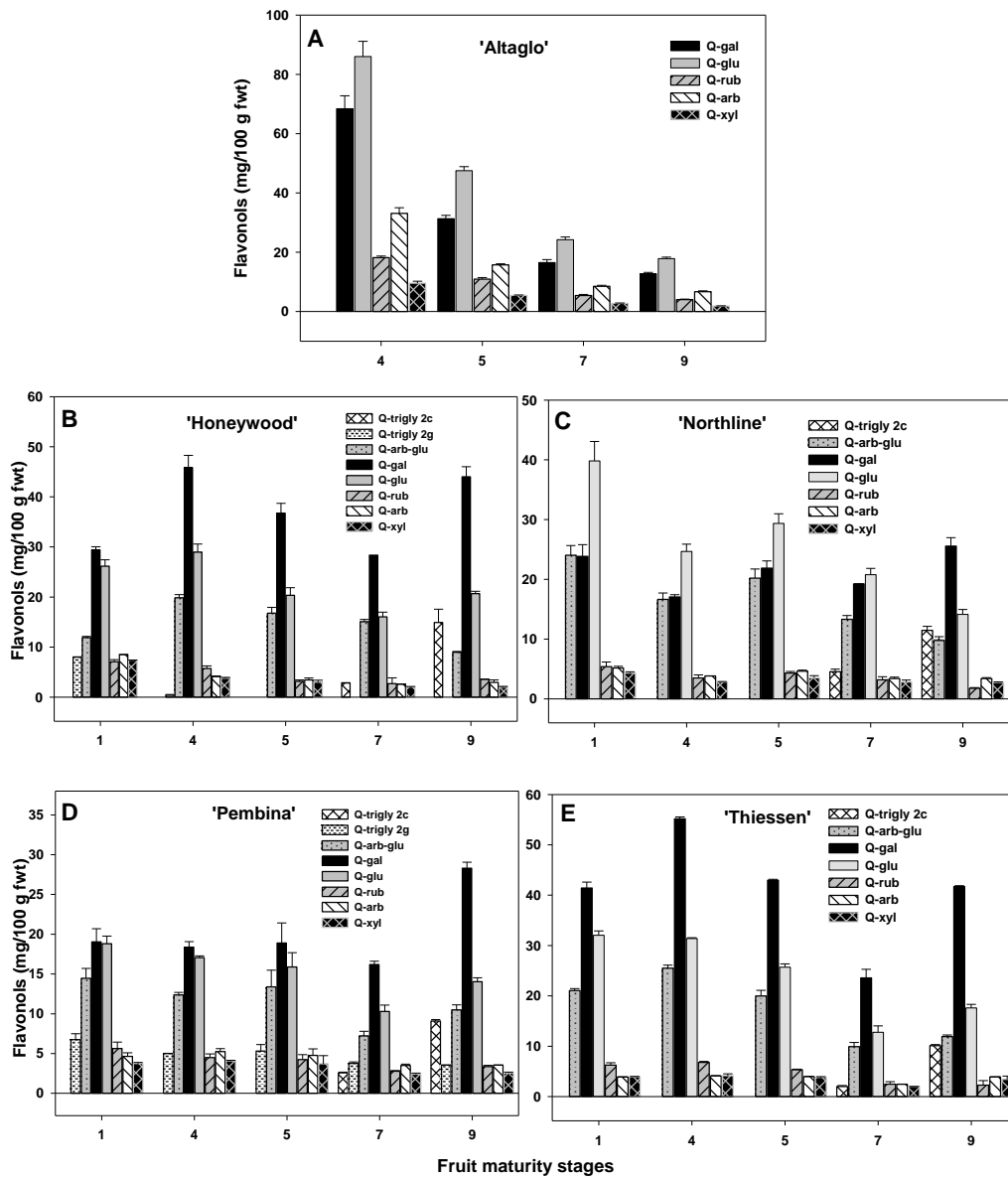


Figure 3.4: Type and content of flavonols in the fruits of (A) 'Altalgo', (B) 'Honeywood', (C) 'Northline', (D) 'Pembina', and (E) 'Thiessen' during fruit

development (stages 1, 4, 5, 7 and 9). Q-trigly 2c, putative quercetin triglycoside; Q-trigly 2g, putative quercetin triglycoside; Q-arb-glu, quercetin 3-*O*-arabinoglucoside; Q-gal, quercetin 3-*O*-galactoside; Q-glu, quercetin 3-*O*-glucoside; Q-rub, quercetin 3-*O*-robinobioside + quercetin 3-*O*-rutinoside; Q-arb, quercetin 3-*O*-arabinoside; Q-xyl, quercetin 3-*O*-xyloside.

Table 3.3: Characteristic retention time and the fragment ion masses of quercetin triglycosides in saskatoon fruit extracts as determined by LC-MS analysis^a.

| Quercetin triglycosides | Sample | t _R (min) ^b | Aglycon (A) | Major fragment and molecular ions [M+H] ⁺ | Fragment ions |
|-------------------------|--|-----------------------------------|---|--|--------------------------|
| 2c | Isolated Fraction from 'Honeywood' stage 9 extract | 10.5 (11.7 in Fig. 3.5) | 303([A+H] ⁺ , 100 ^c) | 812 (A + hex + hex + hex, 60) | 150, 215, 399, 877, 1147 |
| 2g | Stage 1 'Honeywood' Extract | 32.7 (30.9 in Fig. 3.6) | 303([A+H] ⁺ , 34) | 743 (A + rham + hex + pen, 19) 765 (A + rham + hex + pen + Na ⁺ , 29) 633 (A + rham + hex + Na ⁺ , 100) 611 (A + rham + hex, 100) 465 (A + hex, 18) 449 (A + rham, 100) | 766, 649, 579, 147 |

^a MS operated in the positive ion mode; ^b t_R, retention time; ^c Ion abundance. Hex, hexose; pen, pentose.

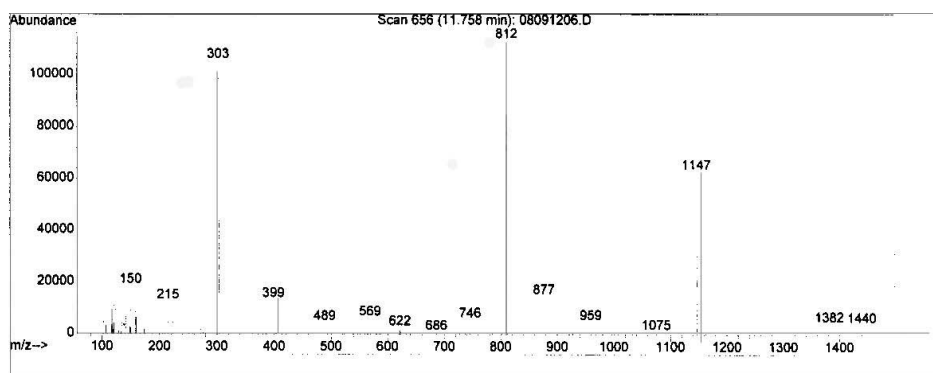


Figure 3.5: Mass spectrum of flavonol-type compound 2c.

Another unknown flavonol-type compound (peak 2g, **Figure 3.2 B**) was detected in 'Honeywood' stage 1 fruits and 'Pembina' fruits throughout development (**Figure 3.4**). This flavonol was further identified by LC-MS

analysis as a quercetin triglycoside of rhamnose, hexose, and pentose with a molecular ion mass of 743 ($302 + 146 + 162 + 132 + 1 =$ quercetin + rhamnose + hexose + pentose + H; **Table 3.3** and **Figure 3.6**). This compound (eluted at 32.7 min in the HPLC system) had similar polarity with that of quercetin 3-*O*-arabinoglucoside, therefore it is reasonable to postulate that this compound is a quercetin 3-*O*-triglycoside. Sequence and linkage among the three sugar units in the trisaccharide, and with quercetin, is hard to confirm by LC-MS analysis since internal monosaccharide loss might happen during the electrospray ionization process (Cuyckens et al., 2001). While isomers of the compound have been identified from various plant samples such as leaves of *Camellia japonica*, seeds of *Chenopodium pallidicaule*, and *Actinidia arguta*, structural confirmation will require further studies using NMR spectroscopy (Webby, 1991; Rastrelli et al., 1995; Onodera et al., 2006).

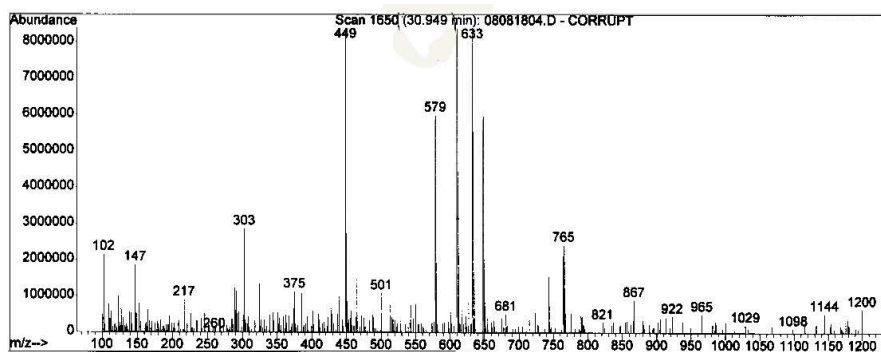


Figure 3.6: Mass spectrum of flavonol-type compound 2g.

In general, the flavonol profile of the pigmented cultivars was relatively similar with quercetin 3-*O*-galactoside, quercetin 3-*O*-glucoside and quercetin 3-*O*-arabinoglucoside dominating the flavonol profile throughout development. The flavonol profile of ‘Altglo’ differed from those of the pigmented-cultivars of fruit in several ways. Quercetin 3-*O*-arabinoglucoside was not detected in ‘Altglo’ (**Figure 3.4 A**) fruits over development, while this flavonol was relatively abundant in the other pigmented cultivars (**Figure 3.4**). Also, quercetin 3-*O*-glucoside was in greater abundance in ‘Altglo’ relative to other flavonols, where as quercetin 3-*O*-galactoside was the most abundance flavonol in the most

pigmented-cultivars (**Figure 3.4**). In flavonol biosynthesis, the glycosyltransferases, which catalyze the transfer of sugars to the flavonol aglycones, may have different preferences for sugars as substrates. The variation in flavonol type between the cultivars and over development within a cultivar may reflect the type and activities of specific glycosyltransferases (Offen et al., 2006). In addition to flavonol peaks, chlorogenic acid isomers were detected (2a, neochlorogenic acid; 2b, chlorogenic acid; 2e, an unknown chlorogenic acid isomer), as previously described by Ozga et al. (2007; **Figure 3.2 B**).

In most of the saskatoon cultivars studied, the maximum fruit flavonol concentration occurred earlier in fruit development (stage 1 to 4; **Figure 3.7**; **Table A.1** in appendix I) followed by a decline in flavonol concentration as the fruit transitioned into ripening (stage 7; **Figure 3.7**). Subsequently, flavonol concentrations increased in the mature fruit (stage 9; **Figure 3.7**). In blueberry (*Vaccinium corymbosum* L.) and bilberry (*Vaccinium myrtillus*), flavonol concentration was also high in early developmental stages of fruits and decreased along with fruit development (Jaakola et al., 2002; Castrejon et al., 2008). The activities of flavonoid biosynthesis enzymes, such as phenylalanine ammonia lyase (PAL), flavonol synthase (FLS), flavonoid 3-*O*-glucosyltransferase (F3GT), and flavonoid 7-*O*-glucosyltransferase (F7GT), were determined in strawberry (*Fragaria × ananassa*) during fruit development (Halbwirth et al., 2006). Most enzyme activities (PAL, F3GT, and F7GT) followed a biphasic pattern, where higher activities were detected both earlier and later in fruit development, with lower activities observed during mid-fruit development. Also, in grape and bilberry fruits, the expression of specific flavonoid biosynthesis pathway genes was high at the beginning of fruit development and at the end of fruit development (Boss et al., 1996; Jaakola et al., 2002). Again, this is likely related to the activity of transcription factors that can up-regulate specific parts of the flavonoid biosynthesis pathway (Bovy et al., 2002).

As the fruit continues to increase in size throughout development, the total flavonol content per fruit increased during development in the pigmented cultivars (**Figure 3.7 B-E**). This was not the case for ‘Altaglo’ fruits, where the total

flavonol content decreased as the fruit matured (stage 4 to 9; **Figure 3.7 A**). In contrast, pink bilberry fruit (colour mutant, pink fruits at maturity) had a greater flavonol content at maturity compared to that in wild type bilberry (dark colour fruits at maturity; Jaakola et al., 2002). The reduction in flavonol content per fruit in ‘Altaglio’ over development is consistent with the loss of function of a ripening-related flavonoid biosynthesis transcription factor(s) that would act to up-regulate flavonoid biosynthesis, leading to flavonol accumulation over development in this cultivar.

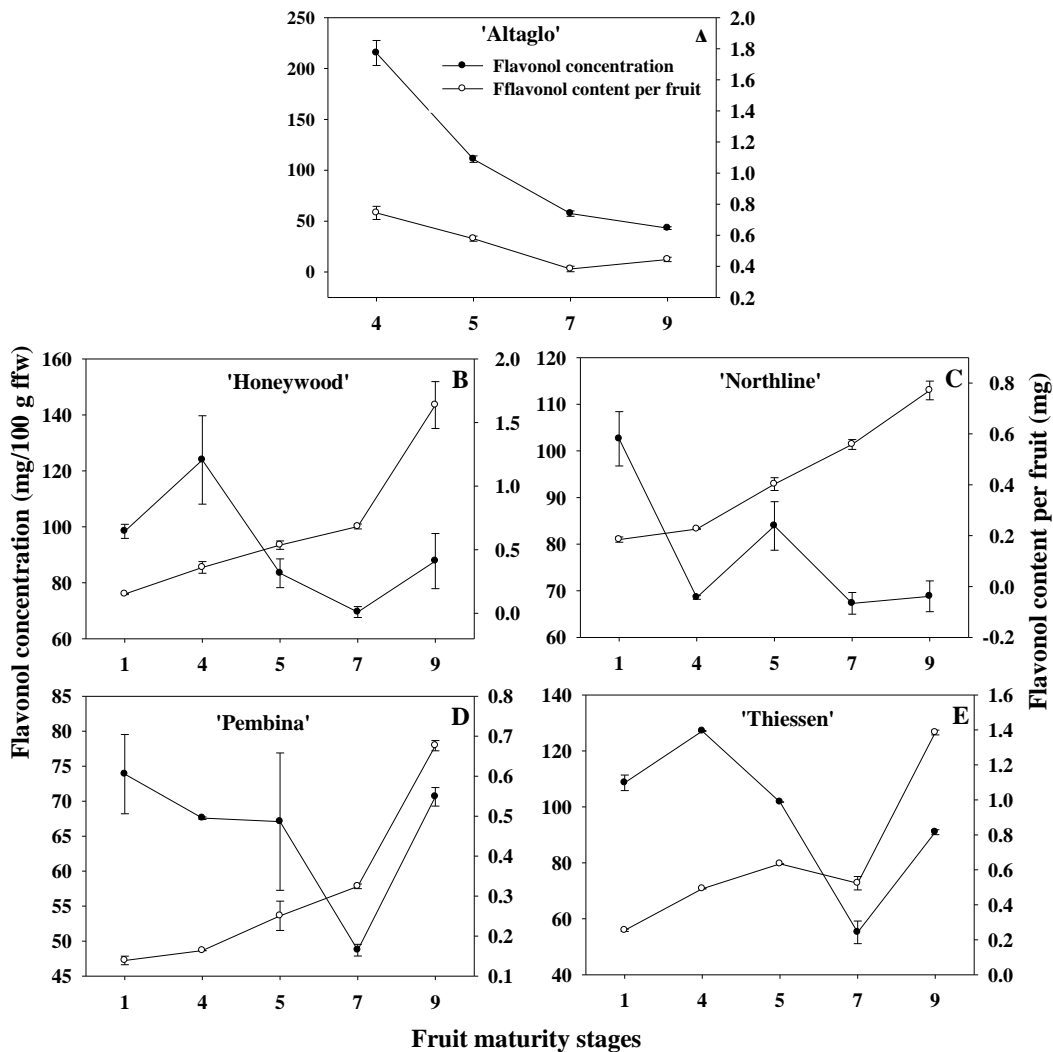


Figure 3.7: Flavonol concentration in 100 g fresh fruit weight (ffw) basis and flavonol content per fruit basis over the development (stages 1, 4, 5, 7, and 9) of

saskatoon fruit. (A) ‘Altaglio’, (B) ‘Honeywood’, (C) ‘Northline’, (D) ‘Pembina’, and (E) ‘Thiessen’.

Localization of flavonols during fruit development

Flavonols have auto-fluorescence and the auto-fluorescence (yellow colour) can be intensified by a flavonol specific staining reagent, diphenylboric acid 2-aminoethylester (DPBA; Schnitzler et al., 1996; Peer et al., 2001). Flavonol auto-fluorescence and enhanced fluorescence by DPBA staining in fruit cross-sections was monitored using a fluorescence microscope (**Figure 3.8**). Flavonols were localized in most of the exocarp and mesocarp tissues (intracellularly, likely in the vacuole) of stage 1 fruits (**Figure 3.8, B and C**). By stage 4, flavonols mainly localized to the epidermis and hypodermal layer (**Figure 3.8, B and C**). At maturity, flavonols were observed mainly in the epidermal/hypodermal layer and cuticle of the fruits (**Figure 3.8, C**). Flavonol localization in the cuticle layer may be the result of flavonol migration from the epidermal to the cuticle layer to provide protection to fruits from UV light damage (Solovchenko and Merzlyak, 2003). Placental tissues (also accumulated flavonols with stage 4 tissues showing the most intense staining for flavonols; **Figure 3.8, D and E**). In seed tissues, flavonols localized to the vacuoles of developing seed coats during early fruit development (stage 4; **Figure 3.8, F and G**). As the seeds develop, seed coat cells undergo sclerification and cell death. Flavonols are likely moving from the vacuoles to the cell walls of the seed coat cells during this process to keep providing protection to the embryo from potential microbial attack during germination. A study of flavonoid deposition in cell walls of flower petals found that flavonols not only accumulate in vacuoles as do other flavonoids, but also in cell walls (Markham et al., 2000). The same pattern of flavonol localization was observed in the pigmented-fruit cultivar ‘Pembina’ as observed in ‘Altaglio’ (data not shown).

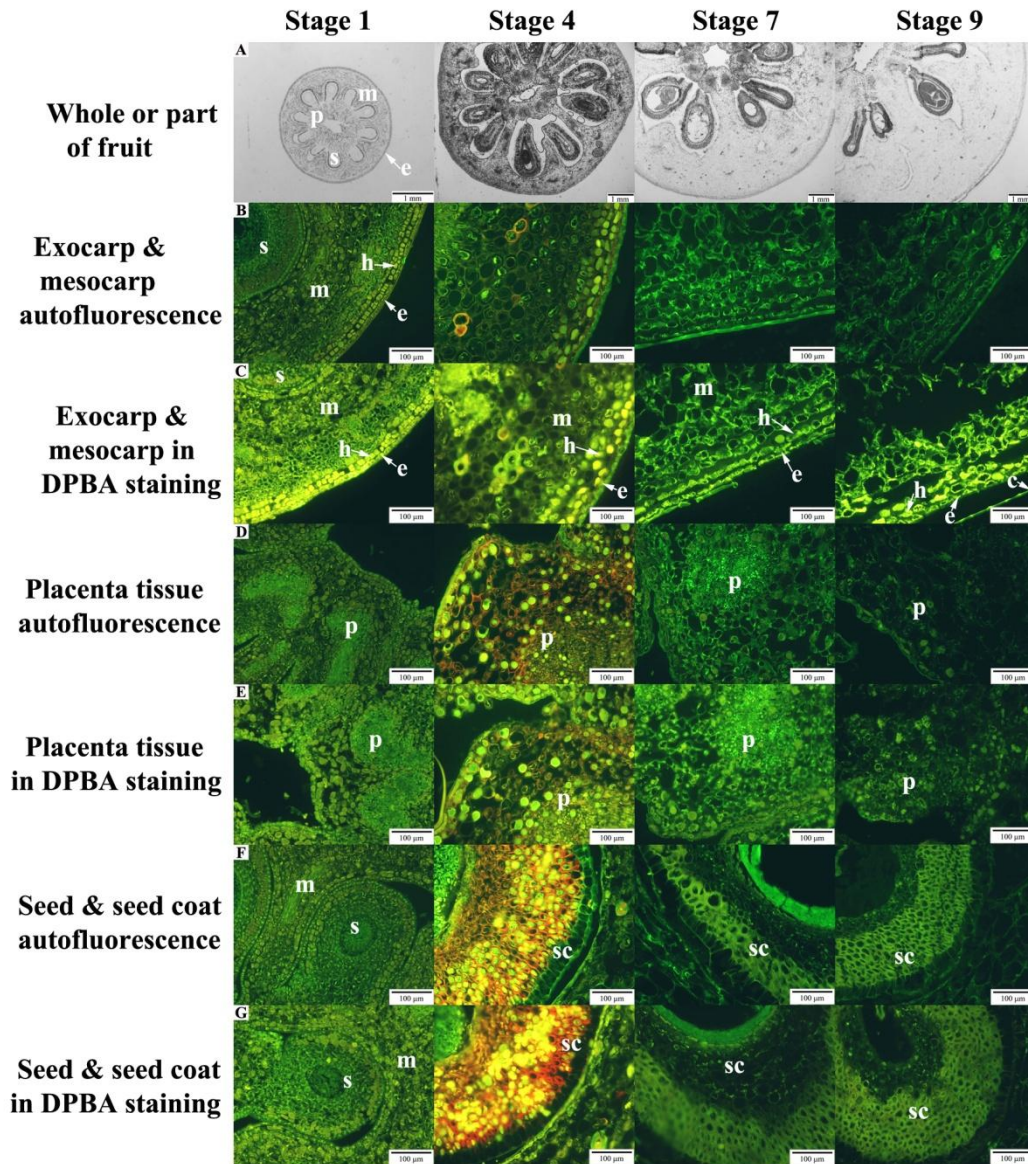


Figure 3.8: Flavonol accumulation in ‘Altagro’ fruit over development. (A) Whole fruit or fruit sections visualized using bright field microscopy; (B-G) Fruit tissues visualized using fluorescence microscopy (excitation filter/BP 420-490; Dichromatic mirror/510; suppression filter/LP 515) at 20× magnification; Exocarp and mesocarp tissue without (B) and with DPBA staining (C); Placenta tissue without (D) and with DPBA staining (E); Seed and seed coat tissue without (F) and with DPBA staining (G). c, cuticle; e, epidermis; h, hypodermis; m, mesocarp; p, placenta; s, seed; sc, seed coat.

Conclusions

In summary, anthocyanin and flavonol accumulation in saskatoon fruits was temporally and spatially regulated during development. Anthocyanin levels were low during early fruit development stages, and dramatically increased during ripening in all pigmented-cultivars. Anthocyanins mainly accumulated in the mature fruit exocarp, locule margin, and mesocarp tissues. In the white-fruited mutant 'Altaglo', anthocyanin content during early fruit development was similar to that of the pigmented cultivars; however, the dramatic increase in anthocyanin content during the ripening phase did not occur. The profiles of the major flavonols were relatively similar among the pigmented cultivars studied. Additionally, two quercetin-triglycosides were identified in the fruit of specific saskatoon cultivars. Flavonol accumulation showed a biphasic pattern, with levels higher earlier and later in fruit development. Flavonols were distributed in all the tissues of the fruit during the early developmental stages, and were mainly localized to the cuticle, exocarp, placental, and seed coat tissues in mature fruit. The temporal and spatial regulation of anthocyanin and flavonol accumulation suggests that these flavonoid compounds play important roles in the fruit during development and in the reproductive strategy of this species.

Literature Cited

- Bakowska-Barczak AM, Kolodziejczyk P** (2008) Evaluation of saskatoon berry (*Amelanchier alnifolia* Nutt.) cultivars for their polyphenol content, antioxidant properties, and storage stability. *Journal of Agricultural and Food Chemistry* **56**: 9933-9940
- Bonaccorsi P, Caristi C, Gargiulli C, Leuzzi U** (2005) Flavonol glucoside profile of southern Italian red onion (*Allium cepa* L.). *Journal of Agricultural and Food Chemistry* **53**: 2733-2740
- Boss PK, Davies C, Robinson SP** (1996) Analysis of the expression of anthocyanin pathway genes in developing *Vitis vinifera* L cv Shiraz grape berries and the implications for pathway regulation. *Plant Physiology* **111**: 1059-1066

- Bovy A, de Vos R, Kemper M, Schijlen E, Pertejo MA, Muir S, Collins G, Robinson S, Verhoeyen M, Hughes S, Santos-Buelga C, van Tunen A** (2002) High-flavonol tomatoes resulting from the heterologous expression of the maize transcription factor genes LC and C1. *Plant Cell* **14**: 2509-2526
- Castrejon ADR, Elchholz I, Rohn S, Kroh LW, Huyskens-Keil S** (2008) Phenolic profile and antioxidant activity of highbush blueberry (*Vaccinium corymbosum* L.) during fruit maturation and ripening. *Food Chemistry* **109**: 564-572
- Crozier A, Jaganath IB, Clifford MN** (2009) Dietary phenolics: chemistry, bioavailability and effects on health. *Natural Product Reports* **26**: 1001-1043
- Cuyckens F, Rozenberg R, de Hoffmann E, Claeys M** (2001) Structure characterization of flavonoid *O*-diglycosides by positive and negative nano-electrospray ionization ion trap mass spectrometry. *Journal of Mass Spectrometry* **36**: 1203-1210
- Deluc L, Bogs J, Walker AR, Ferrier T, Decendit A, Merillon JM, Robinson SP, Barrieu F** (2008) The transcription factor VvMYB5b contributes to the regulation of anthocyanin and proanthocyanidin biosynthesis in developing grape berries. *Plant Physiology* **147**: 2041-2053
- Espley RV, Hellens RP, Putterill J, Stevenson DE, Kutty-Amma S, Allan AC** (2007) Red colouration in apple fruit is due to the activity of the MYB transcription factor, MdMYB10. *Plant Journal* **49**: 414-427
- Halbwirth H, Puhl I, Haas U, Jezik K, Treutter D, Stich K** (2006) Two-phase flavonoid formation in developing strawberry (*Fragaria* × *ananassa*) fruit. *Journal of Agricultural and Food Chemistry* **54**: 1479-1485
- Hosseinian FS, Beta T** (2007) Saskatoon and wild blueberries have higher anthocyanin contents than other Manitoba berries. *Journal of Agricultural and Food Chemistry* **55**: 10832-10838
- Jaakola L, Maatta K, Pirttila AM, Torronen R, Karenlampi S, Hohtola A** (2002) Expression of genes involved in anthocyanin biosynthesis in relation to anthocyanin, proanthocyanidin, and flavonol levels during bilberry fruit development. *Plant Physiology* **130**: 729-739
- Kolb CA, Kopecky J, Riederer M, Pfundel EE** (2003) UV screening by phenolics in berries of grapevine (*Vitis vinifera*). *Functional Plant Biology* **30**: 1177-1186

- Llorach R, Gil-Izquierdo A, Ferreres F, Tomas-Barberan FA** (2003) HPLC-DAD-MS/MS ESI characterization of unusual highly glycosylated acylated flavonoids from cauliflower (*Brassica oleracea* L. var. botrytis) agroindustrial byproducts. *Journal of Agricultural and Food Chemistry* **51**: 3895-3899
- Markham KR, Ryan KG, Gould KS, Rickards GK** (2000) Cell wall sited flavonoids in lisianthus flower petals. *Phytochemistry* **54**: 681-687
- Martineau LC, Couture A, Spoor D, Benhaddou-Andaloussi A, Harris C, Meddah B, Leduc C, Burt A, Vuong T, Le PM, Prentki M, Bennett SA, Arnason JT, Haddad PS** (2006) Anti-diabetic properties of the Canadian lowbush blueberry *Vaccinium angustifolium* Ait. *Phytomedicine* **13**: 612-623
- Mazza G** (1986) Anthocyanins and other phenolic-compounds of saskatoon berries (*Amelanchier alnifolia* Nutt). *Journal of Food Science* **51**: 1260-1264
- McGarry R, Ozga JA, Reinecke DM** (1998) Patterns of saskatoon (*Amelanchier alnifolia* Nutt.) fruit and seed growth. *Journal of the American Society for Horticultural Science* **123**: 26-29
- McGarry R, Ozga JA, Reinecke DM** (2005) The effects of ethephon on saskatoon (*Amelanchier alnifolia* Nutt.) fruit ripening. *Journal of the American Society for Horticultural Science* **130**: 12-17
- Middleton EM, Teramura AH** (1993) The role of flavonol glycosides and carotenoids in protecting soybean from ultraviolet-B damage. *Plant Physiology* **103**: 741-752
- Mol J, Grotewold E, Koes R** (1998) How genes paint flowers and seeds. *Trends in Plant Science* **3**: 212-217
- O' Brien TP, McCully ME** (1981) *The study of plant structure: principles and selected methods*. Termarcarphi, Melbourne, Australia
- Offen W, Martinez-Fleites C, Yang M, Kiat-Lim E, Davis BG, Tarling CA, Ford CM, Bowles DJ, Davies GJ** (2006) Structure of a flavonoid glucosyltransferase reveals the basis for plant natural product modification. *Embo Journal* **25**: 1396-1405
- Onodera K, Hanashiro K, Yasumoto T** (2006) Camellianoside, a novel antioxidant glycoside from the leaves of *Camellia japonica*. *Bioscience Biotechnology and Biochemistry* **70**: 1995-1998

- Ozga JA, Saeed A, Wismer W, Reinecke DM** (2007) Characterization of cyanidin- and quercetin-derived flavonoids and other phenolics in mature saskatoon fruits (*Amelanchier alnifolia* Nutt.). *Journal of Agricultural and Food Chemistry* **55**: 10414-10424
- Peer WA, Brown DE, Tague BW, Muday GK, Taiz L, Murphy AS** (2001) Flavonoid accumulation patterns of transparent testa mutants of *Arabidopsis*. *Plant Physiology* **126**: 536-548
- Prior RL** (2004) Absorption and metabolism of anthocyanins: Potential health effects. *In* *Phytochemicals: Mechanisms of Action*. Crc Press-Taylor & Francis Group, Boca Raton, pp 1-19
- Prior RL, Lazarus SA, Cao GH, Muccitelli H, Hammerstone JF** (2001) Identification of procyanidins and anthocyanins in blueberries and cranberries (*Vaccinium* spp.) using high-performance liquid chromatography/mass spectrometry. *Journal of Agricultural and Food Chemistry* **49**: 1270-1276
- Rastrelli L, Saturnino P, Schettino O, Dini A** (1995) Studies on the constituents of chenopodium pallidicaule (Canihua) Seeds - isolation and characterization of 2 new flavonol glycosides. *Journal of Agricultural and Food Chemistry* **43**: 2020-2024
- Rogiers SY** (1997) Biochemical and physiological studies of saskatoon (*Amelanchier alnifolia* Nutt.) fruit during ripening and storage. University of Alberta, Edmonton
- Rogiers SY, Knowles NR** (1997) Physical and chemical changes during growth, maturation, and ripening of saskatoon (*Amelanchier alnifolia*) fruit. *Canadian Journal of Botany-Revue Canadienne De Botanique* **75**: 1215-1225
- Rogiers SY, Kumar GNM, Knowles NR** (1998) Maturation and ripening of fruit of *Amelanchier alnifolia* Nutt. are accompanied by increasing oxidative stress. *Annals of Botany* **81**: 203-211
- Schaefer HM, Schaefer V, Levey DJ** (2004) How plant-animal interactions signal new insights in communication. *Trends in Ecology & Evolution* **19**: 577-584
- Schnitzler JP, Jungblut TP, Heller W, Kofferlein M, Hutzler P, Heinzmann U, Schmelzer E, Ernst D, Langebartels C, Sandermann H** (1996) Tissue localization of uv-B-screening pigments and of chalcone synthase mRNA in needles of Scots pine seedlings. *New Phytologist* **132**: 247-258

- Solovchenko A, Merzlyak M** (2003) Optical properties and contribution of cuticle to UV protection in plants: experiments with apple fruit. *Photochemical & Photobiological Sciences* **2**: 861-866
- St-Pierre RG** (1997) Growing saskatoons - a manual for orchardists. Fifth edition. Department of Horticulture Science, University of Saskatchewan, Saskatoon, SK. 338 pp.
- Webby RF** (1991) A flavonol triglycoside from *Actinidia arguta* var *Giraldii*. *Phytochemistry* **30**: 2443-2444
- Wu XL, Beecher GR, Holden JM, Haytowitz DB, Gebhardt SE, Prior RL** (2006) Concentrations of anthocyanins in common foods in the United States and estimation of normal consumption. *Journal of Agricultural and Food Chemistry* **54**: 4069-4075

Chapter 4

Characterization of Proanthocyanidins in Saskatoon Fruits (*Amelanchier alnifolia* Nutt.) during Development and at Maturity

Introduction

Saskatoon fruits (*Amelanchier alnifolia* Nutt.) are native fruit species of the Northern prairies and plains of North America (St-Pierre, 1997). Saskatoon fruits have excellent flavour attributes when consumed as fresh fruit or processed food and have potential to be an economically important fruit crop (similar to blueberries) in Canada, since saskatoons can be produced in commercially acceptable amounts in Western Canada (St-Pierre et al., 2005). Saskatoon fruit contain significant levels of flavonoids in the mature fruit including the proanthocyanin (PA) class of flavonoids (Hellstrom et al., 2007; Bakowska-Barczak and Kolodziejczyk, 2008). As one of the main subclasses of flavonoids, PAs (oligomeric and polymeric flavan-3-ols, also known as condensed tannins due to their brown oxidation colour) are widely distributed in many types of fruits, where they provide flavor and astringency to the fruit when consumed (Aron and Kennedy, 2008). Additionally, recent research suggests that PAs may also have beneficial effects on human health (Bagchi et al., 2000; Lee et al., 2008).

The chemical structure of PAs vary by the nature (stereochemistry and hydroxylation pattern) of the flavan-3-ols in the extension and terminal units, the linkages between subunits, the degree of polymerization, and the presence or absence of esterification of the C3 hydroxyl group with gallic acid (refer to **Figure 2.5**). The linkage between flavan-3-ols in PAs is normally between the C4 of the 'upper' unit and the C8 or C6 positions of the 'lower' unit. These types of PAs are called B-type. In the case of A-type PAs, both C2 and C4 of the upper unit and the oxygen at C7 and C6 or C8 are doubly linked (**Figure 2.5**; Gu et al.,

2003). A-type linkages are abundant in PAs from cranberries and peanut seed coats (Koerner et al., 2009), and they are reported to ameliorate the effects of urinary tract infections by hindering certain-classes of bacterial adherence to urinary tract epithelial cells (Foo et al., 2000). Due to the structural complexity of PAs, it is challenging to fully structurally characterize individual PAs. Generally, information about subunit composition and mean degree of polymerization (mDP) provides sufficient knowledge for biologists to study PA biosynthesis and nutritionist to study their health benefits (Lee et al., 2008).

In order to further understand the spatial and temporal dynamics of PA biosynthesis and accumulation in saskatoon fruits, we have identified, quantified, and histochemically localized PAs over fruit development in five cultivars of saskatoons. PA subunit composition and degree of polymerization were characterized and quantified using a method of acid-catalyzed cleavage of the PAs followed by phloroglucinol derivatization (phloroglucinolysis; **Figure 2.9**). Identification and quantitation of the phloroglucinolysis products was performed by reverse-phase (RP) HPLC-DAD analysis and the identification was confirmed by LC-MS/MS. Histochemical localization of PA in saskatoon fruits was performed using the PA-specific stain (DMACA).

Materials and Methods

Plant material

Saskatoon fruits (*Amelanchier alnifolia* Nutt.) from the cultivars Northline, Pembina, Thiessen, Honeywood, and Altaglo were collected from the University of Alberta Experimental Farm, Edmonton, Alberta, Canada and sorted into 9 maturity classes in the manner described in Chapter 3.

Chemicals

All HPLC grade organic solvents (acetone, acetonitrile, methanol, ethyl acetate) and acetic acid (ACS grade) were purchased from Fisher Scientific (Ottawa, ON, Canada). (+)-Catechin hydrate, (-)-epicatechin, (-)-epicatechin gallate, (-)-epigallocatechin, (-)-gallocatechin, (-)-catechin gallate, (-)-

epigallocatechin gallate, (-)-gallocatechin gallate, taxifolin, phloroglucinol, trifluoroacetic acid (TFA), L-(+)-ascorbic acid, hydrochloric acid (HCl, 36.5 ~ 38 %), 1-butanol, DMACA, and TOYOPEARL resin (HW-40F) were purchased from Sigma (Oakville, ON, Canada). The crude cranberry PA and grape skin PA standards were kindly provided by Dr. James Kennedy's lab (Oregon State University). They were prepared following the extraction and purification procedures described in Kennedy and Taylor (2003) and Koerner et al. (2009).

Extraction and purification of PAs

Frozen berries were ground to a fine powder in liquid nitrogen using a mortar and pestle. Ground samples (5-10 g) were extracted with 66% (v/v) aqueous acetone (10 mL per g tissue) in an Erlenmeyer flask. The flask was sparged with nitrogen gas then sealed with a glass stopper and placed on a rotary shaker at 100 rpm in the dark at room temperature for 24 h for extraction. The extract was filtered through Whatman No.1 filter paper under moderate vacuum using a Büchner funnel. The tissue residue was washed with 66% aqueous acetone, extract and wash were pooled, and the acetone was removed using a SpeedVac vacuum concentrator (AES 200, Savant, Farmingdale, NY). The remaining aqueous PA extract was extracted a minimum of 5 times with 100% HPLC grade ethyl acetate (3:1 (v/v), extract: ethyl acetate) to remove chlorophylls, anthocyanins, and flavan-3-ol monomers. The remaining ethyl acetate in the aqueous extract was removed using a SpeedVac vacuum concentrator. The aqueous extract was adjusted to 50% (v/v) aqueous methanol with 0.1% TFA using methanol (100%) and TFA and loaded onto a 4-mL bed volume column of TOYOPEARL (1.5 cm diameter × 12 cm length) preconditioned with 50% (v/v) aqueous methanol with 0.1% TFA. The column was washed with a minimum of 5 column bed volumes of 50% aqueous methanol with 0.1% TFA to remove organic acids and other flavonoids including flavan-3-ol monomers, anthocyanins, and flavonols (eluent from the washing step were monitored with a UV-Vis spectrometer (Scinco, Korea) at two wavelength ranges (260-370 nm and 500-560

nm) and the washing step continued until minimal absorbance was detected in these two wavelength ranges.

For the crude fruit PA extracts from young fruits (stages 1 to 5), 5 column bed volumes of 50% aqueous methanol with 0.1% TFA was sufficient for impurity removal, while PA extracts from mature stage fruits (stages 7 and 9) needed more than 10 bed volumes of washing solution to sufficiently remove the impurities. Following the wash step, the PAs were eluted using 4 bed volumes of 66% acetone with 0.1% TFA. The acetone was removed from the extract using a SpeedVac vacuum concentrator, and the remaining aqueous extract was lyophilized.

Phloroglucinolysis of PAs

The phloroglucinolysis reaction procedure of Koerner et al. (2009) was used with minor modifications. Briefly, approximately 10 mg of the lyophilized PA extract was dissolved in a 2 mL solution of 0.1 N methanolic hydrochloric acid solution containing 100 g L⁻¹ phloroglucinol and 10 g L⁻¹ ascorbic acid. For determining the optimal reaction time for saskatoon fruit PA extracts, the reaction was carried out in a 50 °C water bath for 10, 20, 60, 90, 120, 135, 150, 180, and 300 min. Subsequently, a 200 µL aliquot of the reaction product from each incubation period was added to 1 mL of 40 mM aqueous sodium acetate solution to quench the reaction. The diluted reaction solutions were subjected to HPLC-DAD analysis (see below) for monitoring free-flavan-3-ol (released from PA terminal units) and flavan-3-ol phloroglucinol adduct (from extension PA units) production. Using data from this time-course experiment and that in the literature, the phloroglucinolysis reaction times for monitoring free-flavan-3-ols flavan-3-ol phloroglucinol adducts were as follows: 20 min for B-type and A-type (A₂) terminal units, and B-type phloroglucinol adducts; 120 min for A-type (A₂)-phloroglucinol adducts for saskatoon fruit PA extracts; 20 min for grape fruit skin PA standard extracts (no A-type linkages present), and 135 min for cranberry fruit PA standard extracts.

Identification and quantitation of PAs

A 20 μL aliquot of the diluted reaction mixture was injected onto two Chromolith RP-18e (4.6 x 100 mm) columns connected in series, protected by a guard column (Chromolith RP-18e 4.6 x 10 mm), stabilized at 30°C, using an Agilent 1200 HPLC system equipped with an Agilent G1315B DAD. The HPLC conditions followed that of Kennedy and Taylor (2003) with minor modifications. The samples were eluted at 3 mL min⁻¹ using a linear gradient with 1 % (v/v) aqueous acetic acid (solvent A) and acetonitrile with 1% acetic acid (v/v; solvent B) as follows: isocratic at 3 % B from 0 to 4 min, 3% to 18 % B by 14 min, and 80 % B from 14 to 18 min. Free-flavan-3-ols, A₂ dimers, flavan-3-ol phloroglucinol adducts (from extension subunits), and A₂-phloroglucinol adducts (from extension subunits) were monitored at 280 nm. PA terminal subunits were identified by comparison of HPLC-DAD retention times and absorbance spectra with commercially available flavan-3-ol standards. Phloroglucinol-PA adducts were identified by comparison of HPLC retention times with grape skin and cranberry fruit PA reaction products that have been previously characterized (Koerner et al., 2009). Mean degree of polymerization and conversion yields were calculated according to method of Kennedy and Jones (2001).

To confirm the identification of the flavan-3-ol monomers and phloroglucinol adducts, LC-MS analysis of the phloroglucinolysis reaction products was performed on a 4000 Q-TRAP[®] LC/MS/MS mass spectrometer (MDS SCIEX, Applied Biosystems) connected to an Agilent 1200 HPLC system with G 1315D photodiode array detector, G1312A binary pump, G1379B degasser, G1316A thermostatted column compartment and G1329A autosampler (Agilent Technologies, Palo Alto, CA). HPLC separation was performed on a Symmetry[®] C₁₈ column (250 x 4.6 mm, 5 μm particle size) with a Novapak[®] C₁₈ guard column (10 x 4.6 mm, 4 μm particle size, Waters, MA) at 25 °C and at a flow rate of 1 mL min⁻¹. The compounds were separated using a linear elution gradient of (A) 1 % aqueous acetic acid (v/v) and (B) 100 % methanol as follows: isocratic at 5% B from 0-13 min; 20% B at 33 min; 40 % B at 58 min; 90% B at 58.1 min; isocratic at 90 % B from 58.1 to 68.1 min. MS/MS analysis was carried out in the

negative ion mode using the following mass spectrometer conditions: high-purity nitrogen gas (99.995 %) as nebulising gas (GS1) at 50 psi, heating gas (GS2) at 30 psi, and curtain gas (CUR) at 25 psi for electrospray probe. Ion-spray source temperature was 600 °C and ion spray voltage was 4 kV. Collision-induced dissociation (CID) spectra were acquired using nitrogen as the collision gas under collision energy (CE) of 20 eV. The other MS parameters used were as follows: declustering potential (DP), 70 V; entrance potential (EP), 10 V; and collision exit potential (CXP), 7 V. An information-dependent acquisition (IDA) method, EMS → 4 EPI, was used to profile the phloroglucinol adducts of flavan-3-ols and flavan-3-ol terminal units. The IDA threshold was set at 100 cps, above which enhanced product ion (EPI) spectra were collected from the eight most intense peaks. Both Q1 and Q3 were operated at low and unit mass resolution. The spectra were obtained over a scan range from the mass to charge ratio (m/z) 50 to 1300. The EPI scan rate was 4000 Da/s and the enhanced MS (EMS) scan rate was 1000 Da/s. MS/MS data were acquired and analyzed by Analyst software (version 1.5, Applied Biosystems, CA).

PA terminal subunits (except for the A-type terminal unit dimer; A_2) were identified by comparison of HPLC-DAD retention times, LC-MS fragmentation spectra and absorbance spectra with commercially available flavan-3-ol standards. Epicatechin-(4 β →2)-phloroglucinol (EC-P) was identified by comparison of HPLC retention times and LC-MS fragmentation pattern with grape skin PA phloroglucinolysis reaction products. A_2 and the A_2 -phloroglucinol (A_2 -P) adduct were characterized by comparison of HPLC retention times and LC-MS spectra with cranberry fruit PA phloroglucinolysis products, which have been previously characterized (Kennedy and Jones, 2001; Koerner et al., 2009). The catechin-(4 α →2)-phloroglucinol (C-P) standard was synthesized using a method previously described by Kennedy and Jones (2001) and Li and Deinzer (2006) with minor modifications. Briefly, 20 mg taxifolin was reduced by excessive sodium borohydride (22 mg) in 100 % ethanol (completely dehydrated with anhydrous sodium sulfate) for one hour at room temperature. Phloroglucinol (70 mg dissolved in 4 mL 0.1 N HCl/ethanol solution) was added to the taxifolin

solution and the mixture was stirred 45 min, then diluted with 4 mL Milli-Q water. Catechin-phloroglucinol was extracted from the reaction solution by partition with 10 mL ethyl acetate (4 times), then the ethyl acetate fraction was evaporated to dryness using a SpeedVac vacuum concentrator. Epicatechin was used as an external standard for quantification of the free-PA terminal subunits (catechin, epicatechin, and A₂) and phloroglucinol adducts. The relative molar and mass response factors from Kennedy and Jones (2001) and Koerner et al. (2009) were used for calculating PA subunit concentration, mDP, and conversion yield as described by Kennedy and Jones (2001).

Histochemical localization of PAs

All fruit for the histochemical study were collected at the University of Alberta Experimental Research Station, Edmonton, Alberta and transported to the lab on ice. For stage 5, 7, and 9 fruits, the top (pedicle end) and bottom (calyx end) parts of the fruit were removed and approximately 5 to 10 mm of the central fruit tissue was used for tissue fixation (**Figure 4.1**).

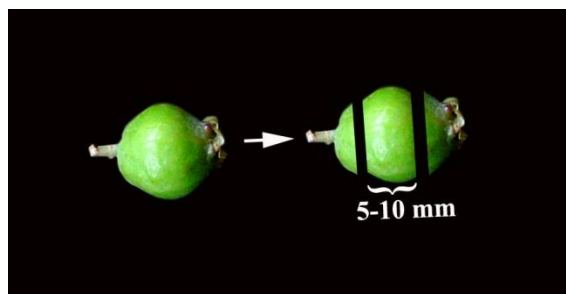


Figure 4.1: A schematic of a typical fruit section (5-10 mm) used for histological fixation for stage 5, 7, and 9 fruits.

The fresh fruit sections were immediately fixed in 3.2 % paraformaldehyde, 1% glutaraldehyde, 2 mM CaCl₂, and 10 mM sucrose in 25 mM PIPES buffer (pH 7.5). After 5 days of fixing solution infiltration under vacuum at room temperature, tissues were rinsed 3 times with 25 mM PIPES buffer (pH 7.5) and dehydrated using a graded ethanol series of 30% and 50% ethanol in 25 mM PIPES buffer (v/v), followed by 70%, 96%, and 100% ethanol in water for 25 min each. After dehydration, specimens were sequentially infiltrated with 2.5%, 5%,

10%, 20%, 50%, 75% 1-butanol in ethanol (v/v) for 20 min each and the infiltration was completed with three washes of 100% 1-butanol for 20 min. The tissues were then embedded in Paraplast[®] Tissue Embedding Medium (Fisher Scientific; Houston, TX) as described by O' Brien and McCully (1981). Briefly, the shavings of Paraplast[®] Tissue Embedding Medium (PEM) were added to the tissue in the final 100% 1-butanol change solution, the vials were sealed, and stored for 2 days at room temperature. PEM was added intermittently to the tissue if all PEM shavings were dissolved into the 1-butanol solution during this period. The vials with the tissue slurry were then placed at 40 °C for 1 day. Subsequently, the vials were unsealed and kept at 40 °C for 2 more days. Then, more PEM shavings were added to the tissue vials and the vials were incubated at 59 °C for 1 day. While keeping the vials at 59 °C, twenty five percent of the infiltration solvent mixture was replaced by freshly melted PEM. After 2 hours, approximately 50% of solvent mixture was replaced by melted PEM. This procedure was repeated 2 more times (at 50% replacement of solvent mixture) and the vials were further incubated overnight at 59 °C. Melted fresh PEM was then added to replace all the mixture solution and the vials were kept at 59 °C for an additional 24 hours (no 1-butanol smell should be detected at this step). After another change of freshly melted PEM, the vials were placed in a 59 °C vacuum oven for 3-5 days (the time in the vacuum oven varied depending on tissue size). Tissues from the vacuum oven were embedded in paraffin blocks using a Tissue-TEK II Embedding centre (Miles Laboratory, IL, USA). Tissue sections were sliced 10 µm to 20 µm thick using a rotary microtome (Reichaert Histo STAT 820), stretched in a 40 °C water bath, affixed onto clean slides, and placed at 37 °C to dry overnight.

For PA localization, the paraffin was removed from the tissue sections using two toluene (100%) washes at 5 min intervals. Tissue sections were stained with 0.1% DMACA/0.5 M H₂SO₄/1-butanol solution prepared as described by Gutmann and Feucht (1991). Briefly, 2.80 mL H₂SO₄ (95~98 %) was added to 50 mL 1-butanol. After this solution cooled down to room temperature, 0.0840 mg

DMACA was added to the solution. This mixture was transferred into a 100 mL glass volumetric flask and brought up to 100 mL with 1-butanol. This staining solution was stored at 4 °C until use (and could be used up to one month). For tissue staining, slides with fruit sections were covered with the DMACA solution and incubated at 60 °C on a hot plate for 15 min. The slides were then washed with 100% ethanol to remove the excess staining solution. The slides were then dipped into two fresh toluene (100%) baths for 5 min each to remove moisture from the tissues. Cover slides were placed on slide-mounted tissue sections using DPX mounting media (BDH Chemicals, NY, USA). Tissue sections were observed using a Zeiss AXIO scope A1 light microscope (Zeiss, Germany) and micrographs were taken with a microscope-mounted Optronics camera (Optronics, USA) controlled by Picture Frame™ Application 2.3 software.

Results and Discussion

Kinetic studies on phloroglucinolysis of PAs from saskatoon fruits

The optimal reaction time for acid-catalyzed depolymerisation in the presence of excess phloroglucinol for PA derivatization varies for PAs with B-type and A-type linkages (Kennedy and Jones, 2001; Koerner et al., 2009). For PAs with B-type linkages, a 20 min reaction time was optimal. Longer reaction times for PA extracts from grape skin and seed resulted in epicatechin terminal units forming an undesirable C-2 phloroglucinol adduct (Kennedy and Jones, 2001). In cranberry juice PA extracts, which contain higher levels of A-type PA linkages, 135 min was found to be the optimal reaction time for the phloroglucinolysis reaction (Koerner et al., 2009). PA polymers with a higher portion of A-type linkages are likely more resistant to the acid-catalyzed cleavage reaction than the PA polymers with only B-type linkage between the flavan-3-ol subunits. This is likely due to the enhanced intermolecular forces resulting from the double linkages between the flavan-3-ol subunits characteristic for the A-type linkage group. Thus, a longer reaction time is required for full conversion of PAs to subsequent depolymerised products. We assumed that the optimal phloroglucinolysis reaction time would vary in accordance to the amount of A-

type linkages in the PA oligomer or polymer. Hence, a kinetic study for PAs extracted from ‘Thiessen’ stage 1 fruits was conducted to determine the optimal reaction time for the phloroglucinolysis reaction for saskatoon fruit extracts. The optimal reaction time for the production of free A_2 dimer from terminal subunits (A_2), epicatechin-($4\beta\rightarrow 2$)-phloroglucinol (EC-P), and epicatechin (EC) was 20 min for PAs from saskatoon fruits, since the levels of these compounds were reduced at longer reaction times (Figure 4.2 B-D). For A_2 dimer phloroglucinol adduct (A_2 -P) formation, 120 min was chosen as optimal for saskatoon fruits, since the majority (approximately 80 %) of the A_2 -P production occurred within this time period (Figure 4.2 A).

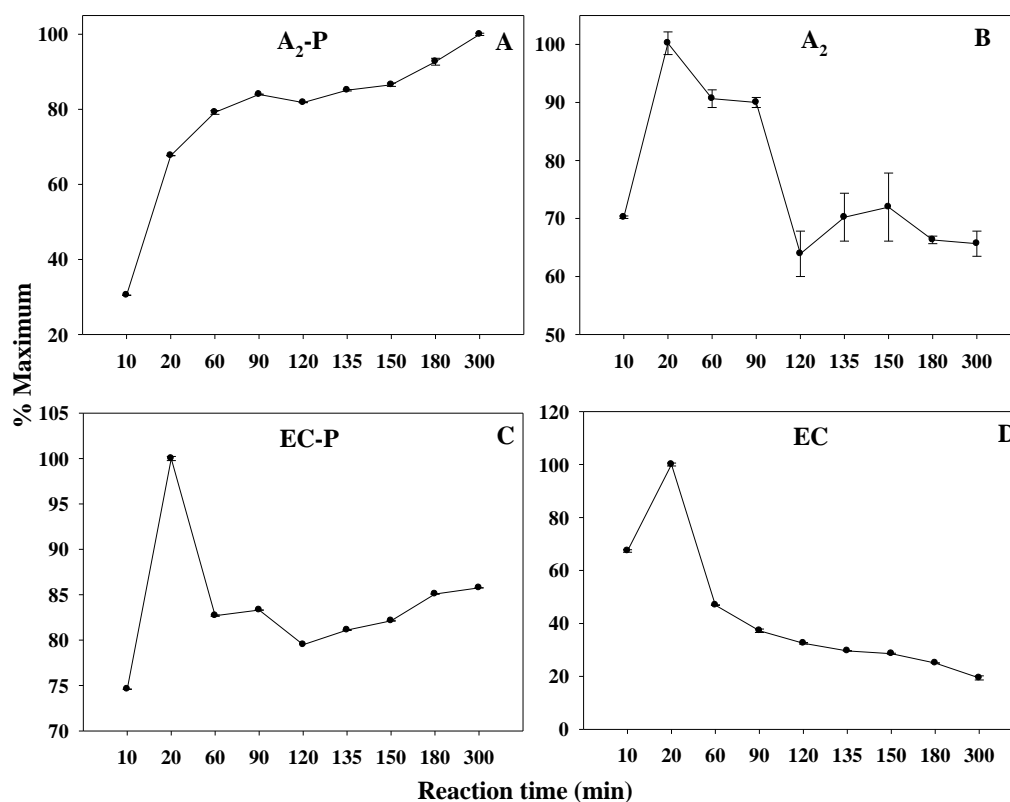


Figure 4.2: Effect of phloroglucinolysis reaction time on the production of flavan-3-ols and flavan-3-ol-phloroglucinol adducts. (A) A_2 dimer phloroglucinol adduct (A_2 -P) (B) A_2 dimer (A_2); (C) epicatechin-($4\beta\rightarrow 2$)-phloroglucinol (EC-P), (D) epicatechin (EC) from ‘Thiessen’ stage 1 fruit extracts. Data are means \pm SE, n=2.

Characterization and quantitation of PAs

Fractionation methods can be used to separate PA oligomer/polymer classes by length, and coupled with LC-MS analysis, the concentration of each PA oligomer class can be estimated (Hellstrom et al., 2007). While the current PA analysis techniques are adequate for separation of PA oligomers (usually 2-7 flavan-3-ol subunits in length) they do not effectively separate PA polymers (PA polymer length greater than 7). Highly polymerized PA mixtures can be characterized by a method that involves acid-catalyzed cleavage of PAs followed by nucleophile stabilization of the cleaved site. Most commonly used nucleophiles in the last two decades are phloroglucinol and benzyl mercaptan for PA analysis. The method that uses phloroglucinol as the derivatization reagent is called phloroglucinolysis (Lee et al., 2008), and the method that uses benzyl mercaptan is called thiolysis (Foo et al., 1996) in PA analysis. PA composition of mature saskatoon fruits has been reported using fractionation with normal-phase semi-preparative HPLC followed by electrospray ionization coupled with tandem mass spectrometry (ESI-MS/MS) analysis of each PA oligomer fraction (Hellstrom et al., 2007), and direct thiolysis of PA extracts with benzyl mercaptan followed by RP-HPLC analysis (Bakowska-Barczak and Kolodziejczyk, 2008). In the above mentioned studies, PAs from mature saskatoon fruits were found to mainly consist of epicatechin subunits, with only B-type linkages reported. In this study, the method of direct phloroglucinolysis followed by RP-HPLC analysis, with confirmation of phloroglucinolysis products by LC-MS/MS, was chosen for characterization of the PA profile during saskatoon fruit development, as it provides information about flavan-3-ol composition and mDP of PAs. Typical RP-HPLC chromatograms of the phloroglucinolysis products of PA extracts of saskatoon fruit ('Northline' stage 1), grape skin standard, and cranberry fruit standard are presented in **Figure 4.3**. The chemical structures of PA phloroglucinolysis products detected in the RP-HPLC chromatograms are presented in **Figure 4.4**. The major products from a 20 min phloroglucinolysis reaction in the saskatoon fruit and grape skin PA extracts are EC-P (peak 3), A₂-P (peak 5), EC (peak 7), A₂ (peak 8) (Figure 4.3A). After the 120 min

phloroglucinolysis reaction, EC levels (peak 7) were reduced, while the A₂-P level (peak 5) increased (**Figure 4.3 B**). These data demonstrate that the 120 min phloroglucinolysis reaction time is optimal for A₂-P quantitation but not for epicatechin quantitation.

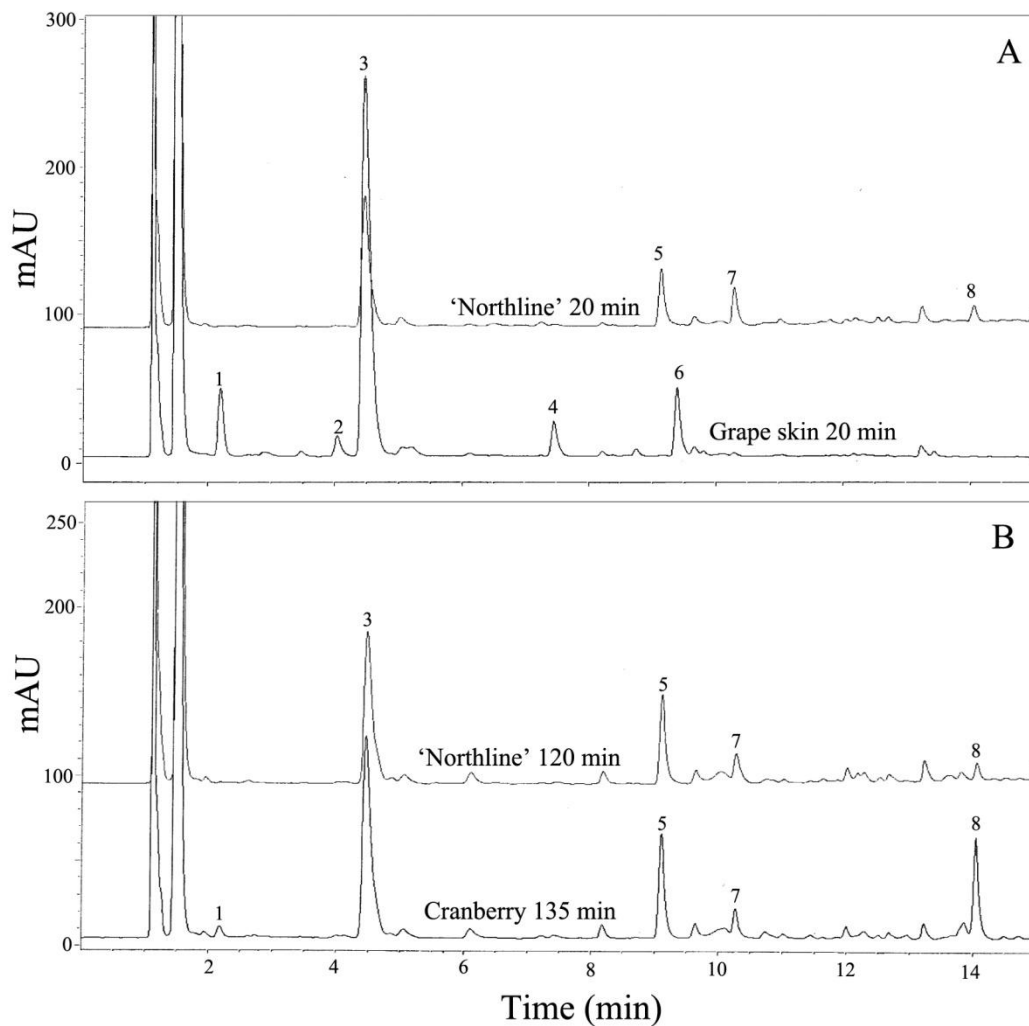


Figure 4.3: RP-HPLC chromatograms (monitored at 280 nm) of the phloroglucinolysis products of PAs from ‘Northline’ stage 1 saskatoon fruits, cranberry fruit standard, and grape skin standard. (A) Comparison of ‘Northline’ 20 min reaction products with grape skin standard 20 min reaction products; (B) Comparison of ‘Northline’ 120 min reaction products with cranberry standard 135 min reaction products. 1. epigallocatechin-(4 β →2)-phloroglucinol (EGC-P); 2. catechin-(4 α →2)-phloroglucinol (C-P); 3. epicatechin-(4 β →2)-phloroglucinol (EC-P); 4. catechin (C); 5. A₂-phloroglucinol (A₂-P); 6. epicatechin gallate-

(4 β →2)-phloroglucinol (ECG-P); 7. epicatechin (EC); 8. A₂. (The two peaks detected prior to peak1 are the reaction components ascorbic acid and phloroglucinol)

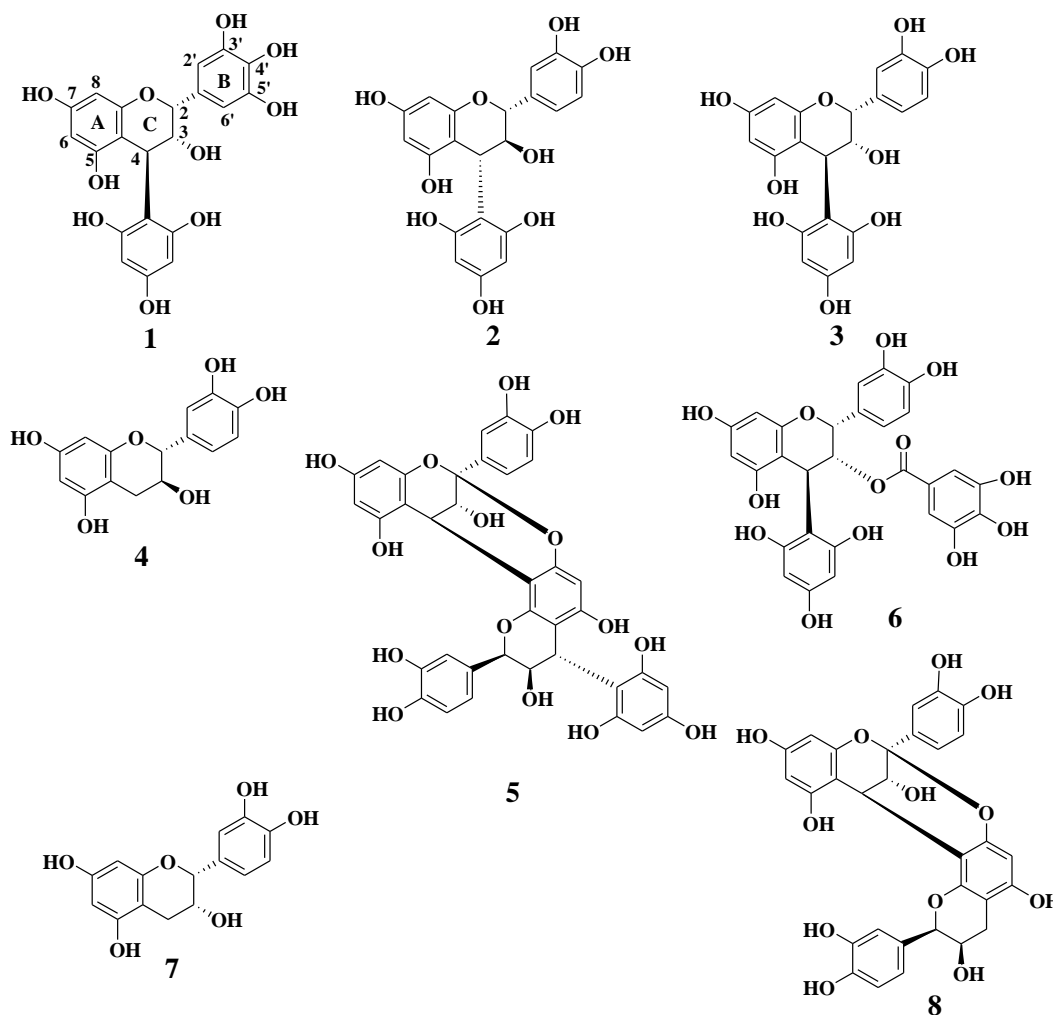


Figure 4.4: Chemical structures of subunit products following phloroglucinolysis of saskatoon fruit, grape skin, and cranberry fruit PA extracts. 1. epigallocatechin-(4 β →2)-phloroglucinol (EGC-P); 2. catechin-(4 α →2)-phloroglucinol (C-P); 3. epicatechin-(4 β →2)-phloroglucinol (EC-P); 4. catechin (C); 5. A₂-phloroglucinol (A₂-P); 6. epicatechin gallate-(4 β →2)-phloroglucinol (ECG-P); 7. epicatechin (EC); 8. A₂.

By comparing RP-HPLC retention times and UV absorption spectra (data not shown) to known grape skin and cranberry standards, saskatoon fruit PA flavan-3-

ol extension units were confirmed to be nearly exclusively procyanidin, specifically that of epicatechin (**Figure 4.3; Table 4.1**). These data are consistent with those reported by Hellstrom et al. (2007) and Bakowska-Barczak and Kolodziejczyk (2008). However, these studies only reported the presence of PA B-type linkages, whereas we found epicatechin flavan-3-ol subunits were linked together by both B-type (peak 3, EC-P) and A-type linkages (peak 5, A₂-P) in the extension units, as well as the terminal units (peak 7, EC; peak 8, A₂) (**Figure 4.3; Table 4.1**). The abundance of A-type PA linkages varies with cultivar, with ‘Pembina’ fruit having the greatest abundance of PA A-type linkages at most stages of fruit development (**Table 4.1**). Additionally, minimal amounts of catechin were detected in the PA extension subunits over fruit development in most cultivars (**Table 4.1**). These PA composition results suggest that the flavonoid biosynthesis enzymes for synthesizing both catechin (leucoanthocyanidin reductase, LAR) and epicatechin (anthocyanidin synthase, ANS/anthocyanidins reductase, ANR) from leucocyanidin are present in saskatoon fruits; however, ANS/ANR must be more active than LAR in PA synthesis. The terminal subunits of PAs from saskatoon fruits mainly consisted of epicatechin (peak 7, **Figure 4.3; Table 4.1**), with a minor portion of epicatechin dimer in A-type configuration (A₂, peak 8, **Figure 4.3; Table 4.1**). Only minimal amounts of catechin (peak 4) from the terminal subunits were detected in saskatoon fruit over development (**Table 4.1**). Interestingly, the presence of epigallocatechin in the PA extension subunits was detected only in ‘Thiessen’ fruits, and it occurred at all developmental stages studied (**Table 4.1**). Epigallocatechin has 3 hydroxyl groups attached to the B-ring, where as epicatechin has two (refer to **Figure 2.4**). This suggests that both B-ring hydroxylases, flavonoid 3'-hydroxylase (F3'H, responsible for producing B-rings with 2 hydroxyl groups attached) and flavonoid 3'5'-hydroxylase (F3'5'H, responsible for producing B-rings with 3 hydroxyl groups attached) (Winkel-Shirley, 2001; **Figure 2.7**), are present in ‘Thiessen’ fruits, where only F3'H is active in the other cultivars studied. PA concentration (mg per 100 g fresh fruit weight) was higher during early fruit development and decreased as the fruit

ripened in the saskatoon cultivars studied (**Table 4.1; Figure 4.5**). Similar PA accumulation patterns were observed over fruit development in bilberry (Jaakola et al., 2002), strawberry (Halbwirth et al., 2006), and grape (Kennedy et al., 2001). As supported by flavonoid gene expression data in blueberry fruits over development (see Chapter 5), a likely scenario is that PA synthesis is limited to the early fruit developmental stages of saskatoon fruits, resulting in decreasing PA concentration as the fruit matures. The average PA polymer length (mDP) was relatively constant at 5-10 among the cultivars and over fruit development (**Table 4.1**). PA composition and concentration of the white-fruited mutant 'Altaglo' was similar to that of the pigmented cultivars (**Table 4.1**), suggesting that PA synthesis is not affected by the mutations.

Table 4.1: A developmental profile of saskatoon fruit PA subunit composition following phloroglucinolysis of cultivars Altagro, Honeywood, Northline, Pembina, and Thiessen.

| Sample | EGC-P | C-P | EC-P | A ₂ -P | C | EC | A ₂ | mDP | Total PA ^a |
|--------------------|-----------------|------------------------|------------|-------------------|-----------|------------|----------------|-----------|-----------------------|
| 'Altagro' | | | | | | | | | |
| Stage 4 | nd ^b | 1.9 ± 0.1 ^c | 78.4 ± 0.2 | 4.9 ± 1.3 | 1.1 ± 0.1 | 11.9 ± 2.1 | 1.8 ± 0.4 | 6.8 ± 0.7 | 321.2 ± 66.5 |
| Stage 5 | nd | 1.9 ± 0.1 | 79.3 ± 3.6 | 3.1 ± 2.5 | 0.8 ± 0.1 | 13.7 ± 0.7 | 1.2 ± 0.4 | 6.4 ± 0.5 | 316.6 ± 93.7 |
| Stage 7 | nd | 2.0 ± 0.1 | 71.4 ± 0.2 | 8.3 ± 0.0 | 1.0 ± 0.0 | 14.5 ± 0.4 | 2.8 ± 0.3 | 5.5 ± 0.0 | 86.4 ± 28.8 |
| 'Honeywood' | | | | | | | | | |
| Stage 1 | nd | 1.1 ± 0.1 | 75.8 ± 0.9 | 8.3 ± 0.0 | 1.1 ± 0.0 | 11.6 ± 0.7 | 2.1 ± 0.2 | 6.8 ± 0.4 | 484.8 ± 45.7 |
| Stage 4 | nd | 1.1 ± 0.1 | 73.4 ± 1.9 | 8.6 ± 1.2 | 0.9 ± 0.1 | 13.1 ± 1.0 | 2.9 ± 0.3 | 6.0 ± 0.3 | 253.2 ± 51.2 |
| Stage 5 | nd | 1.4 ± 0.2 | 75.3 ± 0.6 | 6.8 ± 0.3 | 0.9 ± 0.0 | 13.0 ± 0.0 | 2.6 ± 0.1 | 6.1 ± 0.2 | 147.1 ± 7.4 |
| Stage 7 | nd | 1.2 ± 0.1 | 74.1 ± 1.1 | 8.9 ± 1.1 | 0.5 ± 0.3 | 11.4 ± 0.0 | 3.9 ± 0.4 | 6.4 ± 0.5 | 71.3 ± 5.4 |
| Stage 9 | nd | 1.3 ± 0.0 | 81.5 ± 2.0 | 2.9 ± 1.1 | 1.2 ± 0.1 | 9.5 ± 1.0 | 3.5 ± 0.0 | 7.0 ± 0.4 | 104.2 ± 15.0 |
| 'Northline' | | | | | | | | | |
| Stage 1 | nd | 0.1 ± 0.1 | 72.6 ± 7.4 | 11.1 ± 4.6 | 0.7 ± 0.3 | 12.5 ± 2.0 | 3.1 ± 1.1 | 6.7 ± 1.4 | 246.2 ± 138.8 |
| Stage 4 | nd | 0.7 ± 0.1 | 85.0 ± 0.8 | 2.4 ± 0.4 | 1.2 ± 0.0 | 9.1 ± 0.1 | 1.6 ± 0.1 | 8.4 ± 0.2 | 327.0 ± 11.0 |
| Stage 5 | nd | 0.4 ± 0.2 | 77.8 ± 3.4 | 6.8 ± 2.1 | 0.8 ± 0.4 | 11.4 ± 1.0 | 2.7 ± 0.5 | 6.9 ± 0.7 | 140.2 ± 35.1 |
| Stage 7 | nd | 0.6 ± 0.1 | 80.6 ± 4.1 | 5.7 ± 2.7 | 1.1 ± 0.1 | 8.4 ± 0.9 | 2.2 ± 0.4 | 7.7 ± 0.8 | 73.7 ± 20.0 |
| Stage 9 | nd | 0.7 ± 0.1 | 82.8 ± 2.8 | 5.2 ± 1.8 | 1.0 ± 0.0 | 8.2 ± 0.9 | 2.2 ± 0.2 | 8.8 ± 0.8 | 62.0 ± 16.1 |
| 'Pembina' | | | | | | | | | |
| Stage 1 | nd | 0.4 ± 0.0 | 80.8 ± 0.6 | 5.9 ± 0.3 | 0.9 ± 0.0 | 10.6 ± 0.1 | 1.6 ± 0.2 | 7.7 ± 0.2 | 436.5 ± 64.6 |
| Stage 4 | nd | nd | 66.9 ± 2.2 | 14.8 ± 0.9 | nd | 13.6 ± 1.0 | 4.6 ± 0.4 | 5.5 ± 0.4 | 72.2 ± 16.6 |
| Stage 5 | nd | nd | 64.8 ± 4.5 | 16.1 ± 2.4 | nd | 13.6 ± 1.1 | 5.5 ± 1.1 | 5.4 ± 0.6 | 64.7 ± 13.9 |
| Stage 7 | nd | nd | 58.7 ± 5.2 | 18.1 ± 2.6 | nd | 17.5 ± 2.1 | 5.8 ± 0.9 | 4.5 ± 0.6 | 17.7 ± 4.5 |
| Stage 9 | nd | nd | 63.4 ± 0.7 | 18.2 ± 0.3 | nd | 13.0 ± 1.3 | 5.4 ± 0.3 | 5.4 ± 0.3 | 27.1 ± 0.1 |
| 'Thiessen' | | | | | | | | | |
| Stage 1 | 2.3 ± 0.4 | 1.0 ± 0.0 | 80.9 ± 0.3 | 2.5 ± 0.1 | 0.9 ± 0.0 | 11.8 ± 0.4 | 0.6 ± 0.1 | 7.5 ± 0.2 | 414.4 ± 83.8 |
| Stage 4 | 1.5 ± 0.8 | 1.4 ± 0.1 | 76.0 ± 1.6 | 5.7 ± 1.1 | 0.9 ± 0.0 | 13.0 ± 0.6 | 1.5 ± 0.6 | 6.5 ± 0.5 | 243.1 ± 5.0 |
| Stage 5 | 1.8 ± 0.2 | 1.2 ± 0.1 | 75.6 ± 0.9 | 7.3 ± 0.4 | 0.9 ± 0.1 | 12.0 ± 0.3 | 1.3 ± 0.2 | 7.1 ± 0.3 | 126.7 ± 21.7 |
| Stage 7 | 1.6 ± 0.9 | 1.4 ± 0.1 | 77.2 ± 2.8 | 6.2 ± 2.2 | 0.8 ± 0.1 | 11.2 ± 0.7 | 1.6 ± 0.7 | 7.5 ± 0.7 | 103.5 ± 12.7 |
| Stage 9 | 3.8 ± 1.5 | 0.7 ± 0.7 | 83.0 ± 1.8 | 2.4 ± 0.9 | 0.4 ± 0.4 | 9.3 ± 0.4 | 0.6 ± 0.1 | 9.7 ± 0.1 | 108.1 ± 12.7 |

^a Total PA content in mg per 100 g fresh fruit weight.^b nd, not detected.^c Value of proportional composition (mole %). Data are means ± SE, n=2 to 4.EGC-P, epigallocatechin-(4β→2)-phloroglucinol; C-P, catechin-(4α→2)-phloroglucinol; EC-P, epicatechin-(4β→2)-phloroglucinol; C, catechin; A₂-P, A₂ phloroglucinol; EC, epicatechin; mDP, mean degree of polymerization.

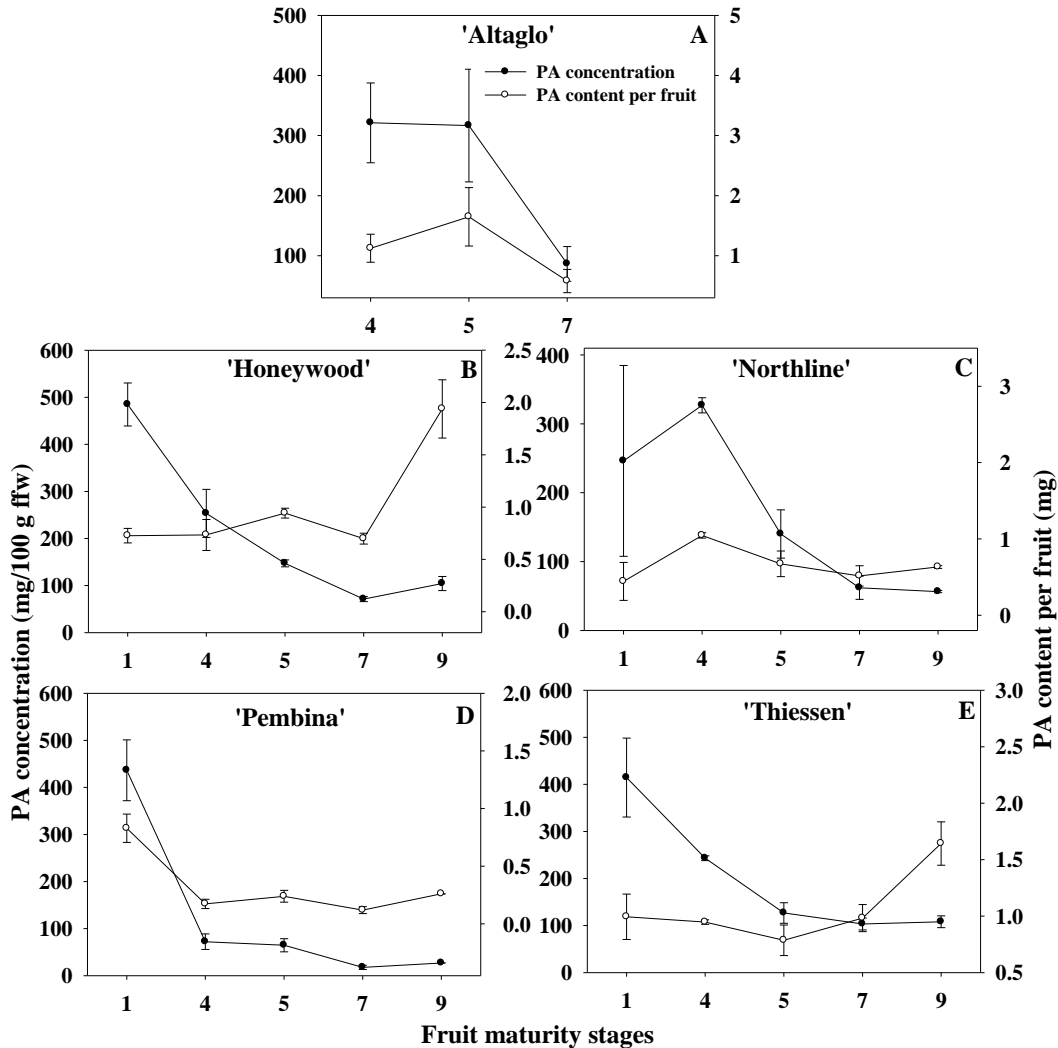


Figure 4.5: PA content in saskatoon fruit expressed as mg per 100 gram fresh weight and mg per fruit over fruit development (A, 'Altaglio'; B, 'Honeywood'; C, 'Northline'; D, 'Pembina'; E, 'Thiessen'). Data are means \pm SE, n=2 or 4.

The phloroglucinolysis reaction products of PAs from saskatoon fruits were further characterized by LC-MS/MS analysis. Saskatoon fruit C-P (RP-HPLC peak 2) and EC-P (RP-HPLC peak 3) had similar retention times, the same molecular ion mass of 413, and similar fragment ions as these compounds in the grape skin and cranberry fruit PA standards (Table 4.2). A₂-P (RP-HPLC peak 5) had the same retention time, molecular ion mass of 699, and fragment ions as this compound in the cranberry fruit standard (Table 4.2), and these data are

consistent with the RP-HPLC, positive ion mode LC-MS, and NMR analysis data for A₂-P for this cranberry fruit extract (Koerner et al., 2009). A₂ (HPLC peak 8) had the same retention time, molecular ion mass of 575, and fragment ions as this compound in the cranberry fruit standard (**Table 4.2**). Possible A₂-P and A₂ ion fragmentation patterns in negative ion mode LC-MS are presented in **Figure 4.6** according to the major fragment ions we have observed (**Table 4.2**).

Table 4.2: Characterization of proanthocyanidin phloroglucinolysis products of ‘Northline’ stage 1 saskatoon fruits, and cranberry fruit and grape skin standards by LC-MS.

| Compound | t _R ^a (min) | Sample | [M-H] ^b | Fragment ions |
|-------------------|-----------------------------------|-------------------------|--------------------|-------------------------|
| EC-P | 23.8 | ‘Northline’ | 413 | 287, 261, 175 |
| | 23.6 | Grape skin ^c | 413 | 287, 261, 175 |
| | 23.7 | Cranberry ^d | 413 | 287, 261, 217, 161, 133 |
| C-P | 22.6 | ‘Northline’ | 413 | 287, 261, 217 |
| | 22.6 | Grape skin | 413 | 287, 261, 217, 161, 133 |
| | 21.9 | Synthesized | 413 | 287, 261, 217, 161 |
| A ₂ -P | 32.3 | ‘Northline’ | 699 | 547, 411, 285 |
| | 32.3 | Cranberry | 699 | 547, 411, 287, 133 |
| Epicatechin | 45.5 | ‘Northline’ | 289 | 245, 137 |
| | 45.5 | Cranberry | 289 | 245, 137 |
| | 45.5 | Grape skin | 289 | 245, 217, 137 |
| Catechin | 34.7 | ‘Northline’ | 289 | 245, 217, 137 |
| | 34.7 | Grape skin | 289 | 245, 161, 137 |
| | 34.7 | Cranberry | 289 | 245, 217, 137 |
| A ₂ | 33.2 | Standard | 289 | 245, 137 |
| | 53.3 | ‘Northline’ | 575 | 539, 445, 423, 285, 133 |
| | 53.2 | Cranberry | 575 | 445, 423, 285, 163 |

^a Retention time; The blueberry, grape skin, and cranberry samples were run at different times leading to some variation in RT between the same compounds in the different samples.

^b MS was run in the negative mode and all the molecular ions are [M-H]⁻.

^c The grape skin PA sample was processed as described by Kennedy and Taylor (2003), fraction 5 was used (eluent from the solvent system consisting of [v/v/v] 20% acetone, 65% methanol, 15% water with the solvent-water mixture containing 0.2% formic acid [v/v]).

^d The cranberry PA sample was processed as described by Koerner et al. (2009). EC-P, epicatechin-(4β→2)-phloroglucinol; C-P, catechin-(4α→2)-phloroglucinol; A₂-P, A₂-phloroglucinol.

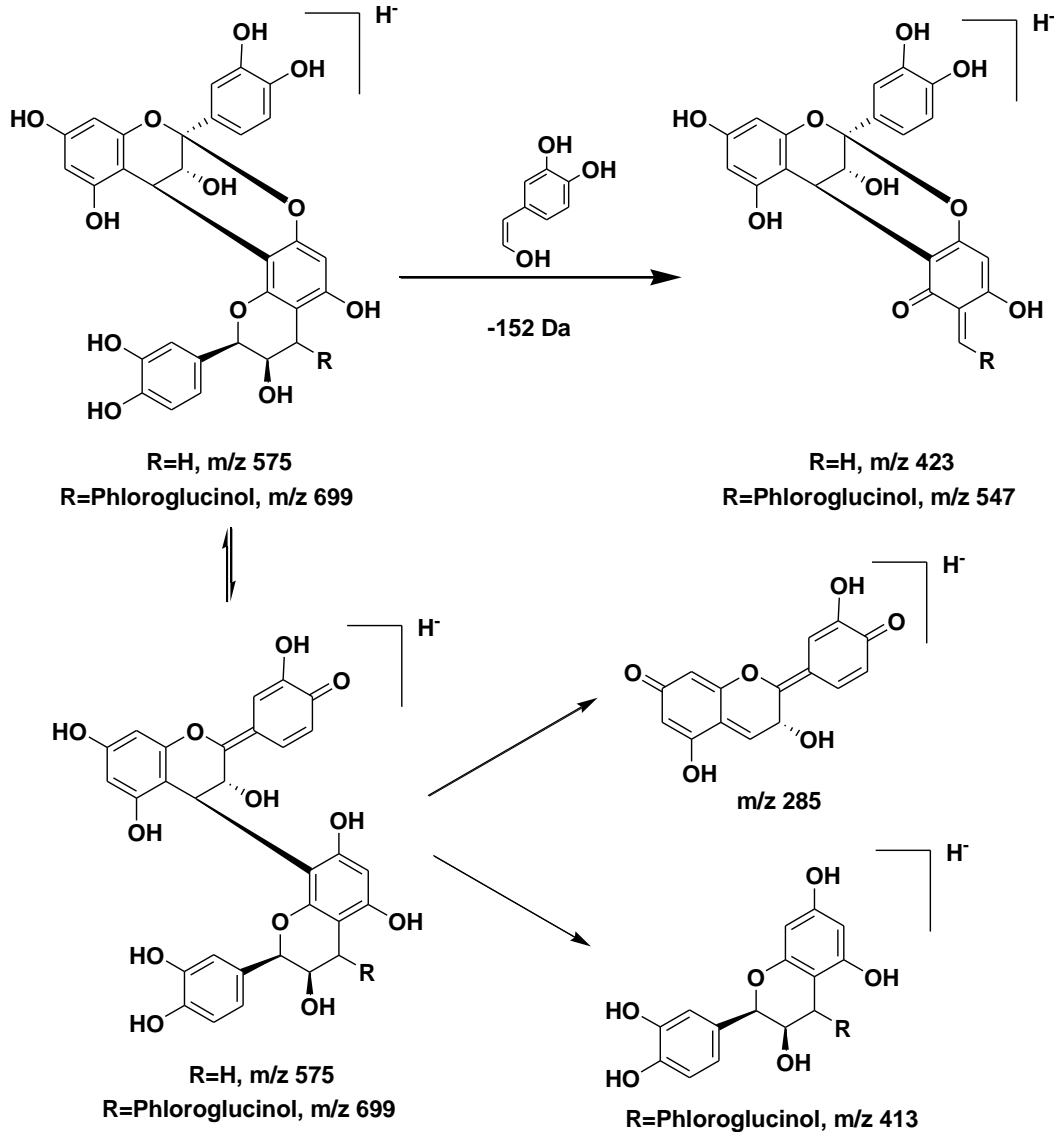


Figure 4.6: Possible fragmentation patterns of A_2 -P and A_2 in a negative ion mode LC-MS system. Modified from Koerner et al. (2009) and Li and Deinzer (2007).

Localization of PAs in saskatoon fruits

‘Altagro’ fruits contain PA levels that are similar to these in the pigmented-fruit cultivars (**Table 4.1**), but the fruits do not accumulate high levels of anthocyanins in the later stages of development. Therefore, PA localization in saskatoon fruits was performed in ‘Altagro’ fruits to avoid anthocyanin interference in the later stages of fruit development. After DMACA staining, PAs

become blue to dark-blue in colour (**Figure 4.7**). PAs accumulated in all the fruit tissues of stage 1 fruit (**Figure 4.7 A and B**), with intense staining in the exocarp, seed coat, and placental tissues. As the fruit continue to develop (by stage 4), PAs mainly accumulated in the hypodermal layer of the exocarp, vascular bundles in mesocarp, placenta tissues, and seed coat tissues (**Figure 4.7 C and D**). At fruit maturity (stage 9), blue staining still can be clearly observed in the exocarp, placenta, and seed coat tissues (**Figure 4.7 E**). However, the total amount of tissue staining for PAs was substantially reduced in the maturing fruit (**Figure 4.7 E**), consistent with lower PA content in the ripening stage of fruits (**Table 4.1**). Interestingly, in the cells of the placental tissue of stage 1 fruits, small vesicle-like structures that stain dark-blue for the presence of PA can be observed (**Figure 4.7 F**). Small PA vesicles have been observed via transmission electron microscopy (TEM) in the endothelial cells of *tds4-1* mutant seeds (Abrahams et al., 2003). It has been suggested that small PA containing vesicles fuse together to form a big PA containing vacuole. In young seed coats (stage 1), PAs are mainly localized intercellularly in the cells of the inner-most cell layer of the seed coat, around the vascular bundle, and in the hypodermal layers of the seed coat (**Figure 4.8 A**). At seed maturity, the PAs in the seed coat hypodermal cell layers were relocated to the cell wall region and/or intracellularly adjacent to the cell wall (**Figure 4.8 B**), similar to that observed for flavonols (**Figure 3.8**). Additionally, a perisperm layer (residual endosperm) was observed in mature saskatoon seeds (**Figure 4.8 B**).

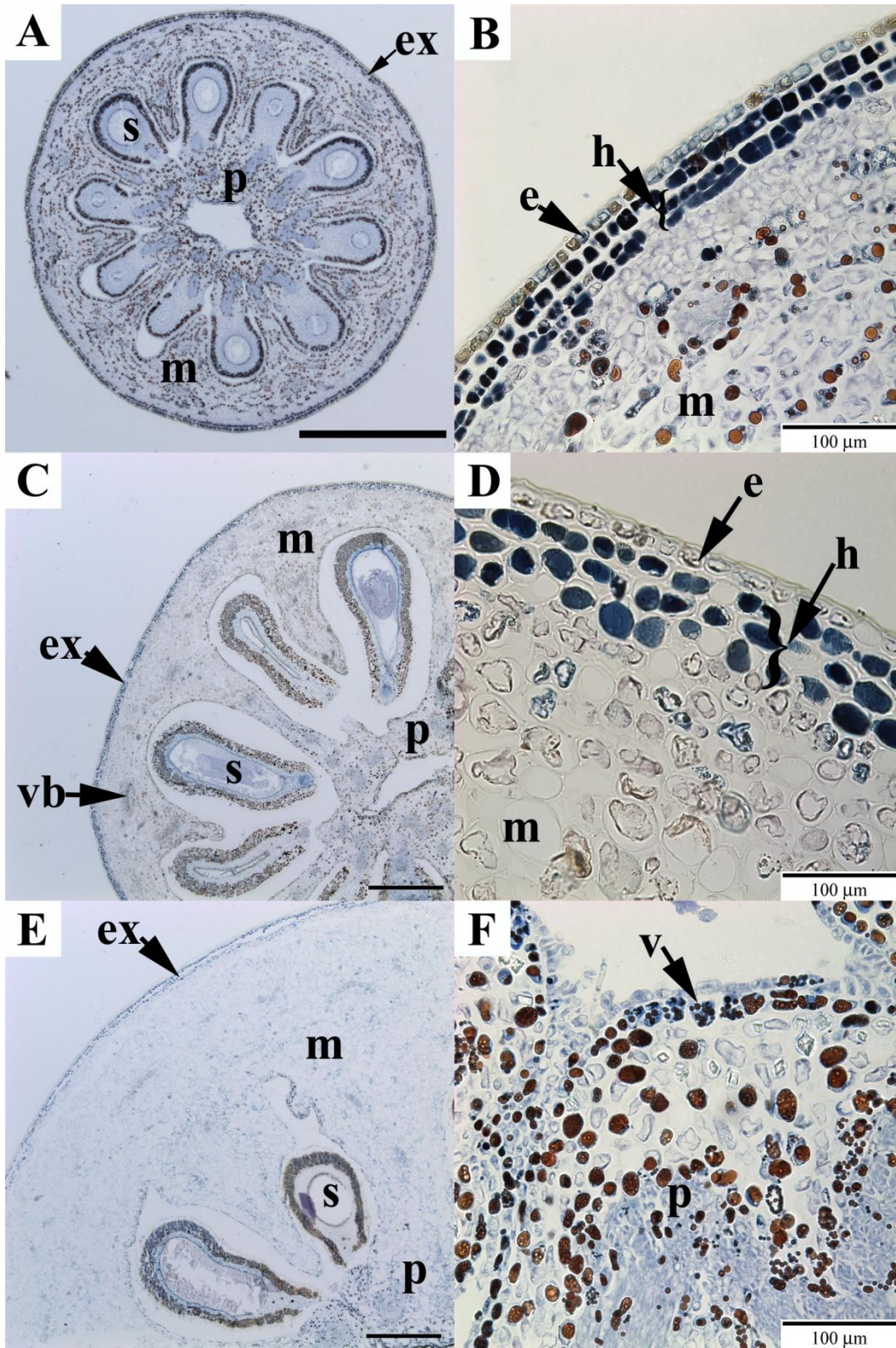


Figure 4.7: Light microscopic images of ‘Altglo’ Saskatoon fruit cross-sections stained with DMACA for PA visualization. (A) stage 1 fruit; (B) stage 1 exocarp

and mesocarp at $40\times$ magnification; (C) stage 4 fruit; (D) stage 4 exocarp and mesocarp at $40\times$ magnification; (E) stage 9 fruit; (F) stage 1 placenta at $40\times$ magnification. Scale bars in A, C, and E are 1 mm. e, epidermis; en, endosperm; ex, exocarp (including cuticle, epidermis, and hypodermis); h, hypodermis; m, mesocarp; p, placenta; s, seed; v, pre-vesicle; vb, vascular bundle.

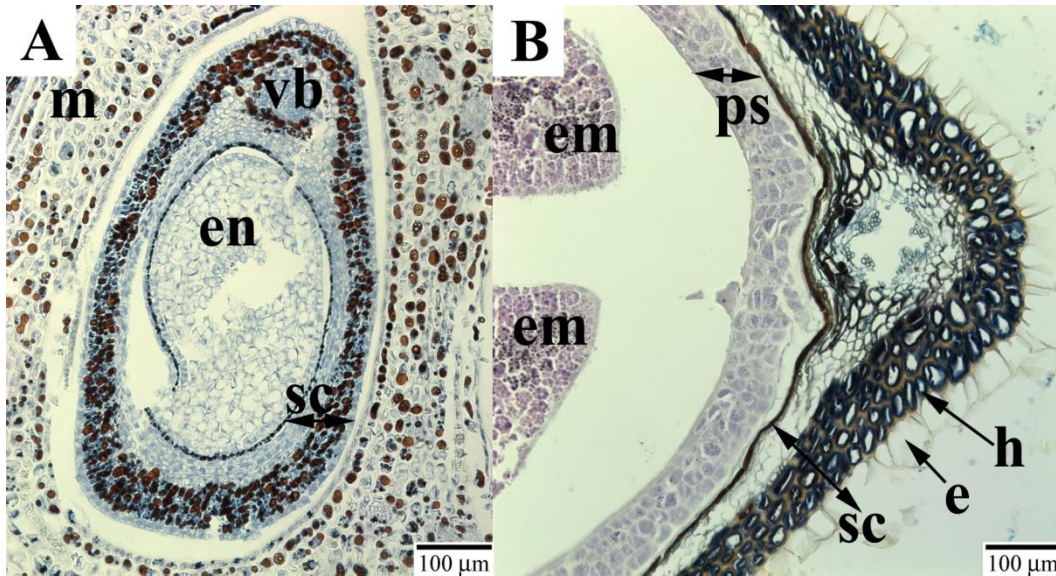


Figure 4.8: Light microscopic images of ‘Pembina’ Saskatoon seed cross-sections stained with DMACA for PA visualization. (A) stage 1 seed at $20\times$ magnification; (B) stage 7 seed at $20\times$ magnification. sc, seed coat; em, embryo; en, endosperm; ps, perisperm; vb, vascular bundle; m, mesocarp; e, epidermis; h, hypodermis.

Conclusions

PA composition varied among cultivars, including variation in the abundance of A-type linkages in the PA polymers, and the presence of epigallocatechin in the PA extension units of only one cultivar. The PA localization and characterization data suggest that PA synthesis and accumulation is tightly regulated over Saskatoon fruit development. PA accumulation profiles were similar to that of flavonols (Chapter 3), suggesting that PAs and flavonols are likely produced early in fruit development and that they are stored in cells of specific fruit tissues throughout development. PAs and flavonols in general localized to similar tissues

throughout development with the exception that only flavonols were detected in the cuticle layer of mature fruit. This suggests that they have overlapping roles in providing protection to the fruit and seed structures, and that they are both important for the reproductive strategy of saskatoons.

Literature cited

- Abrahams S, Lee E, Walker AR, Tanner GJ, Larkin PJ, Ashton AR** (2003) The *Arabidopsis TDS4* gene encodes leucoanthocyanidin dioxygenase (LDOX) and is essential for proanthocyanidin synthesis and vacuole development. *Plant Journal* **35**: 624-636
- Aron PM, Kennedy JA** (2008) Flavan-3-ols: Nature, occurrence and biological activity. *Molecular Nutrition & Food Research* **52**: 79-104
- Bagchi D, Bagchi M, Stohs SJ, Das DK, Ray SD, Kuszynski CA, Joshi SS, Pruess HG** (2000) Free radicals and grape seed proanthocyanidin extract: importance in human health and disease prevention. *Toxicology* **148**: 187-197
- Bakowska-Barczak AM, Kolodziejczyk P** (2008) Evaluation of saskatoon berry (*Amelanchier alnifolia* Nutt.) cultivars for their polyphenol content, antioxidant properties, and storage stability. *Journal of Agricultural and Food Chemistry* **56**: 9933-9940
- Foo LY, Lu YR, Howell AB, Vorsa N** (2000) A-type proanthocyanidin trimers from cranberry that inhibit adherence of uropathogenic P-fimbriated *Escherichia coli*. *Journal of Natural Products* **63**: 1225-1228
- Foo LY, Newman R, Waghorn G, McNabb WC, Ulyatt MJ** (1996) Proanthocyanidins from *Lotus corniculatus*. *Phytochemistry* **41**: 617-624
- Gu LW, Kelm MA, Hammerstone JF, Beecher G, Holden J, Haytowitz D, Prior RL** (2003) Screening of foods containing proanthocyanidins and their structural characterization using LC-MS/MS and thiolytic degradation. *Journal of Agricultural and Food Chemistry* **51**: 7513-7521
- Gutmann M, Feucht W** (1991) A new method for selective localization of flavan-3-Ols in plant-tissues involving glycolmethacrylate embedding and microwave irradiation. *Histochemistry* **96**: 83-86

- Halbwirth H, Puhl I, Haas U, Jezik K, Treutter D, Stich K** (2006) Two-phase flavonoid formation in developing strawberry (*Fragaria x ananassa*) fruit. *Journal of Agricultural and Food Chemistry* **54**: 1479-1485
- Hellstrom J, Sinkkonen J, Karonen M, Mattila P** (2007) Isolation and structure elucidation of procyanidin oligomers from saskatoon berries (*Amelanchier alnifolia*). *Journal of Agricultural and Food Chemistry* **55**: 157-164
- Jaakola L, Maatta K, Pirttila AM, Torronen R, Karenlampi S, Hohtola A** (2002) Expression of genes involved in anthocyanin biosynthesis in relation to anthocyanin, proanthocyanidin, and flavonol levels during bilberry fruit development. *Plant Physiology* **130**: 729-739
- Kennedy JA, Hayasaka Y, Vidal S, Waters EJ, Jones GP** (2001) Composition of grape skin proanthocyanidins at different stages of berry development. *Journal of Agricultural and Food Chemistry* **49**: 5348-5355
- Kennedy JA, Jones GP** (2001) Analysis of proanthocyanidin cleavage products following acid-catalysis in the presence of excess phloroglucinol. *Journal of Agricultural and Food Chemistry* **49**: 1740-1746
- Kennedy JA, Taylor AW** (2003) Analysis of proanthocyanidins by high-performance gel permeation chromatography. *Journal of Chromatography A* **995**: 99-107
- Koerner JL, Hsu VL, Lee JM, Kennedy JA** (2009) Determination of proanthocyanidin A2 content in phenolic polymer isolates by reversed-phase high-performance liquid chromatography. *Journal of Chromatography A* **1216**: 1403-1409
- Lee JM, Kennedy JA, Devlin C, Redhead M, Rennaker C** (2008) Effect of early seed removal during fermentation on proanthocyanidin extraction in red wine: A commercial production example. *Food Chemistry* **107**: 1270-1273
- Lee YA, Cho EJ, Yokozawa T** (2008) Effects of proanthocyanidin preparations on hyperlipidemia and other biomarkers in mouse model of type 2 diabetes. *Journal of Agricultural and Food Chemistry* **56**: 7781-7789
- Li HJ, Deinzer ML** (2006) Structural identification and distribution of proanthocyanidins in 13 different hops. *Journal of Agricultural and Food Chemistry* **54**: 4048-4056
- Li HJ, Deinzer ML** (2007) Tandem mass spectrometry for sequencing proanthocyanidins. *Analytical Chemistry* **79**: 1739-1748

- O' Brien TP, McCully ME** (1981) The study of plant structure: Principles and selected methods. Termarcarphi, Melbourne, Australia
- St-Pierre RG** (1997) Growing saskatoons - a manual for orchardists. Fifth edition. Department of Horticulture Science, University of Saskatchewan, Saskatoon, SK. 338 pp.
- St-Pierre RG, Zatylny AM, Tulloch HR** (2005) Evaluation of growth and fruit production characteristics of 15 saskatoon (*Amelanchier alnifolia* Nutt.) cultivars at maturity. Canadian Journal of Plant Science **85**: 929-932
- Winkel-Shirley B** (2001) Flavonoid biosynthesis. A colourful model for genetics, biochemistry, cell biology, and biotechnology. Plant Physiology **126**: 485-493

Chapter 5

Gene expression and metabolite profiling of developing highbush blueberry (*Vaccinium corymbosum* L.) fruit indicates transcriptional regulation of flavonoid metabolism and ripening-associated activation of abscisic acid metabolism¹

Introduction

Highbush blueberry (*Vaccinium corymbosum* L.; Ericaceae) is one of the most economically important fruit crops in North America. Blueberry fruit have been the focus of much recent attention due to numerous reports of their positive effects on human health. These benefits are generally attributed to high level of polyphenolics, in particular the flavonoids, which act as potent antioxidants (Rasmussen et al., 2005). Highbush blueberries have one of the highest *in vitro* antioxidant capacities of any fruit or vegetable (Prior and Gu, 2005; Wu et al., 2006). The major health benefits linked to consumption of blueberries include a reduced risk for cardiovascular (Basu et al., 2010) and neurodegenerative diseases (Neto, 2007). Furthermore, experiments on rodents suggest that blueberry extracts may also prevent cancer, slow tumor growth, and reverse cognitive and behavioral deficits related to strokes and aging (Lau et al., 2005; Gordillo et al., 2009).

The three common types of flavonoids that accumulate in blueberry fruit are the flavonols, anthocyanins and proanthocyanidins (PAs, also known as condensed tannins). Flavonols are thought to function primarily as protective chemicals against UV-B light in fruit skin (Solovchenko and Schmitz-Eiberger, 2003), but they can also be found in the seed coat (Lepiniec et al., 2006). Ripe blueberries contain quercetin- and myricetin-type flavonols (**Figure 5.1**; Hakkinen et al., 1999). Anthocyanins are flavonoid pigments which give rise to

¹ A version of this chapter has been submitted to the journal 'Plant Physiology' on May 31, 2011 with the following authorship:

Michael Zifkin^a, Alena Jin^a, Jocelyn A. Ozga^b, L. Irina Zaharia, Johann P. Scherthner, Suzanne R. Abrams, James A. Kennedy, C. Peter Constabel^b.

^a These authors contributed equally to this work.

^b These authors are co-corresponding authors.

the red and blue colours of many ripe fruit, which attract frugivores that help disperse seeds (Wilson and Whelan, 1990). The predominant anthocyanins in blueberry are glycosides of delphinidin, cyanidin, peonidin, petunidin, and malvidin (**Figure 5.1**; Prior et al., 2001). The PAs are oligomers and polymers of flavan-3-ols. They are most common in woody plants but can also be found in herbaceous species, and are thought to contribute to defense and stress resistance. In fruit, they are often present in the seed coat, where they function as protectants against desiccation and premature germination (Debeaujon et al., 2000). PAs are also found in the immature fruits, where their astringency and bitterness helps deter frugivores from consuming fruit before they are ripe (Sanoner et al., 1999). The PAs of ripe blueberry fruit are primarily composed of the flavan-3-ol epicatechin, linked *via* a B-type configuration (**Figure 5.1**; Prior et al., 2001; Hosseinian et al., 2007). However, to date little detailed information on blueberry PA and flavonoid structure is available, including tissue specificity and timing of accumulation during fruit development.

Most of the genes and enzymes involved in flavonoid biosynthesis were discovered and characterized in model plants such as *Arabidopsis*, maize and petunia (Lepiniec et al., 2006), but have not yet been investigated in blueberry. Entry into the flavonoid pathway from general phenylpropanoid metabolism is controlled by chalcone synthase (CHS), which condenses *p*-coumaroyl-CoA and three malonyl-CoAs into a chalcone, followed by isomerization by chalcone isomerase (CHI) to form a flavanone (**Figure 5.1**). This intermediate is subsequently hydroxylated by flavanone-3 β -hydroxylase (FHT) to dihydroflavonol. It is further converted to flavonols *via* flavonol synthase (FLS), or reduced by dihydroflavonol reductase (DFR) to leucocyanidins, key intermediates for PAs and anthocyanins. Hydroxylation at the 3' and 5' positions of the B-ring can occur *via* activity of cytochrome P450-dependent flavonoid hydroxylases (**Figure 5.1**; F3'H and F3'5'H), respectively giving rise to di- and tri-hydroxylated B-ring variants of different flavonoid types. In some species such as petunia, F3'5'H also requires a specific cytochrome *b*₅ for optimal activity (de Vetten et al., 1999). The anthocyanidin flavynium ion is produced by

anthocyanidin synthase (ANS), then glycosylated by UDP-glucose: flavonoid-3-*O*-glycosyltransferases (UGFT). Methylation of the 3' and 5' hydroxyl groups of anthocyanins gives rise to peonidin, malvidin and petunidin (**Figure 5.1**). An increased number of B-ring hydroxyl group shifts anthocyanin colour towards the blue, whereas methylation has the opposite effect; free hydroxyls also increase their *in vitro* antioxidant activity (Halbwirth, 2010). Anthocyanidins can be diverted into PA synthesis via anthocyanidin reductase (ANR), which produces epicatechin-type flavan-3-ols (**Figure 5.1**). By contrast, it is thought that catechin-type flavan-3-ols are produced from leucocyanidins by leucoanthocyanidin reductase (LAR) (Tanner et al., 2003). PA precursors are actively moved into the vacuole by MATE transport proteins, where they are polymerized via an as yet unknown mechanism (Zhao et al., 2010). PAs can range in length from two to over 30 units, which are most commonly joined in a B-type orientation, but can also be linked in other configurations including A-type linkages (**Figure 5.1**).

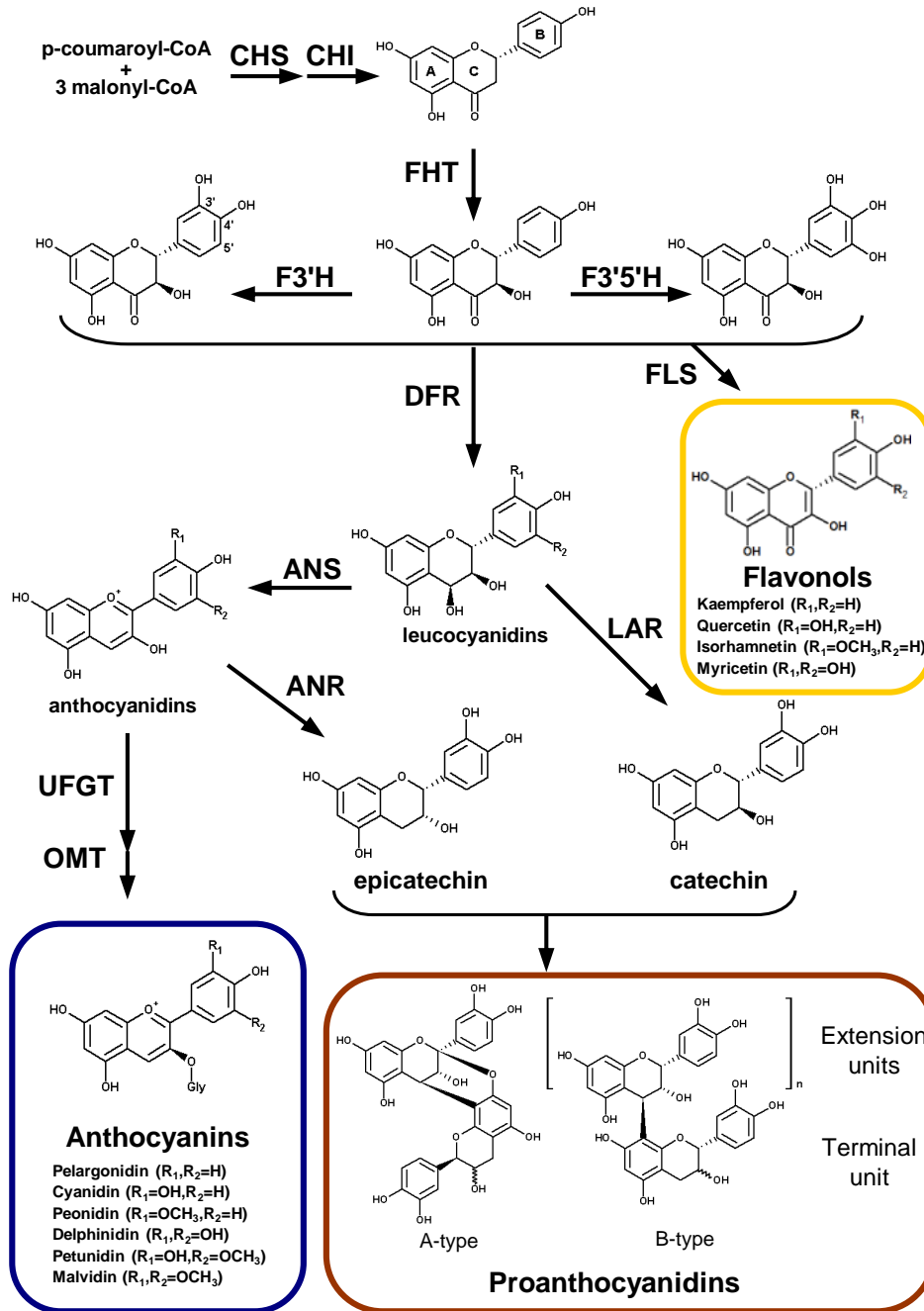


Figure 5.1: General flavonoid biosynthesis pathway leading to flavonols, anthocyanins and proanthocyanidins (PAs). The most common flavonol aglycones and anthocyanins and basic PA linkage types are shown, along with key biosynthetic enzymes. CHS, chalcone synthase; CHI, chalcone isomerase; FHT, flavanone-3 β -hydroxylase; F3'H, flavonoid 3'-hydroxylase; F3'5'H, flavonoid 3'5'-hydroxylase; DFR, dihydroflavonol reductase; FLS, flavonol synthase; ANS, anthocyanidin synthase; LAR, leucoanthocyanidin reductase; ANR, anthocyanidin reductase; UFGT, UDP-glucose:flavonoid-3-*O*-glycosyltransferase; OMT, anthocyanin-*O*-methyltransferase.

Flavonoid synthesis in plants is typically controlled at the transcriptional level by the tissue-specific expression of key transcription factors belonging to the R2R3-MYB, basic helix-loop-helix (bHLH), and WD-repeat protein families (Lepiniec et al., 2006). MYB-bHLH-WDR (MBW) complexes have been shown to be responsible for the regulation of anthocyanins, PAs, and flavonol biosynthesis in a variety of species and tissues including flowers and fruit, with the MYB protein usually providing specificity (Allen et al. 2008; Dubos et al. 2010). Plant MYB gene families are large, with over 126 and 108 genes in *Arabidopsis* and grape, respectively (Dubos et al. 2010). In grape, VvMYBA1 controls anthocyanin accumulation (Kobayashi et al., 2002), whereas at least two other MYBs (VvMYBPA1 and VvMYBPA2) contribute to PA synthesis (Bogs et al., 2007; Terrier et al., 2009). PA-specific MYB regulators have also been described from persimmon (*Diospyrus kaki*) (Akagi et al., 2009b; Akagi et al., 2010) fruit with unusually high PA levels. These studies suggest that a network of MYBs with overlapping specificities is involved in fruit flavonoid synthesis.

The biosynthesis and accumulation of flavonoids and pigments is only one aspect of a complex suite of metabolic changes which occur during fruit maturation. The development and ripening of blueberry fruit is complex and occurs in two main phases: a growth phase characterized by a rapid increase in size, followed by a ripening phase. This second phase begins when seeds have reached maturity; the fruit become soft, blue and edible, with enhanced sugar content, reduced acidity and astringency. In climacteric fruit such as tomato, the ripening phase is marked by an ethylene-mediated respiratory burst. By contrast, in non-climacteric fruit such as grape, cherry, and blueberry, ethylene does not appear to play a prominent role, suggesting the potential involvement of other growth regulators (Coombe and Hale, 1973). An intriguing candidate is abscisic acid (ABA), which accumulates sharply at ripening initiation in cherries and grapes (Coombe and Hale, 1973; Kondo and Inoue, 1997). In grape, this rise is associated with a dramatic activation of ABA-related gene expression (Deluc et al., 2009). Application of ABA to cherries and grapes hastens ripening and increases anthocyanin and sugar content (Kondo and Inoue, 1997; Peppi et al.,

2008), and can modestly enhance flavonol levels (Koyama et al., 2009). Despite similarities to cherries and grapes, however, for blueberry there are no reported studies of ABA and its relation to flavonoid accumulation and ripening.

In order to determine how flavonoid synthesis is regulated during development and ripening of blueberry fruit, we undertook a molecular, biochemical, and histological characterization of flavonoid biosynthesis. We also measured ABA and its catabolites, and quantified a key ABA biosynthesis transcript, to compare kinetics of this growth regulator to the ripening process and flavonoid profiles.

Materials and Methods

Plant material and developmental staging criteria

Highbush blueberry (*Vaccinium corymbosum* L. cv. Rubel) tissue was harvested from an organic blueberry farm (Sweet Briar Farm) near Victoria, British Columbia, Canada during the 2006-2010 growing seasons. Fruits were selected from multiple plants and sorted into an eight stage system reflecting berry development, which was based on size and appearance, following validated methods for other small fruit (Ozga et al., 2006). There were two key phases of fruit growth during each season from which fruits were collected. Fruits from the first phase were sorted into five stages primarily based on size (Stage 1-5), as described in Results. Collection dates were 18 Jun 2007, 20 Jun 2008, 9-12 Jun 2009 and 3 Jun 2010. Fruits in the second phase (Stage 6-8) were sorted by texture and colour, as described in Results. Collection dates were 13 July 2006, 27 Aug 2008, 28 July 2009 and 9 August 2010. Floral buds, flowers and ovaries were also collected. Two stages of floral ovary development were prepared by removing and discarding non-fruit forming floral bud and flower tissue (stigma, style, petals, stamens) from the ovary and calyx. All tissue was frozen on site in liquid N₂ and stored at -80°C until use.

cDNA library construction and EST sequencing

Total RNA was isolated from fruits harvested in 2006 from two separate pools of tissue (stage 5/6, and stage 7/8) using the protocol from Jaakola et al. (2001). PolyA⁺ RNA was isolated using Dynabeads OligodT₂₅ (DynaL A.S., Oslo, Norway) according to the manufacturer's instructions. First strand cDNA synthesis was carried out using Superscript III reverse transcriptase (Invitrogen, Burlington, ON, Canada) according to the manufacturer's protocol with some variations. Briefly, 5 µg PolyA⁺ RNA were primed with 200 pmol attB2Sfi-T20 (AGAGAGGCCCGCCTCGGCCACCACTTTGTACAAGAAAGCTGGGCT₂₀VN) primer at 68°C for 5 minutes. Kit reagents were then added and the reaction was sequentially incubated at 37 °C for 30 min, 45°C for 30 min, and 50°C for 10 min. Second strand synthesis was carried out according to the manufacturer's (Invitrogen) protocol. Following second strand synthesis, the cDNA was blunt-ended for adapter ligation using T4 polymerase (New England Biolabs, Mississauga, ON, Canada) and incubated for 15 minutes at 16°C. The reaction was cleaned up by phenol/chloroform extraction and the DNA precipitated using Poly dA (Roche Diagnostics, Laval, QC, Canada) following the manufacturer's instructions. cDNA quality was assessed by agarose gel electrophoresis. For cDNA library construction, the oligonucleotides attB1-SfiIC-s (AGGCCTACAAGTTTGTACAAAAAAGCAGGCTCTTC) and attB1-SfiIC-as (GAAGAGCCTGCTTTTTTGTACAACTTGTAGGCCTAAA) were first annealed to give adapter attB1-Sfi. 240 pmoles of this adapter were added to 20 µl of second strand DNA and ligated using T4 ligase (Fermentas). The reaction was incubated overnight at 16°C, treated with phenol/chloroform and the DNA ethanol precipitated. The DNA was digested with Sfi I restriction enzyme (New England Biolabs) and following cleanup the cDNA was size separated on a 1% low-melting agarose gel into four size fractions. The gel slices were digested with Agarase (New England Biolabs) and the DNA precipitated according to the manufacturer's protocol. Plasmid pHelix1(+) (Roche Diagnostics) was modified to give pHSX-Ci by inserting an adapter between the Eco RI and Kpn I site that contains two Sfi I sites (ggccgcctcgcc: Sfi I-B and ggccatttagcc: Sfi I-C) to accommodate directional cloning of cDNA inserts. The cDNA fragments were

ligated into pHSX-Ci using T4 ligase, and the ligation mix was cleaned up using High Pure spin columns (Roche Diagnostics). Plasmids containing inserts were transformed into electro-competent DH10B *E. coli* cells (Invitrogen). The quality of the library was verified by plasmid extraction and digestion with Sfi I. The clones were sequenced at the National Research Council's Plant Biotechnology Institute (Saskatoon, SK, Canada).

Annotation and phylogenetic analysis of blueberry ESTs

EST sequences were cleaned, clustered and annotated as described in Nagel et al. (2008). Custom PERL scripts were written to assign Gene Ontology (GO) annotation based on top hits to The Arabidopsis Information Resource (TAIR) database. Blueberry flavonoid ESTs were identified and validated as described in Results. Neighbor-joining phylogenetic trees were constructed using *MEGA* version 4.0 (Tamura et al., 2007). Trees were constructed with the blueberry protein sequences and sequences from functionally characterized proteins of the same class. The tree construction parameters and accession numbers are provided in the figure captions.

RNA isolation and cDNA synthesis for qRT-PCR gene expression analysis

Protocols were designed to conform to the MIQE guidelines for real-time qRT-PCR experiments as much as possible (Bustin et al., 2009). To capture the average transcriptional state of a fruit throughout development, pooled fruits of a given stage were ground in liquid N₂ (100-150 fruits for stage 1-3; 45-80 stage 4-8). Sub-sample(s) of approximately 1 g tissue were aliquoted for RNA extraction. Total RNA was isolated from all tissues using the cetyl-trimethyl-ammonium bromide (CTAB) method originally designed for bilberry fruit, also high in phenolics and carbohydrates (Jaakola et al., 2001). The extraction buffer contained 2% CTAB, 0.3g g⁻¹ polyvinylpyrrolidone, 100 mM Tris-HCl (pH 8.0), 25 mM EDTA, 2.0 M NaCl, and 0.5 g L⁻¹ spermidine. RNA quality and purity was confirmed by denaturing agarose gel electrophoresis and A₂₆₀:A₂₈₀ absorbance ratios (typically 1.90-2.15) using a ND-1000 UV Nanodrop

spectrophotometer (Nanodrop Technologies). Yields ranged from approximately 25–108 $\mu\text{g g fwt}^{-1}$ for ovaries, S1 and S2 fruits, and 6–16 $\mu\text{g g fwt}^{-1}$ for large fruits (S3-S8). RNA was stored at -80°C in TE buffer (pH 7.0).

To remove genomic DNA, 3 μg RNA was DNase treated for 15 min at room temperature with 2-3 μl (2-3 U) Amplification Grade DNase I (Invitrogen) according to the manufacturer's instructions. The DNase was inactivated with 3 μl 25 mM EDTA (pH 8.0) at 65°C for 10 min. The RNA was precipitated overnight at -80°C with 1/9 vol. 3 M sodium acetate and 1 vol. isopropanol. The pellets were washed with 70% ethanol, air-dried, resuspended in Ultrapure water, and quality and purity assessed by Nanodrop $A_{260}:A_{280}$ absorbance ratios, typically 1.7-2.0.

Synthesis of cDNA was carried out using the Superscript II reverse transcriptase kit (Invitrogen) according to the manufacturer's protocol. For each sample, 1 μg total RNA was primed with 2 μl ($534 \mu\text{g mL}^{-1}$) anchored oligo(dT)₂₀VN primers (purchased from Alpha DNA, Montreal, Canada) and 1 μl of 10mM dNTP mix, and then reverse transcribed with 1 μl (200 U) Superscript II reverse transcriptase, without the optional addition of RNaseOUT. Controls for each sample that included RNA and all reagents except reverse transcriptase ('NRT') were included in the reverse transcription protocol to later determine the amount of gDNA contamination. All cDNAs were stored at -20°C .

Primer design

Primers (Alpha DNA) were designed for each gene (**Supplemental Table B5**) using Vector NTI Advance 9 (Invitrogen) according to the following criteria: 19-26 bp per primer, GC content of 40-60%, melting temperature (T_m) generally 60-65 $^{\circ}\text{C}$ (Nearest Neighbor method, Vector NTI settings: 660,000 pM probe concentration, 50 mM salt concentration), and T_m of forward and reverse primers within 3 $^{\circ}\text{C}$ of each other. The primers typically amplified a product of 100-150 bp, did not have a T or a GC run of ≥ 3 at the 3' end of primer, and had minimal or no predicted intra- and inter-primer complementarity, which was determined using Oligo Analyzer 1.2 software (Teemu Kuulasmaa, Finland).

Real time qRT-PCR

Real-time qRT-PCR was performed on an Mx3005p QPCR System (Stratagene) in a 96-well plate using the Quantitect SYBR Green PCR kit (Qiagen), 0.2 mL clear, flat-top 8-well strip caps (Axygen) and 0.2 mL clear, thin wall 8-well PCR strip tubes (Axygen). Each reaction contained 1 μ L of 1:20 diluted cDNA template (5 ng), 1 μ L of 10 μ M forward and reverse primers (667 nM), 7.5 μ L 2X Quantitect master mix (HotStarTaq DNA polymerase, dNTP mix, Sybr Green I dye, ROX reference dye and PCR buffer) and 4.5 μ L Quantitect nuclease-free water in a final volume of 15 μ L. The conditions for each PCR were as follows: 95°C for 15 min, followed by 40-45 cycles of 30 s at 94°C, 30 s at 58 or 60°C, and 30 s at 72°C. Based on results from serial dilution experiments, all primers performed better at 58°C than 55°C, while a few gave best results at 60°C (not shown). At the end of each experiment, a melt curve analysis was performed using the Mx3005p default parameters (60 s at 95°C, 30 s at 55-95°C in one degree increments, 30 s at 95°C), which yielded one peak for each set of primers at a temperature between 77 and 82°C, confirming the amplification of only a single product species during the runs. To further confirm primer specificity, multiple reactions were separated on 2% low-melting agarose gels for each primer set to verify the expected product length. For each gene at least one PCR product was purified and directly sequenced and/or cloned and then sequence-verified.

‘No reverse transcriptase’ (NRT) and ‘no template’ (NTC) controls were systematically included for each primer set to check for unwanted amplification from gDNA, primer dimers, and contamination. Each amplification plot was set to an R_n (ROX normalized) threshold of 0.05 to obtain quantification cycle (C_q) values. All reactions included at least one technical replicate, which typically did not differ by more than 0.2-0.5 C_q . Any plots that did not behave with expected PCR kinetics (rare) were culled. The NTC wells consistently recorded no signal or were at least $\geq 10 C_q$ above target signal. Some of the NRT wells gave signals despite DNase treatment, but the C_q was within 5 C_q of the NTC, indicating negligible levels of gDNA. A conservative absolute minimum limit of quantification (LOQ) threshold for all genes was set at 5 C_q below the lowest C_q

recorded in any of the NRT runs for a particular gene, following the suggestions of Bustin and Nolan (2004). The observable relative transcript abundances reported in the results are calculated from C_q values well above this $\Delta 5 C_q$ threshold.

Relative transcript abundance ratios were calculated using the modified equation $E_{\text{Ref}}^{(C_{q\text{ref}})}/E_{\text{GOI}}^{(C_{q\text{GOI}})}$ from Pfaffl (2001), where E is the efficiency of reaction for each primer set. *LinRegPCR* software version 11 (Ruijter et al., 2009) was used to calculate primer efficiency set taken from the initial log-linear phase of each amplification plot. Efficiencies for each primer set (**Supplemental Table B5**) were calculated by taking the mean of all genuine amplification plots of a given gene that fell within 10 % of the median efficiency. Efficiencies greater than 2.0 were set to 2.0 in the equation, according to Pfaffl (2004). The same efficiency was used for all calculations, as suggested by Peirson et al. (2003). Dilution series were also made for a number of the genes using 2008 pooled fruit cDNA to confirm that recorded C_q values from the experiments were within the linear dynamic range ($R^2 \geq 0.99$) and that efficiencies were consistent with the values calculated using the *LinRegPCR* program (not shown). The C_q value for the reference normalization factor (“Ref”) was calculated by taking the geometric mean of the two most stable reference genes (*VcSAND* and *VcGAPDH*). Reference genes were evaluated as described below.

Reference gene selection and optimization of qRT-PCR expression normalization

In the blueberry EST libraries, unigenes were found with high similarity to reference genes previously found stably expressed throughout grape berry development (Reid et al., 2006); actin, elongation factor-1-alpha (EF-1 α), glyceraldehyde-3-phosphate dehydrogenase (GAPDH), and SAND family protein (SAND) (**Supplemental Table B2**). We also found unigenes for polyubiquitin (UBQ). Transcriptional abundances for all five genes were profiled using qRT-PCR throughout development in both the 2008 and 2009 growing seasons. *VcUBQ* was the first candidate reference gene eliminated due to inconsistent

expression between the two different seasons compared to the other four reference genes (**Supplemental Table B3**).

Two Excel-based programs were then used to evaluate the stability of the top four reference genes. These programs employ statistical measures to compare the stability of each reference gene to all others. For each season, the genes were ranked by *geNorm* (Vandesompele et al., 2002) and *NormFinder* (Andersen et al., 2004) stability values, and compared to the manually-calculated coefficient of variation (CV). The ranking by each of these was averaged into an overall rank for each season and then for all samples including floral tissues (**Supplemental Table B3**). The results indicated that *VcSAND* and *VcGAPDH* were approximately equivalent in stability, followed by *VcEF-1 α* and then *VcActin*, which consistently ranked last. The *geNorm* program was then used to compare the variation in the geometric average of the top two reference genes (*VcSAND* and *VcGAPDH*) to the top three reference genes (*VcSAND*, *VcGAPDH*, *VcEF-1 α*). The *geNorm* program calculated less variation for the *SAND-GAPDH* combination (not shown). Fold expression difference of the *VcSAND-VcGAPDH* combination at each developmental stage (compared to the overall geometric mean *VcSAND-VcGAPDH* expression) showed that the maximum difference from the mean was only 1.24 (0.31 C_q) and 0.91 (0.14 C_q) for the 2008 and 2009 seasons, respectively (**Supplemental Figure B4**). The expression stability of this reference gene combination was statistically confirmed with Analysis of Variance (ANOVA) tests for each growth season (not shown). Since this combination of genes was stable, the expression of each biosynthetic gene was normalized to the geometric mean of *VcSAND* and *VcGAPDH* expression. Based on stability measures, the geometric average of *VcGAPDH* and *VcSAND* was also used for floral tissue expression analysis, while for the tissue separation experiments *VcEF1- α* replaced *VcSAND* (not shown).

Soluble proanthocyanidin (PA) quantification and determination of PA subunit composition and mean degree of polymerization (mDP)

To estimate soluble PA concentrations, three replicates of 50-70 mg of fruit tissue at each stage (from same tissue pool as 2009 qRT-PCR analysis) were ground to a fine powder in liquid nitrogen. The samples were then ground in 10 ml 80% methanol and extracted overnight with shaking. After vortexing the slurry and centrifuging for 5 min at 3320 rcf, the supernatants were used for PA analysis using the method of Porter et al. (1986). Purified *Populus tremuloides* (aspen) PA was used as a standard.

For PA subunit composition and mDP analysis, frozen fruit samples were shipped on dry ice to the University of Alberta, where they were stored at -80 °C until extraction. Frozen berries were ground to a fine powder in liquid nitrogen using a mortar and pestle. Ground samples (5-10 g) were extracted with 66% (v/v) aqueous acetone (8 mL per g tissue) in an Erlenmeyer flask. The flask was sparged with nitrogen gas then sealed with a glass stopper and placed on a rotary shaker at 100 rpm in the dark at 4°C for 24 h for extraction. The extract was filtered through Whatman No.1 filter paper under moderate vacuum using a Buchner funnel. The tissue residue was washed with 66% aqueous acetone, extract and wash were pooled, and the acetone was removed using a SpeedVac vacuum concentrator (AES 200, Savant, Farmingdale, NY). The remaining aqueous PA extract was extracted minimally 5 times with 100% HPLC grade ethyl acetate (3 vol : 1 vol, extract:ethyl acetate) to remove chlorophylls, anthocyanins, and flavan-3-ol monomers. The remaining ethyl acetate in the aqueous extract was removed using a SpeedVac. The aqueous extract was adjusted to 50% (v/v) aqueous methanol with 0.1% TFA using methanol (100%) and TFA and loaded onto a 4 mL bed volume of TOYOPEARL column (1.5 ×12 cm) preconditioned with 50% (v/v) aqueous methanol with 0.1% TFA. The column was washed minimally with 5 column bed volumes of 50% aqueous methanol with 0.1% TFA to remove organic acids and other flavonoids including flavan-3-ol monomers, anthocyanins, and flavonols. PAs were eluted using 4 bed volumes of 66% acetone with 0.1% TFA. The acetone was removed from the extract using a SpeedVac vacuum concentrator, and the remaining aqueous extract was lyophilized.

For acid cleavage and phloroglucinol derivatization of the PA extracts, the method of Koerner et al. (2009) with minor modifications was used. Briefly, the lyophilized semi-purified PA powder (approximately 5 mg) was dissolved in 1 mL solution of 0.1N methanolic hydrochloric acid solution containing 100 g L⁻¹ phloroglucinol and 10 g L⁻¹ ascorbic acid. The reaction was carried out in a 50 °C water bath for 120 min. After 20 min and 120min reactions, a 200 µL aliquot of the reaction mixture was added to 1 mL of 40 mM aqueous sodium acetate to quench the reaction. A 20 µL aliquot of the diluted reaction mixture was injected onto two Chromolith RP-18e (4.6 x 100 mm; Merck, Germany) columns connected in series, protected by a guard column (Chromolith RP-18e 4.6 x 10 mm), stabilized at 30°C, using an Agilent 1200 HPLC system equipped with a Agilent G1315B DAD. The HPLC conditions followed that of Kennedy and Taylor (2003) with minor modifications. The samples were eluted at 3 mL min⁻¹ using a linear gradient with 1 % (v/v) aqueous acetic acid (solvent A) and acetonitrile with 1% acetic acid (v/v; solvent B) as follows: isocratic at 3 % B from 0 to 4 min, 3% to 18 % B in 10 min, and 80 % B from 14 to 18 min. Free-PA (terminal) and phloroglucinol-conjugated-PA (extension) subunits were monitored at 280 nm. PA terminal subunits were identified by comparison of HPLC-DAD retention times and absorbance spectra with commercially available flavan-3-ol standards. Phloroglucinol-PA adducts were identified by comparison of HPLC retention times with grape skin and cranberry fruit PA reaction products that have been previously characterized (Koerner et al., 2009). Mean degree of polymerization and conversion yield were calculated according to method of Kennedy and Jones (2001).

For identification of the flavan-3-ol monomers and phloroglucinol adducts, LC-MS analysis was performed on a 4000 Q-TRAP[®] LC/MS/MS mass spectrometer (MDS SCIEX, Applied Biosystems) connected to an Agilent 1200 HPLC system with a G1315D photodiode array detector, a G1312A binary pump, a G1379B degasser, a G1316A thermostatted column compartment and a G1329A autosampler (Agilent Technologies, Palo Alto, USA). HPLC separation was performed on a Symmetry[®] C₁₈ column (250 × 4.6 mm, 5 µm particle size) with a

Novapak[®] C₁₈ guard column (10 × 4.6 mm, 4 μm particle size, Waters, Massachusetts, USA) at 25 °C and at a flow rate of 1.0 mL min⁻¹. The compounds were separated using a linear elution gradient of (A) 1 % aqueous acetic acid (v/v) and (B) 100 % methanol as follows: isocratic at 5% B from 0-13 min; 20% B at 33 min; 40 % B at 58 min; 90% B at 58.1 min; isocratic at 90 % B from 58.1 to 68.1 min. MS/MS analysis was carried out in the negative ion mode using the following mass spectrometer conditions: high-purity nitrogen gas (99.995 %) as nebulising gas (GS1) at 50 psi, heating gas (GS2) at 30 psi, and curtain gas (CUR) at 25 psi for electrospray probe. Ionspray source temperature was 600 °C and ion spray voltage was 4 kV. Collision-induced dissociation (CID) spectra were acquired using nitrogen as the collision gas under collision energy (CE) of 20 eV. The other MS parameters used were as follows: declustering potential (DP), 70 V; entrance potential (EP), 10 V; and collision exit potential (CXP), 7 V. An information-dependent acquisition (IDA) method, EMS → 4 EPI, was used to profile the phloroglucinol adducts of flavan-3-ols and flavan-3-ol terminal units. The IDA threshold was set at 100 cps, above which enhanced product ion (EPI) spectra were collected from the eight most intense peaks. Both Q1 and Q3 were operated at low and unit mass resolution. The spectra were obtained over a scan range from the mass to charge ratio (m/z) 50 to 1300. The EPI scan rate was 4000 Da/s and the enhanced MS (EMS) scan rate was 1000 Da/s. MS/MS data were acquired and analyzed by Analyst software (version 1.5, Applied Biosystems, California, USA).

Quantification of anthocyanidins and flavonol aglycones

Frozen fruit samples collected in Victoria, British Columbia were shipped on dry ice to the University of Alberta. Samples were ground to a fine powder in liquid nitrogen using a mortar and pestle. Ground samples (2-4 g) were extracted with 8 mL of the HPLC grade solvent mixture, acetone: methanol: water: formic acid (40:40:20:0.1, v/v/v/v). The extracts were vortexed for 2 min then filtered through a Whatman No. 1 filter paper using a Büchner funnel under moderate vacuum. The tissue residue was washed 3 times with 4 mL of the solvent mixture,

extracts and washes pooled, and evaporated to dryness using a SpeedVac vacuum concentrator. The extract residue was solubilized in 10 mL deionized water and a 1 mL aliquot was loaded onto a Sep-Pak C18 cartridge (Waters Scientific, Mississauga, Ontario), which had been preconditioned with 2 mL of 100% methanol followed by 5 mL deionized water. The column was washed with 5 mL deionized water to remove sugars and organic acids. Subsequently, the anthocyanins and flavonols were eluted from the column with 10 mL of 0.1% formic acid in methanol (v/v) and this elutant was evaporated under vacuum to near dryness. The residue was dried completely under a stream of nitrogen gas. For hydrolysis of anthocyanins and flavonols to their aglycones, 3 mL of 2 N HCl in 50% aqueous methanol (v/v) was added to the sample residue followed by sonication or vortexing to aid sample solubilization. The samples were then incubated in a pre-heated dry-bath at 100 °C for 1 hour. The samples were cooled using an ice-bath and the volume of each sample was adjusted to 10 mL using deionized water prior to HPLC analysis. The extracts (20 µL per sample) were injected onto a Zorbex SB-C18, 4.6 x 250 mm (5 µm; Agilent) C18 column fitted with a Zorbex SB-C18, 4.6 x 12.5 mm (5 µm; Agilent) guard column, using an HPLC system (Agilent 1200, USA) equipped with a photodiode array (DAD; Agilent G1315B) detector. The samples were eluted at a flow rate of 1 mL min⁻¹ using a linear gradient of 0.4% aqueous trifluoroacetic acid (TFA; solvent A) and acetonitrile with 0.4% TFA (solvent B) as follows: isocratic at 18% B from 0 to 10 min, 20% B by 25 min; 30% B by 35 min; 40% B by 40 min. The column temperature was maintained at 35 °C. Quantification of the anthocyanin aglycones was conducted by monitoring absorption at 530 nm, and 350 nm was used for the flavonol aglycones. Commercial standards of anthocyanin and flavonol aglycones were used for comparison of HPLC retention times and UV-VIS absorption spectra. The standards pelargonidin chloride, malvidin chloride, cyanidin chloride, delphinidin chloride, peonidin chloride, and quercetin were purchased from Extrasynthese (Genay Cedex, France), petunidin chloride from Polyphenol Laboratories (Sandnes, Norway), and kaempferol and myricetin were purchased from Sigma (Oakville, Canada).

Histological procedures and PA and flavonol tissue localization

Fresh fruit were shipped on ice to the University of Alberta, where they were processed immediately. Fresh fruits from stages 1 to 8 were dissected into 5 to 10 mm-thick cross sections and immediately fixed in 3.2 % paraformaldehyde (v/v), 1% glutaraldehyde (v/v), 2 mM CaCl₂, and 10 mM sucrose in a 25 mM Pipes buffer (pH 7.5). After 5 days of fixing solution infiltration under vacuum at RT, tissues were rinsed 3 times with 25 mM Pipes buffer and dehydrated using a graded ethanol series of 30% and 50% ethanol in 25 mM Pipes buffer (pH 7.5; v/v), followed by 70%, 96%, and 100% ethanol in water for 25 min each. After dehydration, specimens were sequentially infiltrated with 2.5%, 5%, 10%, 20%, 50%, 75% 1-butanol in ethanol (v/v) for 20 min each and the infiltration was completed with three washes of 100% 1-butanol for 20 min. The tissues were then embedded in Paraplast[®] Tissue Embedding Medium (Fisher) as described by O'Brien and McCully (1981). Tissues from the infiltration were embedded in paraffin blocks using a Tissue-TEK II Embedding centre (Tissue Tek, USA). Tissue sections were sliced 10 to 20 µm thick using a rotary microtome (Reichaert Histo STAT 820), stretched in a 40 °C water bath, affixed onto slides, and placed at 37°C to dry overnight.

For PA localization, the paraffin was removed from the tissue sections using two toluene (100%) washes at 5 min intervals. Tissue sections were stained with 0.1% 4-dimethylamino-cinnamaldehyde (DMACA) solution (prepared as described by Gutmann and Feucht (1991) and incubated at 60 °C for 15 min. The slides were then washed with 100% ethanol and two changes in toluene for 5 min each. Cover slides were placed on slide-mounted tissue sections using DPX mounting medium (BDH Chemicals). Tissue sections were observed using a Zeiss AXIO scope A1 light microscope (Zeiss, Germany) and micrographs were taken with a microscope-mounted Optronics camera (Optronics, USA) controlled by Picture Frame[™] Application 2.3 software. For flavonol localization, cover slides were directly placed on slide-mounted tissue sections after removal of paraffin with toluene. Flavonol auto-fluorescence (Schnitzler et al., 1996) was observed under green fluorescence (excitation filter/BP 420-490; dichromatic

mirror/510; suppression filter: LP 515) using a Leica DMRXA microscope (Leica, Germany) in the fluorescence configuration, and micrographs were taken with a microscope-mounted Nikon camera (Nikon, Japan) controlled by ACT-1 software (Nikon, USA). Tissue sections were also stained with the flavonol-specific stain diphenylboric acid 2-aminoethylester (DPBA), using the method of Peer et al. (2001).

Quantification of abscisic acid and its catabolites

Fruits collected during the 2009 growing season were used for the analysis of ABA and metabolites. For replication, three batches of 5-15 fruits from several stages of development (Stage 1, 3, 5-8) were analyzed separately. Pooled tissues from each stage were analyzed in parallel for ABA and catabolites (2008 season). All pre-frozen tissues were freeze-dried prior to extraction. For tissue-specific hormone analysis, seeds were separated from the flesh of eight freeze-dried stage 5 and stage 8 fruits each.

The sample preparation for the plant hormone analysis was performed as described in detail in Owen et al., 2009. The MS analysis was carried out by UPLC/ESI-MS/MS utilizing a Waters ACQUITY UPLC system, equipped with a binary solvent delivery manager and a sample manager coupled to a Waters Micromass Quattro Premier XE quadrupole tandem mass spectrometer via a Z-spray interface. MassLynx™ and QuanLynx™ (Micromass, Manchester, UK) were used for data acquisition and data analysis. The analytical UPLC column was ACQUITY UPLC® HSS C18 (2.1x100 mm, 1.8 µm) with an ACQUITY HSS C18 VanGuard Pre-column (2.1x5 mm, 1.8 µm). Mobile phase A comprised 0.025 % acetic acid in HPLC-grade water and mobile phase B comprised 0.025 % acetic acid in HPLC-grade acetonitrile. Sample volumes of 10 µL were injected onto the column at a flow rate of 0.40 mL min⁻¹ under initial conditions of 2% B, which was maintained for 0.2 min, then increased to 15% B at 0.4 min, and then increased to 50%B at 5 min and 100% B by 5.5 min. 100%B was maintained until 6.2 min then decreased to 2% by 6.5 min and held until 8 min for column equilibration before the next injection.

The procedure for quantification of ABA phytohormone and metabolites using deuterium labeled internal standards (synthesized as described in Abrams et al. (2003) and Zaharia et al. (2005a), has been presented in detail elsewhere (Ross et al., 2004, Owen et al., 2009). The mass spectrometer was set to collect data in Multiple Reaction Monitoring (MRM) mode controlled by MassLynx v4.1 (Waters Inc). The analytes were ionized by negative-ion electrospray using the following conditions: capillary potential 1.75 kV; desolvation gas flow 1100 L/h; cone gas flow 150L/h; source and desolvation gas temperatures, 120 °C and 350 °C, respectively. The resulting chromatographic traces are quantified off-line with the QuanLynx v4.1 software (Waters Inc), wherein each trace is integrated and the resulting ratio of signals (non-deuterated/internal standard) is compared with a previously constructed calibration curve to yield the amount of analyte present (ng per sample). Calibration curves were generated from the MRM signals obtained from standard solutions based on the ratio of the chromatographic peak area for each analyte to that of the corresponding internal standard, as described by Ross et al. (2004). The QC samples, internal standard blanks and solvent blanks were also prepared and analyzed along each batch of tissue samples.

Results

For this chapter, my contribution to the data and research was the determination of PA subunit composition and mean degree of polymerization (mDP), quantification of PAs and anthocyanidin and flavonol aglycones, and localization of PAs and flavonols over fruit development. The Supplement data for this chapter are in Appendix B.

Phenology of blueberry fruit development

Fruits from cultivar Rubel were chosen for our study because this cultivar is known to have superior antioxidant capacity and flavonoid content (Prior et al., 1998). Fruit set and ripening initiation in ‘Rubel’ is temperature-dependent and asynchronous; therefore, fruits were harvested in batches during the two main phases of the growing season and sorted into maturation classes by size and fruit

colour (**Figure 5.2 A**). During the initial 'expansion' phase, young fruit were hard and dark green and differed primarily by size. In the 'maturation' phase, enlarged light green fruits began to soften and accumulate red and then blue pigments (**Figure 5.2 A**). Stages 1-5 were staged by increasing size (Stage 1: 2-3.5 mm in diameter, Stage 2: 3-4 mm, Stage 3: 4-7 mm, Stage 4: 7-9 mm, Stage 5: 9-13 mm; **Figure 5.2 B**). Stages 6-8 were sorted by fruit colour (Stage 6: 25-50 % red skin, Stage 7: predominately purple skin with some red or blue, Stage 8: entirely dark blue and soft texture), as previously validated for other small fruits (Ozga et al., 2006). The initiation of seed coat browning (Stage 5) slightly preceded the beginning of skin pigmentation (Stage 6). Floral buds were collected approximately one to two weeks before full bloom (anthesis; **Figure 5.2 C**).

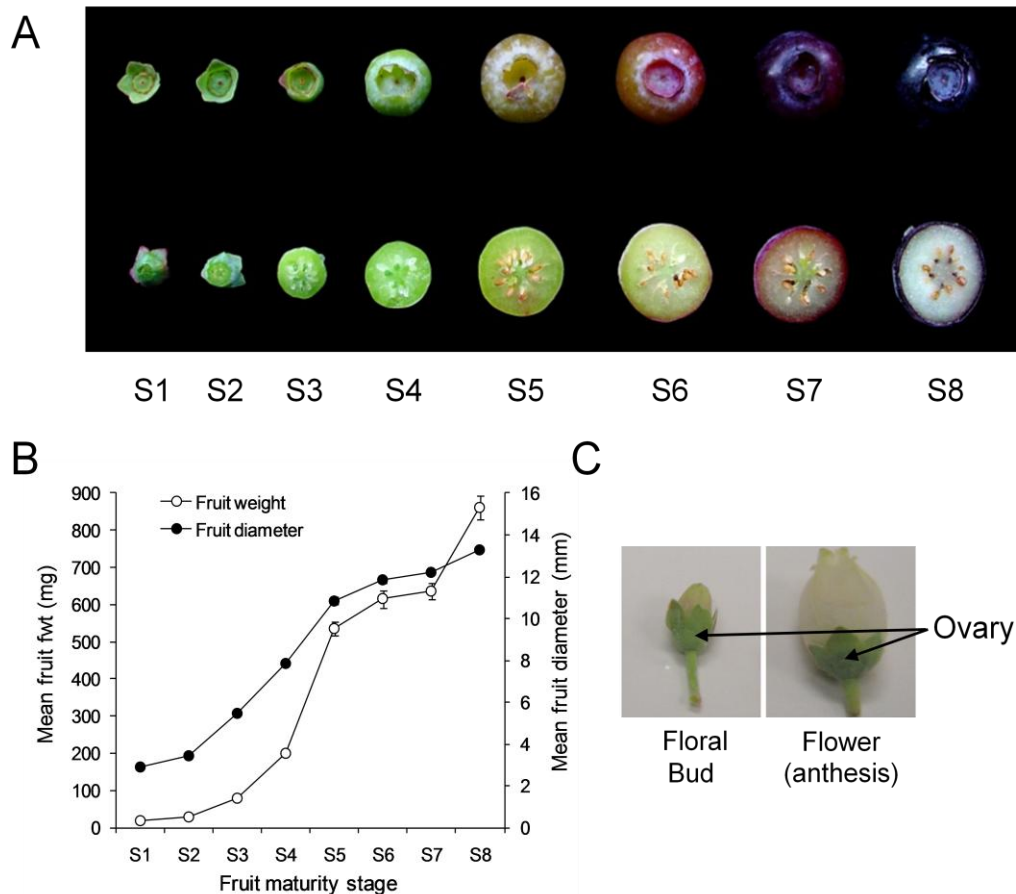


Figure 5.2: Developmental stages of blueberry (cv. Rubel) fruit and flowers used for molecular, chemical, and histological analyses. (A) Whole and bisected fruit separated into eight stages. (B) Mean fresh fruit weight and diameter throughout development. Data are means \pm SE, $n = 28-30$. (C) Floral buds, and flowers at anthesis, with ovary tissue indicated.

Construction, annotation and analysis of blueberry ESTs

Prior to this project, only a limited number of blueberry EST sequences were available in public databases, primarily from floral buds. In order to obtain additional gene sequences, we constructed and sequenced two cDNA libraries, one each from S5/6 and S7/8 pooled fruit mRNA. Following removal of low quality, vector and short sequences, a total of 17,134 high-quality ESTs were generated. After clustering, this yielded a total of 8,500 unique gene sequences (unigenes) with an average length of 610 bp (**Table 5.1**). Of these, 2,570 ESTs could be compiled into contiguous assemblies (contigs) of two or more ESTs, and 5,930 remained as singletons. Annotation for 89% of the unigenes based on similarity to sequences in the GenBank database was performed using the BLASTX algorithm. Using custom PERL scripts, assignment to three major gene ontology (GO) categories (biological process, cellular component and molecular function) was possible for 4,769 (56%) of the sequences, based on hits to proteins in the TAIR protein database (**Supplemental Figure B1**).

Table 5.1: Blueberry fruit cDNA library statistics.

| | Stage 5/6 | Stage 7/8 | Total |
|---------------------|-----------|-----------|--------|
| ESTs | 9,814 | 7,320 | 17,134 |
| Unigenes | 5,941 | 3,989 | 8,500 |
| Contigs | 1,354 | 1,174 | 2,570 |
| Singletons | 4,587 | 2,815 | 5,930 |
| Ave. GC % | 45.2 | 43.0 | 44.4 |
| Ave. length (bp) | 711 | 407 | 610 |
| GO annotated | 4,208 | 1,345 | 4,769 |
| TAIR v.8 hits | 5,778 | 3,115 | 7,602 |
| Uniprot v.14.6 hits | 5,642 | 2,632 | 7,076 |

To gain insight into which genes were most highly expressed in developing blueberry fruit, the genes were first ranked by the number of ESTs in each unigene (**Supplemental Table B1**). Eleven of the 40 most highly represented unigenes corresponded to genes that encode cruciferin-type seed nutrient storage proteins. Since most of the ESTs contributing to these cruciferin unigenes (over 870 total ESTs) came from the S5/6 library, it is likely that there was a significant contribution of seed cDNA to this EST library. Unigenes with matches predicted

to encode metallothionein, polygalacturonase, NADP-malic enzyme, and catalase were represented by 20 or more S5/6 ESTs.

Although the S7/8 library contained approximately 2,500 fewer ESTs than the S5/6 library, there were a number of unigenes in this library supported by at least 20 ESTs (**Supplemental Table B1**). Several of these were predicted to encode proteins without well-defined physiological functions, such as a protease inhibitor/seed storage/lipid transfer protein and a senescence-associated protein (SAG29). Other highly represented genes in the S7/8 cDNA library include a pathogenesis-related basic chitinase, succinate dehydrogenase, fructose-bisphosphate aldolase, and calcium-binding EF hand family protein. The libraries also contained numerous ESTs that were predicted to encode other proteins involved in important ripening-related processes, such as carbohydrate and sugar metabolism, tissue softening, cell wall metabolism, aroma synthesis, and pathogen defense (not shown). The presence of many ripening-related ESTs confirmed the utility of the libraries for studying blueberry fruit development and ripening.

Identification of genes for blueberry flavonoid biosynthesis

The major aim in producing the blueberry EST libraries was to identify genes involved in flavonoid biosynthesis. Annotations of partial and full-length blueberry genes predicted to encode most of the enzymes of the flavonoid pathway, as well as one putative flavonoid R2R3-MYB transcription factor, were substantiated by performing TBLASTX searches of the NCBI reference sequence protein database. In all cases, the top hit was an ortholog from *Arabidopsis*, grapevine or petunia, whose function had previously been experimentally verified (**Table 5.2**). In the S7/8 (mature fruit) EST library, many of the ESTs encoding enzymes for anthocyanin biosynthesis (CHS, FHT, F3'5'H, cytochrome *b₅*, ANS and UFGT) were enriched relative to the S5/6 stage library (**Table 5.2**). Surprisingly, genes encoding the PA-specific enzymes ANR and LAR were absent from both EST libraries. However, these genes were present in a highbush blueberry floral bud EST set in GenBank (**Table 5.2**). To confirm the annotations of the new flavonoid-related blueberry genes, phylogenetic trees were constructed

with the translated blueberry sequences and functionally characterized proteins involved in important biosynthetic steps. The putative blueberry F3'H and F3'5'H genes, both part of the P450 gene family, were each embedded within their respective subclades (**Figure 5.3**). Similarly, ANR and DFR, which both belong to a large superfamily of enzymes (NADPH-dependent reductases/epimerases/dehydrogenases), clustered within the predicted subclade (**Figure 5.4**). The predicted blueberry UFGT sequence was embedded in a subclade of flavonoid-3-*O*-glycosyltransferases with demonstrated activity toward anthocyanidins (**Supplemental Figure B2**). Therefore, we are confident in our annotations and suggest it is highly likely the blueberry genes encode functional enzymes. We also note that the blueberry *VcDFR*, *VcANR* and *VcUFGT* genes grouped most closely with sequences of genes from species within the same order (Ericales), such as persimmon (*D. kaki*), tea (*Camellia sinensis*), and cranberry (*Vaccinium macrocarpon*). To our knowledge, no hydroxylases from plants in Ericales have been functionally investigated.

Table 5.2: Blueberry unigenes used for qRT-PCR analysis.

| Gene | REFSEQ match | Accession No. | <i>E</i> value | ID (%) ^a | Region of ID ^b | Coverage (%) ^c | Amplicon Region ^d | Unigenes & ESTs ^e |
|----------|--------------|---------------|----------------|---------------------|---------------------------|---------------------------|------------------------------|------------------------------|
| VcCHS | AtTT4 | AT5G13930 | 0.0 | 84 | *7-395* | 100 | 213-327 (1170) | 2 (2/31) |
| VcFHT | AtTT6 | AT3G51240 | 2e-109 | 84 | *1-231 | 65 | 18-117 (701) | 1 (1/5) |
| VcF3'H | VvF3'H | XP_002284165 | 0.0 | 83 | 37-506 | 92 | 620-774 (1428) | 1 (2/5) |
| VcF3'5'H | VvF3'5'H | XP_002263919 | 0.0 | 74 | *1-431 | 85 | 743-886 (1296) | 1 (0/6) |
| VcCytob5 | PhDIF-F | AAD10774 | 5e-54 | 69 | *1-148* | 100 | 28-178 (443) | 1 (0/26) |
| VcDFR | AtTT3 | AT5G42800 | 2e-133 | 74 | *7-328* | 100 | 843-980 (993) | 1 (2/2) |
| VcANS | AtLDOX | AT4G22880 | 3e-148 | 77 | *1-347 | 97 | 741-879 (1065) | 1 (1/21) |
| VcUFGT | VvF3GT | XP_002277035 | 1e-72 | 58 | 200-450* | 55 | 707-853 (777) | 1 (0/4) |
| VcANR | VvANR | XP_002271372 | 2e-154 | 81 | 10-338* | 97 | 906-1046 (993) | 0 (0/0) |
| VcLAR | VvLAR1 | XP_002281447 | 5e-73 | 70 | 162-346* | 53 | 387-532 (558) | 0 (0/0) |
| VcMYB1 | VvMYBPA1 | XP_002266014 | 3e-76 | 60 | *1-286* | 100 | 409-602 (822) | 1 (0/1) |
| VcNCED1 | AtNCED3 | AT3G14440 | 4e-106 | 76 | 253-493 | 40 | 186-313 (722) | 2 (3/4) |

^a Percent sequence identity (ID), based on amino acid sequence.

^b Stars (*) at left and right of region indicate presence of predicted start and stop codons, respectively.

^c Percentage of total predicted protein length present in unigene sequences.

^d Percent coverage: Nucleotide region within each unigene that qRT-PCR primers were designed to amplify with total unigene coding sequence length in brackets.

^e Predicted number of unique gene copies (unigenes) present within the blueberry fruit EST libraries. The ANR and LAR sequences were retrieved from NCBI. The number of ESTs in each EST library that comprise the unigenes are shown in brackets (S5/6 to S7/8).

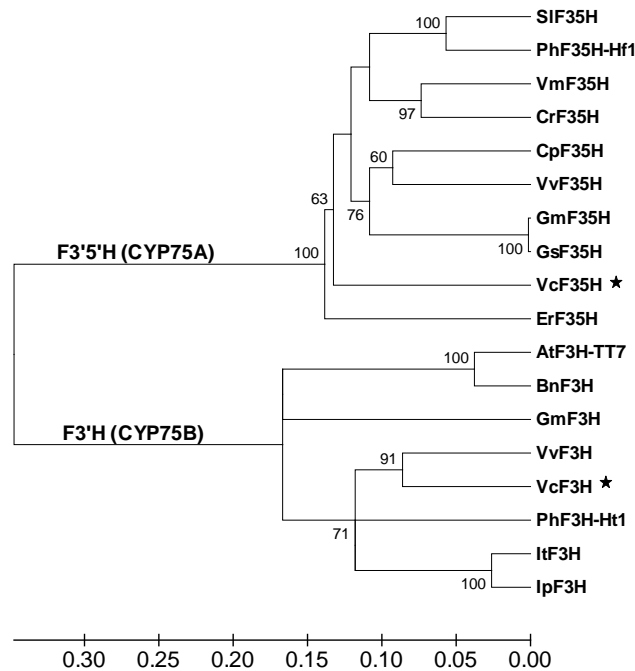


Figure 5.3: Phylogeny of F3'H and F3'5'H – the cytochrome P450 flavonoid hydroxylases. Protein sequences for functionally characterized flavonoid hydroxylases were obtained from GenBank and aligned with partial coding sequences for the putative blueberry VcF3'H and VcF3'5'H (indicated with stars) using ClustalW. The linearized neighbour-joining tree was produced with *MEGA* software version 4.0 (Tamura et al., 2007). Nodes were evaluated with 1,000 bootstrap replicates. Bootstrap values for nodes are shown as numbers on branches (only those > 50% are shown). Evolutionary distances (Poisson-correction method) are shown as number of substitutions per amino acid site. GenBank accession numbers are as follows: SIF35H (*Solanum lycopersicum*, GQ904194), PhF35H-Hf1 (*Petunia hybrida*, Z22544), VmF35H (*Vinca major*, AB078781), CrF35H (*Catharanthus roseus*, AJ011862), CpF35H (*Cyclamen persicum*, GQ891056), VvF35H (*Vitis vinifera*, DQ786631), GmF35H (*Glycine max*, AB540111), GsF35H (*Glycine soja*, AB540112), ErF35H (*Eustoma russellianum*, BAA03439), AtF3H-TT7 (*A. thaliana*, NM_120881), BnF3H (*Brassica napus*, DQ324378), GmF3H (*G. max*, AB061212), VvF3H (*V. vinifera*, XM_002284129), PhF3H-Ht1 (*P. hybrida*, AF155332), ItF3H (*Ipomoea tricolor*, BAD00189), IpF3H (*I. purpurea*, AB113265).

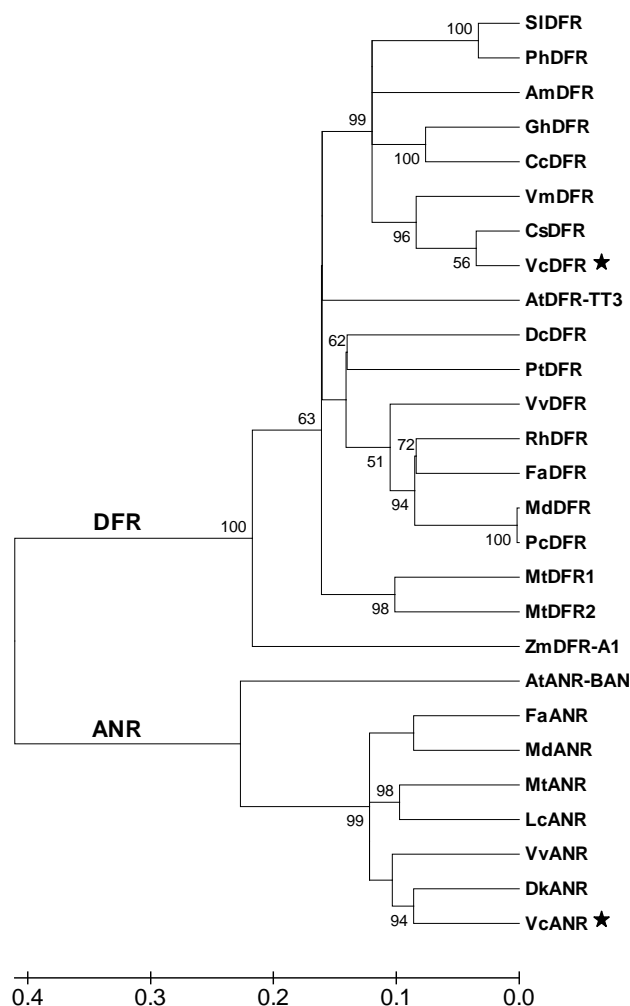


Figure 5.4: Phylogeny of dihydroflavonol reductase (DFR) and anthocyanidin reductase (ANR) protein family. Sequences for full-length functionally characterized DFR and ANR enzymes were obtained from GenBank and aligned with putative VcDFR and VcANR sequences (stars) with ClustalW. A linearized neighbour-joining tree was produced with *MEGA* software version 4.0 (Tamura et al., 2007) as described in **Figure 5.3**. Bootstrap values for nodes are shown as numbers on branches (only those > 50% are shown). Evolutionary distances (Poisson-correction method) are shown as number of substitutions per amino acid site. GenBank accession numbers are as follows: SIDFR (*Solanum lycopersicum*, Z18277), PhDFR (*petunia*, AF233639), AmDFR (*Antirrhinum majus*, X15536), GhDFR (*Gerbera hybrida*, Z17221), CcDFR (*Callistephus chinensis*, Z67981), VmDFR (*Vaccinium macrocarpon*, AF483835), CsDFR (*Camellia sinensis*, AB018685), AtDFR-TT3 (*A. thaliana*, NM_123645), DcDFR (*Dianthus caryophyllus*, Z67983), PtDFR (*Populus tremuloides*, AY147903), VvDFR (*V. vinifera*, XM_002281822), RhDFR (*Rosa hybrida*, D85102), FaDFR (*Fragaria x*

ananassa, AF029685), MdDFR (*Malus x domestica*, AF117268), PcDFR (*Pyrus communis*, AY227730), MtDFR1 (*Medicago truncatula*, AY389346), MtDFR2 (*M. truncatula*, AY389347), ZmDFR-A1 (*Zea mays*, NM_001158995), AtANR-BAN (*Arabidopsis*, NM_104854), FaANR (*F. ananassa*, DQ664192), MdANR (*M. domestica*, DQ139835), MtANR (*M. truncatula*, AY184243), LcANR (*Lotus corniculatus*, DQ349113), VvANR (*V. vinifera*, BN000166), and DkANR (*Diospyrus kaki*, AB195284

In a phylogenetic analysis of R2R3-MYB proteins, the blueberry *VcMYB1* sequence grouped most closely with regulators of PA synthesis from grapevine (*VvMYBPA1*) and persimmon fruit (*DkMYB4*), rather than flavonol, anthocyanin and general flavonoid MYB regulators (Bogs et al., 2007; Akagi et al., 2009b; **Supplemental Figure B3**). This suggests a function for *VcMYB1* in blueberry PA synthesis. These MYBs are all within a subclade that is phylogenetically distinct from a second type of MYB PA regulator, which contains the *Arabidopsis* TT2, grapevine *VvMYBPA2*, and aspen *PtMYB134* sequences (Mellway et al., 2009). However, we found no other MYBs belonging to any flavonoid regulatory group in our EST collection.

PA biosynthetic genes are expressed very early in blueberry fruit development

To study the transcriptional regulation of PA and flavonoid biosynthesis in highbush blueberry, the expression of flavonoid pathway genes was profiled over the eight stages of development using quantitative real-time reverse transcription-PCR (qRT-PCR). To ensure reliability of expression results, qRT-PCR was performed for all genes on three separate 2008 cDNA preparations for each developmental stage. For additional replication, the analysis was repeated for most genes on two cDNA preparations from the 2009 season. All gene expression values were efficiency-corrected.

Reference gene selection was a critical factor in our qRT-PCR analysis, in particular because of the broad physiological and cellular changes that occur during fruit development. This made the evaluation of several reference genes for qRT-PCR imperative (Gutierrez et al., 2008). After evaluating five possible genes

as implemented by Reid et al. (2006) (**Supplemental Table B2**), we determined that the average relative transcriptional abundance of genes encoding glyceraldehyde-3-phosphate dehydrogenase (GAPDH) and SAND family protein (SAND) was the most constant and did not differ statistically across the berry developmental stages (**Supplemental Figure B4, Supplemental Table B3**). The reference gene selection process and statistical methods used to evaluate the genes are described in detail in the Materials and Methods. All expression data were calculated as an expression ratio relative to the geometric mean of the two most stable reference genes.

We first analyzed the gene expression profiles for *VcDFR* and *VcANS* genes, which encode enzymes required for both PA and anthocyanin synthesis. Transcript abundance of the genes followed a biphasic pattern in both 2008 and 2009 growing seasons (**Figure 5.5 A, B**). Expression was high early in development (S1 and S2), decreased to a minimum by mid-fruit development (S5), then increased again as the fruit matured (S6-8). By contrast, the PA-specific *VcANR* and *VcLAR* genes showed a different profile, as their transcripts were detected only early in fruit development, in stages S1-S4 (**Figure 5.5 C, D**). These transcriptional profiles imply that PA synthesis is most active in young fruit. *VcMYB1* transcripts were also highly abundant in very young stages, together with *VcANR* and *VcLAR* (**Figure 5.5 E**), supporting the idea that it functions in PA synthesis. However, after decreasing to minimal levels at stage 5, *VcMYB1* transcripts were again found at higher levels in ripening fruit (S6-S8), the period when anthocyanins are synthesized (**Figure 5.2 A**). Since transcripts of the PA-specific genes *VcANR* and *VcLAR* were already present at high levels in S1 fruit, we further assessed PA gene expression in the fruit-forming tissues (ovary and calyx) of floral buds and flowers. In floral buds, bud ovaries and S1 fruits, transcript abundance of *VcANS* and *VcANR* was relatively high, suggesting a capacity to produce epicatechin-type flavan-3-ols for PA synthesis early in fruit development (**Figure 5.5 F**). Based on these results, it appeared that PA biosynthetic gene expression had already commenced in the ovaries by the time floral buds had formed. *VcLAR* transcript abundance was much greater in whole

floral buds and flowers than fruit-forming ovaries, suggesting that *VcLAR* was more abundant in floral tissues other than the ovary and attached calyx (i.e. petals, stamens, stigma, style).

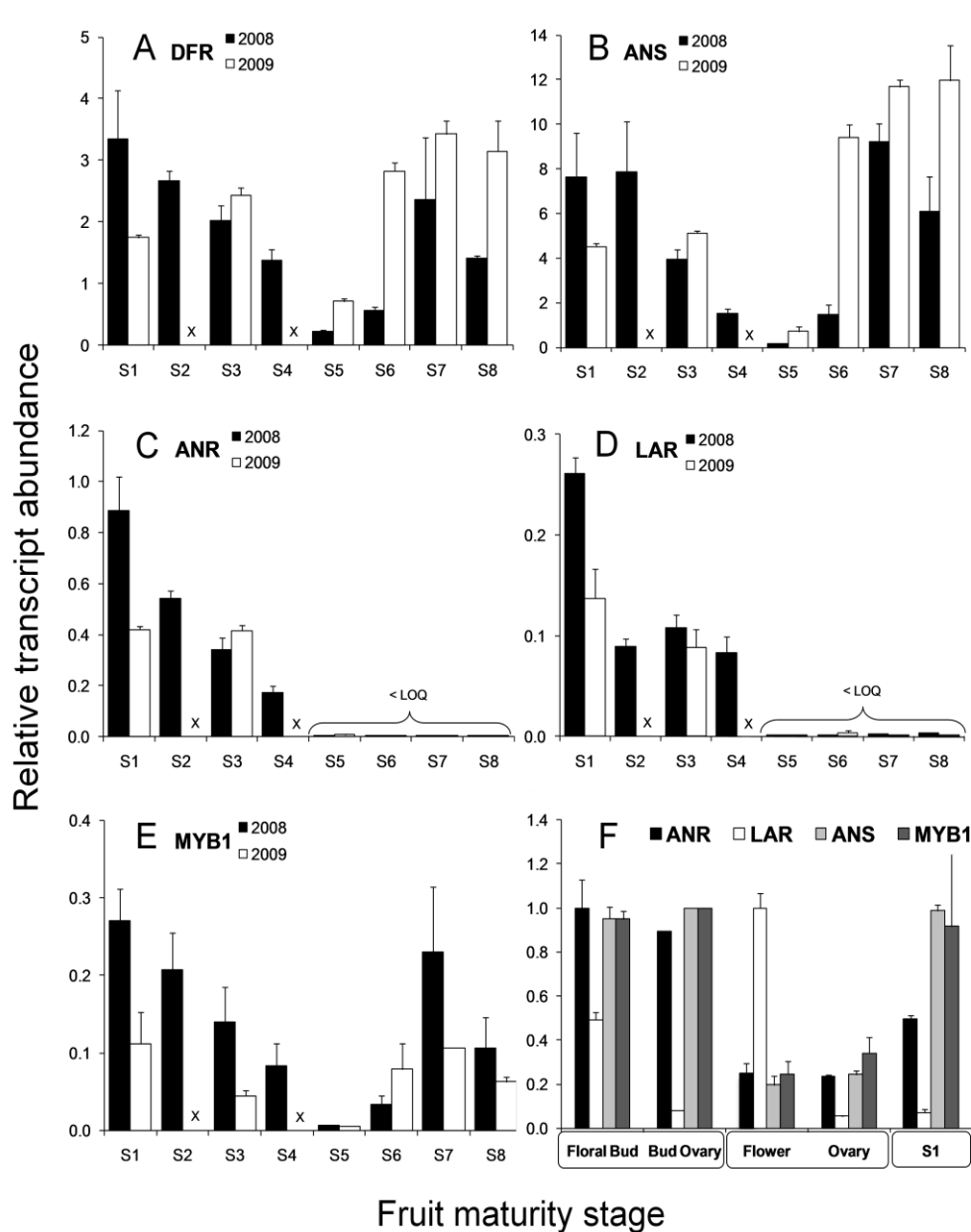


Figure 5.5: Proanthocyanidin gene transcript abundance during blueberry fruit development and ripening. (A) *VcDFR*, (B) *VcANS*, (C) *VcANR*, (D) *VcLAR*, and (E) *VcMYB1* transcripts throughout the 2008 (\pm SE, $n=3$) and 2009 (\pm SE, $n=2$) growing seasons. S2 and S4 fruits were not measured in the 2009 season and are marked with an x. (F) Relative abundance of select transcripts in floral tissues (\pm SE, $n=2$ except floral buds) relative to their abundances in 2009 S1 fruit. These

values were normalized for each gene relative to the maximum abundance in the five samples shown, which was set to 1.0. All values are reported relative to the geometric mean abundance of *VcGAPDH* and *VcSAND* at each stage. LOQ, limit of quantification.

Quantification and chemical characterization of PAs

To correlate PA gene expression profiles with PA accumulation, total soluble PA concentration was assayed at each developmental stage (Porter et al., 1986). On a fresh weight basis, the PA concentration as measured using the butanol-HCl method declined from a maximum in ovaries at flowering (30 mg g fwt⁻¹) to substantially lower levels in large green S5 fruit (**Figure 5.6 A**). PA concentrations continued to decline gradually from S5 to a minimum at S8 (2.5 mg g fwt⁻¹). However, since the berries were also rapidly expanding until S5, the total calculated amount of soluble PA per fruit still increased over this time period (**Figure 5.6 A**). PA concentration was further analyzed by reverse-phase HPLC after acid catalysis in the presence of phloroglucinol (phloroglucinolysis; Kennedy et al., 2001). This method allows the determination of PA subunit composition and concentration by comparison of product retention properties to known products (**Supplemental Table B4**). Flavan-3-ols in the extension units form phloroglucinol adducts at their C-4 position, while terminal flavan-3-ol units are released as flavan-3-ol monomers. After HPLC analysis and LC-MS confirmation of the PA phloroglucinolysis reaction products, the mean degree of polymerization (mDP) of PAs was also calculated. In blueberry PAs, the extension units were almost exclusively epicatechin in fruit at all stages (**Table 5.3**), and the majority of these subunits were linked in a B-type configuration (C₄→C₈ or C₄→C₆). The epicatechin-phloroglucinol adduct molecular mass [M-H] as assessed by LC-MS was 413, which is consistent with this adduct (**Supplemental Table B4**).

Table 5.3: Summary of blueberry PA subunit composition following acid hydrolysis and phloroglucinol derivatization

| Compound | Stage 3 | Stage 4-5 | Stage 6 | Stage 7 | Stage 8 |
|-------------------------------------|--------------|--------------|--------------|--------------|---------------------------------|
| Epigallocatechin in extension units | <i>a</i> | <i>a</i> | <i>a</i> | <i>a</i> | 3.35 ^{<i>b</i>} ± 0.68 |
| Catechin in extension units | 0.64 ± 0.03 | 0.67 ± 0.01 | 0.64 ± 0.02 | 0.91 ± 0.04 | 0.92 ± 0.12 |
| Epicatechin in extension units | 83.44 ± 0.06 | 83.49 ± 0.08 | 81.66 ± 0.06 | 85.48 ± 0.66 | 82.93 ± 0.56 |
| A2 in extension units | 1.85 ± 0.00 | 2.23 ± 0.12 | 3.80 ± 0.16 | 1.43 ± 0.14 | 1.06 ± 0.03 |
| Catechin in terminal units | 6.94 ± 0.17 | 6.78 ± 0.00 | 6.64 ± 0.03 | 6.97 ± 0.21 | 6.96 ± 0.06 |
| Epicatechin in terminal units | 5.26 ± 0.05 | 4.90 ± 0.14 | 5.33 ± 0.12 | 3.45 ± 0.17 | 3.00 ± 0.15 |
| A2 in terminal units | 1.86 ± 0.31 | 1.93 ± 0.05 | 1.93 ± 0.07 | 1.76 ± 0.08 | 1.78 ± 0.05 |

Data are means ± SE (n=2).

^{*a*} Under the detection limit.

^{*b*} Value of proportional composition (mole %).

Linkages of the terminal unit to the first extension units were also primarily B-type, as flavan-3-ols with the molecular mass of 289 were the main non-derivatized compounds detected after phloroglucinolysis. Terminal units were slightly enriched in catechin compared to epicatechin, with the relative amount of epicatechin decreasing over development (37.4 mole % in S3 to 25.6 mole % in S8; **Table 5.3**). A minor proportion of the fruit PAs had A-type interflavan linkages (Koerner et al., 2009) in both the extension and terminal units. A-type interflavonoid bonds are resistant to acid-cleavage, resulting in the presence of the A-type dimer-phloroglucinol adduct (M-H, 699) for the extension units after the acid-cleavage and phloroglucinol addition reaction, and the A-type dimer for the terminal units (M-H, 575; **Supplemental Table B4**). The calculated mDP of the blueberry fruit PAs was relatively stable between S3 and S6 (7 - 7.5) and then increased to a maximum of 8.5 in S8 fruit (**Figure 5.6 B**). Using the phloroglucinolysis data to calculate total PA concentrations, we again observed a sharp decline as the fruits matured, consistent with the PA profile over fruit development determined with the butanol-HCl method (**Figure 5.6A**). Overall, the pattern of PA accumulation was consistent with the profiles of PA-specific transcript accumulation early in berry development.

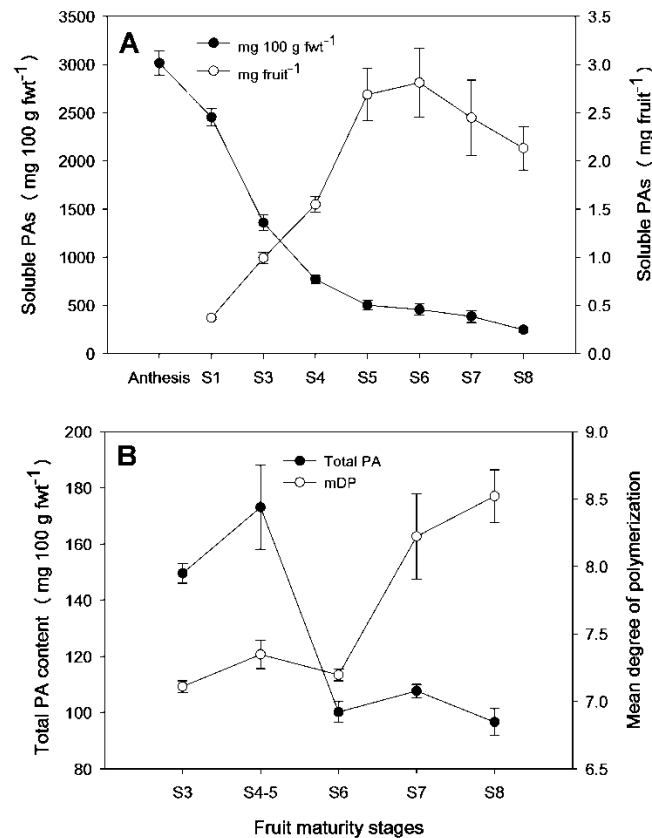


Figure 5.6: Proanthocyanidin accumulation during blueberry fruit development. (A) Total soluble PA content as determined with the butanol-HCl method (assayed using aspen tannin as standard) and PA content per fruit (data are means \pm SE, n=3). (B) PA concentration and mean degree of polymerization (mDP) for blueberry PAs as determined by phloroglucinolysis (data are means \pm SE, n=2).

General flavonoid and anthocyanin-specific transcript profiles and end product accumulation are distinct from those in PA synthesis

The *VcCHS* and *VcFHT* genes encode enzymes at the entry-point of the flavonoid pathway and are necessary for the biosynthesis of all flavonoids, including PAs, anthocyanins and flavonols. *VcCHS* gene transcripts exhibited a biphasic abundance profile (**Figure 5.7 A**), with early and late peak profiles similar to *VcDFR* and *VcANS*. By contrast, *VcFHT* transcript abundance was lower during early fruit development and then increased substantially as the fruit matured (**Figure 5.7 A**). *VcF3'H* gene transcripts, which encode the flavonoid 3' B-ring hydroxylase, also exhibited a biphasic expression pattern during fruit development, consistent with a function in both anthocyanin and PA accumulation

(**Figure 5.7 B**). *Cytochrome b₅* (*VcCytob₅*) transcripts were also detected in a biphasic pattern similar to *VcF3'H* (**Figure 5.7 D**). By contrast, transcripts of the *VcF3'5'H* gene (responsible for the third hydroxylation of the B-ring) were abundant only during the ripening fruit stages S5-S8 (**Figure 5.7 C**), closely paralleling the appearance of anthocyanins (**Figure 5.2 A**). This pattern was similar to the *VcUFGT* gene (**Figure 5.7 E**). All of the general flavonoid genes including *VcF3'5'H* and *VcCytob₅* were most highly expressed during ripening (S5-S8). Overall, the gene expression profiles determined by qRT-PCR confirm a clear separation of PA and anthocyanin synthesis in developing blueberry fruit.

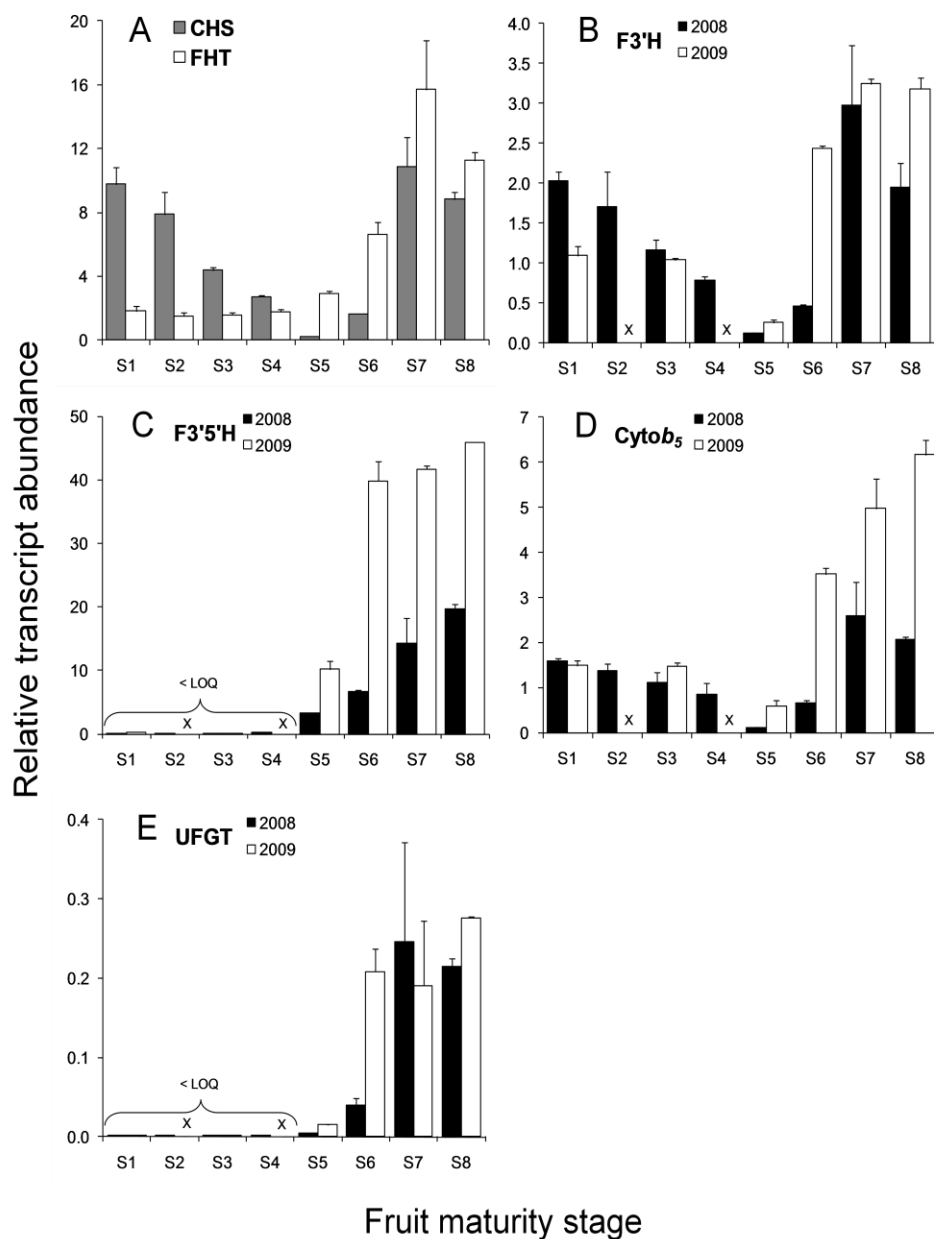


Figure 5.7: Transcript abundance of genes involved in general flavonoid metabolism including B-ring hydroxylation and anthocyanin synthesis. (A) *VcCHS* and *VcFHT* (data are means \pm SE, $n=3$, 2008). (B) *VcF3'H*, (C) *VcF3'5'H*, (D) *VcCytob5* and (E) *VcUFGT* (data are means \pm SE, $n=3$ for 2008, $n=2$ for 2009). All values are relative to the geometric mean of abundance of *VcGAPDH* and *VcSAND* reference gene transcripts. Both 2008 and 2009 data are shown for panels B-F, but stages S2 and S4 were not sampled in 2009. LOQ, limit of quantification.

Next, we tested if anthocyanins accumulate in accordance with the pattern of gene expression observed above. Anthocyanin and flavonol aglycones were

identified and quantified at several developmental stages. Even in the green berry stages (S1- S5), cyanidin-type anthocyanins were detected at low levels, likely accounting for the red blush to some parts of the green fruit (**Figure 5.2 A**, **Figure 5.8 A** and **B**). As the fruit ripened and the exocarp colour changed from mostly green to partially pink (**Figure 5.2 A**, S6), blue-purple delphinidin-type anthocyanins began to accumulate (**Figure 5.8 B**). In accordance with their deep colouration, in mature S8 fruit the anthocyanidin levels peaked dramatically. Delphinidin was the most abundant, followed by cyanidin, malvidin, petunidin and minor quantities of peonidin (**Figure 5.8 A** and **B**). The appearance of the tri-hydroxylated anthocyanidins and derivatives (for structures see **Figure 5.1**) was coordinated and likely driven by the abundance of *VcF3'5'H* transcripts beginning at stage S5. We also assayed flavonols, which were most abundant in young fruit (**Figure 5.8 C**). Quercetin was predominant, with only minor quantities of myricetin observed (**Figure 5.8 C** and **D**), indicating that the F3'5'H enzyme was not significantly impacting flavonol structure.

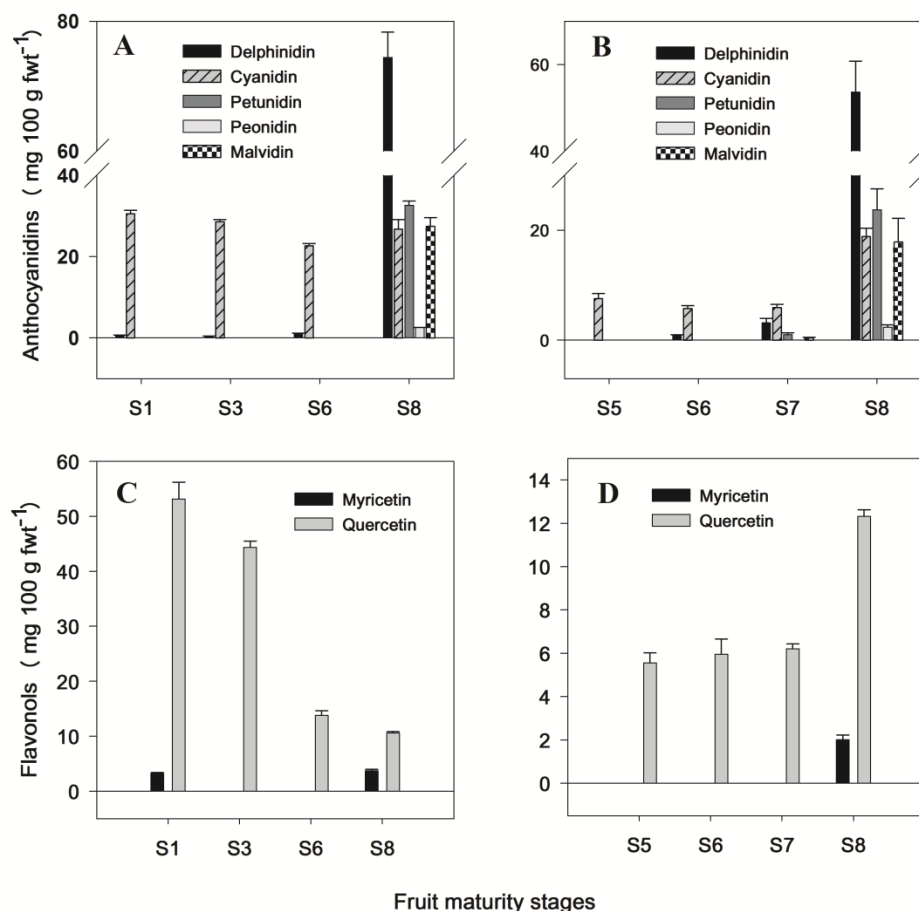


Figure 5.8: Anthocyanin and flavonol aglycone concentrations in blueberry fruit over development. (A) Anthocyanin aglycone concentrations in 2010 fruit (stages S1, S3, S6 and S8). (B) Anthocyanin aglycone concentrations in 2009 fruit (S5, S6, S7 and S8). (C) Flavonol aglycone concentrations in 2010 fruit (stages S1, S3, S6 and S8). (D) Flavonol aglycone concentrations for 2009 fruit (stages S5, S6, S7 and S8). Data are means \pm SE, $n=3$.

PAs, flavonols, and flavonoid gene transcripts are localized to distinct regions of blueberry fruit

The tight temporal control of gene transcription observed above suggested that PAs and other flavonoids might also be under precise tissue-specific control. To determine the localization of PAs, fruits were histologically fixed, sectioned, and incubated with the PA-specific stain 4-dimethylamino-cinnamaldehyde (DMACA). PAs were localized throughout the entire fruit (dark blue colouration upon reaction with PAs) at S1 (**Figure 5.9 A-C**). As fruit development progressed to stage 3 (S3), PA staining became minimal in the mesocarp, but remained

intense in the seed coats, placentae and the exocarp (**Figure 5.9D-F**). At S5 to S8 the volume of the mesocarp tissue increased substantially, thus diluting PA concentration and reducing intensity of DMACA staining at S6-S8 (**Figure 5.9 G-L**). A change in colour from dark blue to brown in the placental and seed coat tissues suggests localized oxidation of the PAs occurred by stage 6 (**Figure 5.9 G, H, J, and K**; see also **Figure 5.2 A**). At fruit maturity (Stage 8, **Figure 5.9 L**), the dark-blue staining in the epidermis is likely due to DMACA-staining of PAs as well as anthocyanins that occur at high levels in this tissue at this stage. The purple staining in the hypodermis in stage 8 fruit is likely mainly due to the presence of anthocyanins.

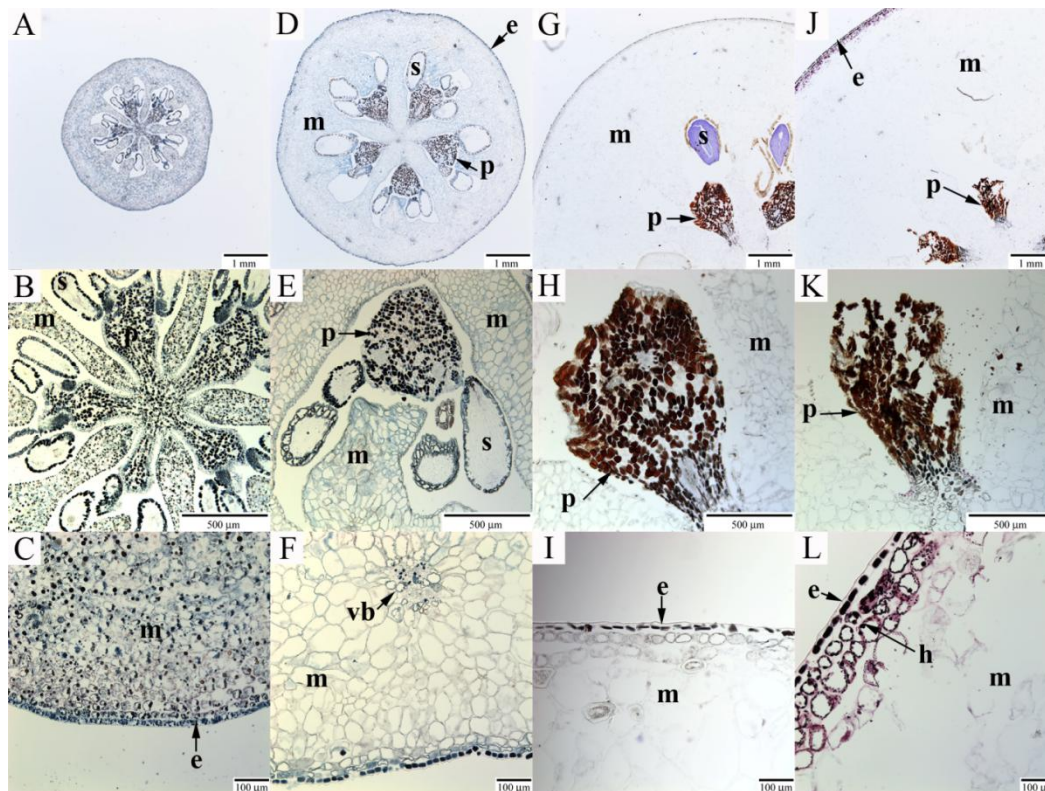


Figure 5.9: Localization of PAs in blueberry fruit at major developmental stages. Fruit tissue cross-sections were treated with DMACA to visualize PAs, and light micrographs of fruit cross-sections from stages S1 (panels A-C), S3 (panels D-F), S6 (panels G-I), and S8 (panels J-L) are shown. Middle row (panels B, E, H, and K) shows details of stained placental and seed tissues, bottom row (panels C, F, I, and L) shows fruit flesh and epidermal tissue. e, exocarp; h, hypodermis; m, mesocarp; p, placenta; s, seed; vb, vascular bundle.

For flavonol localization, flavonol autofluorescence was monitored using fluorescence microscopy in fruit cross-sections after histological fixation. To verify the yellow-coloured fluorescence signal derived from flavonols, we also stained all fruit sections with a flavonol-specific stain (diphenylboric acid 2-aminoethylester; DPBA). After DPBA staining, the same yellow-coloured fluorescence signal dramatically intensified (**Supplemental Figure B5**), confirming the yellow-autofluorescence was specific to the flavonols. As the intensity of the DPBA-stained sections often blurred the cellular detail of the sections, here we show the non-DPBA-stained autofluorescence micrographs, where both cellular structure and flavonol autofluorescence (yellow colour) are clear. Intense flavonol-specific autofluorescence (yellow) was detected in the exocarp, mesocarp, and placental tissues of stage 1 fruit (S1; **Figure 5.10 A-C**), apparently co-localizing with PA staining. Flavonol-specific autofluorescence became minimal in the mesocarp by stage 3, but remained intense in the placentae and exocarp of stage 6 fruit (**Figure 5.10 D-I**), and placentae and cuticle at stage 8 (**Figure 5.10 J-L**). Thus, flavonol localization generally followed the pattern of PAs. In addition, we detected flavonols in the developing seed. S1 seed coats show fluorescence intracellularly (likely vacuolar; **Figure 5.10 D**), which redistributes towards the periphery of the cell (**Figure 5.10 H**), and eventually being focussed in the seed coat (**Figure 5.10 L, P**). Also, we noted yellow autofluorescence in stage 3 seeds at the base of the seed attachment to the placental tissue (**Figure 5.10 H**).

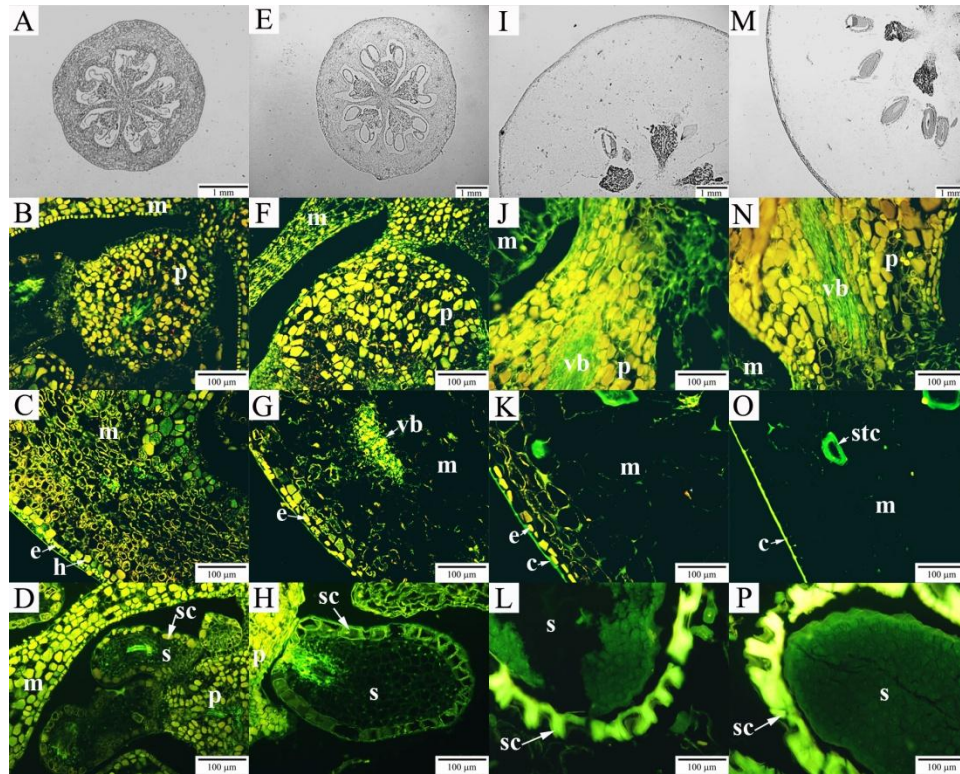


Figure 5.10: Flavonol localization in blueberry fruit cross-sections during development. Flavonols were visualized by autofluorescence (yellow colour). Light micrographs from S1 (panels A-D), S3 (panels E-H), S6 (panels I-L), and S8 (panels M-P) are shown. Light micrographs depicting the entire fruit over development (A, E, I, and M; size bar=1 mm). Fluorescence micrographs show detail of placental tissues (panels B, F, J, and N), fleshy fruit tissues (panels C, G, K, and O), and seed tissues (panels D, H, L, and P) over development (size bars=100 μ m). Brightness was adjusted for panels B, C, D, and H for better cellular structure observation. c, cuticle; e, exocarp; m, mesocarp; p, placenta; s, seed; sc, seed coat; stc, stone cell; vb, vascular bundle.

To investigate the relation between flavonoid gene transcript abundance and PA and flavonoid localization, the abundance of flavonoid gene transcripts was measured in samples enriched in specific fruit tissues. Approximately 60 early stage fruits (S3) were coarsely dissected into “inner fruit tissue” (primarily developing seeds and placentae) and “skin” (primarily exocarp and hypodermis) tissue. In addition, 45 S7 fruits were separated into seeds and skin while the mesocarp and placental tissues were discarded. The abundance of key flavonoid gene transcripts was then profiled in these tissues and compared to whole, undissected S3 and S7 fruit (**Figure 5.11**). In S3 fruit, *VcANR* and *VcLAR* gene

transcripts were detected at greater levels in the inner fruit tissues than in the skin and whole fruit (**Figure 5.11 A**), which is consistent with intense PA staining localizing to the developing seed coats and placentae (**Figure 5.9 D-F**).

Furthermore, *VcF3'H* and *VcMYB1* transcripts were abundant in both the inner fruit tissue and skin (**Figure 5.11 A**), which matches the localization of both PAs and flavonols in young fruit (S1, S3).

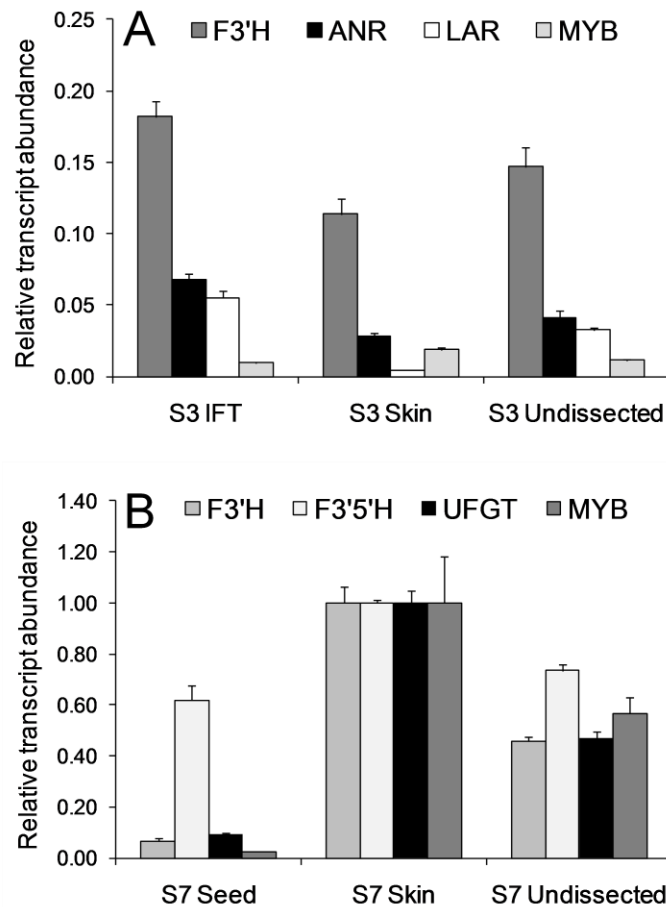


Figure 5.11: Tissue-specific flavonoid gene expression. (A) Relative abundance of *VcANR*, *VcLAR*, *VcF3'H*, and *VcMYB1* in stage 3 (S3) tissues relative to whole, undissected S3 fruits. IFT, inner fruit tissue (mainly seeds and placentae) and skin (exocarp and some mesocarp). (B) Relative abundance of *VcF3'H*, *VcF3'5'H*, *VcUFGT* and *VcMYB1* in S7 seed and skin tissues relative to whole, undissected S7 fruits. Transcript abundances are relative to geometric mean abundance of *GAPDH* and *EF1- α* reference transcripts (data are means \pm SE, n=3). In panel B the values are further normalized to the highest abundance in the three samples (set to 1.0 for each gene).

In S7 fruit, *VcANR* and *VcLAR* were not detected in appreciable amounts in any tissue (not shown), despite the presence of PAs in the exocarp and placentae of S6 and S8 fruits (**Figure 5.9 I and L**; see also **Figure 5.6**). These data support the idea that PAs are synthesized early in fruit development and are stored in cells of specific tissues throughout development including at maturity. Also in stage 7 fruit, *VcUFGT*, *VcF3'H* and *VcMYB1* transcripts were nearly exclusive to the skin tissue (**Figure 5.11 B**), which is the site of anthocyanin-based colouration in ripening fruit. However, *VcF3'5'H* transcripts were also detected in S7 seeds, as well as in the skin of S7 fruit. It is possible that some of the B-ring trihydroxylated anthocyanins, or the minor quantities of trihydroxylated flavonols (myricetin) and PAs (epigallocatechin PA subunits) found in ripe fruit were seed-derived.

Abscisic acid biosynthesis and metabolism throughout blueberry development

Like grape and other non-climacteric fruit, highbush blueberries do not exhibit a significant rise in ethylene and respiration during ripening (Frenkel, 1972). In grape berries, ABA accumulates sharply at ripening initiation (Coombe and Hale 1973) and appears likely to have a more prominent role than ethylene in this process. The similarities in growth and ripening patterns with grape prompted us to investigate the potential role of ABA in blueberry fruit. Using a previously described LC/ESI-MS/MS method (Ross et al., 2004, Owen et al., 2009), we quantified the amount of ABA throughout blueberry fruit development. Physiologically active *cis*-ABA (hereafter referred to as free ABA; **Figure 5.12 A**) began to increase at ripening initiation and peaked in S7 fruit, reaching a substantial concentration of more than 30 $\mu\text{g g DW}^{-1}$ (**Figure 5.12 B**). On a per fruit basis, the rise in free ABA starting at ripening initiation was dramatic, increasing by nearly six times between S5 and S6 (**Figure 5.12 B**). Free ABA content was maximal at S6, indicating that free ABA synthesis immediately preceded the rapid increase in anthocyanin synthesis (**Figure 5.2 A and Figure 5.8 B**).

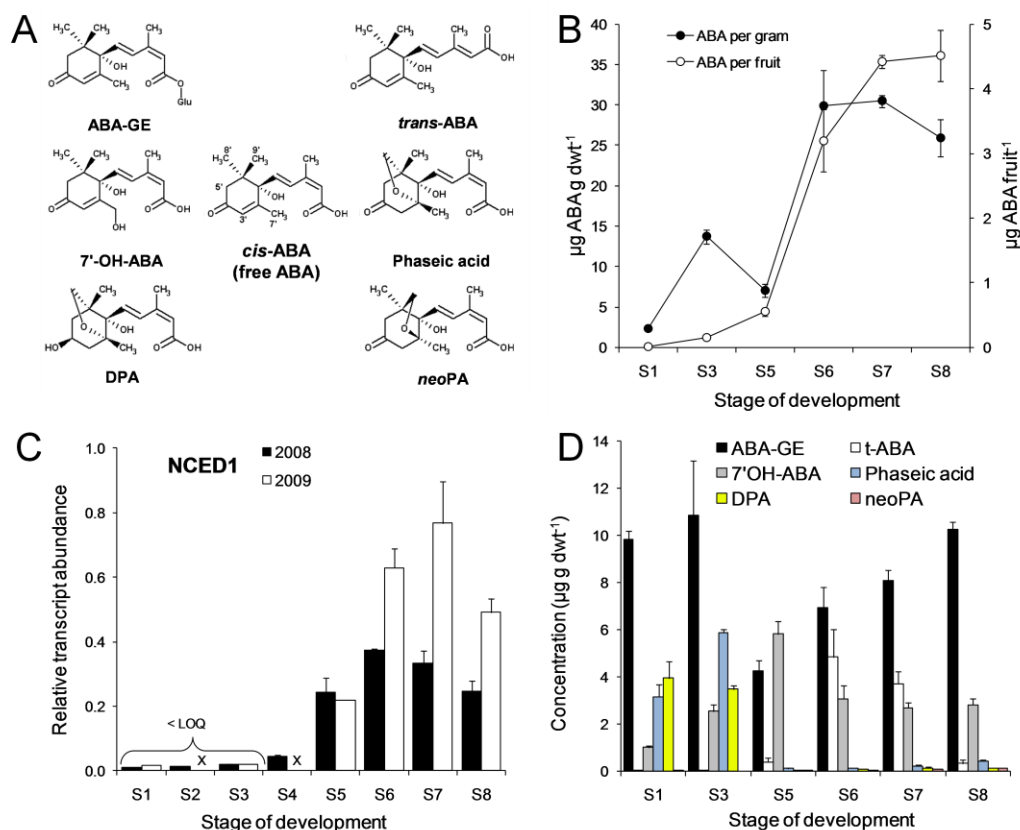


Figure 5.12: ABA metabolism and related gene expression in ripening blueberry fruit. (A) Structures of ABA and ABA metabolites. Catabolites can be produced *via* 7' hydroxylation (7'-OH-ABA), 8' hydroxylation (phaseic acid, DPA), 9' hydroxylation (*neo*PA) and conjugation (ABA-GE) pathways. (B) Free ABA concentration ($\mu\text{g g dry weight}^{-1}$) and quantity of ABA per fruit at each stage of development (data are means \pm SE, $n=3$). (C) Expression of *VcNCED1* relative to the geometric mean of *VcGAPDH* and *VcSAND* reference genes (data are means \pm SE, $n=3$ for 2008, $n=2$ for 2009). (D) Concentration of ABA metabolites and catabolites ($\mu\text{g g dry weight}^{-1}$) during development (data are means \pm SE, $n=3$). ABA-GE, ABA-glucose ester; 7'-OH-ABA, 7'-hydroxy-ABA; DPA, dihydrophaseic acid; *t*-ABA, *trans*-ABA; *neo*PA, *neo*-phaseic acid.

Free ABA is synthesized from carotenoids *via* a number of enzymatic steps, but its synthesis is rate-limited by 9-*cis*-epoxycarotenoid dioxygenase (NCED) activity (Nambara and Marion-Poll, 2005). We searched the blueberry ESTs for homologues of NCED genes, identifying one 723 bp contig (*VcNCED1*, CL1643Contig1) in the EST library that was 76.8% identical (*E* value: $1\text{e-}108$) to *Arabidopsis NCED3* (Table 5.2). The enzyme encoded by *AtNCED3* has been

functionally characterized as a 9-*cis*-epoxycarotenoid dioxygenase (Iuchi et al., 2001). Therefore, qRT-PCR was carried out to assay blueberry *VcNCEDI* transcript abundance during development. The relative *VcNCEDI* transcript abundance was very low in young, pre-ripening fruit, but then substantially increased around ripening initiation, beginning at S5 and peaking at S6 - S7 (**Figure 5.12 C**). This trend was consistent in two growing seasons; in both cases the pattern of *VcNCEDI* expression paralleled the upwards trend in free ABA accumulation. It was also similar to the rise of the anthocyanin-specific transcript *VcUFGT* (**Figure 5.7 E**), but interestingly, the *VcNCEDI* transcripts accumulated slightly earlier.

The concentration of biologically active ABA in plant tissues is the result of a combination of transport, biosynthesis, and catabolism. ABA can be metabolized through three major catabolic pathways: (a) 8'-hydroxylation leading to the formation of phaseic acid and dihydrophaseic acid (DPA); (b) 7'-hydroxylation leading to the formation of 7'-hydroxy-ABA (7'-OH-ABA); and (c) conjugation of ABA with glucose to form ABA-glucose ester (ABA-GE) (**Figure 5.12 A**). Less common is 9'-hydroxylation to form *neo*-phaseic acid (*neo*PA), though this also occurs (Nambara and Marion-Poll, 2005). The relative activity of each of these pathways depends on the plant species, tissue, developmental stage, and biological process involved (Zaharia et al., 2005b). Consequently, we measured the concentrations of all the major ABA catabolites, conjugates and isomers, including ABA-GE, 7'-OH-ABA, phaseic acid, DPA, *neo*PA and *trans*-ABA (*t*-ABA), to determine potential routes for ABA metabolism during the maturation/ripening process. All of these metabolites were detected (**Figure 5.12 D**), indicating that the three main catabolic pathways function during blueberry fruit ripening.

Early developmental stages S1 and S3 are characterized by substantial amounts of ABA-GE (around 9.8 $\mu\text{g g DW}^{-1}$) as well as increasing amounts of phaseic acid and DPA. At S1 the amount of ABA-GE was much higher relative to the amount of free ABA (**Figure 5.12 D** and **Supplemental Figure B6**). Levels of 7'-OH-ABA also increased during early maturation stages, such that at S5 the

ratio between free-ABA:7'-OH-ABA:ABA-GE was 1.7:1.4:1. During ripening (S5-S8), phaseic acid and DPA were no longer detected in significant quantities, suggesting that flux through the 8'-hydroxylation catabolic pathway is reduced during fruit ripening. ABA-GE appears to be the major catabolite during the maturation stages, peaking at $10.2 \mu\text{g g DW}^{-1}$ in S8 fruit. Notably, *trans*-ABA began to increase at S5, reaching a ratio of 6:1 for *cis:trans* forms of ABA at S6. While the presence of *trans*-ABA is thought to be due to isomerisation of natural ABA under UV light, its presence in such large amounts is intriguing. *neo*PA was detected in minute amounts, mostly in the later stages of ripening, which shows that little flux was occurring through the 9'-hydroxylation catabolic pathway.

The tissue distribution of the ABA metabolites was probed by separating seeds from fleshy ovary tissue of S5 and S8 fruits. Free ABA content was 2- and 3-fold enriched in the fruit flesh compared to the seeds of S5 and S8 fruits, respectively, and the increase in free ABA between S5 and S8 was most substantial in the flesh tissue (**Supplemental Figure B6**). Moreover, it appears that ABA catabolism was higher in the flesh of berry fruits as seeds contain low levels of catabolites. In S5 flesh, 7'-OH-ABA appears to be a major ABA catabolite along with ABA-GE, while at the ripe stage S8, conjugation to ABA-GE seems to predominate.

Discussion

While blueberry flavonoids and PAs have been studied by chemical analyses, the underlying molecular biology and developmental context have not been investigated. We have used genomics and molecular tools to identify relevant flavonoid genes, and correlated accumulation of flavonoid transcripts with flavonoid end-products over blueberry fruit development. Our results show that PA biosynthetic genes are expressed early in fruit development, and that their expression is clearly separated in time from anthocyanin-specific genes. While the signal(s) for this change in flavonoid gene expression and ripening in general are not known, the substantial and dynamic levels of ABA suggest involvement of this growth regulator in blueberry fruit ripening.

PA synthesis is developmentally and spatially delimited in blueberry fruit

PAs were present in the fruit throughout development (**Figure 5.6** and **Figure 5.9**), but PA gene transcripts (*VcANR* and *VcLAR*) were only detected very early in the developmental profile, prior to ripening (up to S4; **Figure 5.5**). PA concentration steadily declined from early development to ripening initiation, corresponding to a decline in *VcANR*, *VcLAR* and general flavonoid gene expression as well as a rapid expansion of the fruit mesocarp. However, the total amount of PAs per fruit increased until S5 (**Figure 5.6 A**). This implies that early in development sufficient pools of flavan-3-ols were produced for PA synthesis to continue through to S5. The lack of *VcANR* and *VcLAR* transcripts, decreased PA concentration, and reduced PA staining in ripening fruit (S5-S8) suggests that PA synthesis occurred exclusively early in fruit development. This also explains the absence of ESTs with similarity to ANR and LAR genes in our EST libraries, which were derived from mid- and late-stage berries.

The limitation of PA gene expression to young blueberry fruit is similar to the pattern in grapes, where *VvANR* and *VvLAR* gene expression is high in seeds and skin until just after ripening initiation (véraison) (Bogs et al., 2005). Interestingly, in grape seeds there is a dramatic spike in *VvF3'H*, *VvDFR*, and *VvLAR2* expression at ripening initiation, while *VvANR* and *VvANS* are also expressed at high levels (Bogs et al., 2005; 2006). It has been suggested that this might correspond to a burst in flavan-3-ol monomer synthesis in seeds (Downey et al., 2003a; Bogs et al., 2007). By contrast, we detected very little expression of *VcANR* or *VcLAR* at ripening initiation (S5/6) or in the seeds of S7 fruit, suggesting some differences in development of grape and blueberry seeds.

The reason why PA synthesis declines at ripening initiation is not entirely clear. It is generally assumed that PAs in young fruit skin function as feeding deterrents while seeds are still immature (Wrangham and Waterman, 1983). Since maturing seeds in S5/6 fruit had begun the browning process, *de novo* PA synthesis is likely unnecessary after this stage, and high PA levels in skin may hinder consumption by seed-dispersers. Skin PAs may also function more broadly

as antimicrobials to protect against pathogens and other fungi (Treutter, 2006), and thus help keep fruit palatable for dispersers.

DMACA staining showed that in S1 fruit PAs accumulated in all the ovary tissues as well as in developing seed coats, but that as the fruit matured, PAs in the ovary were primarily concentrated in placentae and the exocarp (skin) (**Figure 5.9**). Flavonol localization (**Figure 5.10**) and early accumulation (**Figure 5.8C and D**) during fruit development paralleled that of PAs (**Figure 5.6 and Figure 5.9**). Therefore, the same general flavonoid genes (*VcCHS*, *VcFHT* and *VcF3'H*) could contribute to both PA and flavonol synthesis. Cranberries, grapes and apples also synthesize relatively high amounts of flavonols early in ovary and fruit development (Downey et al., 2003b; Solovchenko and Schmitz-Eiberger, 2003; Vvedenskaya and Vorsa, 2004). We also detected flavonols in placentae and the seed coat, and there appeared to be redistribution of flavonols toward the cell periphery in early seed development. In *Arabidopsis* seeds, flavonols are localized in proximity to PAs, where they both become imbedded in mature seed coats by enzyme-catalyzed oxidative polymerization (Pourcel et al., 2005).

PA subunit composition reflects biosynthetic gene expression and suggests transcriptional control of PA synthesis

Blueberry PAs were composed almost entirely of epicatechin units, with only a small amount of catechin present, mostly as terminal units of PA polymers (**Table 5.3**). The predominance of epicatechin units in the polymers seems to parallel the substantially higher relative abundance of *VcANR* transcripts compared to *VcLAR* transcripts. ANR has been characterized as producing epicatechin-type flavan-3-ol monomers in a number of species (Xie et al., 2004; Bogs et al., 2005; Akagi et al., 2009a), while LAR is thought to make catechin-type flavan-3-ol monomers in species that make this compound (Tanner et al., 2003). It is tempting to hypothesize that the ANR activity is associated with PA synthesis in blueberry; however, the exact origin of the flavan-3-ol extension subunits in PA polymers is still in question.

During early fruit development when PA biosynthesis predominates, transcript abundance of *VcF3'H* was high and that of *VcF3'5'H* minimal (**Figure 5.7**). Correspondingly, fruit PA subunit composition consisted of *ortho*-dihydroxylated flavan-3-ols (mainly epicatechin) produced by B-ring hydroxylation by *F3'H*. As the fruit matured (stage 6 to 8), transcript abundance of both *VcF3'H* and *VcF3'5'H* increased. This may explain the small amounts of the trihydroxylated epigallocatechin that were detected in mature fruits (**Table 5.3**). The control of B-ring hydroxylation by *F3'H* and *F3'5'H* gene expression has been observed in other fruit. In apple, the PA hydroxylation pattern is the result of high *F3'H* gene expression and the apparent lack of an *F3'5'H* gene (Han et al., 2010). By contrast, persimmon fruit PAs are composed primarily of trihydroxylated subunits, corresponding to a high expression of a *F3'5'H* gene (Akagi et al., 2009a). Grape berries express *F3'5'H* genes only in the skin, precluding formation of trihydroxylated PA subunits in the seed (Bogs et al., 2005; 2006). Thus, the species- and tissue-specific PA subunit hydroxylation patterns appear to be largely dependent on the regulation of flavonoid hydroxylase genes, consistent with our results in blueberry. The functional significance of these hydroxylation patterns in fruit PAs needs to be studied further. Previous work has shown that flavonoids with a trihydroxylated B-ring are more efficient *in vitro* antioxidants than dihydroxylated counterparts (Halbwirth, 2010). Similarly, trihydroxylation of PAs may enhance their effectiveness as feeding deterrents against insects (Ayres et al., 1997).

The average length of blueberry fruit PAs was approximately seven subunits, linked mainly via B-type linkages, and their structure showed little variation through development (**Figure 5.6** and **Table 5.3**). It is not yet known what regulates PA length and linkage type, but these can vary depending on species and tissue (Aron and Kennedy, 2008). The blueberry mDP range is similar to polymer lengths reported for apple fruits (3-13; Sanoner et al., 1999; Hamazu et al., 2005) and grape seeds (3-9; Kennedy et al., 2000; Downey et al., 2003a). By contrast, the skin of ripe persimmon, quince and grape contain PAs with mDPs of 30 or greater (Downey et al., 2003a; Hamazu et al., 2005; Akagi et al., 2009a). Such

larger PA polymers impart astringency to these fruit, while lower MW PAs (< 6) are perceived as bitter (Robichaud and Noble, 1990).

Coexpression of VcUFGT, VcF3'5'H, and VcCytob₅ implicate these genes in anthocyanin synthesis in blueberry

While PA and flavonol levels were greater in immature blueberry fruit, anthocyanins accumulated in substantial quantities only in ripening fruit (Stage 6-8). Many of the ESTs associated with general flavonoid biosynthesis (CHS, FHT, F3'H and ANS) were enriched in the ripe berry (S7/8) EST library relative to S5/6 (**Table 5.2**), suggesting that the corresponding genes are involved in anthocyanin biosynthesis. Expression profiles of *VcCHS*, *VcFHT*, *VcDFR* and *VcANS* confirmed that these general flavonoid transcripts were highly abundant in anthocyanin-rich maturing fruits (Stage 6-8). Anthocyanin synthesis also takes place rapidly following ripening initiation in grape and bilberry, which is likewise reflected in a concerted activation of anthocyanin gene expression (Boss et al., 1996; Jaakola et al., 2002). Blueberry ripening also included the rapid accumulation of *VcUFGT* transcripts, primarily in the skin. The orthologous gene in grape (*VvF3GT*) was demonstrated to code for an anthocyanidin glycosyltransferase enzyme, and is also rapidly expressed following ripening initiation concomitant with colour development (Ford et al., 1998; Kobayashi et al., 2001). Based on sequence similarity to other functionally characterized anthocyanidin glycosyltransferases (**Supplemental Figure B2**) and the tight correlation between transcript abundance and anthocyanin accumulation, it is likely the *VcUFGT* gene product is responsible for anthocyanidin glycosylation in blueberry fruit.

Similar to *VcUFGT*, ESTs predicted to encode *VcF3'5'H* were found exclusively in the S7/8 EST library, and qRT-PCR analysis indicated that corresponding transcripts are abundant only during ripening. This pattern predicts a role in anthocyanin biosynthesis, consistent with our observation that the predominant anthocyanins in ripe fruit were glycosides of delphinidin, petunidin, and malvidin, which all require a trihydroxylated (3'4'5) B-ring produced by an

F3'5'H enzyme. As mentioned above, restriction of *VcF3'5'H* expression to the ripening stages could explain why the dihydroxylated B-ring structure predominates in PAs and flavonols.

Our expression profiles also implicate *cytochrome b₅* (*VcCytob₅*) in ripening. This gene is most homologous to *DIF-F* from petunia, which was shown to encode a specific cytochrome b₅ necessary for full activity of F3'5'H (de Vetten et al., 1999). Interestingly, *VcCytob₅* transcripts were also highly abundant early in blueberry development during PA and flavonol synthesis, which could imply its involvement in F3'H activity as well. Likewise, the putative grape ortholog of petunia *DIF-F* also displays a biphasic developmental expression pattern (Bogs et al., 2006).

VcMYB1 phylogeny and expression pattern suggest a broad role in regulation of flavonoid synthesis

The synthesis of PAs, anthocyanins and flavonols is known to be regulated by a network of MYB transcription factors. Two main types of MYB factors have been implicated in PA regulation in plants. The *Arabidopsis TT-2* gene defines the first type, and regulates genes encoding general flavonoid and PA-specific enzymes in the seed coat. It is closely related to the stress-inducible *PtMYB134* gene which regulates leaf PAs in *Populus* (Mellway et al. 2009). A second type of PA-regulatory MYB was defined by the grape *VvMYBPA1* gene (Bogs et al., 2007). However, grape was subsequently shown to also require a TT-2 like MYB (*VvMYBPA2*) to regulate PAs in berries, which works in concert with *VvMYBPA1* (Terrier et al. 2009). Anthocyanin-regulatory MYBs (*VvMYBA1/2*) have also been characterized in grape (Kobayashi et al., 2002).

Surprisingly, in the blueberry EST libraries we did not find a homolog of the anthocyanin-specific MYB factors such as *VvMYBA1*. Rather, we identified *VcMYB1*, a likely ortholog of grapevine *VvMYBPA1* (**Supplemental Figure B3**). The latter is highly expressed in young fruit, and acts by activating promoters of *VvANR*, *VvLAR* and general flavonoid genes (Bogs et al., 2007; Terrier et al., 2009). Likewise, preliminary *in vivo* transcriptional activation assays using

promoter-luciferase fusion constructs indicated that *VcMYB1* activated the *Arabidopsis ANR* promoter, but not an anthocyanin *UFGT* gene promoter from apple (M. Zifkin, A. Gesell, and C.P. Constabel, unpublished data). This would be consistent with a role of *VcMYB1* in PA synthesis. Nevertheless, the *VcMYB1* gene is also highly expressed during ripening initiation (in skin), when *VcANR* and *VcLAR* transcript abundance is low (**Figure 5.5**). A similar expression pattern was observed for the grape *VvMYBPA1* (Bogs et al. 2007). Therefore, these MYBs may act as activators of PA synthesis early in development, but also contribute to anthocyanin synthesis during ripening via activation of general flavonoid genes. This would likely necessitate a negative regulator of PA-specific genes during ripening to prevent reactivation of the PA pathway (Terrier et al., 2009). Further work is necessary to unequivocally demonstrate the functionality and specificity of *VcMYB1* in the context of blueberry fruit development.

Activation of ABA metabolism during blueberry ripening

Our analysis revealed a dramatic increase in ABA at ripening initiation, reaching concentrations exceeding $30 \mu\text{g g DW}^{-1}$ in ripe fruits, primarily in flesh tissue (**Figure 5.12** and **Supplemental Figure B6**). This concentration of free ABA is much greater than that typically reported from other plant parts. For example, the concentration of free ABA in wild-type *Arabidopsis* seeds is generally less than $0.05 \mu\text{g g DW}^{-1}$ (Chiwocha et al., 2005), and in tomato (a climacteric fruit) the reported concentration is $0.2\text{-}0.5 \mu\text{g g DW}^{-1}$ throughout ripening (Zhang et al., 2009). The levels of ABA in blueberry fruit surpassed those found in grape by six-fold (Owen et al., 2009) and appear excessive for normal physiological requirements. Furthermore, ABA turnover in young green fruit (S1-S4) appears to be high, as indicated by the presence of a relatively high proportion of ABA catabolites, produced mostly *via* the 8'- and 7'-hydroxylation pathways and conjugation to glucose. At ripening initiation, by contrast, the overall quantities of catabolites were lower in comparison to the amount of free ABA. Therefore, it appears that later in berry development the ABA turnover rate is slowed. During ripening, the relative importance of the catabolic pathways

changed, so that the 8'-hydroxylation pathway products phaseic acid and DPA were reduced while *trans*-ABA increased. Moreover, we note that ABA-GE is an abundant catabolite in blueberry fruit flesh, but not seed (**Supplemental Figure B6**). The significance of these alternate catabolic pathways in the context of fruit development needs further investigation.

The accumulation pattern of ABA was consistent between two growing seasons, suggesting that the rise of ABA is part of a normal developmental program. This was confirmed by the sharp rise in expression of the *VcNCEDI* gene, which encodes 9-*cis*-epoxycarotenoid dioxygenase, the rate-limiting enzyme of ABA synthesis (Nambara and Marion-Poll, 2005). The strong correlation between ABA and *VcNCEDI* transcript levels also suggests that the ABA is synthesized locally in the fruit, rather than transported from elsewhere in the plant. Since ABA levels in blueberry are likely to be influenced by drought stress as they are in grape (Castellarin et al., 2007), some of the variation we observed in absolute levels of ABA metabolites between years may be due to water availability.

While this is the first report on ABA metabolism and biosynthetic gene expression in blueberry, in grape a rise in *VvNCEDI* and ABA accumulation around ripening initiation has been reported (Deluc et al., 2009). Furthermore, free ABA levels are enhanced by external ABA application and low water availability (Castellarin et al., 2007; Deluc et al., 2009; Koyama et al., 2009). Interestingly, both exogenous and drought-stimulated ABA lead to elevated anthocyanin synthesis and anthocyanin-related gene expression, providing a link between ABA metabolism and anthocyanin synthesis (Coombe and Hale, 1973; Peppi et al., 2008; Koyama et al., 2009; Wheeler et al., 2009). ABA application may also hasten flavonol synthesis if applied at véraison, but the effect on flavonols is much less pronounced compared to anthocyanins (Koyama et al., 2009). Likewise, there appears to be little effect of ABA on PA synthesis and gene expression (Koyama et al., 2009; Lacampagne et al., 2010). This is analogous to our results for blueberry fruit, where we found a tight correlation between *VcNCEDI* expression, ABA, and the expression of anthocyanin genes

and anthocyanin concentration, but not PA biosynthetic genes or PA concentration.

Collectively, these results implicate ABA as a key plant growth regulator in blueberry fruit development, and suggest that modulation of *VcNCED1* gene expression is a regulatory mechanism for ABA synthesis in the fruit. Whether ABA could act as a general trigger of ripening or only as an activator of some metabolic pathways is not known. The application of ABA or genetic manipulation of ABA metabolism may provide a way to modulate ripening, as well as increase the flavonoid-based antioxidant activity of blueberry fruit.

Conclusion

Our work shows that flavonoid biosynthetic pathways leading to PAs and anthocyanins are tightly regulated in developing blueberries, and that this regulation occurs at the level of gene expression. Developmental profiles and localization studies emphasize that these pathways are controlled in both time and space, suggesting important functions for their end products. The observation that PAs, anthocyanins, and flavonols are all present in the skin (exocarp) of ripe fruits, suggests this tissue is a key site for blueberry organoleptic and antioxidant properties, and general health-promoting benefits. Our study also links ABA metabolism to ripening in blueberry, corroborating the importance of this growth regulator in non-climacteric fruit ripening. Ultimately, this may provide practical benefits for control of ripening or the manipulation of fruit for enhanced flavonoids.

LITERATURE CITED

- Abrams SR, Nelson K, Ambrose SJ** (2003) Deuterated abscisic acid analogs for mass spectrometry and metabolism studies. *J Label Compd Radiopharm* **46**: 273–283
- Akagi T, Ikegami A, Suzuki Y, Yoshida J, Yamada M, Sato A, Yonemori K** (2009a) Expression balances of structural genes in shikimate and flavonoid

biosynthesis cause a difference in proanthocyanidin accumulation in persimmon (*Diospyrus kaki* Thunb.) fruit. *Planta* **230**: 899–915

Akagi T, Ikegami A, Tsujimoto T, Kobayashi S, Sato A, Kono A, Yonemori K (2009b) DkMyb4 is a Myb transcription factor involved in proanthocyanidin biosynthesis in persimmon fruit. *Plant Physiol* **151**: 2028–2045

Akagi T, Ikegami A, Yonemori K (2010) DkMyb2 wound-induced transcription factor of persimmon (*Diospyros kaki* Thunb.), contributes to proanthocyanidin regulation. *Planta* **232**: 1045–1059

Allen AC, Hellens RP, Laing WA (2008) MYB transcription factors that colour our fruit. *Trends Plant Sci* **13**: 99–102

Andersen CL, Jensen JL, Orntoft TF (2004) Normalization of real-time quantitative reverse transcription PCR data: a model-based variance estimation approach to identify genes suited for normalization, applied to bladder and colon cancer data sets. *Cancer Res* **64**: 5245

Aron PM, Kennedy JA (2008) Flavan-3-ols: nature, occurrence and biological activity. *Mol Nutr Food Res* **52**: 79–104

Ayres MP, Clausen TP, MacLean SF, Redman AM, Reichardt PB (1997) Diversity of structure and antiherbivore activity in condensed tannins. *Ecology* **78**: 1696–1712

Basu A, Rhone M, Lyons TJ (2010) Berries: emerging impact on cardiovascular health. *Nutr Rev* **68**: 168–177

Bogs J, Downey MO, Harvey JS, Ashton AR, Tanner GJ, Robinson SP (2005) Proanthocyanidin synthesis and expression of genes encoding leucoanthocyanidin reductase and anthocyanidin reductase in developing grape berries and grapevine leaves. *Plant Physiol* **139**: 652–663

Bogs J, Ebadi A, McDavid D, Robinson SP (2006) Identification of the flavonoid hydroxylases from grapevine and their regulation during fruit development. *Plant Physiol* **140**: 279–291

Bogs J, Jaffe FW, Takos AM, Walker AR, Robinson SP (2007) The grapevine transcription factor VvMYBPA1 regulates proanthocyanidin synthesis during fruit development. *Plant Physiol* **143**: 1347–1361

- Boss PK, Davies C, Robinson SP** (1996) Analysis of the expression of anthocyanin pathway genes in developing *Vitis vinifera* L. cv Shiraz grape berries and the implications for pathway regulation. *Plant Physiology* **111**: 1059–1066
- Bustin SA, Benes V, Garson JA, Hellemans J, Huggett J, Kubista M, Mueller R, Nolan T, Pfaffl MW, Shipley GL, Vandesompele J, Wittwer CT** (2009) The MIQE guidelines: minimum information for publication of quantitative real-time PCR experiments. *Clin Chem* **55**: 611–622
- Bustin SA, Nolan T** (2004) Pitfalls of quantitative real-time reverse-transcription polymerase chain reaction. *J Biomol Tech* **15**: 155–165
- Castellarin SD, Matthews MA, Di Gaspero G, Gambetta GA** (2007) Water deficits accelerate ripening and induce changes in gene expression regulating flavonoid biosynthesis in grape berries. *Planta* **227**: 101–112
- Chiwocha SDS, Cutler AJ, Abrams SR, Ambrose SJ, Yang J, Ross ARS, Kermode AR** (2005) The *ert1-2* mutation in *Arabidopsis thaliana* affects the abscisic acid, auxin, cytokinin and gibberellin metabolic pathways during maintenance of seed dormancy, moist-chilling and germination. *Plant J* **42**: 35–48
- Coombe BG, Hale CR** (1973) The hormone content of ripening grape berries and the effects of growth substance treatments. *Plant Physiol* **51**: 629–634
- Debeaujon I, Léon-Kloosterzie KM, Koornneef M** (2000) Influence of the testa on seed dormancy, germination, and longevity in *Arabidopsis*. *Plant Physiol* **122**: 403–414
- Deluc LG, Quilici DR, Decendit A, Grimplet J, Wheatley MD, Schlauch KA, Merillon J, Cushman JC, Cramer GR** (2009) Water deficit alters differentially metabolic pathways affecting important flavor and quality traits in grape berries of Cabernet Sauvignon and Chardonnay. *BMC Genomics* **10**: 212
- de Vetten N, ter Horst J, van Shaik H, de Boer A, Mol J, Koes R** (1999) A cytochrome *b*₅ is required for full activity of flavonoid-3'5'-hydroxylase, a cytochrome P₄₅₀ involved in the formation of blue flower colours. *Proc Nat Acad Sci* **96**: 778–783
- Downey MO, Harvey JS, Robinson SP** (2003a) Analysis of tannins in seeds and skins of Shiraz grapes throughout berry development. *Aust J Grape Wine R* **9**: 15–27

- Downey MO, Harvey JS, Robinson SP** (2003b) Synthesis of flavonols and expression of flavonol synthase genes in the developing grape berries of Shiraz and Chardonnay (*Vitis vinifera* L.). *Aust J Grape Wine Res* **9**: 110–121
- Dubos C, Stracke R, Grotewold E, Weisshaar B, Martin C, Lepiniec L** (2010) MYB transcription factors in Arabidopsis. *Trends Plant Sci* **15**: 573–581
- Ford CM, Boss PK, Hoj PB** (1998) Cloning and characterization of *Vitis vinifera* UDP–glucose:flavonoid–3–*O*–glucosyltransferase, a homolog of the enzyme encoded by the maize bronze–1 locus that may primarily serve to glucosylate anthocyanidins in vivo. *J Biol Chem* **273**: 9224–9233
- Frenkel C** (1972) Involvement of peroxidase and indole-3-acetic acid oxidase isozymes from pear, tomato, and blueberry fruit in ripening. *Plant Physiol* **49**: 757–763
- Gordillo G, Fang H, Khanna S, Harper J, Phillips G, Sen CK** (2009) Oral administration of blueberry inhibits angiogenic tumor growth and enhances survival of mice with endothelial cell neoplasm. *Antiox Redox Signal* **11**: 47–58
- Gutierrez L, Mauriat M, Guenin S, Pelloux J, Lefebvre JF, Louvet R, Rusterucci C, Moritz T, Guerineau F, Bellini C, Van Wuytswinkel** (2008) The lack of a systematic validation of reference genes: a serious pitfall undervalued in reverse transcription-polymerase chain reaction (RT-PCR) analysis in plants. *Plant Biotechnol J* **6**: 609–618
- Gutmann M, Feucht W** (1991) A new method for selective localization of flavan-3-ols in plant-tissues involving glycolmethacrylate embedding and microwave irradiation. *Histochemistry* **96**: 83–86
- Hakkinen SH, Karenlampi SO, Heinonen IM, Mykkanen HM, Torronen AR** (1999) Content of the flavonols quercetin, myricetin, and kaempferol in 25 edible berries. *J Agric Food Chem* **47**: 2274–2279
- Halbwirth H** (2010) The creation and physiological relevance of divergent hydroxylation patterns in the flavonoid pathway. *Int J Mol Sci* **11**: 595–621
- Hamauzu Y, Yasui H, Inno T, Kume C, Omanyuda M** (2005) Phenolic profile, antioxidant property, and anti-influenza viral activity of Chinese quince (*Pseudocydonia sinensis* Schneid.), quince (*Cydonia oblonga* Mill.), and apple (*Malus domestica* Mill.) fruits. *J Agric Food Chem* **53**: 928–934

- Han Y, Vimolmangkang S, Elena Soria-Guerra R, Rosales-Mendoza S, Zheng D, Lygin AV, Korban SS** (2010) Ectopic expression of apple F3'H genes contributes to anthocyanin accumulation in the *Arabidopsis tt7* mutant grown under nitrogen stress. *Plant Physiol* **153**: 806–820
- Hosseinian FS, Li W, Hydamaka AW, Tsopmo A, Lowry L, Friel J, Beta T** (2007) Proanthocyanidin profile and ORAC values of manitoba berries, chokecherries, and seabuckthorn. *J Agric Food Chem* **55**: 6970–6976
- Hou D-X** (2003) Potential mechanisms of cancer chemoprevention by anthocyanins. *Curr Mol Med* **3**: 149–159
- Iuchi S, Kobayashi M, Taji T, Naramoto M, Seki M, Kato T, Tabata S, Kakubari Y, Yamaguchi-Shinozaki K, Shinozaki K** (2001) Regulation of drought tolerance by gene manipulation of 9-*cis*-epoxycarotenoid dioxygenase, a key enzyme in abscisic acid biosynthesis in *Arabidopsis*. *Plant J* **27**: 325–333
- Jaakola L, Pirttila AM, Halonen M, Hohtola A** (2001) Isolation of high quality RNA from bilberry (*Vaccinium myrtillus* L.) fruit. *Mol Biotech* **19**: 201–203
- Jaakola L, Maatta K, Pirttila AM, Torronen R, Karenlampi S, Hohtola A** (2002) Expression of genes involved in anthocyanin biosynthesis in relation to anthocyanin, proanthocyanidin, and flavonol levels during bilberry fruit development. *Plant Physiol* **130**: 729–739
- Kennedy JA, Matthews MA, Waterhouse AL** (2000) Changes in grape seed polyphenols during fruit ripening. *Phytochemistry* **55**: 77–85
- Kennedy JA, Hayasaka Y, Vidal S, Waters EJ, Jones GP** (2001) Composition of grape skin proanthocyanidins at different stages of berry development. *J Agric Food Chem* **49**: 5348–5355
- Kennedy JA, Jones GP** (2001) Analysis of proanthocyanidin cleavage products following acid-catalysis in the presence of excess phloroglucinol. *J Agric Food Chem* **49**: 1740–1746
- Kennedy JA, Taylor AW** (2003) Analysis of proanthocyanidins by high-performance gel permeation chromatography. *J Chromatogr A* **995**: 99–107
- Kobayashi S, Ishimaru M, Ding CK, Yakushiji H, Goto N** (2001) Comparison of UDP-glucose:flavonoid 3-O-glucosyltransferase (UFGT) gene sequences between white grapes (*Vitis vinifera*) and their sports with red skin. *Plant Sci* **160**: 543–550

- Kobayashi S, Ishimaru M, Hiraoka K, Honda C** (2002) Myb-related genes of the Kyoho grape (*Vitis labruscana*) regulate anthocyanin biosynthesis. *Planta* **215**: 924–933
- Koerner JL, Hsu VL, Lee JM, Kennedy JA** (2009) Determination of proanthocyanidin A2 content in phenolic polymer isolates by reversed-phase high-performance liquid chromatography. *J Chromatogr A* **1216**: 1403–1409
- Kondo S, Inoue K** (1997) Abscisic acid (ABA) and 1-aminocyclopropane-1-carboxylic acid (ACC) content during growth of 'Satohnishiki' cherry fruit, and the effect of ABA and ethephon application on fruit quality. *J Hort Sci* **72**: 221–227
- Koyama K, Sadamatsu K, Goto-Yamamoto N** (2009) Abscisic acid stimulated ripening and gene expression in berry skins of the Cabernet Sauvignon grape. *Funct Integr Genomics* **10**: 367–381
- Lacampagne S, Gagné S, Gény L** (2010) Involvement of abscisic acid in controlling the proanthocyanidin biosynthesis pathway in grape skin: new elements regarding the regulation of tannin composition and leucoanthocyanidin reductase (LAR) and anthocyanidin reductase (ANR) activities and expression. *J Plant Growth Reg* **29**: 81–90
- Lau FC, Shukitt-Hale B, Joseph JA** (2005) Beneficial effects of fruit polyphenols on brain aging. *Neurobiol Aging* **26**: 128–132
- Lepiniec L, Debeaujon I, Routaboul JM, Baudry A, Pourcel L, Nesi N, Caboche M** (2006) Genetics and biochemistry of seed flavonoids. *Annu Rev Plant Biol* **57**: 405–430
- Mellway RD, Tran LT, Prouse MB, Campbell MM, Constabel CP** (2009) The wound-, pathogen-, and ultraviolet B-responsive MYB134 gene encodes an R2R3 MYB transcription factor that regulates proanthocyanidin synthesis in poplar. *Plant Physiol* **150**: 924–941
- Nagel J, Culley LK, Lu Y, Liu E, Matthews PD, Stevens JF, Page JE** (2008) EST analysis of hop glandular trichomes identifies an *O*-methyltransferase that catalyzes the biosynthesis of xanthohumol. *Plant Cell* **20**: 186–200
- Nambara E, Marion-Poll A** (2005) Abscisic acid biosynthesis and catabolism. *Annu Rev Plant Biol* **56**: 165–185

- Neto CC** (2007) Cranberry and blueberry: Evidence for protective effects against cancer and vascular diseases. *Mol Nutr Food Res* **51**: 652–664
- O'Brien TP, McCully ME** (1981) The study of plant structure, principles and selected methods. Melbourne, Australia: Termarcarphi Pty. Ltd
- Owen SJ, Lafond MD, Bowen P, Bogdanoff C, Usher K, Abrams SR** (2009) Profiles of abscisic acid and its catabolites in developing Merlot grape (*Vitis vinifera*) berries. *Am J Enol Vitic* **60**: 277–284
- Ozga JA, Saeed A, Reinecke DM** (2006) Anthocyanins and nutrient components of saskatoon fruits (*Amelanchier alnifolia* Nutt.). *Can J Plant Sci* **86**: 193–197
- Peer WA, Brown DE, Tague BW, Muday GK, Taiz L, Murphy AS** (2001) Flavonoid accumulation patterns of transparent testa mutants of Arabidopsis. *Plant Physiology* **126**: 536–548
- Peirson SN, Butler JN, Foster RG** (2003) Experimental validation of novel and conventional approaches to quantitative real-time PCR data analysis. *Nucleic Acids Res* **31**: e73
- Peppi MC, Walker MA, Fidelibus MW** (2008) Application of abscisic acid rapidly upregulated UFGT gene expression and improved colour of grape berries. *Vitis* **47**: 11–14
- Pfaffl MW** (2001) A new mathematical model for relative quantification in real-time RT-PCR. *Nucleic Acids Res* **29**: 2002–2007
- Pfaffl MW** (2004) Quantification strategies in real-time PCR. In A-Z of Quantitative PCR (Bustin, S.A., ed.). La Jolla, CA: International University Line, pp. 87–112
- Porter LJ, Hrstich LN, Chan BG** (1986) The conversion of procyanidins and prodelphinidins to cyanidin and delphinidin. *Phytochemistry* **25**: 223–230
- Pourcel L, Routaboul JM, Kerhoas L, Caboche M, Lepiniec L, Debeaujon I** (2005) TRANSPARENT TESTA10 encodes a laccase-like enzyme involved in oxidative polymerization of flavonoids in Arabidopsis seed coat. *Plant Cell* **17**: 2966–2980
- Prior RL, Cao G, Martin A, Sofic E, McEwen J, O'Brien C, Lischner N, Ehlenfeldt M, Kalt W, Krewer G, Mainland CM** (1998) Antioxidant capacity as influenced by total phenolic and anthocyanin content, maturity, and variety of *Vaccinium* species. *J Agric Food Chem* **46**: 2686–2693

- Prior RL, Lazarus SA, Cao G, Muccitelli H, Hammerstone JF** (2001) Identification of procyanidins and anthocyanins in blueberries and cranberries (*Vaccinium spp.*) using high-performance liquid chromatography/mass spectrometry. *J Agric Food Chem* **49**: 1270–1276
- Prior RL, Gu L** (2005) Occurrence and biological significance of proanthocyanidins in the American diet. *Phytochemistry* **66**: 2264–2280
- Rasmussen SE, Frederiksen H, Krogholm KS, Poulsen L** (2005) Dietary proanthocyanidins: occurrence, dietary intake, bioavailability, and protection against cardiovascular disease. *Mol Nutr Food Res* **49**: 159–174
- Reid KE, Olsson N, Schlosser J, Peng F, Lund ST** (2006) An optimized grapevine RNA isolation procedure and statistical determination of reference genes for real-time RT-PCR during berry development. *BMC Plant Biol* **6**: 27
- Robichaud JL, Noble AC** (1990) Astringency and bitterness of selected phenolics in wine. *J Sci Food Agric* **53**: 343–353
- Ross ARS, Ambrose SJ, Cutler AJ, Feurtado JA, Kermode AR, Nelson K, Zhou R, Abrams SR** (2004) Determination of endogenous and supplied deuterated abscisic acid in plant tissues by high performance liquid chromatography-electrospray ionization tandem mass spectrometry with multiple reaction monitoring. *Anal Biochem* **329**: 324–333
- Ruijter JM, Ramakers C, Hoogaars WMH, Karlen Y, Bakker O, van den Hoff MJB, Moorman AFM** (2009) Amplification efficiency: linking baseline and bias in the analysis of quantitative PCR data. *Nucleic Acids Res* **37**: e45
- Sanoner P, Guyot S, Marnet N, Molle D, Drilleau JF** (1999) Polyphenol profiles of French cider apple varieties (*Malus domestica* sp.). *J Agric Food Chem* **47**: 4847–4853
- Schnitzler JP, Jungblut TP, Heller W, Kofferlein M, Hutzler P, Heinzmann U, Schmelzer E, Ernst D, Langebartels C, Sandermann H** (1996) Tissue localization of uv-B-screening pigments and of chalcone synthase mRNA in needles of Scots pine seedlings. *New Phytol* **132**: 247–258
- Solovchenko A, Schmitz-Eiberger M** (2003) Significance of skin flavonoids for UV-B protection in apple fruits. *J Exp Bot* **54**: 1977–1984

- Tamura K, Dudley J, Nei M, Kumar S** (2007) MEGA4: Molecular Evolutionary Genetics Analysis (MEGA) software version 4.0. *Mol Biol Evol* **24**: 1596–1599
- Tanner GJ, Francki KT, Abrahams S, Watson JM, Larkin PJ, Ashton AR** (2003) Purification of legume leucoanthocyanidin reductase and molecular cloning of its cDNA. *J Biol Chem* **278**: 31647–31656
- Terrier N, Torregrosa L, Ageorges A, Violet S, Verries C, Cheynier V, Romieu C** (2009) Ectopic expression of VvMYBPA2 promotes proanthocyanidin biosynthesis in grapevine and suggests additional targets in the pathway. *Plant Physiol* **149**: 1028–1041
- Treutter D** (2006) Significance of flavonoids in plant resistance: a review. *Environ Chem Lett* **4**: 147–157
- Vandesompele J, De Preter K, Pattyn F, Poppe B, Van Roy N, De Paepe A, Speleman F** (2002) Accurate normalization of real-time quantitative RT-PCR data by geometric averaging of multiple internal control genes. *Genome Biol* **3**: 0034.1–0034.11
- Vvedenskaya IO, Vorsa N** (2004) Flavonoid composition over fruit development and maturation in American cranberry, *Vaccinium macrocarpon* Ait. *Plant Sci* **167**: 1043–1054
- Wheeler S, Loveys B, Ford C, Davies C** (2009) The relationship between the expression of abscisic acid biosynthesis genes, accumulation of abscisic acid and the promotion of *Vitis vinifera* L. berry ripening by abscisic acid. *Aust J Grape Wine Res* **15**: 195–204
- Wilson MF, Whelan CJ** (1990) The evolution of fruit colour in fleshy-fruited plants. *Am Nat* **136**: 790–809
- Wrangham RW, Waterman PG** (1983) Condensed tannins in fruits eaten by chimpanzees. *Biotropica* **15**: 217–222
- Wu X, Beecher GR, Holden JM, Haytowitz GB, Gebhardt SE, Prior RL** (2006) Concentrations of anthocyanins in common foods in the United States and estimation of normal consumption. *J Agric Food Chem* **54**: 4069–4075
- Xie DY, Sharma SB, Dixon RA** (2004) Anthocyanidin reductases from *Medicago truncatula* and *Arabidopsis thaliana*. *Arch Biochem Biophys* **422**: 91–102

- Zaharia LI, Galka MM, Ambrose SJ, Abrams SR** (2005a) Preparation of deuterated abscisic acid metabolites for use in mass spectrometry and feeding studies. *J Label Cmpd Radiopharm* **48**: 435–445
- Zaharia LI, Walker-Simmons MK, Rodríguez CN, Abrams SR** (2005b) Chemistry of abscisic acid, abscisic acid catabolites and analogs. *J Plant Growth Reg* **24**: 274–284
- Zhang M, Yuan B, Leng P** (2009) The role of ABA in triggering ethylene biosynthesis and ripening of tomato fruit. *J Exp Bot* **60**: 1579–1588
- Zhao J, Pang Y, Dixon RA** (2010) The mysteries of proanthocyanidin transport and polymerization. *Plant Physiol* **153**: 437–443

Chapter 6

Characterization of Proanthocyanidins in Pea (*Pisum sativum* L.), Lentil (*Lens culinaris* L.), and Faba bean (*Vicia faba* L.) Seeds

Introduction

PAs are present in many plant tissues and they have diverse physiological and ecological functions (Xie and Dixon, 2005). PAs accumulate in the mature seed coats of a number of plant species (Shirley, 1998; Lepiniec et al., 2006) and they likely function as protective agents against biotic and abiotic stresses (Pourcel et al., 2007). The presence of PAs in seed coats can be assessed by the appearance of brownish colouration, which is the result of PA oxidation by polyphenol oxidase (Marles et al., 2008). Seed coat-derived PAs can be soluble or insoluble at seed maturity (Naczka et al., 2000). PA insolubility is the result of oxidative cross-linking with other cell components as the seed matures (Spencer et al., 1988; Li et al., 1996; Zhao et al., 2010).

As one of the main flavonoid subclasses, PAs are widely distributed in legume species (Amarowicz et al., 2000; Prati et al., 2007). Historically, PAs were considered to be anti-nutritional components in pulse (grain legume seeds) nutritional studies because of their ability to precipitate proteins and reduce the bioavailability of some minerals (Wang et al., 1998). However, recent research on the role of PAs as beneficial plant-based components in the human diet has led to renewed interest in this class of flavonoids in food crops (Ariga, 2004). Several recent nutritional studies have found that PAs in common fresh fruits (including grapes, blueberries, and apples), wines, grape seed extract, and chocolate, have potential beneficial health effects including antioxidant, anti-diabetic, anti-carcinogenic, and anti-inflammatory activities (Foo et al., 2000; Murphy et al., 2003; Lee et al., 2008). PAs in legume seeds exhibit remarkable antioxidant activity *in vitro* (Amarowicz et al., 2000); however, more detailed PA structural

information is needed for a better understanding of the PA structure-bioactivity relationship. The characterization of PAs in grain legume seeds has, in general, received minimal attention to date. The majority of PA studies in legume seeds used approximate analysis methods to estimate total PA content (Wang et al., 1998).

The first objective of this study was to better understand PA diversity and accumulation in the seeds of the commonly consumed grain legumes of pea (*Pisum sativum* L.), lentil (*Lens culinaris* L.), and faba bean (*Vicia faba* L.). To this end, PAs in the mature seeds of specific cultivars of these grain legumes were identified and quantified. The second objective was to determine the temporal and spatial profiles of PA accumulation in pea seed coat tissue over development, with the goal of further understanding PA biosynthesis and accumulation in this PA accumulating tissue for potential manipulation of PA type and amount through genetic means or cultural practices.

Materials and methods

Plant material

Mature air-dried seeds of all legume species used for PA analysis were grown in Barrhead or Namao, Alberta, Canada in 2008. The pea (*Pisum sativum* L.) cultivars studied were ‘Canstar’, a yellow-seeded field pea with clear-coloured seed coats and yellow embryos; ‘Cebeco 1478’, an orange-seeded orange pea with clear-coloured seed coats and orange embryos; ‘Courier’, ‘CDC Acer’, and ‘CDC Rocket’, maple-type field peas consisting of brown-speckled seed coats and yellow embryos; ‘Solido’, a marrowfat-type field pea with brown seed coats and yellow embryos; and ‘Lan3017’, a field pea with brown seed coats and yellow embryos (**Figure 6.1**). The lentil (*Lens culinaris* L.) cultivars used were ‘CDC LeMay’, a small-seeded French-type with dark green/brown speckled seed coats and yellow embryos; ‘CDC Redberry’, a small-seeded type with brown seed coats and red embryos; and ‘CDC Plato’, a large-seeded type with greenish brown seed coats and yellow embryos (**Figure 6.1**). The faba bean (*Vicia faba* L.) cultivars used were ‘CDC Fatima’, a small-seeded type with brown seed coats and yellow

embryos; and ‘Snowbird’, a small-seeded type with pale-yellow seed coats and greenish yellow embryos (Figure 6.1).

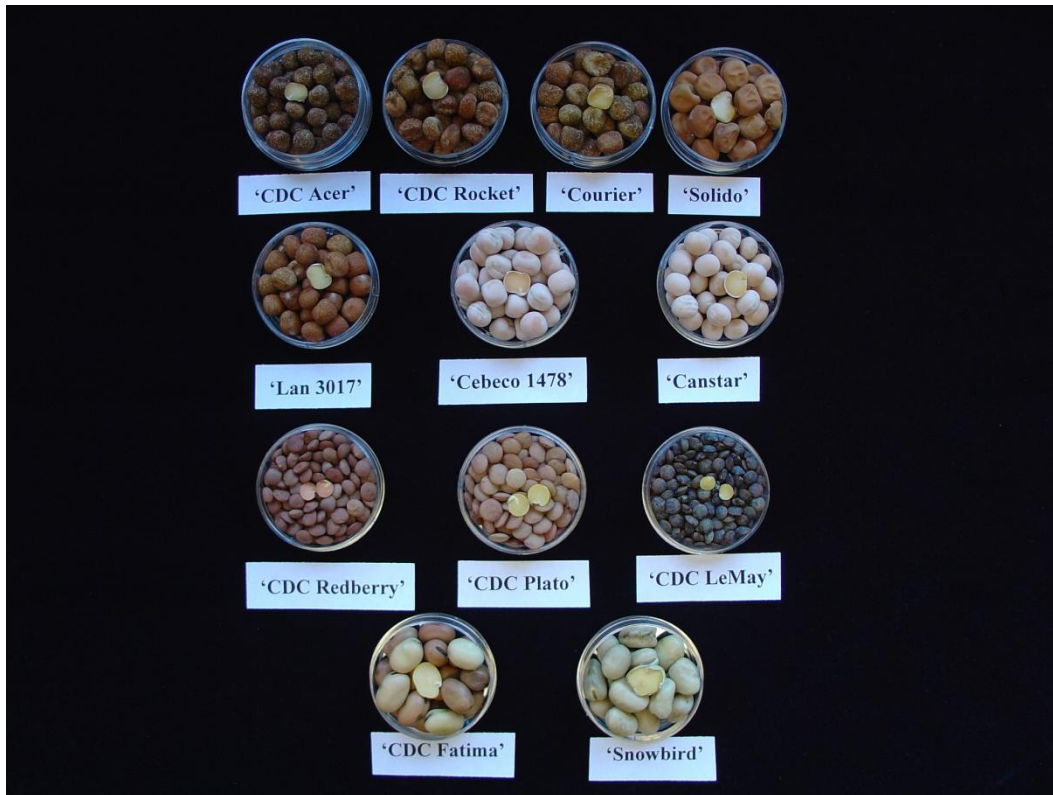


Figure 6.1: Mature legume grain seeds from pea (*Pisum sativum* L.), lentil (*Lens culinaris* L.), and faba bean (*Vicia faba* L.) used in this study. The pea cultivars are CDC Acer, CDC Rocket, Courier, Solido, Lan3017, Cebeco 1478, and Canstar. The lentil cultivars are CDC Redberry, CDC Plato, and CDC LeMay. The faba bean cultivars are CDC Fatima and Snowbird.

For PA characterization in developing pea seed coats, seeds of ‘Canstar’ and ‘Courier’ were planted at an approximate depth of 2.5 cm in 3-L plastic pots (3 seeds per pot) in Sunshine #4 potting mix (Sun Gro Horticulture, Vancouver, Canada) and sand (1:1). Plants were grown in a climate-controlled growth chamber at the University of Alberta with a 16 h-light/8 h-dark photoperiod (19°/17°C) with an average photon flux density of 383.5 $\mu\text{E}/\text{m}^2\text{s}$ (measured with a LI-188 photometer, Li-Cor Biosciences, Lincoln, NE). Flowers at anthesis (full bloom) were tagged daily and pods 10, 12, 15, 20, 25, 30, and 35 days after anthesis (DAA) were harvested onto ice. The seed coats were separated from the

embryos (immediately after harvesting) and seed coat cross sections approximately 1 mm wide and 3 mm long were dissected out from the middle region of cotyledon side for use in the PA localization study. These sections were merged into a fixing solution and the remaining seed coat material was stored at -80°C. Mature green leaves of black currant (*Ribes nigrum*) which were extracted to provide a gallicocatechin-(4 α →2)-phloroglucinol (GC-P) standard were collected from the University of Alberta Research Farm, Edmonton, Alberta.

Chemicals

All organic solvents (used for extraction, purification, and HPLC mobile phases) and formic acid (ACS grade) were purchased from Fisher Scientific (Ottawa, ON, Canada). (+)-Catechin hydrate, (-)-epicatechin, (-)-epicatechin gallate, (-)-epigallocatechin, (-)-gallocatechin, (-)-catechin gallate, (-)-epigallocatechin gallate, (-)-gallocatechin gallate, taxifolin, phloroglucinol, trifluoroacetic acid (TFA), L-ascorbic acid, hydrochloric acid (36.5 ~ 38 %), 1-butanol, 4-(dimethylamino)cinnamaldehyde (DMACA), and TOYOPEARL resin (HW-40F) were purchased from Sigma (Oakville, ON, Canada). Formaldehyde, glutaraldehyde, and Spurr's resin were purchased from Electron Microscopy Sciences (Hatfield, PA, USA). Crude grape skin PA standard was kindly provided by Dr. J. Kennedy (California State University, Fresno, CA, USA) and the standard was prepared following the extraction and purification procedures described in Kennedy and Jones (2001).

Extraction and purification of proanthocyanidins

Whole seeds of pea, lentil, and faba bean (5-10 g) were ground to a fine powder in a small food processor, and frozen seed coats of 'Courier' (approximately 5 g) were ground to a fine powder in liquid nitrogen using a mortar and pestle. These samples were extracted with 66% (v/v) aqueous acetone (10 mL per g sample) in a 250 mL Erlenmeyer flask. Flasks containing the extraction mixture were immediately sparged with nitrogen to minimize the oxygen content in the flask head-space and closed with glass stoppers.

Subsequently, the flasks were placed on a rotary shaker at 100 rpm at 4 °C in the dark for 24 hours. Extracts were then filtered through a Buchner funnel with Whatman[®] # 1 filter paper under moderate vacuum. The residue was rinsed with 66 % aqueous acetone, the extracts and rinses were pooled, and the acetone was removed under vacuum using a Speed-Vac concentrator (AES 2000, Savant, NY, USA). The remaining aqueous extract was partitioned with chloroform (1:3 v/v, chloroform:extract) five times using a separatory funnel to remove lipophilic compounds and flavan-3-ol monomers. The extracts were further purified by passing them through a 4-mL bed volume column of TOYOPEARL HW 40-F resin (Supelco; column, 1.5 cm diameter × 12 cm length) preconditioned with 50% (v/v) aqueous methanol containing 0.1 % (v/v) TFA. The extract was placed onto the column and washed with five bed volumes of 50% v/v aqueous methanol with 0.1% v/v TFA and eluted with four bed volumes of 66% aqueous acetone with 0.1% v/v TFA. The acetone/TFA was removed from the extract under vacuum using a SpeedVac concentrator and the remaining aqueous extracts were freeze dried to a fine powder.

Phloroglucinolysis and HPLC analysis of PA subunits

The PA extract powder was subjected to acidic conditions to cleave the PAs into their constitutive subunits, followed by derivatization with excessive phloroglucinol (phloroglucinolysis) according to Kennedy and Jones (2001). The phloroglucinolysis reaction conditions and procedures were the same as described in Chapter 4, using a 40 min reaction time for pea seed coat PA extracts, and a 20 min reaction time for the whole legume seed samples. A 200 µL aliquot of the above reaction mixture was added to 1 ml of 40 mM sodium acetate solution to quench the reaction. A 20 µL aliquot of the diluted reaction mixture was injected onto two Chromolith RP-18e (4.6 x 100 mm) columns connected in series, protected by a guard column (Chromolith RP-18e 4.6 x 10 mm), stabilized at 30°C, using an Agilent 1200 HPLC system equipped with a Agilent G1315B diode array detector (DAD). The RP-HPLC conditions followed that described in Chapter 4. PA terminal subunits were identified by comparison of RP-HPLC-

DAD retention times and absorbance spectra with commercially available flavan-3-ol standards. Flavan-3-ol-phloroglucinol adducts were identified by comparison of RP-HPLC retention times with grape skin PA reaction products that were previously characterized. The mean degree of polymerization and the conversion yield were calculated according to the method of Kennedy and Jones (2001).

Identification of PA subunits by LC-MS/MS

For identification of the PA-derived flavan-3-ol monomers and phloroglucinol adducts, LC-MS/MS analysis was performed as described in Chapter 4. The flavan-3-ols from PA terminal subunits were identified by comparison of LC-MS/MS spectrum, RP-HPLC retention time, and DAD absorbance spectra with authentic flavan-3-ol standards. Epicatechin-(4 β →2)-phloroglucinol (EC-P) and epigallocatechin-(4 β →2)-phloroglucinol (EGC-P) were identified by the comparison of RP-HPLC retention times, DAD absorbance spectra, and mass spectrum data with grape skin PA phloroglucinol derivatization products (Kennedy and Jones, 2001). Gallocatechin-(4 α →2)-phloroglucinol (GC-P) was identified by the comparison with the RP-HPLC retention time and DAD absorbance spectra with black currant leaf PA phloroglucinol derivatization products. The presence of gallocatechin in the PA extension units of black current leaves has been previously identified by Tits et al. (1992).

PA localization in pea seed coats

Fresh seed coat tissues of 'Courier' (10, 12, 15, 20, 25, 30, and 35 DAA) and 'Canstar' (30 DAA) located adjacent to the mid-region of the cotyledons were dissected into 1 × 3 mm cross sections and immediately immersed into a fixing solution prepared according to Van Dongen et al. (2003). Briefly, the fixing solution consisted of 2.9 % paraformaldehyde, 0.2 % glutaraldehyde, 2 mM calcium chloride (CaCl₂), 10 mM sucrose, and 25 mM PIPES. The pH of the fixing solution was adjusted to 7.5 using sodium hydroxide. After five days of fixing solution infiltration under vacuum at room temperature, the tissues were rinsed three times with 25 mM PIPES buffer and dehydrated using a graded

ethanol series of 30% and 50% ethanol in 25 mM PIPES buffer (pH 7.5; v/v), followed by 70%, 96%, and 100% ethanol in water for 15 min each. After two more changes in 100% ethanol followed by two changes in propylene oxide, the tissues were then merged into 1:1 Spurr's resin and propylene oxide mixture for 2 hours. Then, the tissues were properly oriented into Spurr's resin bath and cured at 60 °C for 3 days. Tissue sections were sliced into 4 µm-thick sections using a Reichert Jung Ultracut E ultra microtome (Scotia, NY, USA), affixed onto clean slides, and placed at 60 °C until dry. For comparing PA localization in 30 DAA 'Canstar' and 'Courier' seed coats, tissue sections were stained directly with 0.1% 4-dimethylamino-cinnamaldehyde (DMACA) solution, prepared as described in Chapter 4, by incubating at 60°C for 15 min. The slides were then washed with 100% ethanol and two changes of toluene for 5 min each. Cover slides were placed on slide-mounted tissue sections using DPX mounting media (BDH Chemicals, ON, Canada). Tissue sections were observed using a Leica DMRXA microscope (Leica, Germany) with Nomarski configuration and micrographs were taken with a microscope-mounted Nikon camera (Nikon, Japan) controlled by ACT-1 software (Nikon, USA). For PA localization in developing pea seed coats, a celloidin coating was applied to all slides prior to the staining process to improve the adherence of tissue sections to the glass slides. Briefly, the slides were submerged in absolute ethanol for 10 seconds, then coated with celloidin solution (0.5% celloidin in 1:1 ethanol:ethyl ether) for 5 min, and rinsed with 70% ethanol. Tissue sections were then stained with 0.1% DMACA solution at 60°C for 30 min. The slides were washed with 100% ethanol and dehydrated with two changes of toluene for 5 min each. Cover slides were placed on slide-mounted tissue sections using DPX mounting media. Tissue sections were observed using a Zeiss AXIO scope A1 light microscope (Zeiss, Germany) and micrographs were taken with a microscope-mounted Optronics camera (Optronics, CA, USA) controlled by Picture Frame™ Application 2.3 software.

Results and Discussion

PA subunit composition and quantitation in mature pea seeds

Estimates of the PA content of various cultivars of pea have previously been reported using either a Vanillin-Hydrochloric acid (HCl) method (Igbasan et al., 1997; Wang et al., 1998) or buthanol-HCl-Fe³⁺ method (Troszynska et al., 2002). The vanillin-HCl method can overestimate PA levels because of the use of catechin as a standard and the existence of different reaction kinetics for PAs and catechin (Sun et al., 1998). The buthanol-HCl-Fe³⁺ method can underestimate PA content due to incomplete conversion of PAs into anthocyanidins (Butler et al., 1982; Makkar et al., 1999). These colourimetric-based assays are considered to be approximate assays and they do not provide data on PA subunit composition or degree of polymerization. PA concentration can also be estimated by acid-catalyzed cleavage followed by phloroglucinol derivatization (Kennedy and Jones, 2001). This method allows the determination of PA subunit composition and concentration by the comparison of the reaction product retention properties with those of flavan-3-ol standards and other well characterized PA standard reaction products. Flavan-3-ols in the PA extension units form phloroglucinol adducts at their C4 position, while terminal flavan-3-ol units are released as flavan-3-ol monomers (see **Figure 2.9**). After HPLC analysis and LC-MS confirmation of the PA phloroglucinolysis reaction products, the mean degree of polymerization (mDP) of PAs can be calculated.

Among the seven pea cultivars studied, ‘Canstar’ and ‘Cebeco 1478’ had clear-coloured seed coats. No PA subunits were detected in the RP-HPLC chromatograms of ‘Canstar’ (**Figure 6.2 A**) or ‘Cebeco 1478’ (data not shown) extracts after phloroglucinolysis. However, PA subunits were detected in the seeds of cultivars ‘Courier’, ‘Solido’, ‘Lan3017’, ‘CDC Acer’, and ‘CDC Rocket’ that had brown or brown-speckled seed coats (**Figure 6.2; Table 6.1**).

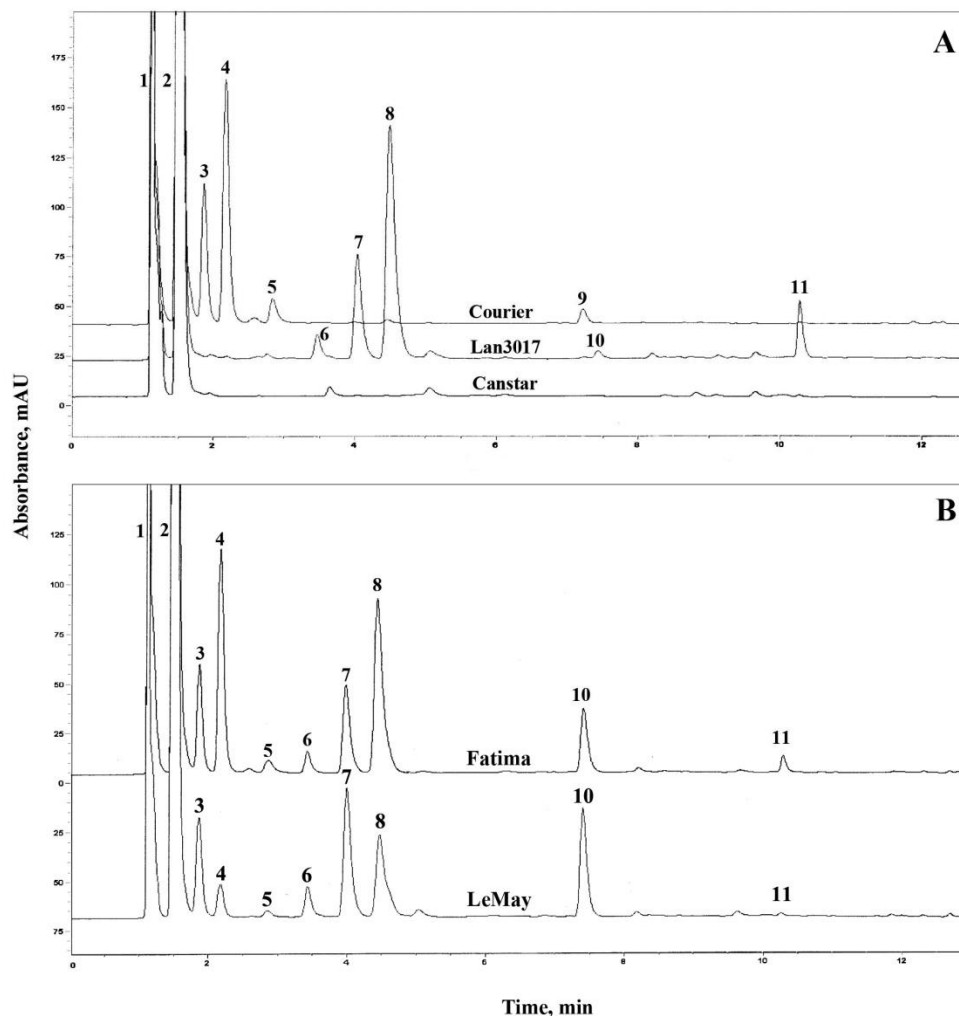


Figure 6.2: RP-HPLC-DAD chromatograms of the phloroglucinolysis products from pea (‘Courier’, ‘Lan3017’, and ‘Canstar’; A), lentil (‘LeMay’; B), and faba bean (‘Fatima’; B) seeds. 1. L-Ascorbic acid (1.1 min); 2, phloroglucinol (1.5 min); 3, gallocatechin-(4 α →2)-phloroglucinol (1.8 min); 4, epigallocatechin-(4 β →2)-phloroglucinol (2.2 min); 5, gallocatechin (2.9 min); 6, putative catechin-(4 α →2)-phloroglucinol isomer (3.4 min); 7, catechin-(4 α →2)-phloroglucinol (4.0 min); 8, epicatechin-(4 β →2)-phloroglucinol (4.4 min); 9, epigallocatechin (7.2 min); 10, catechin (7.4 min); 11, epicatechin (10.3 min).

Table 6.1: Summary of PA subunit composition following phloroglucinolysis and RP-HPLC-DAD analysis in the seeds of pea, lentil and faba bean.^a

| Peak ID | Compound | 'Courier' | 'CDC Acer' | 'CDC Rocket' | 'Solido' | 'Lan3017' | 'CDC LeMay' | 'CDC Redberry' | 'CDC Plato' | 'Fatima' |
|---------|-------------------------------|---------------------------|--------------|--------------|--------------|-----------------|--------------|----------------|--------------|--------------|
| 3 | GC-P | 29.23 ± 0.73 ^b | 30.86 ± 0.83 | 30.05 ± 0.37 | 28.99 ± 0.88 | 1.36 ± 0.02 | 32.90 ± 0.35 | 36.75 ± 0.10 | 33.83 ± 0.01 | 18.52 ± 0.30 |
| 4 | EGC-P | 55.38 ± 1.05 | 50.13 ± 1.88 | 49.63 ± 1.26 | 51.16 ± 1.27 | 0.79 ± 0.05 | 11.77 ± 0.19 | 7.62 ± 0.01 | 6.68 ± 0.47 | 42.18 ± 1.27 |
| 5 | GC | 9.88 ± 0.29 | 10.21 ± 0.60 | 10.52 ± 0.42 | 10.53 ± 0.14 | nd ^c | 4.28 ± 0.04 | 4.86 ± 0.50 | 5.75 ± 0.01 | 6.10 ± 0.70 |
| 6 | C-P isomer | nd | nd | nd | nd | 4.98 ± 0.00 | 3.87 ± 0.02 | 5.30 ± 0.07 | 5.79 ± 0.01 | 1.56 ± 0.10 |
| 7 | C-P | nd | 0.29 ± 0.01 | 0.23 ± 0.00 | 0.22 ± 0.01 | 21.41 ± 0.01 | 17.87 ± 0.05 | 24.10 ± 0.18 | 25.84 ± 0.06 | 6.93 ± 0.48 |
| 8 | EC-P | 0.37 ± 0.01 | 0.88 ± 0.02 | 0.85 ± 0.01 | 0.60 ± 0.02 | 65.37 ± 0.03 | 15.03 ± 0.06 | 7.65 ± 0.11 | 8.93 ± 0.01 | 18.41 ± 1.03 |
| 9 | EGC | 5.13 ± 0.04 | 7.41 ± 0.48 | 8.51 ± 0.45 | 8.24 ± 0.21 | nd | nd | nd | nd | nd |
| 10 | C | nd | nd | nd | nd | 0.94 ± 0.00 | 14.03 ± 0.17 | 13.57 ± 0.18 | 12.98 ± 0.36 | 5.13 ± 0.10 |
| 11 | EC | nd | 0.21 ± 0.00 | 0.21 ± 0.01 | 0.27 ± 0.02 | 5.15 ± 0.02 | 0.25 ± 0.00 | 0.15 ± 0.00 | 0.21 ± 0.03 | 1.18 ± 0.08 |
| | mDP | 6.7 ± 0.2 | 5.6 ± 0.3 | 5.2 ± 0.2 | 5.3 ± 0.1 | 16.4 ± 0.0 | 5.4 ± 0.0 | 5.4 ± 0.1 | 5.3 ± 0.1 | 8.1 ± 0.5 |
| | Conversion yield ^d | 83.9 ± 1.6 | 90.1 ± 4.6 | 87.6 ± 1.4 | 78.3 ± 4.9 | 59.1 ± 0.9 | 80.1 ± 3.5 | 82.1 ± 0.0 | 79.5 ± 1.9 | 74.1 ± 2.3 |
| | Total PA ^e | 416.0 ± 7.7 | 367.4 ± 45.6 | 293.7 ± 26.4 | 264.1 ± 14.6 | 96.7 ± 13.2 | 269.0 ± 23.9 | 377.8 ± 8.1 | 341.4 ± 15.6 | 654.3 ± 41.9 |

^aNo PA subunits were detected in the RP-HPLC chromatograms of 'Canstar' or 'Cebeco 1478' extracts after phloroglucinolysis; ^b molar % ± SE (n=2); ^c nd, not detected; ^d yield of PA extract calculated; ^e Total PA content based on characterized PA subunit, mg/ 100 g dry weight.

GC-P, galliccatechin-(4 α →2)-phloroglucinol; GC, galliccatechin; EGC-P, epigallocatechin-(4 β →2)-phloroglucinol; EGC, epigallocatechin; C-P, catechin-(4 α →2)-phloroglucinol; C, catechin; EC-P, epicatechin-(4 β →2)-phloroglucinol; EC, epicatechin.

In the seeds of pea cultivars ‘Courier’, ‘CDC Acer’, ‘CDC Rocket’ and ‘Solido’, similar PA flavan-3-ol extension and terminal unit profiles were detected (**Table 6.1**). The PA flavan-3-ol extension units were nearly exclusively prodelphinidin, where epigallocatechin (peak 4) was the most abundant flavan-3-ol extension subunit followed by gallocatechin (peak 3; **Figure 6.2 A**). The PA terminal subunits of these pea cultivars mainly consisted of gallocatechin (peak 5) and epigallocatechin (peak 9, **Figure 6.2 A; Table 6.1**). A minimal amount of epicatechin also occurred in the PA extension subunits (peak 8) in these four cultivars, and in the terminal subunits (peak 11) of three of the four pea cultivars (**Figure 6.2 A; Table 6.1**). The PA flavan-3-ol extension and terminal subunit profile of ‘Lan3017’ seeds was markedly different than that of the other pea cultivars studied (**Figure 6.2 A; Table 6.1**). ‘Lan3017’ contained nearly exclusively procyanidin moieties in the PA polymers, with the majority of the PA extension subunits consisting of epicatechin (peak 8, **Figure 6.2 A**) followed by catechin (peak 7, **Figure 6.2 A; Table 6.1**). The mDP of the PA polymers was similar in the pea cultivars ‘Courier’, ‘CDC Acer’, ‘CDC Rocket’ and ‘Solido’ at 5-7 subunits in length. However, the PA mDP was 2 to 3 times greater in ‘Lan3017’ than that in the other pea cultivars studied (**Table 6.1**). Also, ‘Lan3017’ had the lowest PA content of the five-PA containing pea cultivars (**Table 6.1**). The PA extension and terminal subunits in all PA-containing pea cultivars are assumed to be linked in a B-type configuration ($C_4 \rightarrow C_8$ or $C_4 \rightarrow C_6$, **Figure 2.8**), as the PA interflavonoid bonds were readily cleaved under the acid-hydrolysis conditions.

Mature ‘Courier’ seeds had the highest PA concentration among the seven cultivars of pea studied (**Table 6.1**). The total PA concentration in mature ‘Courier’ seeds (416.0 mg/100g fresh weight) is comparable to that of blueberries (331.9 mg/100g fresh weight), cranberries (418.8 mg/100g fresh weight), small red beans (456.6 mg/100g fresh weight), sorghum (high tannin whole grain extrudate, 447.3 mg/100g fresh weight) and hazelnuts (500.7 mg/100g fresh weight) (Gu et al., 2004).

PA subunit composition and quantitation in developing pea seed coats

PAs in legume seeds generally accumulate in the seed coat (Duenas et al., 2003); thus, this tissue was selected for studying PA accumulation over development. Similar subunit composition was observed in developing pea seed coats from 12 to 30 DAA as that found in mature seed coats of ‘Courier’ (Table 6.1 and 6.2). As discussed above, the extension subunits of PAs from both immature and mature ‘Courier’ pea seeds consist primarily of epigallocatechin followed by galliccatechin. The main flavan-3-ol subunits that occupy the terminal position in the PA polymers were also epigallocatechin and galliccatechin, the former being more abundant. Interestingly, a small amount of epicatechin was detected in the terminal subunits of PAs from immature pea seed coats, whereas none was detected in the mature seed coat tissues (**Table 6.2**).

Table 6.2: Summary of PA subunit composition following phloroglucinolysis of ‘Courier’ pea seed coats over development.

| | GC-P | EGC-P | EC-P | GC | EGC | EC |
|----------------------------|-------------------------|------------|-------------|------------|-------------|-------------|
| 12 DAA ^a | 20.5 ± 1.1 ^b | 55.8 ± 1.1 | 0.42 ± 0.01 | 17.3 ± 0.2 | 5.65 ± 0.15 | 0.38 ± 0.02 |
| 15 DAA | 24.8 ± 0.4 | 55.2 ± 0.0 | 0.38 ± 0.02 | 15.0 ± 0.2 | 4.35 ± 0.21 | 0.32 ± 0.06 |
| 20 DAA | 27.5 ± 0.3 | 52.9 ± 0.4 | 0.36 ± 0.02 | 14.4 ± 0.4 | 4.47 ± 0.11 | 0.29 ± 0.04 |
| 25 DAA | 29.2 ± 0.4 | 51.6 ± 0.6 | 0.22 ± 0.11 | 14.3 ± 0.2 | 4.51 ± 0.09 | 0.21 ± 0.01 |
| 30 DAA | 30.8 ± 1.0 | 49.8 ± 1.3 | 0.31 ± 0.02 | 14.1 ± 0.3 | 4.76 ± 0.12 | 0.19 ± 0.03 |

^a DAA, days after anthesis; ^b molar % ± SE (n=3).

GC-P, galliccatechin-(4 α →2)-phloroglucinol; EGC-P, epigallocatechin-(4 β →2)-phloroglucinol; EC-P, epicatechin-(4 β →2)-phloroglucinol; GC, galliccatechin; EGC, epigallocatechin; EC, epicatechin.

The molar percent of galliccatechin in the extension units increased as seed development progressed, while that of epigallocatechin decreased. This change in PA composition over development may reflect an increase in flow of metabolites through LAR versus ANS/ANR branch points in the flavonoid biosynthesis pathway as the seed coat matures. The mDP of PAs from young seed coats at 12

DAA was less than five, then it increased slightly (about one subunit in length) by 15 DAA and it remained at this level until 30 DAA (**Figure 6.3**). At seed maturity, the mDP increased to approximately seven. The total PA yield was calculated using the PA extract yield values and the conversion yield of PAs to known subunits. Using this calculation, we determined that the PA content increased during development, reaching a maximum level at 20 DAA. After 20 DAA, the PA content steadily decreased until seed maturation. This reduction in PA concentration may be due to the oxidation of PAs in pea seed coats by polyphenol oxidase activity (Marles et al., 2008), resulting in the brown oxidation colour observed in the seed coats of mature ‘Courier’ pea seeds.

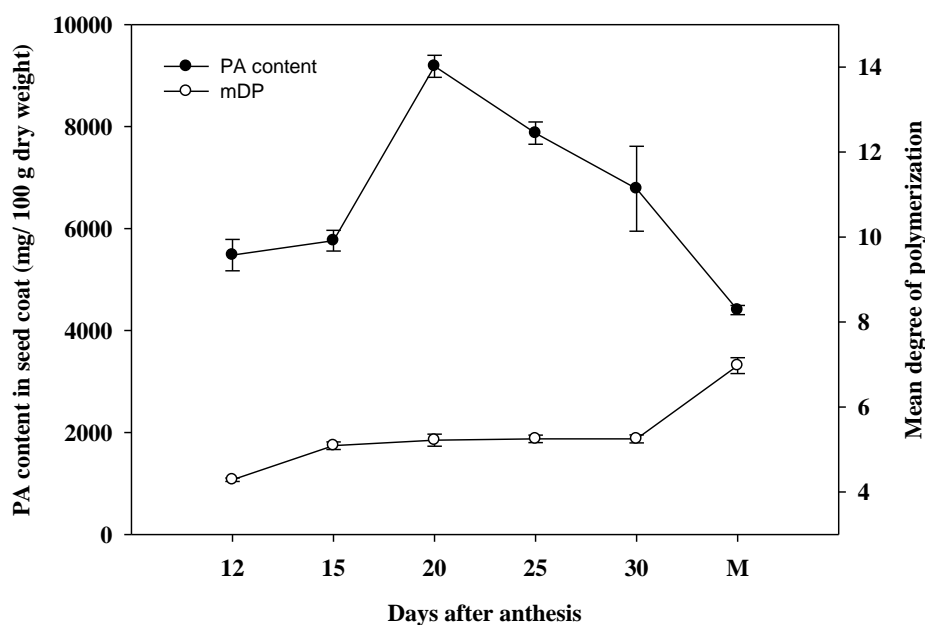


Figure 6.3: The change in PA content and mDP over seed coat development in ‘Courier’. mDP, mean degree of polymerization.

PA subunit composition and quantitation in lentil seeds

PA composition of lentil seed coats from two cultivars has been studied using a fractionation method based on C18 mini cartridges followed by both the Vanillin-HCl assay and thiolysis-HPLC analysis (Duenas et al., 2003). This method can provide an approximate range of PA polymer distribution and information about subunit composition and the mDP. Though many lentil

polyphenols with purported health benefits have been found exclusively in the seed coat (Duenas et al., 2002), lentil seeds are mostly commonly consumed after the seed coats are removed. An understanding of PA composition in lentil seeds, particularly those grown in Western Canada, will be useful for more effective use of this by-product in the future.

After phloroglucinolysis, PA subunit derivatives from the seeds of three lentil cultivars ‘CDC Lemay’, ‘CDC Redberry’, and ‘CDC Plato’ were analyzed by RP-HPLC-DAD. All cultivars exhibited similar PA extension and terminal subunit flavan-3-ol profiles (**Table 6.1**). The PA extension subunits consisted of four common flavan-3-ols: galliccatechin (peak 3), epigallocatechin (peak 4), catechin (peak 7), and epicatechin (peak 8) (**Figure 6.2 B**). The PA terminal subunits mainly consisted of galliccatechin (peak 5) and catechin (peak 10) with a minimal amount of epicatechin (peak 11) (**Figure 6.2 B; Table 6.1**). The mDP of the PAs was also similar in the three lentil cultivars studied at 5-6 subunits (**Table 6.1**). The PA polymers are assumed to be linked in a B-type configuration, similar to that in pea cultivars, as the PA interflavonoid bonds were readily cleaved under the acid-hydrolysis conditions. Among the three lentil cultivars studied, ‘CDC Redberry’ had the most darkly-coloured seed coats (**Figure 6.1**), and consistent with the colouration, the seed of this cultivar had the highest PA content (**Table 6.1**). Interestingly, both 2, 3-*trans*-flavan-3-ols (catechin and galliccatechin) and 2, 3-*cis*-flavan-3-ols (epicatechin and epigallocatechin; see **Figure 2.6**) were found in both PA extension and terminal subunits (**Figure 6.2 B; Table 6.1**). This result is in agreement with that reported by Duenas et al. (2003) for two different lentil cultivars (Pardina and Castellana). Higher abundance of 2, 3-*trans*-flavan-3-ols compared to 2, 3-*cis*-flavan-3-ols in the lentil PA subunits might be due to a higher amount of PA precursors flowing through the LAR versus the ANS/ANR branch of the flavonoid biosynthesis pathway (see **Figure 2.6**).

PA subunit composition and mDP in faba bean seeds

‘CDC Fatima’ and ‘Snowbird’ were the two faba bean cultivars used for this study. ‘CDC Fatima’ seed coats were brown and ‘Snowbird’ seed coats were pale

yellow (**Figure 6.1**). No PAs were detected in the extracts from the seeds of ‘Snowbird’ (data not shown). However, PA subunits were detected in the seeds of ‘CDC Fatima’. The PA extension subunits identified in faba bean seeds were similar to that in lentil seeds (**Figure 6.2 B; Table 6.1**). The PA terminal subunits consisted of galliccatechin (peak 5), catechin (peak 10), and epicatechin (peak 11, **Figure 6.2 B; Table 6.1**), which is in agreement with the published values for the cultivar ‘Alfred’ (Merghem et al., 2004). However, in ‘Alfred’, catechin (2, 3-*trans*-flavan-3-ols) was the most abundant PA extension subunit (Merghem et al. 2004), while in ‘Fatima’ epigallocatechin (2, 3-*cis*-flavan-3-ol) was the most abundant PA extension subunit (**Figure 6.2 B**). The differences observed between these cultivars may be due to differences in the activities of F3'5'H and F3'H (responsible for B-ring hydroxylation) as well as LAR versus ANS/ANR branch pathway activities between these genotypes.

Phloroglucinolysis product confirmation by LC-MS

Table 6.3 summarizes the molecular ion and fragment ion masses of the legume PA phloroglucinolysis products obtained using LC-MS analysis. The following compound structures were confirmed by their HPLC retention times and molecular ion and fragment ion masses: epigallocatechin-(4 β →2)-phloroglucinol, galliccatechin, catechin-(4 α →2)-phloroglucinol, catechin, epicatechin-(4 β →2)-phloroglucinol, epigallocatechin, and epicatechin. The presence of galliccatechin (GC) in the PA extension subunits was previously described in black currant (*Ribes nigrum*) leaves (Tits et al., 1992). In this study, a PA extract of black currant leaves was subjected to phloroglucinolysis followed by RP-HPLC-DAD analysis to serve as a reference standard for GC-P. The putative GC-P compound from the pea, lentil and faba bean extracts (peak 3; **Figure 6.2 A and B**) had an identical retention time and absorbance spectra as the GC-P reaction product from the black current PA extract (data not shown). Consistent with these data, the molecular ion mass of the putative GC-P was 429 ([M-H]) with fragment ions 303, 261, and 177, and the putative GC-P eluted from the RP-HPLC column prior to EGC-P, as expected for GC-P (**Table 6.3**).

Another unknown compound (peak 6 in **Figure 6.2 A** and **6.2 B**) had a molecular ion mass of 413 and fragment ion masses of 287 and 261. These ion masses are consistent with that of C-P and EC-P. However, the retention time of the peak 6 compound precedes that of both C-P and EC-P. This compound was found in the phloroglucinolysis products of ‘Lan3017’, the three lentil cultivars, and the faba bean cultivar CDC Fatima. In a previous study, after thiolysis of a PA extract of lentil seed coats Duenas et al. (2003) found that catechin from the PA extension units formed two catechin thiol adducts (benzyl mercaptan-derivatives) in an approximately 1: 4 ratio, while epicatechin formed only one thiol 3, 4-*trans*-adduct (personal communication). It appears that the formation of flavan-3-ol 3, 4-*trans*-adducts is less stereo-specifically limited for catechin than for epicatechin, and it is likely that the compound in peak 6 (**Figure 6.2 A** and **6.2 B**) is an isomer of C-P (**Figure 6.4**). NMR would be required to confirm the structure of the C-P isomer. Possible gallocatechin-(4 α →2)-phloroglucinol and catechin-(4 α →2)-phloroglucinol ion fragmentation patterns in negative ion mode LC-MS are presented in **Figure 6.5** according to the major fragment ions we have observed (**Table 6.3**).

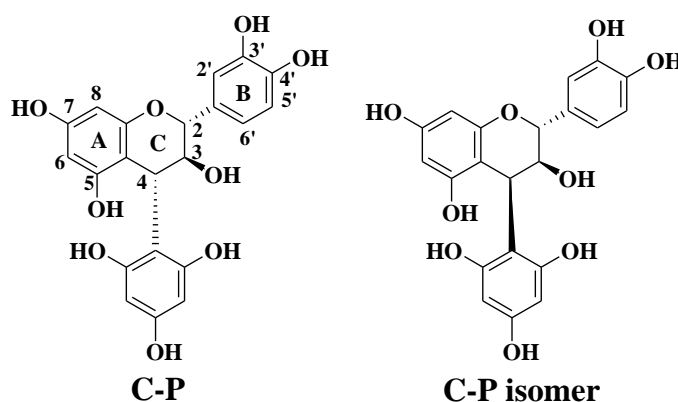


Figure 6.4: Chemical structures of catechin-(4 α →2)-phloroglucinol and putative catechin-(4 α →2)-phloroglucinol isomer. C-P, catechin-(4 α →2)-phloroglucinol.

Table 6.3: Characterization of phloroglucinolysis products from pea, faba bean and lentil seeds using LC-MS analysis.

| Compound | Species | Cultivar | t_R (min) ^a | [M-H] ^{-b} | Fragment ions |
|------------|-----------|-----------|--------------------------|---------------------|-------------------------|
| GC-P | pea | 'Solido' | 7.4 | 429 | 303, 261, 177 |
| | lentil | 'LeMay' | 7.6 | 429 | 303, 261, 177 |
| | faba bean | 'Fatima' | 7.5 | 429 | 303, 261, 177 |
| EGC-P | pea | 'Solido' | 9.6 | 429 | 303, 261, 177 |
| | lentil | 'LeMay' | 9.7 | 429 | 303, 261, 177 |
| | faba bean | 'Fatima' | 9.7 | 429 | 303, 261, 177 |
| GC | pea | 'Solido' | 16.8 | 305 | 219, 137 |
| | lentil | 'LeMay' | 16.7 | 305 | 287, 219, 163, 137 |
| | Faba bean | 'Fatima' | 16.8 | 305 | 261, 170, 137 |
| | Standard | | 18.1 | 305 | 231, 219, 179 |
| C-P isomer | pea | 'Lan3017' | 17.2 | 413 | 287, 261, 161, 135 |
| | lentil | 'LeMay' | 17.3 | 413 | 287, 261, 161, 133 |
| | faba bean | 'Fatima' | 17.2 | 413 | 287, 261, 163 |
| C-P | pea | 'Lan3017' | 21.3 | 413 | 287, 261, 217, 175 |
| | lentil | 'LeMay' | 21.2 | 413 | 287, 261, 217, 125 |
| | Faba bean | 'Fatima' | 21.2 | | 287, 261, 217, 175, 133 |
| EC-P | pea | 'Lan3017' | 22.1 | 413 | 287, 261, 175 |
| | lentil | 'LeMay' | 22.2 | 413 | 287, 261, 161 |
| | Faba bean | 'Fatima' | 22.2 | 413 | 287, 261, 217, 175, 133 |
| EGC | pea | 'Solido' | 33.4 | 305 | 219, 137 |
| | Standard | | 34.4 | 305 | 219, 179, 137 |
| C | pea | 'Lan3017' | 33.3 | 289 | 245, 173, 137 |
| | lentil | 'LeMay' | 33.4 | 289 | 245, 203, 137 |
| | faba bean | 'Fatima' | 33.5 | 289 | 245, 137 |
| | Standard | | 33.2 | 289 | 245, 205, 137 |
| EC | pea | 'Lan3017' | 44.3 | 289 | 245, 137 |
| | lentil | 'LeMay' | 44.4 | 289 | 245, 174, 137 |
| | faba bean | 'Fatima' | 44.4 | 289 | 245, 203, 137 |

^a Retention time on LC-MS. The gallicocatechin and epigallocatechin standards were run at different times with the legume samples leading to some variation in retention time between the same compounds in the standards and samples.

^b MS was run in the negative mode and all the molecular ions are [M-H]⁻.

GC-P, gallicocatechin-(4 α →2)-phloroglucinol; EGC-P, epigallocatechin-(4 β →2)-phloroglucinol; EC-P, epicatechin-(4 β →2)-phloroglucinol; C-P, catechin-(4 α →2)-phloroglucinol; C, catechin; GC, gallicocatechin; EGC, epigallocatechin; EC, epicatechin.

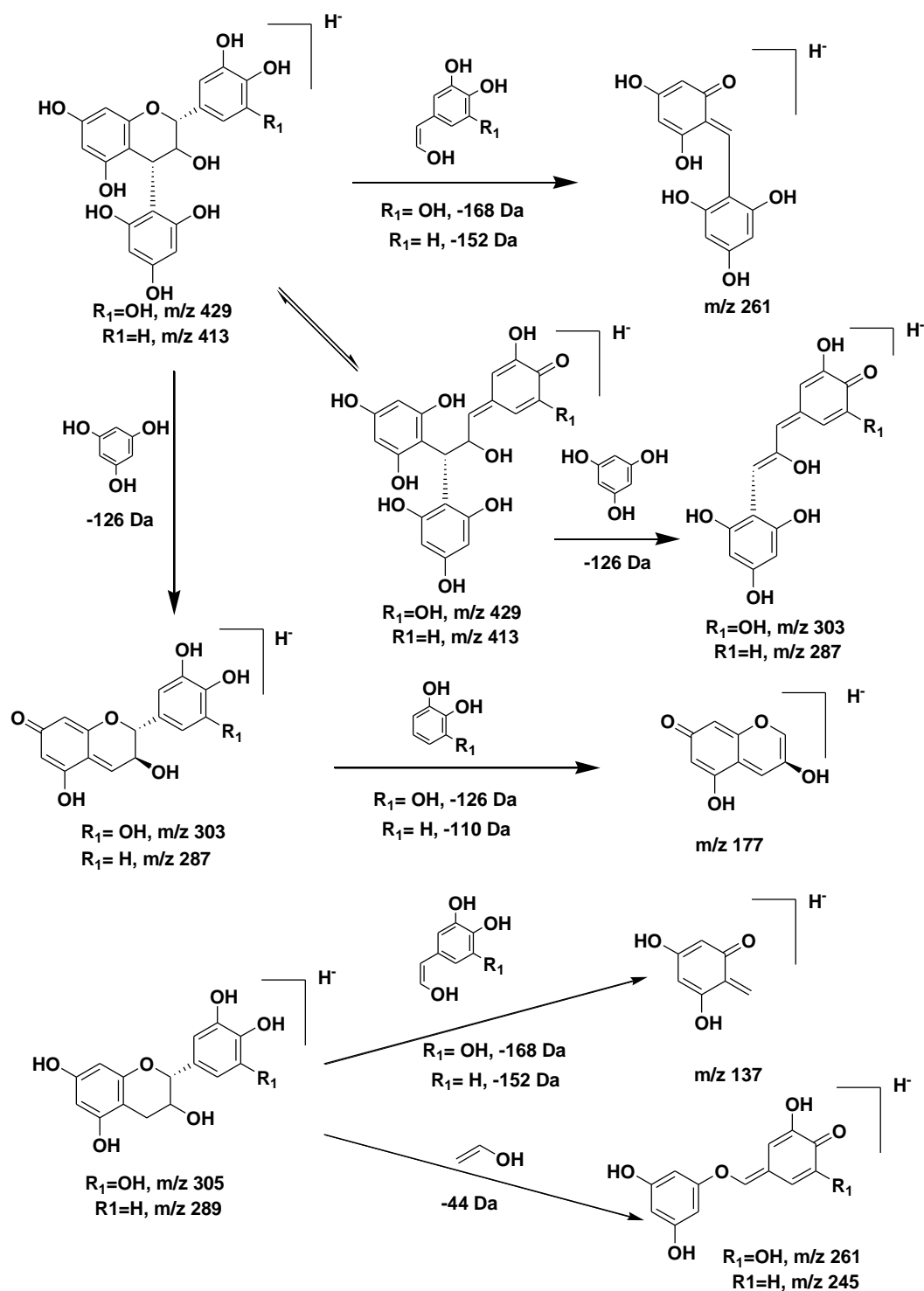


Figure 6.5: Proposed MS fragmentation patterns of gallocatechin-(4α→2)-phloroglucinol, catechin-(4α→2)-phloroglucinol, gallocatechin, and catechin.

Localization of PAs in developing 'Courier' pea seed coats

During pea seed development, seed coats protect the embryo from various stresses and provide nutrients to sustain embryo growth (Van Dongen et al., 2003). In *Medicago truncatula*, a model legume plant, the majority of PAs are found in the seed coat, with only a minimal level of PAs in the other parts of the seed (Pang et al., 2007). However, minimal information exists on the sites of PA accumulation within the seed coat, and how PA localization changes over development. In order to address these questions, we localized PAs in 'Courier' pea seed coats over development using a DMACA staining method (Gutmann and Feucht, 1991). PAs mainly accumulated intracellularly (likely the vacuole) in the cells of the epidermal and ground parenchyma layers of the seed coat throughout development (**Figure 6.6**). As the seed matures, the cells of epidermal layer of the seed coat sclerify and the intercellular space and vacuolar size decreases. As a result, the vacuolar-localized PAs are visualized in the inner side of the epidermal layer (non-sclerified portion of the epidermal cells; **Figure 6.6**). As PAs can serve as protective agents during biotic and abiotic stress conditions, it is understandable that PAs localize to the outer-most layer (epidermal layer) of the seed. As parenchyma cells often function in a storage capacity, PAs may be stored in the vacuoles of the cells of the ground parenchyma layer of the seed coat where they could be transported to their site of function during various stress conditions. It may be that the PAs stored in the ground parenchyma cells account for the majority of the soluble PAs detected in the seed coats.

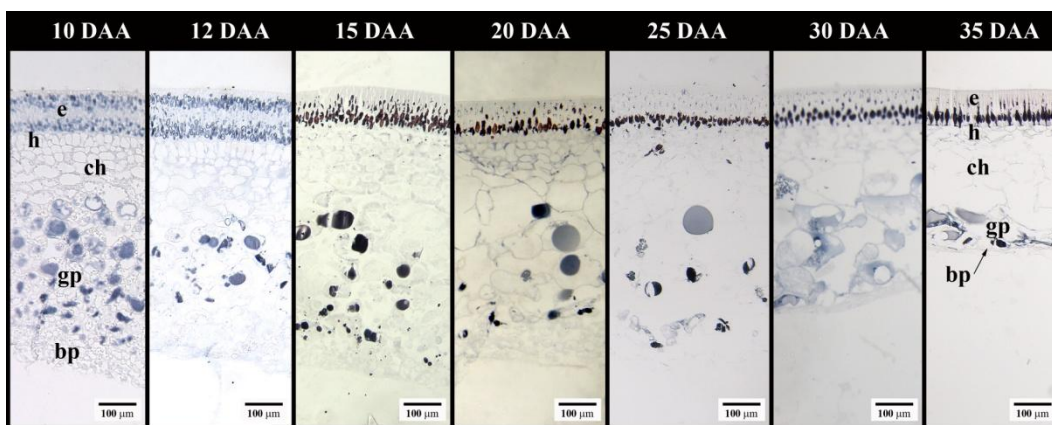


Figure 6.6: Cotyledon mid-region cross sections of ‘Courier’ pea seed coats. e, epidermal layer; h, hypodermal layer; ch, chlorenchyma layer, gp, ground parenchyma layer; bp, branched parenchyma layer.

Localization of PAs in ‘Courier’ and ‘Canstar’ seed coats

30 DAA, ‘Courier’ and ‘Canstar’ seed coats were sectioned and stained with PA specific DMACA staining solution for understanding the difference of PA accumulation in these two cultivars. DMACA can stain not only PAs but also precursors of PAs (Abrahams et al., 2002). ‘Courier’ seed coat sections exhibited dark-blue staining in the inner epidermal and the ground parenchyma cell layers (**Figure 6.7**). However, no PA-specific staining was observed in the seed coat sections of ‘Canstar’. These data are consistent with our analytical data that suggest that PAs do not accumulate in ‘Canstar’ pea seed coats. Data of seed coat development morphology of these two cultivars of pea are presented in Appendix C.

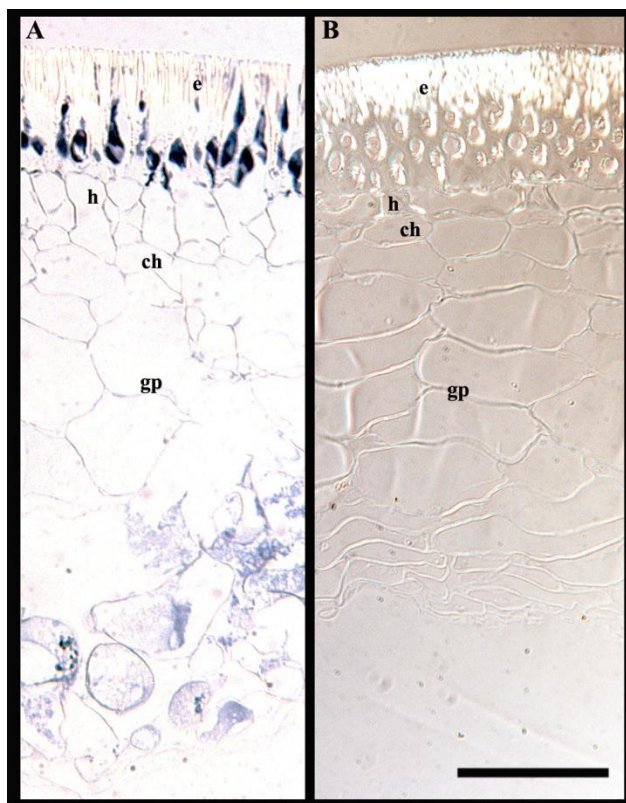


Figure 6.7: Micrographs of 'Courier' and 'Canstar' seed coats stained with DMACA and observed under a Nomarski microscope. A, 30 DAA 'Courier' seed coat, showing PA-specific staining (dark-blue colour) in the epidermal and ground parenchyma layers. B, 30 DAA 'Canstar' seed coat, showing no evidence of staining. e, epidermis; h, hypodermis; ch, chlorenchyma layer; gp, ground parenchyma layer; Black scale bar = 100 μ m.

Conclusions

In summary, the results from this study indicate that seed PA accumulation profiles varied between and within legume species. Pea can be a very good legume model plant for studying PA biosynthesis since a marked variation in PA composition and levels exists among different pea cultivars. With this genetic variation within agronomically acceptable pea cultivars, there is great potential to extend the usage of these pulses in human and animal diets. Across species, pea and faba bean seeds were found to contain more 2, 3-*cis*-flavan-3-ols than 2, 3-*trans*-flavan-3-ols in their PAs. This result indicates that more substrate flows

through the ANS/ANR branch point of than the LAR branch point for the production of subunits for PA biosynthesis.

Literature cited

- Abrahams S, Tanner GJ, Larkin PJ, Ashton AR** (2002) Identification and biochemical characterization of mutants in the proanthocyanidin pathway in Arabidopsis. *Plant Physiology* **130**: 561-576
- Amarowicz R, Naczek M, Zadernowski R, Shahidi F** (2000) Antioxidant activity of condensed tannins of beach pea, canola hulls, evening primrose, and faba bean. *Journal of Food Lipids* **7**: 195-205
- Ariga T** (2004) The antioxidative function, preventive action on disease and utilization of proanthocyanidins. *Biofactors* **21**: 197-201
- Butler LG, Price ML, Brotherton JE** (1982) Vanillin assay for proanthocyanidins (condensed tannins) - Modification of the solvent for estimation of the degree of polymerization. *Journal of Agricultural and Food Chemistry* **30**: 1087-1089
- Duenas M, Hernandez T, Estrella I** (2002) Phenolic composition of the cotyledon and the seed coat of lentils (*Lens culinaris* L.). *European Food Research and Technology* **215**: 478-483
- Duenas M, Sun BS, Hernandez T, Estrella I, Spranger MI** (2003) Proanthocyanidin composition in the seed coat of lentils (*Lens culinaris* L.). *Journal of Agricultural and Food Chemistry* **51**: 7999-8004
- Foo LY, Lu YR, Howell AB, Vorsa N** (2000) A-type proanthocyanidin trimers from cranberry that inhibit adherence of uropathogenic P-fimbriated *Escherichia coli*. *Journal of Natural Products* **63**: 1225-1228
- Gu LW, Kelm MA, Hammerstone JF, Beecher G, Holden J, Haytowitz D, Gebhardt S, Prior RL** (2004) Concentrations of proanthocyanidins in common foods and estimations of normal consumption. *Journal of Nutrition* **134**: 613-617
- Gutmann M, Feucht W** (1991) A new method for selective localization of flavan-3-ols in plant-tissues involving glycolmethacrylate embedding and microwave irradiation. *Histochemistry* **96**: 83-86

- Igbasan FA, Guenter W, Slominski BA** (1997) Field peas: Chemical composition and energy and amino acid availabilities for poultry. *Canadian Journal of Animal Science* **77**: 293-300
- Kennedy JA, Jones GP** (2001) Analysis of proanthocyanidin cleavage products following acid-catalysis in the presence of excess phloroglucinol. *Journal of Agricultural and Food Chemistry* **49**: 1740-1746
- Lee YA, Cho EJ, Yokozawa T** (2008) Effects of proanthocyanidin preparations on hyperlipidemia and other biomarkers in mouse model of type 2 diabetes. *Journal of Agricultural and Food Chemistry* **56**: 7781-7789
- Lepiniec L, Debeaujon I, Routaboul JM, Baudry A, Pourcel L, Nesi N, Caboche M** (2006) Genetics and biochemistry of seed flavonoids. *Annual Review of Plant Biology* **57**: 405-430
- Li YG, Tanner G, Larkin P** (1996) The DMACA-HCl protocol and the threshold proanthocyanidin content for bloat safety in forage legumes. *Journal of the Science of Food and Agriculture* **70**: 89-101
- Makkar HPS, Gamble G, Becker K** (1999) Limitation of the butanol-hydrochloric acid-iron assay for bound condensed tannins. *Food Chemistry* **66**: 129-133
- Marles MAS, Vandenberg A, Bett KE** (2008) Polyphenol oxidase activity and differential accumulation of polyphenolics in seed coats of pinto bean (*Phaseolus vulgaris* L.) characterize postharvest colour changes. *Journal of Agricultural and Food Chemistry* **56**: 7049-7056
- Merghem R, Jay M, Brun N, Voirin B** (2004) Qualitative analysis and HPLC isolation and identification of procyanidins from *Vicia faba*. *Phytochemical Analysis* **15**: 95-99
- Murphy KJ, Chronopoulos AK, Singh I, Francis MA, Moriarty H, Pike MJ, Turner AH, Mann NJ, Sinclair AJ** (2003) Dietary flavanols and procyanidin oligomers from cocoa (*Theobroma cacao*) inhibit platelet function. *American Journal of Clinical Nutrition* **77**: 1466-1473
- Naczki M, Amarowicz R, Pink D, Shahidi F** (2000) Insoluble condensed tannins of canola/rapeseed. *Journal of Agricultural and Food Chemistry* **48**: 1758-1762
- Pang YZ, Peel GJ, Wright E, Wang ZY, Dixon RA** (2007) Early steps in proanthocyanidin biosynthesis in the model legume *Medicago truncatula*. *Plant Physiology* **145**: 601-615

- Pourcel L, Routaboul JM, Cheynier V, Lepiniec L, Debeaujon I** (2007) Flavonoid oxidation in plants: from biochemical properties to physiological functions. *Trends in Plant Science* **12**: 29-36
- Prati S, Baravelli V, Fabbri D, Schwarzinger C, Brandolini V, Maietti A, Tedeschi P, Benvenuti S, Macchia M, Marotti I, Bonetti A, Catizone P, Dinelli G** (2007) Composition and content of seed flavonoids in forage and grain legume crops. *Journal of Separation Science* **30**: 491-501
- Shirley BW** (1998) Flavonoids in seeds and grains: physiological function, agronomic importance and the genetics of biosynthesis. *Seed Science Research* **8**: 415-422
- Spencer CM, Cai Y, Martin R, Gaffney SH, Goulding PN, Magnolato D, Lilley TH, Haslam E** (1988) Polyphenol complexation - some thoughts and observations. *Phytochemistry* **27**: 2397-2409
- Sun BS, Ricardo-da-Silva J M, Spranger I** (1998) Critical factors of vanillin assay for catechins and proanthocyanidins. *Journal of Agricultural and Food Chemistry* **46**: 4267-4274
- Tits M, Angenot L, Poukens P, Warin R, Dierckxsens Y** (1992) Prodelphinidins from *Ribes nigrum*. *Phytochemistry* **31**: 971-973
- Troszynska A, Estrella I, Lopez-Amores ML, Hernandez T** (2002) Antioxidant activity of pea (*Pisum sativum* L.) seed coat acetone extract. *Lebensmittel-Wissenschaft Und-Technologie-Food Science and Technology* **35**: 158-164
- Van Dongen JT, Ammerlaan AMH, Wouterlood M, Van Aelst AC, Borstlap AC** (2003) Structure of the developing pea seed coat and the post-phloem transport pathway of nutrients. *Annals of Botany* **91**: 729-737
- Wang XF, Warkentin TD, Briggs CJ, Oomah BD, Campbell CG, Woods S** (1998) Total phenolics and condensed tannins in field pea (*Pisum sativum* L.) and grass pea (*Lathyrus sativus* L.). *Euphytica* **101**: 97-102
- Xie DY, Dixon RA** (2005) Proanthocyanidin biosynthesis - still more questions than answers? *Phytochemistry* **66**: 2127-2144
- Zhao J, Pang YZ, Dixon RA** (2010) The mysteries of proanthocyanidin transport and polymerization. *Plant Physiology* **153**: 437-443

Chapter 7

Summary and Conclusions

Summary of the thesis work

This thesis aims to gain new insight into the study of the biosynthesis of flavonoids (specifically anthocyanins, flavonols, and PAs) and their accumulation in fruit and seeds during growth and maturation processes. For this purpose, fruits and seeds were categorized into different developmental and maturation stages prior to further chemical analyses and localization studies. Various cultivars of saskatoon fruits were sorted into nine maturation stages, while 'Rubel' blueberry fruits were grouped into eight developmental stages according to fruit size, colour, and firmness. Pea seed samples were collected during seed development according to the length of growing date from anthesis (full bloom of flowers). Individual anthocyanins and flavonols in different cultivars of saskatoon fruits were identified using HPLC-DAD/LC-MS analysis and quantified using HPLC-DAD during fruit development and maturity in order to understand the variation of flavonoid profile across the cultivars and fruit developmental stages. After effective extraction and purification, anthocyanins and flavonols in blueberry fruits were hydrolyzed with acidic aqueous methanol, and subsequent anthocyanidins and flavonol aglycones were identified and quantified using HPLC-DAD during the fruit maturation process for matching the flavonoid profile with the flavonoid biosynthesis gene expression study. PAs are oligomers and polymers of flavan-3-ols. Due to the limitations of current analytical methods for direct PA polymer identification, PAs from saskatoon fruits, blueberry fruits, and legume seeds underwent acid-catalyzed cleavage and then cleaved products were derivatized with phloroglucinol to their subsequent flavan-3-ol phloroglucinol adducts and free flavan-3-ols. The reaction products were identified using HPLC-DAD/LC-MS, and subunit composition, average degree of polymerization, and conversion yield were determined using HPLC-DAD analysis. Anthocyanin localization was studied through direct observation of colour

distribution in the cross sections of different stages of saskatoon and blueberry fruits. Flavonol localization was studied using flavonol auto-fluorescence, and flavonols in saskatoon and blueberry fruits were stained with DPBA in order to enhance the auto-fluorescence. Cross sections of saskatoon fruits, blueberry fruits, and pea seed coats were stained with DMACA solution for localizing PAs.

General conclusions

Overall, the thesis sought to answer the following original hypotheses:

1. Flavonoid synthesis and accumulation in the fruits of *Amelanchier alnifolia* (saskatoon) and *Vaccinium corymbosum* (blueberry), and the seeds of *Pisum sativum* (pea), are developmentally and spatially regulated.

Saskatoon fruits

From the study of anthocyanin and flavonol profiles of saskatoon fruit over development (Chapter 3), we have found that anthocyanin numbers and concentrations increased in pigmented-cultivars of fruit along with fruit development and maturation process. For example, cyanidin 3-*O*-xyloside only appeared and accumulated during the ripening stages of fruit, but not in the early developmental stages of fruit. Also, total anthocyanin concentration was minimal in the early developmental stages, drastically increased in fruit ripening stages, and reached its maximum in mature fruits. Flavonol accumulation showed a biphasic pattern in saskatoon fruits during fruit development. Generally, a high level of flavonols was achieved in early fruit developmental stages; it decreased mid-way through fruit development, then increased again in the mature stages of the pigmented-cultivar fruit. PA synthesis and accumulation also followed the biphasic pattern of flavonol accumulation in saskatoon fruits. In early developmental fruits, flavonols and PAs were localized in most tissues of saskatoon fruits. In the later developmental stages, PAs and flavonols in fruit mesocarp tissues decreased and these flavonoids were more tissue-specifically accumulated, likely in the vacuoles of epidermal and placental tissues and cell

walls of seed coats. Based on these results, we can conclude that flavonoid synthesis and accumulation is tightly correlated with saskatoon fruit developmental and maturation stages.

Blueberry fruits

In the study of flavonoid accumulation during the development and ripening of blueberry fruits, we were able to combine the expression of flavonoid biosynthesis genes with the corresponding metabolite profiles. The combination of flavonoid composition, concentration, localization, and gene expression data suggests that flavonoid biosynthesis is tightly regulated at the gene expression level during fruit development. The types of anthocyanidins varied in different stages of blueberry fruits. In the early stages of blueberry fruits, anthocyanins consisted of two anthocyanin aglycones, cyanidin and delphinidin, while cyanidin was a major anthocyanidin. Methoxylated anthocyanidins such as peonidin, petunidin, and malvidin only appeared in the later maturation stages of fruits. The anthocyanidin level was low in early green fruits and reached its maximum point in mature fruits. Flavonol and PA concentrations were high in early developmental fruit and low in later maturation stages. In the ripening stages of blueberry fruit, PAs and flavonols were mainly localized in the exocarp (epidermis and hypodermis), the seed coat, and the placental tissues, while these flavonoids were ubiquitous in all the fruit tissues in early fruits. These flavonoid accumulation patterns demonstrate that flavonoid biosynthesis in blueberry fruits is also controlled in time and space.

Pea seeds

PA composition was studied in the seed coats of developing pea seed. The PA content in 'Courier' pea seed coats varied during pea seed development. The PA level was lower in early pea seed coats and reached its maximum level in 20 DAA seed coats, and then gradually decreased, possibly due to the oxidation of PAs. The average polymer length of PAs increased along with pea seed development, while PA subunit composition was consistent over pea seed development. PAs in

pea seed coat tissues were localized in the vacuoles of the epidermal layer and the ground parenchyma layer. The result shows that PA accumulation in peas is closely associated with seed growth, development, and tissue type.

2. Variation exists in the type and amount of specific flavonoids between different cultivars of the same species (among fruits of *Amelanchier alnifolia* [saskatoon] and among seeds of *Pisum sativum* [pea]), as well as among seeds of different species within the grain legume crops (pea, faba bean and lentil).

Flavonoid profiles in the various cultivars of saskatoon fruits

Anthocyanin profiles were similar among four pigmented cultivars of saskatoon fruits, while total anthocyanin contents in developing and mature fruits were different among these cultivars. Flavonols found in saskatoon fruits were all quercetin glycosides, and the glycosylation profiles of flavonols were slightly different among various saskatoon cultivars. This might be due to the fact that glycosylation was controlled by different UFGT enzyme activities and different saskatoon varieties might have different UFGT enzymes.

PA composition in different pea cultivars of pea seeds

PA subunit composition in pea seeds was different among cultivars. ‘Courier’ pea seeds contained prodelphinidin type PAs while PAs in pea *cv.* Lan3017 seeds were exclusively procyanidins. The difference might be caused by the presence and activity of B-ring hydroxylation enzymes, F3'H and F3'5'H, in different cultivars of pea seeds.

PA profile variation among legume species

Chapter 6 of the thesis examined variations of PA compositions in legume seeds. Flavan-3-ol subunit composition in PAs from pea and faba bean seeds had more 2, 3-*cis* flavan-3-ols than 2, 3-*trans* flavan-3-ols. PAs from lentil seeds consisted of more 2, 3-*trans* flavan-3-ols than 2, 3-*cis* flavan-3-ols in the three

cultivars we have studied. The variation might be due to difference in gene expressions and transcription factors in flavonoid biosynthesis.

Our work shows that flavonoid biosynthesis and accumulation in saskatoon fruits, blueberry fruits, and pea seed coats were tightly regulated temporally and tissue-specifically, and that this regulation is controlled by genes, enzymes, and transcription factors present in certain plant species, cultivars, and developmental stages. In the future, we can extend our study to the area of molecular biology and investigate genes and transcription factors involved in saskatoon fruit and legume seed flavonoid biosynthesis in order to find correlations between accumulated flavonoids and the underlying genetic control system. It is hoped that our flavonoid chemical analysis and localization data can be used in the future by metabolic engineers to find specific genes producing certain flavonoid compounds and to improve health beneficial flavonoid levels by working with tissues and developmental stages in which they are highly accumulating flavonoid compounds. The variation of PA composition within pea cultivars is an ideal model for the nutritional study of the relationship between flavonoid structure and bioactivity.

Appendix A

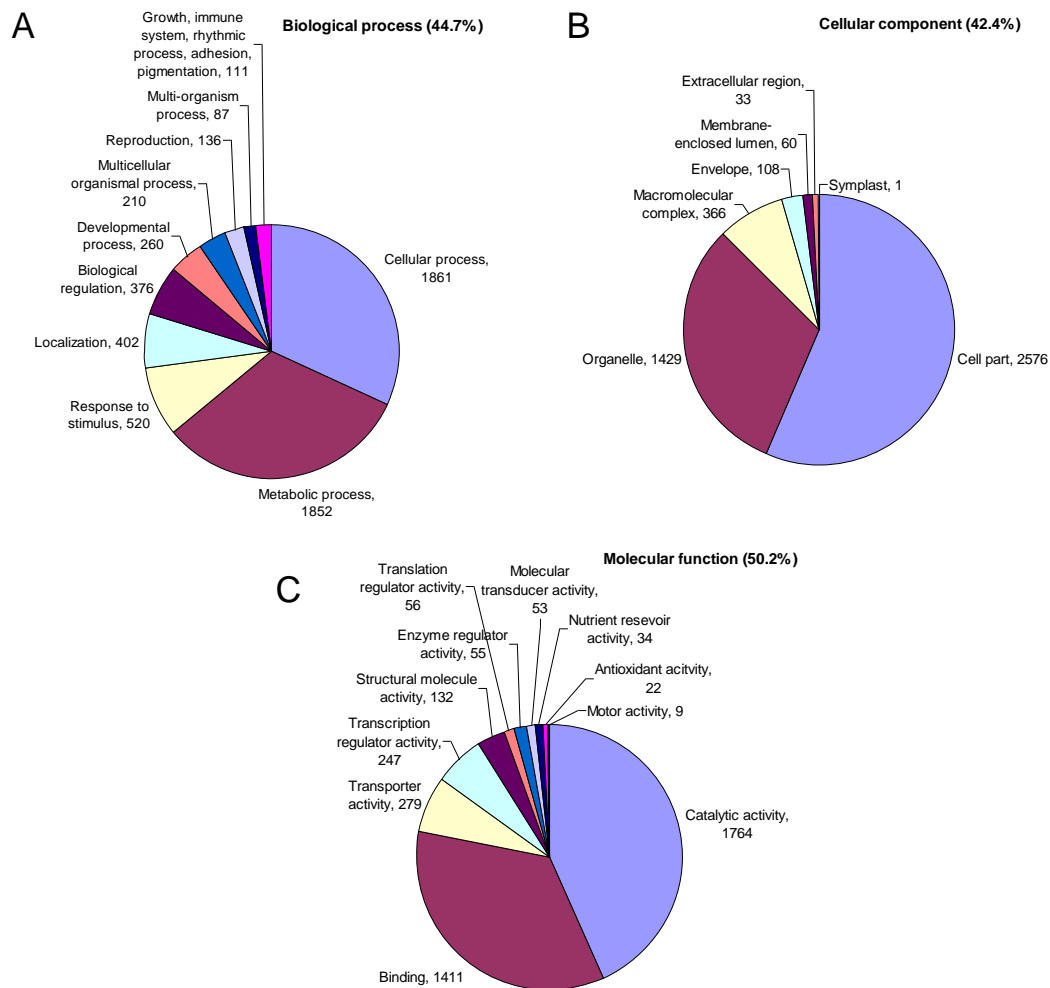
Supplement Data for Flavonoid Analysis in Saskatoon Fruits (*Amelanchier alnifolia* Nutt.)

Table A1: Total flavonol concentration over fruit development (mg/100 g fwt)^a.

| Cultivar | Stage 1 | Stage 4 | Stage 5 | Stage 7 | Stage 9 |
|-----------|-----------------|---------------------------|-------------|-------------|------------|
| Altaglo | nd ^b | 215.2 ± 12.3 ^c | 110.9 ± 3.1 | 57.4 ± 2.6 | 43.2 ± 1.3 |
| Honeywood | 98.4 ± 2.5 | 108.6 ± 5.5 | 83.4 ± 5.1 | 69.54 ± 1.9 | 97.1 ± 4.6 |
| Northline | 102.6 ± 5.8 | 68.6 ± 0.4 | 83.9 ± 5.2 | 67.3 ± 2.3 | 68.8 ± 3.3 |
| Pembina | 73.1 ± 5.7 | 66.6 ± 0.3 | 66.2 ± 9.7 | 48.7 ± 0.8 | 74.9 ± 1.5 |
| Theissen | 108.6 ± 2.8 | 127.1 ± 0.2 | 101.7 ± 0.1 | 55.2 ± 4.0 | 91.0 ± 0.9 |

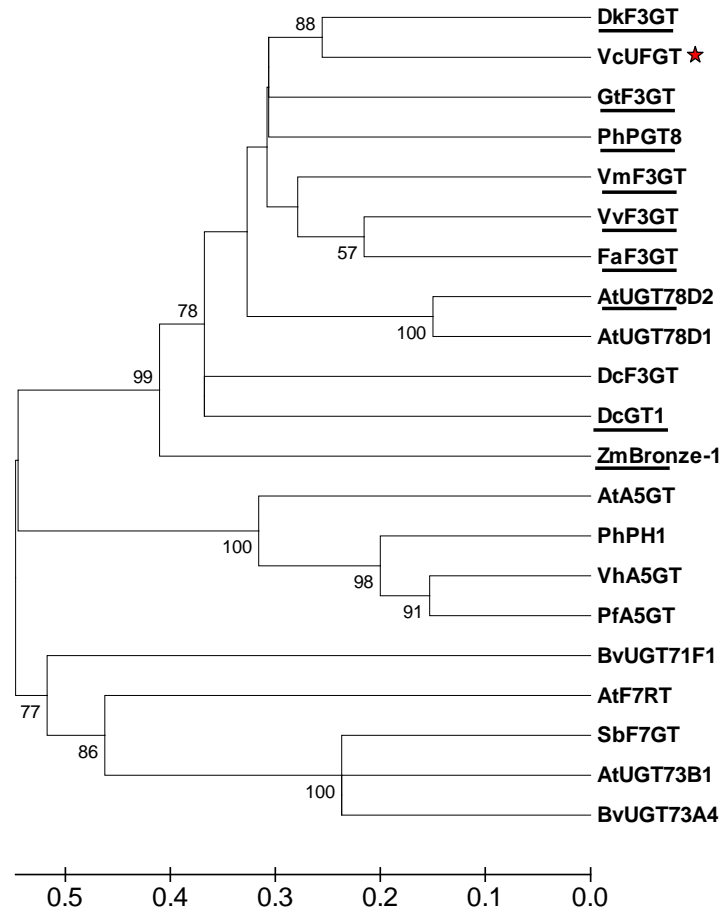
^a Flavonol content estimated as quercetin-3-*O*-glucoside (for all flavonols except Q-gal) and quercetin-3-*O*-galactoside equivalents; ^b nd=not determined; ^c Data are means ± SE, n=2 to 4.

Appendix B



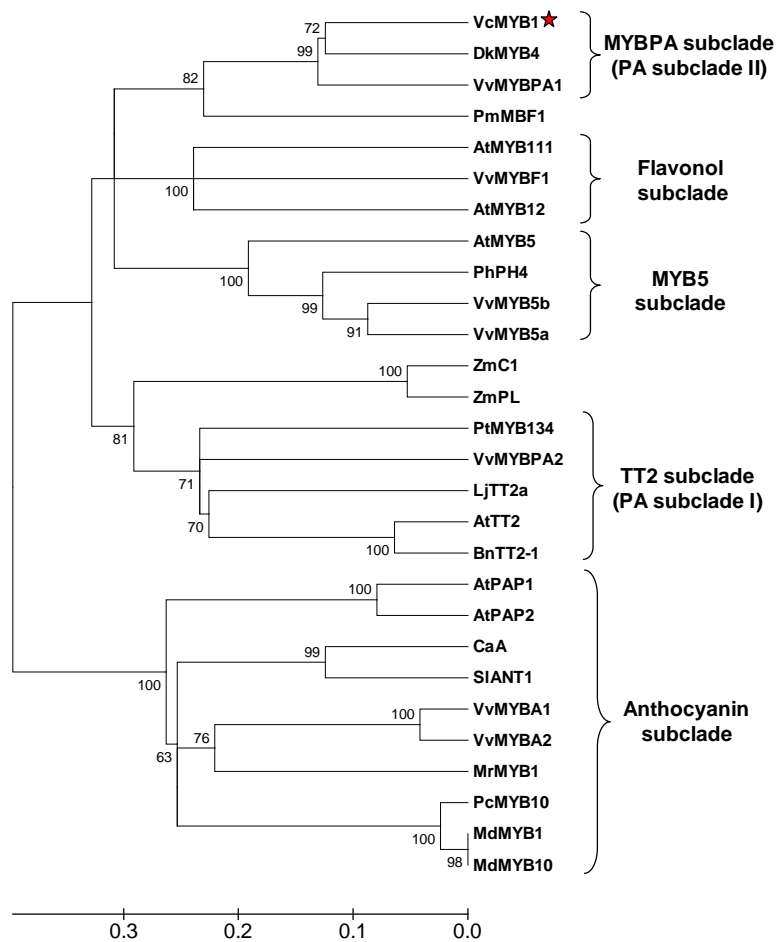
Supplemental Figure B1. Gene ontology (GO) categorization of blueberry unigenes.

Values are number of unigenes in each category. Percentage values are the proportion of unigenes that could be matched to a process, component or function within each category.



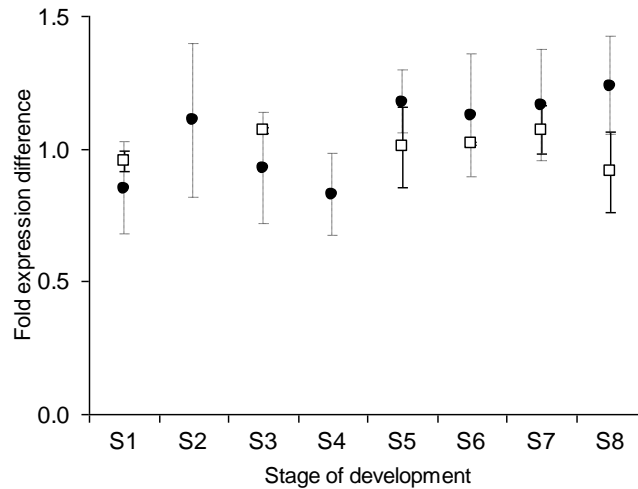
Supplemental Figure B2. Phylogeny of a subset of the flavonoid-O-glycosyltransferase family. Partial length sequences for functionally characterized flavonoid glycosyltransferases and the putative blueberry UFGT (black star). Sequences were trimmed to match the consensus region of the blueberry UFGT sequence (200-450 aa region). Enzymes that are involved in glycosylation at the 3-*O* position of at least anthocyanidins are underlined. Protein sequences were aligned with ClustalW and the linearized Neighbour-joining tree was produced with *MEGA* software version 4.0 (Tamura et al., 2007), as described for Fig. 3. GenBank accession numbers are as follows: DkF3GT (*Diospyrus kaki*, BAF49284), GtF3GT (*Gentiana triflora*, BAA12737), PhPGT8 (petunia, AB027454), VmF3GT (*Vigna mungo*, BAA36972), VvF3GT (*V. vinifera*, AAB81682), FaF3GT (*Fragaria x ananassa*, AAU09442), AtUGT78D2 (Arabidopsis, At5G17050), AtUGT78D1 (Arabidopsis, At1g30530), DcF3GT (*Dianthus caryophyllus*, BAD52005), DcGT1 (*D. caryophyllus*, BAD52003), ZmBronze-1 (*Zea mays*, X13502), AtA5GT (Arabidopsis, AAM91686), PhPH1 (petunia, BAA89009), VhA5GT (*Verbena hybrida*, BAA36423), PfA5GT (*Perilla frutescens*, BAA36421), BvUGT71F1 (*Beta vulgaris*, AY526081), AtF7RT (Arabidopsis, NP_563756), SbF7GT (*Scutellaria baicalensis*, BAA83484), AtUGT73B1 (Arabidopsis, At4g34138), and BvUGT73A4 (*B. vulgaris*, AY526080). F3GT, flavonoid 3-*O*-glycosyltransferase; A5GT,

anthocyanidin 5-*O*-glycosyltransferase, F7R(G)T, flavonoid 7-*O*-rhamnosyl(glycosyl)transferase.



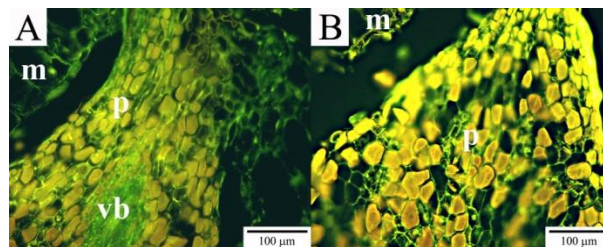
Supplemental Figure B3. Phylogeny of the flavonoid R2R3-MYB transcription factor family. The putative blueberry flavonoid regulator VcMYB1 is marked with a black star. Trimmed protein sequences were aligned with ClustalW and the linearized Neighbour-joining tree was produced with *MEGA* software version 4.0 (Tamura et al., 2007), as described for Fig. 3. GenBank accession numbers are as follows: DkMYB4 (*Diospyrus kaki*, AB503671), VvMYBPA1 (*Vitis vinifera*, AM259485), PmMBF1 (*Picea mariana*, AAA82943), AtMYB111 (Arabidopsis, NP_199744), VvMYBPF1 (*V. vinifera*, FJ948477), AtMYB12 (Arabidopsis, NP_182268), AtMYB5 (Arabidopsis, NM_112200), PhPH4 (petunia, AAY51377), VvMYB5b (*V. vinifera*, AY555190), VvMYB5a (*V. vinifera*, AAS68190), ZmC1 (*Zea mays*, AAK09327), ZmPL (*Z. mays*, AAB67721), PtMYB134 (*Populus trichocarpa*, FJ573151), VvMYBPA2 (*V. vinifera*, EU919682), LjTT2a (*Lotus japonicus*, BAG12893), AtTT2 (Arabidopsis, Q9FJA2), BnTT2-1 (*Brassica napus*, DQ778643), AtPAP1 (Arabidopsis, AAG42001), AtPAP2 (Arabidopsis, NP_176813), CaA (*Capsicum annuum*, AJ608992), SIANT1 (*Solanum lycopersicum*, AAQ55181), VvMYBA1 (*V.*

vinifera, BAD18977), VvMYBA2 (*V. vinifera*, BAD18978), MrMYB1 (*Myrica rubra*, GQ340767), PcMYB10 (*Pyrus communis*, EU153575), MdMYB1 (*Malus x domestica*, DQ886414), and MdMYB10 (*M. domestica*, ABB84753).

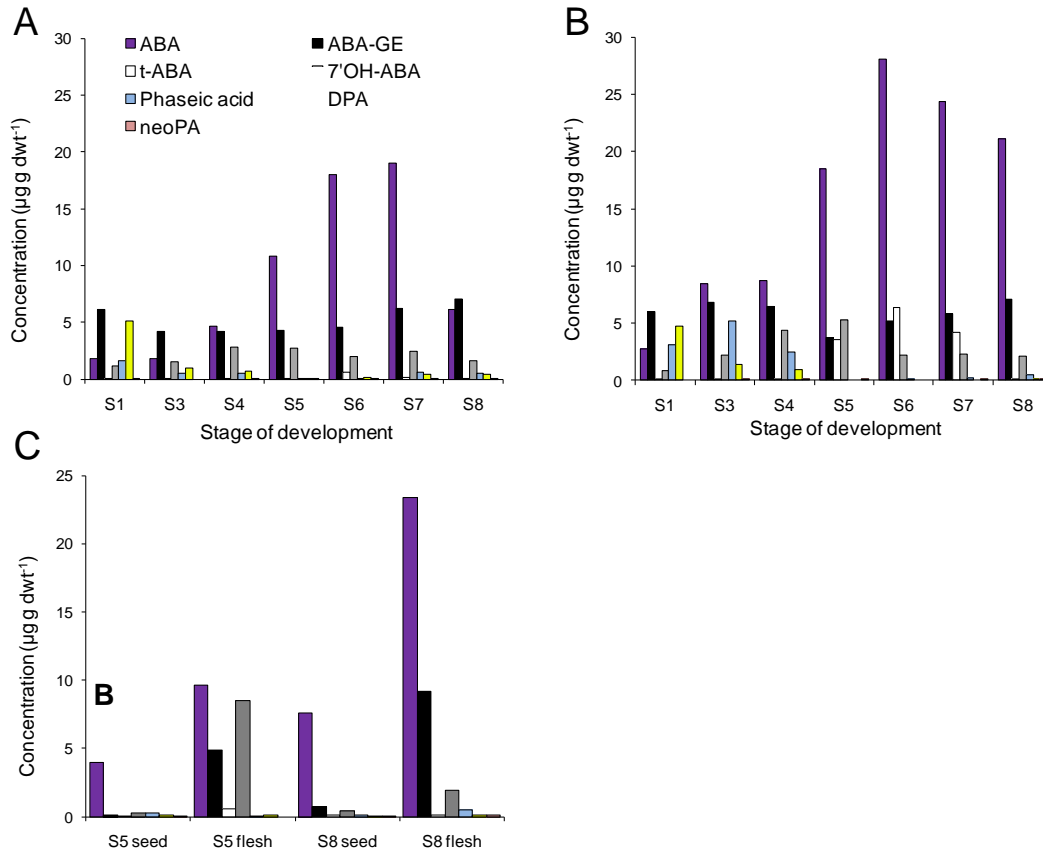


Supplemental Figure B4. Evaluation of reference genes for qPCR.

To show the relative stability of the best reference gene combination, the fold geometric mean C_q difference for *GAPDH* and *SAND* in each sample was calculated with respect to the overall mean C_q in each season (dark circles, 2008; open squares, 2009). A fold difference of 1.0 indicates no difference, 0.0-1.0 lower abundance, and > 1.0 higher abundance. Bars indicate standard error of the mean (dotted lines, 2008; solid lines, 2009).



Supplemental Figure B5. Fluorescence microscopy images of Stage 6 fruit cross-sections. (A) Blueberry fruit flavonol auto-fluorescence appears as a golden-yellow colour. (B) DPBA-stained stage 6 fruit fluorescence image. Flavonol fluorescence appears as a bright golden-yellow colour. Green colour is likely attributed to lignin fluorescence. m=mesocarp, p= placenta, vb= vascular bundle.



Supplemental Figure B6. Concentrations of ABA and ABA catabolites from pooled fruit tissue (also used for RNA extractions) for the 2008 (A) and 2009 (B) growing seasons. (C) Concentration of ABA and metabolites in seeds and flesh (skin and pulp) of 2009 S5 and S8 fruits.

Supplemental Table B1. Top 40 represented unigenes in the two blueberry fruit EST libraries.

| | Unigene | Total ESTs | S5/6 | S7/8 | Blast annotation | Arabidopsis Locus ID | E value |
|----|--------------|------------|------|------|--|----------------------|---------|
| 1 | CL1Contig166 | 172 | 165 | 7 | CRU1; cruciferin; nutrient resevoir | AT5G44120 | 1e-109 |
| 2 | CL1Contig27 | 140 | 122 | 18 | MT2A; metallothionein | AT3G09390 | 4e-11 |
| 3 | CL1Contig363 | 127 | 127 | 0 | CRU1; cruciferin; nutrient resevoir | AT5G44120 | 1e-103 |
| 4 | CL2Contig1 | 122 | 118 | 4 | CRU1; cruciferin; nutrient resevoir | AT5G44120 | 5e-32 |
| 5 | CL1Contig144 | 114 | 52 | 62 | TT6/metallothionein-like | AT3G51240 | 6e-22 |
| 6 | CL1Contig76 | 109 | 28 | 81 | protease inhibitor/seed storage/LTP | AT2G45180 | 7e-32 |
| 7 | CL1Contig356 | 106 | 103 | 3 | CRU1; cruciferin; nutrient resevoir | AT5G44120 | 1e-102 |
| 8 | CL1Contig382 | 82 | 82 | 0 | CRU1; cruciferin; nutrient resevoir | AT5G44120 | 1e-98 |
| 9 | CL1Contig216 | 78 | 1 | 77 | SAG29; senescence associated protein | AT5G13170 | 3e-65 |
| 10 | CL2Contig2 | 74 | 73 | 1 | CRU1; cruciferin; nutrient resevoir | AT5G44120 | 5e-75 |
| 11 | CL1Contig160 | 63 | 43 | 20 | MT3; metallothionein | AT3G15353 | 6e-17 |
| 12 | CL4Contig1 | 59 | 59 | 0 | CRU3; cruciferin | AT4G28520 | 6e-66 |
| 13 | CL1Contig357 | 52 | 49 | 3 | UBQ3; polyubiquitin | AT5G03240 | 1e-142 |
| 14 | CL1Contig381 | 50 | 50 | 0 | CRU1; cruciferin; nutrient resevoir | AT5G44120 | 1e-104 |
| 15 | CL1Contig285 | 49 | 41 | 8 | Polygalacturonase | AT1G70370 | 0 |
| 16 | CL1Contig361 | 48 | 44 | 4 | PAP85; vicilin-like seed storage protein | AT3G22640 | 2e-54 |
| 17 | CL1Contig195 | 45 | 0 | 45 | PR3; chitinase | AT3G12500 | 4e-97 |
| 18 | CL1Contig239 | 38 | 5 | 33 | Putative fructose-bisphosphate aldolase | AT2G36460 | 1e-167 |
| 19 | CL5Contig4 | 34 | 19 | 15 | TUA2; Tubulin alpha-2 chain | AT1G50010 | 0 |
| 20 | CL1Contig167 | 34 | 34 | 0 | CRU1; cruciferin; nutrient resevoir | AT5G44120 | 2e-44 |
| 21 | CL1Contig146 | 33 | 0 | 33 | SDH1-1; Succinate dehydrogenase 1-1 | AT5G66760 | 4e-84 |
| 22 | CL1Contig296 | 29 | 5 | 24 | Calcium-binding EF hand family protein | AT4G38810 | 1e-129 |
| 23 | CL10Contig1 | 26 | 21 | 5 | NADP-ME4; NADP-malic enzyme | AT1G79750 | 0 |
| 24 | CL9Contig1 | 26 | 10 | 16 | CYP2; cyclophilin-like | AT2G21130 | 8e-76 |
| 25 | CL1Contig343 | 25 | 6 | 19 | Gibberellin-regulated family protein | AT5G59845 | 2e-26 |
| 26 | CL1Contig360 | 24 | 24 | 0 | CRU1; cruciferin; nutrient resevoir | AT5G44120 | 7e-51 |
| 27 | CL1Contig92 | 24 | 7 | 17 | PM-associated cation-binding protein | AT4G20260 | 2e-27 |
| 28 | CL1Contig71 | 23 | 17 | 6 | RD22; responsive to dessication | AT5G25610 | 8e-77 |
| 29 | CL1Contig75 | 23 | 4 | 19 | NTF2B; nuclear transport factor | AT1G27970 | 1e-57 |
| 30 | CL12Contig2 | 22 | 1 | 21 | TDS 4; TT18; anthocyanidin synthase | AT4G22880 | 1e-145 |
| 31 | CL1Contig23 | 22 | 13 | 9 | Pectinesterase inhibitor | AT1G14890 | 3e-51 |
| 32 | CL1Contig2 | 22 | 10 | 12 | GRP7/CCR2; glycine rich protein | AT2G21660 | 4e-37 |
| 33 | CL1Contig366 | 21 | 21 | 0 | CRU1; cruciferin; nutrient resevoir | AT5G44120 | 1e-104 |
| 34 | CL1Contig243 | 21 | 2 | 19 | STF2; stromal cell-derived factor-like | AT2G25110 | 5e-90 |
| 35 | CL24Contig1 | 20 | 20 | 0 | CAT2; catalase | AT4G35090 | 1e-142 |
| 36 | CL20Contig1 | 20 | 20 | 0 | RPL2; ribosomal protein L2 | ATCG01310 | 1e-120 |
| 37 | CL1Contig244 | 20 | 1 | 19 | SKS5; SKU5 Similar 5 | AT1G76160 | 2e-92 |
| 38 | CL1Contig241 | 20 | 1 | 19 | glycine cleavage system H protein | AT2G35120 | 7e-64 |
| 39 | CL25Contig1 | 20 | 20 | 0 | RBCS1A; RUBISCO small chain | AT1G67090 | 4e-54 |
| 40 | CL1Contig151 | 20 | 0 | 20 | B5 #3; cytochrome B5 B isoform D | AT5G48810 | 4e-29 |

Supplemental Table B2. Reference genes evaluated for qRT-PCR transcript abundance normalization.

| Gene | Top REFSEQ match | Arabidopsis Locus ID | E value | % ID ^a | Region of ID ^b | Coverage (%) ^c | Amplicon Region ^d | No. of similar genes ^e |
|---------------|---------------------|----------------------|---------|-------------------|---------------------------|---------------------------|------------------------------|-----------------------------------|
| Actin | AtActin7 | AT5G09810 | 2e-119 | 95 | 85-318 | 62 | 95-222 (705) | 2 |
| EF-1 α | AtEF-1 α | AT5G60390 | 0.0 | 88 | *1-433 | 96 | 1097-1272 (1323) | 2 |
| GAPDH | AtGAPDH2 | AT1G13440 | 6e-168 | 93 | *2-336* | 100 | 501-602 (1011) | 3 |
| SAND | AtSAND family prot. | AT2G28390 | 4e-42 | 74 | 337-465 | 21 | 98-208 (420) | 0 |
| UBQ | AtUBQ4 | AT5G20620 | 2e-122 | 100 | *1-228 | 60 | 466-595 (777) | TNTD |

^a Based on amino acid sequence.

^b Stars (*) at left and right of region indicate presence of predicted start and stop codons, respectively.

^c Percentage of total predicted protein length present in unigene sequences.

^d Nucleotide region within each unigene that qPCR primers were designed to amplify with total unigene coding sequence length in brackets.

^e Predicted number of similar unique genes present within the blueberry fruit EST libraries. TNTC, too numerous to determine.

Supplemental Table B3. Reference gene statistics, stability values and rankings.

| | Mean Cq | Min Cq | Max Cq | SD (\pm Cq) | CV (%) Cq | NormFinder stability | geNorm stability | Rank |
|---------------|---------|--------|--------|----------------|-----------|----------------------|------------------|------|
| Actin | 200 | | | | | | | |
| | 8 | 23.34 | 21.61 | 25.21 | 0.99 | 4.26 | 0.382 | 4 |
| | 200 | | | | | | | |
| | 9 | 21.04 | 20.20 | 22.45 | 0.67 | 3.19 | 0.262 | 4 |
| | All | 22.58 | 20.20 | 25.21 | 1.41 | 6.26 | 0.384 | 4 |
| EF-1 α | 200 | | | | | | | |
| | 8 | 19.80 | 18.58 | 20.91 | 0.65 | 3.30 | 0.249 | 3 |
| | 200 | | | | | | | |
| | 9 | 17.84 | 17.16 | 18.32 | 0.37 | 2.08 | 0.168 | 3 |
| | All | 19.03 | 17.16 | 20.91 | 1.04 | 5.45 | 0.206 | 3 |
| GAPDH | 200 | | | | | | | |
| | 8 | 19.77 | 19.12 | 20.69 | 0.45 | 2.27 | 0.211 | 1 |
| | 200 | | | | | | | |
| | 9 | 18.72 | 18.41 | 19.23 | 0.24 | 1.29 | 0.233 | 2 |
| | All | 19.38 | 18.41 | 20.69 | 0.60 | 3.11 | 0.244 | 2 |
| SAND | 200 | | | | | | | |
| | 8 | 25.82 | 24.70 | 26.73 | 0.60 | 2.31 | 0.243 | 2 |
| | 200 | | | | | | | |
| | 9 | 24.41 | 23.96 | 24.63 | 0.19 | 0.80 | 0.164 | 1 |
| | All | 25.24 | 23.96 | 26.73 | 0.81 | 3.20 | 0.168 | 1 |
| UBQ | 200 | | | | | | | |
| | 8 | 21.76 | 20.88 | 23.27 | 0.67 | 3.08 | - | - |
| | 200 | | | | | | | |
| | 9 | 18.81 | 18.36 | 19.62 | 0.39 | 2.07 | - | - |
| | All | 20.78 | 18.36 | 23.27 | 1.53 | 7.36 | - | 5 |

Supplemental Table B4. LC-MS retention time and characteristic ions of stage 3 (S3) blueberry fruit PA acid-cleavage phloroglucinol derivatization products.

| Compound | Sample | t _R (min) ^a | Molecular ion ^b | Fragment ions |
|----------------------------|-------------------------|-----------------------------------|----------------------------|---------------|
| Catechin-phloroglucinol | Blueberry | 20.9 | 413 | 287, 261, 217 |
| | Grape skin ^c | 22.7 | 413 | 287, 261, 217 |
| Epicatechin-phloroglucinol | Blueberry | 21.7 | 413 | 287, 261 |
| | Grape skin | 23.61 | 412 | 287, 261 |
| A2-phloroglucinol | Blueberry | 31.1 & 37.0 | 699 | 573, 547, 411 |
| | Cranberry ^d | 32.4 | 699 | 573, 547, 411 |
| A2 | Blueberry | 52.3 | 575 | 137, 163 |
| | Cranberry | 53.28 | 575 | 423, 163 |
| Catechin | Blueberry | 33.1 | 289 | 245, 137, 59 |
| | Cranberry | 34.7 | 289 | 245, 217, 137 |
| Epicatechin | Blueberry | 44.2 | 289 | 245, 137, 59 |
| | Cranberry | 45.5 | 289 | 245, 137 |

^a t_R=Retention time; the blueberry, grape skin, and cranberry samples were run at different times leading to some variation in retention time between the same compounds in the different samples.

^b MS was run in the negative mode and all the molecular ions are [M-H]⁻.

^c The grape skin PA sample was processed as described by Kennedy and Taylor (2003), fraction 5 was used (eluent from the solvent system consisting of [v/v/v] 20% acetone, 65% methanol, 15% water with the solvent-water mixture containing 0.2% formic acid [v/v]).

^d The cranberry PA sample was processed as described by Koerner et al. (2009).

Supplemental Table B5. Gene-specific primers used for qRT-PCR.

| Gene | Forward primer | Reverse primer | Mean E ^a | Amplico length (bp) | T _a ^b (°C) |
|----------------------|-------------------------|-------------------------|---------------------|---------------------|----------------------------------|
| CHS | CTTGACTGAGGAAATCTTGAAGG | AGCCTCTTTGCCCAATTG | 2.02 | 115 | 58 |
| FHT | AACGTCACCTGCACTAGCAG | CTCGTTGCTGAATTCGTTGTAG | 1.78 | 100 | 60 |
| F3'H _G | CGAGATTCGATGCGTTTCTGAGT | GATTCGGTATCGGTGAGCTTC | 2.04 | 155 | 60 |
| F3'5'H _{AG} | GCAAGTGGGATGATTTGATAACG | TGTTGGTGAGGCTAAGTGATCC | 2.10 | 144 | 60 |
| Cytob5 | TCACAGGTCGCTCAACACAAGTC | CATCAAACCTCCTGGTTGCGTC | 1.99 | 149 | 60 |
| DFR | CACTGAGTTTAAGGGGATTCCTA | CCCTTCTCCCTACAAGTGCAA | 2.04 | 138 | 60 |
| | AGG | TGG | | | |
| ANS | CTTCATCCTCCACAACATGGT | GCTCTTGACTTCCCATTGCTC | 1.90 | 139 | 58 |
| UFGT | AGTTTGCTTTGAAGGCTGTTG | ATGTGCTGGTGTGCATTTG | 1.90 | 147 | 58 |
| ANR | CAAAGAGGGATTCAGCTACAAGT | ACAGACACACAGTGGCACATTA | 1.75 | 141 | 58 |
| | A | G | | | |
| LAR | TGATGAAGTTGAAGTGTGCGA | AATCCATTGGCGGTTACG | 1.81 | 146 | 58 |
| VcMYB ₁ | CCACCAAAGAAGAGGAGGAC | CCATTGCCATCGAATTTAGAC | 1.94 | 194 | 60 |
| NCED1 | GTCGTTCAAGAAGCCGTATCTC | ACGACGTAGTTCTGAGTGATCG | 1.86 | 128 | 58 |
| Actin | AGGCTAACCGTGAGAAGATGAC | AGAGTCCAGCACGATTCCAG | 2.09 | 127 | 58 |
| EF-1α | AGTTTGCTGAGATCTTGACCAAG | GTCCCTGACAGCAAACCTTC | 2.10 | 175 | 58 |
| GAPDH | GGTTATCAATGATAGGTTTGGA | CAGTCCTTGCTTGATGGACC | 2.04 | 102 | 58 |
| SAND | AAGCATCTCTTCATCCTGATGA | GATTGTATCTTGGCAGGCAA | 1.95 | 110 | 58 |
| UBQ | CATCTGGTGCTGAGGTTGA | CCTCCTTATCCTGTATCTTAGCC | 2.05 | 107 | 58 |

^a Mean E is the mean efficiency of reaction for each primer set (shown as 2008/2009 if different between seasons).

^b T_a is the annealing temperature used in each PCR for a given primer set.

Appendix C

Seed Coat Structure Changes over Pea (*Pisum sativum* L.) Seed Development

Introduction

In order to better understand the relationship between PA accumulation in the seed coats of pea (*Pisum sativum* L.) and pea seed coat structure, pea seed coat structure and the change of the structure over pea seed development were studied in the PA containing cultivar ‘Courier’ and the PA-deficient cultivar ‘Canstar’.

Material and methods

Plant material

Mature dry seeds of the pea (*Pisum sativum* L.) cultivars ‘Canstar’ and ‘Courier’ were planted in a growth chamber and grown under conditions as described in Chapter 6. Pea flowers were tagged at full bloom (anthesis) at the same time each day (10 am). Pea fruit were also harvested at the same time as flower tagging. Pea fruit were harvested onto ice at 4, 6, 8, 10, 15, 20, and 30 days after anthesis (DAA). Approximately 1 mm wide and 3 mm long seed coat cross sections were manually dissected out from the mid-cotyledon region of the whole seed immediately after harvesting, and immersed into a fixing solution.

Methods

The fixing solution was prepared in the same manner as described in Chapter 6. After 5 days of fixing, the seed coat sections were rinsed, dehydrated, and embedded using the same procedure as described in chapter 6. Sections of 2 to 4 μm thickness were obtained using an ultra microtome and the sections were mounted onto Superfrost[®] plus microscope slides. Drops of Richardson staining solution were placed on the slides and these slides were placed on a 60 °C hot plate for 2 min. After 2 min of staining, excess staining solution was washed out using distilled water. The slides were dried on the the 60 °C hot plate and

micrographs were obtained using Zeiss AXIO scope A1 light microscope (Zeiss, Germany) and with a microscope-mounted Optronics camera (Optronics, USA) controlled by Picture Frame™ Application 2.3 software.

Results and discussion

Some cultivars of pea accumulate flavonoids in their seed coats, especially proanthocyanidins (PAs), while other cultivars do not. In order to determine if any physiological/structural attributes are associated with PA accumulation in pea seed coats, seed coat cellular structure was assessed over development in ‘Courier’, a PA-accumulating cultivar, and ‘Canstar’, a PA-deficient cultivar. The pea seed coat tissues were processed according to a modified histological procedure (Chapter 6), and stained with Richardson stain for anatomical feature observation under a light microscope. In ‘Canstar’, the five seed coat tissue layers (Van Dongen et al., 2003), epidermis, hypodermis, chlorenchyma, ground parenchyma, and branched parenchyma, were well differentiated by 10 DAA (Figure C.1). In the later developmental stages (20 and 30 DAA), the branched parenchyma layer was crushed by the enlarging embryo and is no longer present. Maximum seed coat thickness was observed in 10 to 15 DAA ‘Canstar’ seed coats. Numerous starch granules were observed early in seed coat development (6 to 15 DAA), but by 20 DAA, only a few can be discerned.

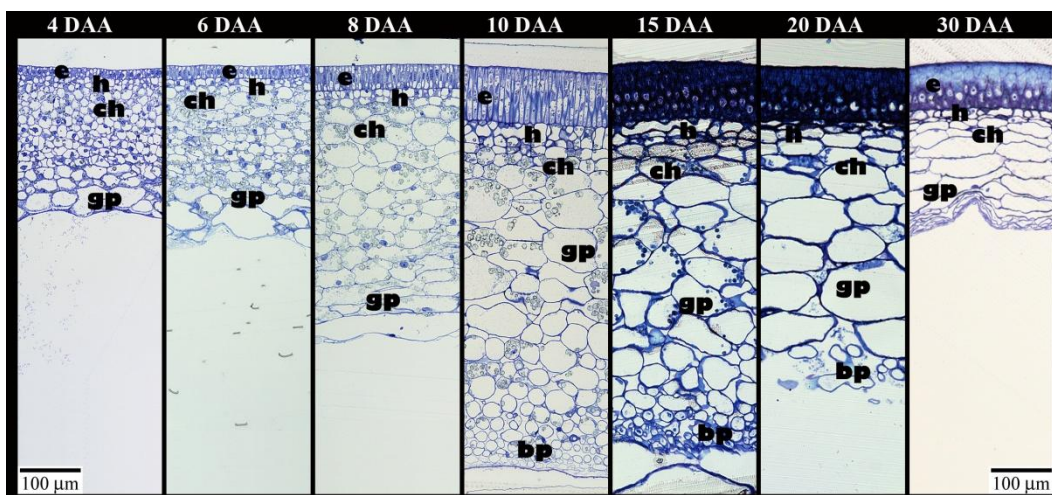


Figure C.1: Micrographs of ‘Canstar’ seed coat cross sections over pea seed

development (4 to 30 DAA). e, epidermis; h, hypodermis; ch, chlorenchyma layer; gp, ground parenchyma layer; bp, branched parenchyma layer.

In the PA-containing cultivar ‘Courier’, the five tissue layers, epidermis, hypodermis, chlorenchyma, ground parenchyma, and branched parenchyma, were well differentiated by 6 DAA compared to 10 DAA for ‘Canstar’ (Figure C.2). However, the reduction in seed coat inner tissues due to embryo expansion occurred later in development in ‘Courier’ compared to ‘Canstar’ (Figure C.2). Since ‘Canstar’ and ‘Courier’ have different genetic backgrounds, it is not possible to state if these differences in seed coat development between these two cultivars are due to PA synthesis and accumulation, or due to other genetic factors.

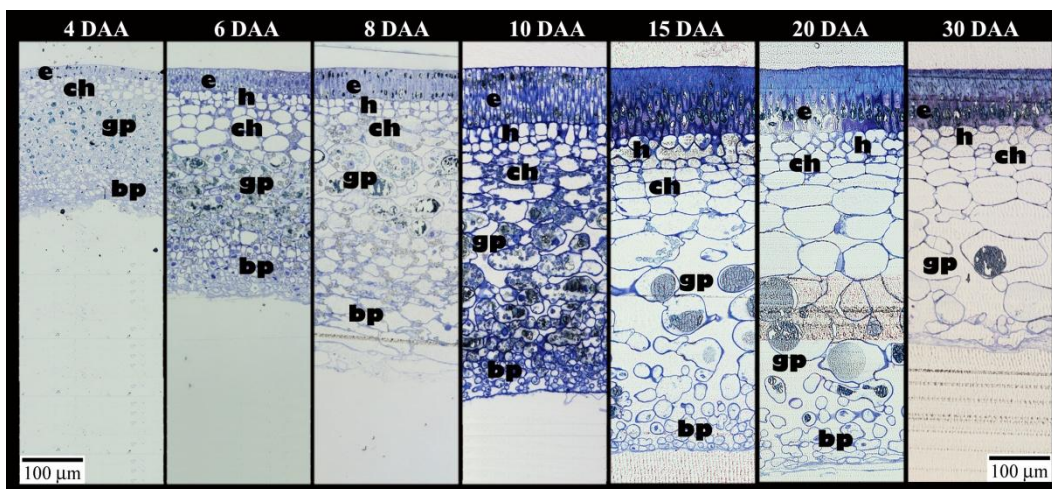


Figure C.2: Micrographs of ‘Courier’ seed coat cross sections over pea seed development (4 to 30 DAA). e, epidermis; h, hypodermis; ch, chlorenchyma layer; gp, ground parenchyma layer; bp, branched parenchyma layer.

Literature cited

Van Dongen JT, Ammerlaan AMH, Wouterlood M, Van Aelst AC, Borstlap AC (2003) Structure of the developing pea seed coat and the post-phloem transport pathway of nutrients. *Annals of Botany* **91**: 729-737